FIBRIN CLOT STRUCTURE ALTERATIONS AFTER PARTICULATE MATTER EXPOSURE

Xiaoxi Pan

Submitted in accordance with the requirements for the degree of
Doctor of Philosophy

University of Leeds

School of Medicine

2016

The Candidate confirmed that the work submitted is her own and that appropriate credit has been given where reference has been made on the work of others.

Data presented in chapter 4 has been published in the journal Environment International; doi:10.1016/j.envint.2016.03.030

ACKNOWLEDGEMENT

in patients with venous thrombosis" which was successfully accepted and published in the Environment International in July 2016.

ABSTRACT

Particulate matter (PM) as an important part of ambient air pollution has been associated with increased risks of cardiovascular diseases. Fibrin clot structure alteration is an emerging risk factor of many cardiovascular diseases, especially thrombosis. Therefore, the aim of this study was to investigate whether and how air particulate matter affects fibrin clot structure and endothelial cell behaviour.

Turbidity assay, turbidity lysis assay and laser scanning confocal microscopy were used to analyse clots formed from normal pooled plasma or purified fibrinogen, in the presence of varying concentrations of PM. It was found that clots formed from plasma with higher concentrations of particles led to prolonged lysis time compared to control. No differences were seen for clots formed from fibrinogen.

In a study of clots formed from plasma samples collected as part of a previous study on the effects of air pollution on deep vein thrombosis (DVT), alterations were observed in clots formed from plasma of DVT patients exposed to high levels of PM compared to those exposed to low levels, but the same differences were not observed in clots formed from plasma of control subjects.

To investigate the potential role of venous endothelial cells in moderating clot structure following exposure to PM, human umbilical vein endothelial cells (HUVEC) were treated with PM for 24 hours and clots subsequently formed on the cells. Clots formed from plasma on the treated cells were altered compared to controls. RT-PCR and ELISA results showed increased gene expression of tissue factor (TF), protein expression of von Willebrand Factor (VWF) and

plasminogen activation inhibitor-1 (PAI-1) and decreased thrombomodulin mRNA expression which were consistent with changes observed in clot structure.

Engineered SiO_2 nanoparticles caused denser clot structure in clots formed from normal pooled plasma. The gene expression of thrombomodulin was inhibited by SiO_2 nanoparticles, but there were no significant difference in the TF mRNA expression between control and treated cells. Silica NPs caused increased concentrations of VWF, but not PAI-1 produced by endothelial cells.

The results presented here show that PM can induce changes to clot structure and function, and that changes in gene expression induced in endothelial cells may be a mechanism by which a prothrombotic state is induced in response to PM exposure. Furthermore, some, but not all, similar changes were observed in clots and cells exposed to SiO_2 nanoparticles, raising the possibility that such engineered nanoparticles may also have the potential to contribute to cardiovascular toxicity.

CONTENT

LIST OF TABLES

LIST OF FIGURES

LIST OF ABBREVIATIONS

A2AP – α2-Antiplasmin

ACTB – Beta Actin

ADP – Adenosine Diphosphate

Ag(O) – Silver (Oxide)

APHEA – Agency for Public Health Education Accreditation

ATP – Adenosine Triphosphate

Au(O) – Gold (Oxide)

BMI – Body Mass Index

$CaCl_2$ – Calcium Chloride

CAD – Coronary Artery Disease

CDC – Centre for Disease Control and Prevention

CeO_2 – Cerium Dioxide

CHF – Congestive Heart Failure

Chk1 – Checkpoint Kinase 1

CI – Confidence Interval

CNTs – Carbon Nanotubes

CO – Carbon Monoxide

CRP – C Reactive Protein

CVD – Cardiovascular Disease

CVS – Cardiovascular System

DMSO – Dimethyl Sulfoxide

DPBS – Dulbecco's Phosphate Buffered Saline

DVT – Deep Vein Thrombosis

ECGS – Endothelial Cell Growth Supplements

ELISA – Enzyme-Linked Immune-Sorbent Assay

ENPs – Engineered Nanoparticles

F – Factor

FBS – Fetal Bovine Serum

Fe(O) – Iron (Oxide)

FITC – Fluorescein Isothiocyanate

FpA – Fibrinopeptide A

FpB – Fibrinopeptide B

GAPDH – Glyceraldehyde 3-Phosphate Dehydrogenase

GP – Glycoprotein

HBCD – Hexabromocyclododecane

HR – Hazard Ratio

HUVEC – Human Umbilical Vein Endothelial Cells

ICAM – Intercellular Adhesion Molecule

IL – Interleukin

Ks – Darcy Constant

LSCM – Laser Scanning Confocal Microscope

MCP – Monocyte Chemoattractant Protein

NIST – National Institute of Standards and Technology

Nitro-PAHs – Nitro-substituted Polycyclic Aromatic Hydrocarbons

NMMAPS – National Morbidity, Mortality, and Air Pollution Study

NO – Nitric Oxide

NO_x – Nitric Oxides

NPs – Nanoparticles

O_3 – Ozone

PAHs – Polycyclic Aromatic Hydrocarbons

PAI – Plasminogen Activator Inhibitor

PAR – Protease Activated Receptor

PBDE – Polybrominated Diphenyl Ether

PCDD – Polychlorinated Dibenzo-p-Dioxin

PCDF – Dibenzofuran

PE – Pulmonary Embolism

PM – Particulate Matter

$PM_{0.1}$ – Particulate Matter less than 100 nm in diameter

$PM_{0.2}$ – Particulate Matter less than 200 nm in diameter

$PM_{2.5}$ – Particulate Matter less than 2.5 μm in diameter

PM_{10} – Particulate Matter less than 10 μm in diameter

ROS – Reactive Oxygen Species

RR – Relative Risk

RT-PCR – Real-Time Polymerase Chain Reaction

Si(O) – Silicon (Oxide)

SiO_2 – Silicon Dioxide

SO_2 – Sulphur Dioxide

TF –Tissue Factor

TNF – Tumour Necrosis Factor

TAFI – Thrombin Activated Fibrinolysis Inhibitor

TFPI – Tissue Factor Pathway Inhibitor

THBD – Thrombomodulin

TiO_2 – Titanium Dioxide

Tm – Melting Temperature

tPA – Tissue-type Plasminogen Activator

UFPs – Ultrafine Particles

uPA – Urokinase-type Plasminogen Activator

VCAM – Vascular Cell Adhesion Molecule

VSMC – Vascular Smooth Muscle Cells

VWF – Von Willebrand Factor

WHO – World Health Organisation

ZnO – Zinc Oxide

1 Introduction

1.1 Air Pollution

Air pollution is a combination of gases and particulate matter (PM) varying in chemical compositions and concentrations that originate from man-made and natural resources (Brook, 2008; Gold and Samet, 2013). Air pollution is significantly associated with increased risk of mortality and morbidity (Franchini and Mannucci, 2012; Peters, 2005). The World Health Organisation described the worldwide impact of air pollution with 3.6 million premature deaths being attributable to ambient air pollution each year in both rural and urban areas (Mills et al., 2009; Newby et al., 2014; World Health Organisation, 2011). Many studies have shown that exposure to air pollution could lead to adverse effects on the pulmonary and cardiovascular systems. It is estimated that there are 80% of premature deaths related to ischaemic heart diseases and strokes, 14% of deaths caused by chronic obstructive pulmonary diseases or acute lower respiratory infections, and 6% of deaths due to lung cancer (World Health Organisation, 2011). Ambient air pollution ranked ninth among the modifiable disease risk factors, with other commonly recognized factors such as low physical activity, high cholesterol and drug use were all listed below air pollution (Newby et al., 2014). The American Heart Association writing group in 2004 illustrated that short-term air pollution exposure, especially to the PM, contributes to acute cardiovascular mortality and morbidity. For the long-term exposure, life expectancy would be reduced by a few years by high PM exposure (Brook et al., 2004).

Air pollution includes both indoor air pollution and outdoor air pollution. Indoor air pollution refers to the air pollution found in indoors and they are mainly from insufficient combustion of biomass fuels such as wood, charcoal, and animal/crop residues for cooking, lighting and heating, as well as fabric of buildings, and emissions from building materials such as chemical pollutants (Jones, 1999; Rajagopalan and Brook, 2012; World Health Organisation, 2015a, 2014). According to the World Health Organization, there are still approximately 3 billion people using open fires and simple stoves burning biomass and coal for cooking and heating. 76% of these people are from low- and middle- income countries. The house-hold air pollution exposure is particularly high among women and young children (Rajagopalan and Brook, 2012; World Health Organisation, 2015b). After exposure to the house-hold air pollution, children under five are susceptible to acute lower respiratory infections. And for the adults, ischaemic heart disease, stroke, chronic obstructive pulmonary disease and lung cancer are associated with the exposure. In 2012, household air pollution contributed 7.7% to global mortality (World Health Organisation, 2015b). Outdoor air pollution is an important cause of indoor air pollution, similarly, indoor air pollution also contributes to the outdoor air quality (World Health Organisation, 2014). In this study, we mainly focused on outdoor air pollution but there may be cross over for effects of indoor pollutants, especially from combustion.

1.1.1 Historical Perspective

As early as 1273, the use of coal as a fuel in London raised concerns regarding the bad influences of air pollution on health (Routledge and Ayres, 2005). In 1872, Robert Angus Smith published one of the first feature length air pollution related books, which was entitled "Air

and Rain, The Beginning of Chemical Climatology" (Simkhovich et al., 2008; Smith, 1872). There were several major air pollution incidents in the 20th century that highlighted the impact of air pollution on human health. In the December of 1930, high atmospheric pressure mixed with mild winds created a thick and motionless fog in the Meuse Valley in Belgium, the fog caused 60 deaths. This air pollution incident was caused by the thick low fog which entrapped pollutants from chimney exhausts and created a toxic cloud (Nemery et al., 2001; Simkhovich et al., 2008). On the 26th of October, 1945, industrial pollutants from a local smelting plant started to accumulate in the air over Donora, Pennsylvania. This incident caused 20 fatalities, with approximately 5,000 to 7,000 people (of 14,000 residents) becoming ill (Helfand et al., 2001; Simkhovich et al., 2008). In 1952, a dramatic air pollution event, referred to as the Great Smog, occurred in Greater London. From 5th to 9th of December, the entire city was almost paralysed by the heavy fog carrying pollutants from local industrial plants. The PM_{10} level was between 3,000 to 14,000 $\mu g/m^3$. The hospital admission rate was increased by 48%, especially the respiratory disease related admissions increased by 163%. In three months' time (from December 1952 to February 1953), 12,000 more deaths induced by this environmental incident (Davis et al., 2002; Simkhovich et al., 2008; Utell et al., 2002).

Figure 1-1. Great Smog in Great London, December 1952

Source: Elliot Wagland, 2013

After these environmental incidents, at the early 1970s, many countries started to introduce

and enforce regulations aimed at limiting the effects of air pollutants (Simkhovich et al., 2008;

Utell et al., 2002).

1.1.2 Air Pollutants

Urban air pollution is a heterogeneous mixture of gaseous pollutants and PM (Sun et al., 2010).

The components of the air pollutants are various depend on the meteorological conditions,

time of the day, industrial operations, traffic density, etc. (Langrish et al., 2012). But, in

general, the main components of gaseous pollution include ozone (O_3), nitrogen oxides (NO_x),

sulphur dioxide (SO_2), carbon monoxide (CO), carbonyl compounds, and organic solvents

(Newby et al., 2014; Polichetti et al., 2009; Sun et al., 2010). The primary pollutants originate

from the combustion of fossil fuels, releasing pollutants such as soot particles and oxides of

nitrogen and sulphur directly into the air (Newby et al., 2014). The major sources of these

gaseous pollutants, NOx, SO_2, and CO are from high temperature industrial processes (Brook et al., 2010). The secondary pollutants are recombined in the atmosphere, for example, ozone is formed by complex photochemical reactions of nitrogen oxides and volatile organic compound (Newby et al., 2014).

The PM in air pollution is a mixture of particles, with different sizes, shapes, surface area, chemical composition, solubility, and different origins that are suspended in the air (Pope 3rd, 2009). PM is categorized by aerodynamic diameter to include coarse particles with a diameter range less than 10 μm (PM_{10}), fine particles with a diameter less than 2.5 μm ($PM_{2.5}$), and ultrafine particles with a diameter less than 100 nm ($PM_{0.1}$) (Brook, 2008; Polichetti et al., 2009). Hence, PM_{10} contains both $PM_{2.5}$ and $PM_{0.1}$. PM_{10} and $PM_{2.5}$ are measured in their mass per volume of air ($μg/m^3$). However, in consideration of the particle size, ultrafine particulate matter are measured by their number per cubic meter (Brook et al., 2010).

PM consists of many chemical compounds, including organic carbon species, elemental or black carbon, and trace metals (e.g. lead and arsenic) (Brook et al., 2010). In terms of the origins of PM, coarse particles are mainly from a number of human and natural activities, such as mechanical grinding in industries and transportation (Shah et al., 2013). Non-combustion surface or randomly releases that arise from agriculture emissions and industrial processes, as well as waste management all contribute to the production of coarse particles or even larger sizes (Brook et al., 2010). $PM_{2.5}$ represents approximately 50-70% of the total mass of PM_{10}, which is worth noting that $PM_{2.5}$ can travel larger distances (over 100 km) compared to PM_{10} (Newby et al., 2014). $PM_{2.5}$ is mainly originated from combustion processes of fossil and bio-fuels, as well as high temperature industrial processes and can contribute to smoke and

haze in urban areas (Pope, 2009, Brook et al., 2010). The ultrafine particulate matter is mainly from fresh combustion and traffic–related pollution (Brook et al., 2010). $PM_{0.1}$ is very short-lived and found mainly within only a few hundred meters of its sources (Brook, 2008). Ultrafine PM are included in both coarse and fine PM, nevertheless $PM_{0.1}$ contribute particle numbers instead of the mass as they have negligible weight. For the same mass concentration of PM, ultrafine PM have much larger surface area and high number of particles compared to the larger size of PM. Ultrafine PM acts as a carrier to the lung for absorbed reactive gases, free radicals, and metal or organic compounds (Wichmann and Peters, 2000).

According to the World Health Organisation statistics, the guideline values for PM_{10} and $PM_{2.5}$ are 50 $\mu g/m^3$ and 25 $\mu g/m^3$ as the 24-hour mean concentrations; 20 $\mu g/m^3$ and 10 $\mu g/m^3$ as the annual concentrations (World Health Organisation, 2011). According to the database of WHO in 2014, ambient air pollution was monitored in approximately 1600 cities in 91 countries from 2008 to 2012. The world's average level of PM_{10} was 71 $\mu g/m^3$, region range from 26 to 208 $\mu g/m^3$. Compared to high-income countries, middle- and low- income countries had higher PM_{10} levels, especially those in the Eastern Mediterranean reached the highest PM_{10} level, 208 $\mu g/m^3$. Africa and South-East Asia also had high levels of PM_{10} which were 78 and 128 $\mu g/m^3$ respectively (World Health Organisation, 2014). The details of PM_{10} levels in other regions are shown in the following figure.
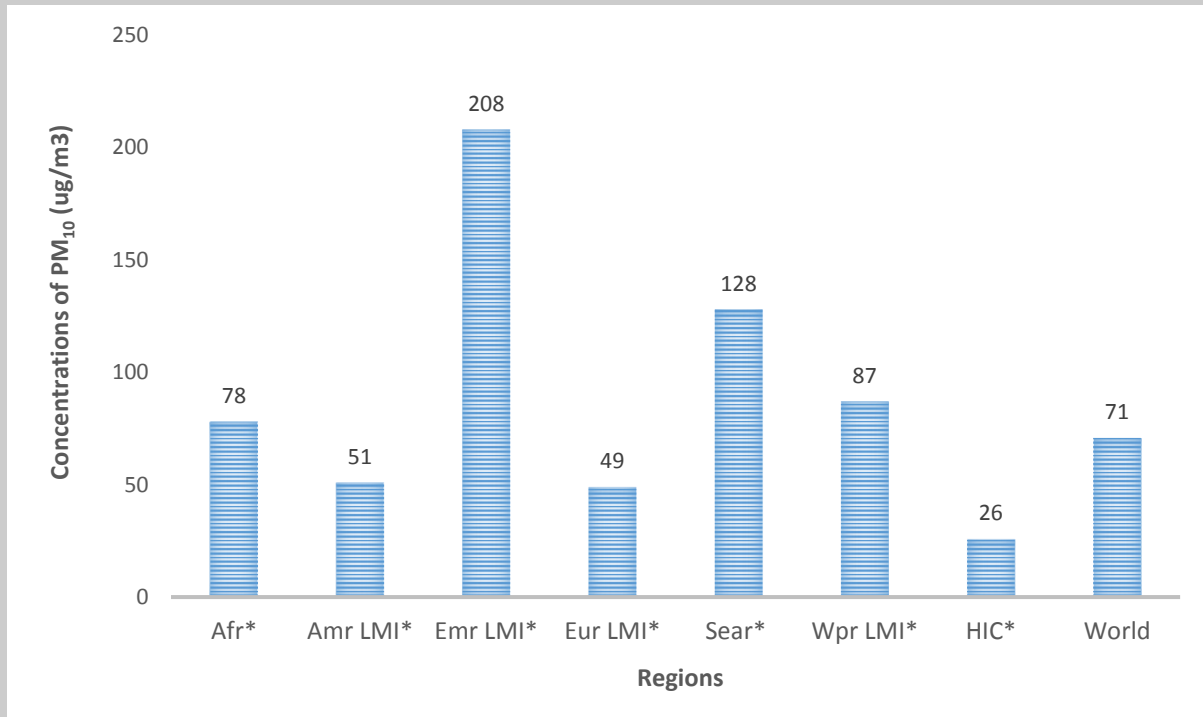
Figure 1-2: PM$_{10}$ levels by region (2008-2012)

* PM10 values are regional urban population-weighted.

Afr: Africa;

Amr: America,

Emr: Eastern Mediterranean,

Sear: South-East Asia,

Wpr: Western Pacific;

LMI: Low- and Middle-Income countries;

HIC: High-Income Countries.

Source: Adapted from World Health Organisation, 2014 (World Health Organisation, 2014)

PM$_{10}$ are identified as "inhalable particles" (Mills et al., 2009) as they are able to enter into the lung through the respiratory tract (Shah et al., 2013). Coarse particles most likely deposit in upper and larger airways. Fine particulate matter can transfer into deeper respiratory tract, with deposition in the alveolar region (Snow et al., 2014, Sun et al., 2010) then affect the cardiovascular system (Shah et al., 2013). PM$_{0.1}$ is able to be inhaled deeply into the lungs.

Due to the small size, those particles are difficult to be cleared by alveolar macrophages as alveolar macrophages may not be able to recognize particles with a diameter less than 500nm (Snow et al., 2014), hence, ultrafine PM is able to be exempted from phagocytosis. While $PM_{0.1}$ deposits in the deeper alveolar region, particles may interfere with cells, fluids, and tissues of the lungs due to their large surface area. Also, the ultrafine particles may be able to translocate to different organs by crossing into the circulatory and/or lymphatic systems (Wichmann and Peters, 2000).

Population and individual level of exposure to the air pollutants are different due to greatest impact on concentrations by multiple time scales, weather patterns, seasonal cycles in solar radiation and temperature (Brook et al., 2010). Compared to PM_{10} and $PM_{0.1}$, $PM_{2.5}$ has the longest atmospheric lifetime and can be spread by the prevailing winds over large geographic regions and leads to greater number of people being exposed to similar levels (Brook et al., 2010). Also, actual exposure to all pollutants vary at the personal level can be various depending on the different microenvironments or activities an individual experiences (Brook et al., 2010).

Air particulate matter could increase the risks of cardiovascular diseases through two pathways. Firstly, PM may have direct effects on the lung and cardiovascular system. Alternatively, particles may provoke either pulmonary inflammation or oxidative stress or both, with release of prothrombotic and inflammatory cytokines into the circulation (Chuang et al., 2007, Mills et al., 2009). But there are limited evidence in the specific particulate constituents and sources responsible (Brook et al., 2010).

1.1.3   Routes of Exposure

Humans are exposed to air pollutants mainly through the respiratory system. Food and water are contaminated by the ambient air pollutants; therefore, ingestion can be the second major route of air pollutants intake (Kampa and Castanas, 2008; Thron, 1996). Also, dermal contacts may also be taken into account as a minor route of exposure to air pollutants. To a certain degree, the air pollutants can be eliminated though excretion (Kampa and Castanas, 2008; Madden and Fowler, 2000).

1.2   Cardiovascular System and Diseases

The cardiovascular system is composed of the heart, blood vessels and blood (Aaronson and Ward, 2007). The heart includes two muscle pumps, the right and left ventricles (Aaronson and Ward, 2007; Levy et al., 2007). Each pump is connected with a contractile reservoir, the right or left atrium; and serves different circulations (Aaronson and Ward, 2007). The pulmonary circulation starts from the right ventricle. The deoxygenated blood is pumped through the pulmonary trunk to the lungs, four pulmonary veins return oxygenated blood from the lungs to the left atrium to complete the short and low pressure circulation (Aaronson and Ward, 2007). The left ventricle propels the oxygenated blood to all other tissues of the body. The tissues absorb some of the oxygen, and partly deoxygenated blood returns via two great veins, the superior vena cava and inferior vena cava, to the right atrium. This second, systemic circulation loop is under higher pressure and is longer compared to the pulmonary circulation (Aaronson and Ward, 2007; Levick, 2003).

The primary function of the cardiovascular system (CVS) is distributing oxygen, glucose, amino acids, fatty acids, hormones, vitamins and water to the tissues; and removing the metabolic by-products from the tissues (carbon dioxide, urea, creatinine) (Aaronson and Ward, 2007; Levy et al., 2007). Secondly, the CVS regulates the body temperature through transporting the heat from deep organs to the skin surface and regulate heat loss from the skin. Thirdly, the CVS maintains the body under homeostatic stasis by controlling the humoral communication throughout the body (Aaronson and Ward, 2007; Levick, 2003; Levy et al., 2007).

According to World Health Organisation (WHO), a group of disorders affecting the heart, brain, and blood vessels are classified as cardiovascular diseases (CVDs), such as coronary heart disease, cerebrovascular disease, raised blood pressure, venous thrombosis, pulmonary embolism, peripheral artery disease, rheumatic heart disease, congenital heart disease and heart failure (World Health Organisation, 2011). According to the WHO Statistics, CVDs are the number one cause of death around the world. About 17.3 million people died from CVDs in 2008 representing 30% of all deaths worldwide. CVDs are projected to be the single leading cause of death and it is estimated that 25 million people will die from CVDs by 2030 (World Health Organisation, 2011).

In the UK, CVD accounted for about 180,000 deaths in 2010 – about one in three of all deaths that year (British Heart Foundation, 2012). In addition, the report from the Centre for Disease Control and Prevention (CDC) in the U.S demonstrated that CVD caused 761,085 deaths in 1981 and 700,142 in 2001 (Brook et al., 2010). The main types of CVD are coronary artery disease (CAD) and stroke, of which 45% of CVD mortality is from CAD and 28% is from stroke

(British Heart Foundation, 2012). There are also a variety of cardiovascular diseases, but atherosclerosis and hypertension are the most common types (Ajjan and Ariens, 2009). Many factors increase the risks for developing CVDs, including tobacco use, physical inactivity, diabetes, obesity and raised blood pressure (Frayn et al., 2005). Modern lifestyle changes lead to the increase of many of these CVD risk factors.

1.2.1 Coronary Artery Disease

The coronary artery disease also known as coronary heart disease, is a condition in which the walls of the coronary arteries supplying the oxygen-rich blood to the muscle of the heart become thickened, therefore, the coronary artery lumen gets narrowed and the blood flow reduces (Libby and Theroux, 2005). The presence of atherosclerosis plaque leads to coronary artery disease that is a chronic process starting from early of adolescent life and continues to develop throughout the life time (Libby and Theroux, 2005).

CAD causes the highest mortality rate in the UK which is approximately 82,000 deaths per year. Men have higher mortality rate of CAD which is one in five compared to women's one in ten (British Heart Foundation, 2012). However, after the age of 50, men and women have a similar risk rate. One recent study showed there were about 2.7 million people suffering from CAD, in which about 2 million people were affected by angina in the UK (Mahmood, 2009). There are also two other common symptoms as well as angina, heart attacks and heart failure (Frayn et al., 2005).

1.2.2   Thrombosis

Thrombus formation is a dynamic process and in which shear stress, flow, turbulence, and the number of platelets in the circulation greatly impact the structure of the clot. Thrombosis refers to the clot formation within the vessel that reduces the blood flow or blocks the vessel completely therefore leading to myocardial tissue infarction (Mackman, 2012). The two most common types of thrombosis occur in the arteries and veins.

Arterial thrombosis refers to the thrombus forms in the arteries. In most cases, arterial thrombosis is caused by the rupture of plaques. Myocardial infarction, unstable angina, ischemia stroke, arterial fibrillation and peripheral arterial diseases are all belonging to arterial thrombosis. The risk factors of arterial thrombosis include age, smoking, obesity, high blood pressure, lack of physical activity, high cholesterol level, and diabetes (Celinska-Lowenhoff et al., 2011; Meltzer et al., 2007).

Venous thromboembolic diseases include deep vein thrombosis (DVT), which occurs in the legs or arms, and pulmonary embolism, which occurs when a piece of the deep vein thrombus in the leg (or arm) breaks off (embolism) and travels to the lung through the vena cava, right atrium/ventricle and pulmonary artery to block a blood vessel in the lung (Mackman, 2012). Venous thrombosis begins at the venous valves (Esmon, 2009). A triad of causes for venous thrombosis was proposed by Virchow in 1856 including 1) changes in blood coagulability, 2) changes in vessel wall and 3) circulatory stasis (Esmon, 2009). Elevated level of coagulation factors and defects of natural anti-coagulants are both associated with risk of venous thrombosis (Esmon, 2009). However, compared to age and carcinoma, these factors are less frequent contributors to venous thrombosis. Cancer is able to increase the risks of venous

thrombosis about 6 to 10 fold through three pathways: generating tissue factor (TF) to initiate the coagulation, shedding procoagulant lipid microparticles, or impairing blood flow (Esmon, 2009). Venous thrombosis is the second leading cause of death in patients with cancer (Furie and Furie, 2008). High levels of FVIII, FIX and FXII are able to increase the risk of venous thrombosis two-fold (Bouma and Mosnier, 2006; Koster et al., 1995; Meijers et al., 2000; van Hylckama Vlieg et al., 2000). Factor V Leiden is a gene defect which is found in one third of the Caucasian patients with venous throboembolism. Factor V Leiden has a mutation Arg506 which is between Arg to Gln mutation. This form of FV is not be able to be cleaved by activated protein C, thus can not support the APC-driven inactivation of FVIIIa. Subjects with heterozygous or homozygous FV Leiden will have 5 and 50 fold increased risks of venousm thrombosis, respectively (Bertina et al., 1994; Dahlbäck and Villoutreix, 2005; Rosendaal and Reitsma, 2009; Versteeg et al., 2013).

1.3   PM Effects on Cardio-respiratory System

Many epidemiological and experimental studies have shown that the cardiovascular system and the respiratory system are particularly influenced by PM (Kampa 2008, Cohen 2005, Huang 2006, Kunzli 2005, Sharma 2005).

The PM in urban air pollution has been associated with cardiovascular mortality and morbidity in a number of studies (Brook et al., 2010; Newby et al., 2014). There are several cardiovascular diseases where exposure to PM has been shown to contribute to risk, including

ischemic heart disease, heart failure, cerebrovascular disease, cardiac arrhythmias, peripheral arterial and venous diseases (Brook et al., 2010; Mills et al., 2009; Newby et al., 2014).

The epidemiological studies can be broadly categorized to short-term exposure studies and long-term exposure studies. Different types of effects may be expected with different exposure terms. For the short-term exposure, acute effects can be induced such as autonomic imbalance and systematic inflammation (Brook, 2008). Both initiation and aggravation of diseases are caused after long term air pollution exposure, for example, the progression of atherosclerosis. Also, carcinogenesis is another possible latent effect (Brook, 2008; Routledge and Ayres, 2005). Observational studies and experimental studies of different sizes of PM are described respectively as follows.

1.3.1 PM_{10}

There are many epidemiological studies focused on the long-term effects of PM_{10} on the cardiovascular system. Several key studies are summarised in the table 1-1.

There is a study focused on the associations between air pollution and cardiovascular hospital admissions for people aged over 65 years from 1986 to 1989 in Michigan, U.S, an increase of 32 $\mu g/m^3$ of PM_{10} concentrations were associated with increased ischemic heart disease hospitalisation (adjusted relative risk (RR) = 1.018, 95% confidence interval (CI) = 1.005--1.032) (Schwartz and Morris, 1995). A German cohort study carried out from 1985-2003 showed cardiopulmonary mortality was associated with residents living within a 50-meter radius of a major road (RR = 1.70; 95% CI = 1.02--2.81) and with PM_{10} exposure (adjusted RR = 1.34; 95%

CI = 1.06--1.71 for 1-year average) (Gehring et al., 2006). A 67% increase in risk of deep vein thrombosis for each 10 μg/m^3 elevation of PM_{10} was observed in a large cohort study with 16 year follow up (from 1995 to 2005) in the Lombardy region (OR = 1.70; 95% CI = 1.30--2.23) (Baccarelli et al., 2008). A retrospective cohort study carried out from 1998-2009 in Shenyang, China, reported that every 10 μg/m^3 of PM_{10} caused a 55% increased cardiovascular mortality (hazard ratio HR = 1.55; 95% CI = 1.51--1.60) and 49% increase in cerebrovascular morbidity (HR = 1.49; 95% CI = 1.45--1.53), respectively (Zhang et al., 2011). A census mortality study from New Zealand from 1996-1999 showed that every 10 μg/m^3 increase in average PM_{10} exposure was related to a 7% (95% CI = 3%--10%) increase of all-cause mortality in adults aged 30-74 years at census (Hales et al., 2012). According to another cohort study from 1985 to 2008, an increase of 10 μg/m^3 PM_{10} was associated with an increased hazard ratio for all-cause mortality (HR = 1.15, 95% CI = 1.04--1.27), cardiopulmonary mortality (HR = 1.39, 95% CI = 1.17--1.64), and lung cancer mortality (HR = 1.84, 95% CI = 1.23--2.74) (Heinrich et al., 2013). In a prospective cohort study of 71,431 middle-aged Chinese men who were studied from 1990 to 2006, PM_{10} was significantly correlated with mortality from cardiopulmonary diseases, with every 10 μg/m^3 of PM_{10} increase being associated with 1.6% increased total mortality rate (95% CI = 0.7%--2.6%), 1.8% increased cardiovascular mortality rate (95% CI = 0.8%--2.9%), and 1.7% increased respiratory mortality rate (95% CI = 0.3%--3.2%) (Zhou et al., 2014). Another retrospective cohort study focused on the association between long-term PM_{10} exposure and cardiovascular mortality rate in 4 cities of China from 1998-2009. Each elevated 10 μg/m^3 of PM_{10} lead to the increase of relative risk ratios (RRs) of all-cause mortality, 1.24 (95% CI = 1.22--1.27), cardiovascular disease mortality, 1.23 (95% CI = 1.19--1.26), ischemic heart disease mortality, 1.37 (95% CI = 1.28--1.47), heart failure disease

mortality, 1.11(95% CI = 1.05--1.17), and cerebrovascular disease mortality, 1.23(95% CI = 1.18--1.28) (Zhang et al., 2014). Every 10 μg/m^3 elevation of PM_{10} concentration increases the risks of hospitalization for myocardial infarction (Mu et al., 2014; Polichetti et al., 2009).

This meta-analysis showed that every 10 μg/m^3 elevation in PM_{10} concentration was associated with 1.63% increased heart failure hospitalisation or death rate (95% CI = 1.20%--2.07%) (Morris, 2001). Also, a systematic review focused on the Chinese population and 1464 articles and indicated that every 10 μg/m^3 increase in PM_{10} results in 23–67% increase in the risk of total mortality (Lu et al., 2015).

There are a few epidemiological studies focused on short-term exposure of PM_{10} (Table 1-1).

Schwartz investigated admissions to all hospitals in Tucson, Arizona, for cardiovascular disease in people aged over 65 years. An inter-quartile range increase (23 micrograms per m^3) in PM_{10} was associated with increased hospital admissions by 2.75% (95% CI = 0.52%--5.04%) (Schwartz, 1997). Revised Analysis of National Morbidity, Mortality, and Air Pollution Study (NMMAPS) recruited from 20 to 100 cities in the U.S. Data was collected from 1987 to 1994. The results showed that PM_{10} significantly increased the risks of both cardiovascular and respiratory deaths. Every 10 μg/cm^3 elevation of PM_{10} increased 0.68% of death (95% posterior interval, 0.20 to 1.16 percent) (Samet et al., 2000). The European Approach 2 (Agency for Public Health Education Accreditation APHEA2) project conducted in eight European cities (Barcelona, Birmingham, London, Milan, the Netherlands, Paris, Rome, and Stockholm) focused on the short-term effects of ambient PM on the mortality rate in 29 European countries. For all ages, every daily increase of 10 μg/m^3 of PM_{10} or black smoke were associated with 0.6% increase in daily deaths (95% CI = 0.4--0.8%), for the elderly it was

slightly higher (Katsouyanni et al., 2001). It also found that 0.5% (95% CI = 0.2--0.8) of cardiac hospital admissions for all ages was correlated with 10 μg/m^3 of PM$_{10}$, and 0.7% (95% CI = 0.4--1.0) for cardiac admissions over 65 years (Le Tertre et al., 2002). Another study was conducted in 7 United States cities from 1986 and 1999 focused on the association between daily levels of PM$_{10}$ and the rate of hospitalization for congestive heart failure (CHF) in Medicare recipients (age > or = 65 years). It indicated a 10 μg/m^3 increase in PM$_{10}$ was associated with a 0.72% (95% CI = 0.35%--1.10%) increase in the rate of admission for CHF on the same day (Wellenius et al., 2006). From 1987 to 1993, Ponka *et al.* investigated the association between daily concentrations of SiO$_2$, NO$_2$, O$_3$, and PM$_{10}$, and the daily number of deaths from all causes and cardiovascular causes. The results showed that every 10 μg/m^3 of PM$_{10}$ were associated with 3.5% (95% CI = 1.0--5.8) and 4.1% (95% CI = 0.4--10.3) increases of total mortality and cardiovascular mortality respectively (Pönkä et al., 2010). Analitis *et al.* investigated the short-term effects of ambient particle concentrations (on cardiovascular and respiratory mortality from 29 European cities. The results showed 10 μg/m^3 increase of PM$_{10}$ was associated with increases of 0.76% (95% CI = 0.47%--0.05%) in cardiovascular deaths and 0.58% (0.21 to 0.95%) in respiratory deaths (Rajzer et al., 2012). PM$_{10}$ includes particles derived from non-anthropogenic sources such as salt and dust particles. In a study conducted in 13 south-European cities the association between PM$_{10}$ originating from desert and from other sources with daily mortality and emergency hospitalizations rate was investigated. The results showed that increases of 10 μg/m^3 in non-desert and desert PM$_{10}$ were associated with increases in natural mortality of 0.55% (95% CI = 0.24%--0.87%) and 0.65% (95% CI = 0.24%--1.06%), respectively (Stafoggia et al., 2015).

A systemic review focused on the association between short term exposures of fine PM and morbidity and mortality rate of heart failure. This review contains 1146 articles in 5 databases. It showed every 10 μg/m^3 increase in PM_{10} caused 1.63% (95% CI = 1.20%--2.07%) increase of total heart failure mortality and morbidity rate (Shah et al., 2013). Wang et al. focused on the short term effects of ambient particulate matter on cerebrovascular events which contained all observational human studies from January 1966 to January 2014. Meta-analysis was performed to evaluate the associations in this systematic review that each 10 μg/m^3 increase in PM_{10} was associated with 0.5% (95% CI = 0.3%--0.7%) increased in total cerebrovascular deaths (Wang et al., 2014). Another systematic review and meta-analysis focused on the Chinese population and 1464 articles were included from PubMed, Web of Science, and China National Knowledge Infrastructure databases. For the short term effects, cardiovascular mortality and respiratory mortality increased 0.36% (95%CI = 0.24%--0.49%), and 0.42% (95%CI = 0.28%--0.55%) after 10 μg/m^3 increase in PM_{10} (Lu et al., 2015).

Study	Key Findings	Year	References
Long-term Study: Study in Michigan, US	An increase of 32 µg/m^3 of PM$_{10}$ concentrations were associated with ischemic heart disease hospitalisation (RR = 1.018, 95% CI = 1.005--1.032)	1986-1989	Schwartz & Morris, 1995
Long-term Study: German cohort study	Cardiopulmonary mortality was associated with living within a 50-meter radius of a major road (RR = 1.70; 95% CI = 1.02--2.81) with PM$_{10}$ (RR = 1.34; 95% CI = 1.06--1.71 for 1-year average)	1985-2003	Gehring et al., 2006
Long-term Study: Cohort Study in Lombardy, Italy	A 70% increase in risk of deep vein thrombosis for each 10 µg/m^3 elevation of PM$_{10}$ was observed with 16 year follow up (OR = 1.70; 95% CI = 1.30--2.23)	1995-2005	Baccarelli et al., 2008
Long-term Study: Retrospective Cohort Study in Shenyang, China	An increase of every 10 µg/m3 of PM10 caused 55% increased cardiovascular mortality (HR = 1.55; 95% CI = 1.51--1.60) and 49% increase in cerebrovascular mobility (HR = 1.49; 95% CI = 1.45--1.53)	1998-2009	Zhang et al., 2011
Long-term Study: New Zealand Census Mortality Study	Every 10 µg/m^3 increase in average PM$_{10}$ exposure increased 7% (95% CI = 3%--10%) of all-cause mortality in adults (aged 30-74 years at census)	1996-1999	Hales et al., 2012

Long-term Study: German Women Perspective Cohort Study	An increase of 10 µg/m³ PM_{10} was associated with an increased hazard ratio (HR) for all-cause (HR = 1.15, 95% CI = 1.04--1.27), cardiopulmonary (HR = 1.39, 95% CI = 1.17--1.64), and lung cancer mortality (HR = 1.84, 95% CI = 1.23--2.74)	1985-2008	Heinrich et al., 2013
Long-term Study: Retrospective cohort Study in 4 cities of China	For each elevated 10 µg/m³ of PM_{10} lead to the increase of relative risk ratios of all-cause mortality, cardiovascular disease mortality, ischemic heart disease mortality, heart failure disease mortality, and cerebrovascular disease mortality were 1.24 (95% CI = 1.22--1.27), 1.23 (95% CI = 1.19--1.26), 1.37 (95% CI = 1.28--1.47), 1.11(95% CI = 1.05--1.17), and 1.23(95% CI = 1.18--1.28), respectively.	1998-2009	Zhang et al., 2014
Long-term Study: Systematic Review & Meta-Analysis	Every 10 µg/m³ elevation in PM_{10} concentration was associated with 1.63% increased heart failure hospitalisation or death rate (95% CI = 1.20%--2.07%).		Morris, 2001
Long-term Study: Systematic Review & Meta-Analysis in Chinese Population	After the long term exposure, 10 µg/m³ increase in PM_{10} result in 23–67% increase in the risk of total mortality.		Lu et al., 2015
Short-term Study: Tucson	An inter-quartile range increase (23 micrograms per m³) in PM_{10} was associated with increased hospital admissions by 2.75% (95% CI = 0.52%--5.04%)		Schwartz, 1997

Short-term Study: NMMAPS Study	PM_{10} significantly increased the risks of both cardiovascular and respiratory caused deaths. Every 10 µg/cm^3 elevation of PM_{10} increased 0.68% of death (95% posterior interval = 0.20%--1.16%).	Samet et al., 2000
Short-term Study: APHEA2 Study	For all ages, every daily increase of 10 µg/m^3 of PM_{10} or black smoke were associated with 0.6% of daily deaths (95% CI = 0.4--0.8%), for the elderly it was slightly higher	Katsouyanni et al., 2001
Short-term Study: APHEA2 Study	The association between PM and cardiovascular caused hospital admissions. 0.5% (95% CI = 0.2--0.8) of cardiac admissions for all ages was correlated with 10 µg/m^3 of PM_{10}, and 0.7% (95% CI = 0.4--1.0) for cardiac admissions over 65 years	Le Tertre et al., 2002
Short-term Study: 7 United States cities	10 µg/m^3 Increase in PM_{10} was associated with a 0.72% (95% CI = 0.35%--1.10%) increase in the rate of admission for CHF on the same day	Wellenius et al., 2006
Short-term Study: Helsinki, Finland	Every 10 µg/m^3 of PM_{10} were associated with 3.5% (95% CI = 1.0--5.8) and 4.1% (95% CI = 0.4--10.3) increases of total mortality and cardiovascular mortality respectively	Pönkä et al., 2010
Short-term Study: 29 European cities	10 µg/m^3 Increase of PM_{10} was associated with increases of 0.76% (95% CI = 0.47--0.05%) in cardiovascular deaths and 0.58% (0.21 to 0.95%) in respiratory deaths	Rajzer et al., 2012
Short-term Study: 13 South-European Cities	Increases of 10-µg/m^3 in non-desert and desert PM_{10} were associated with increases in natural mortality of 0.55% (95% CI = 0.24%--0.87%) and 0.65% (95% CI = 0.24%--1.06%), respectively	Stafoggia et al., 2015

Short-term Study: **Systematic Review**	Every 10 µg/m^3 increase in PM$_{10}$ caused 1.63% (95% CI = 1.20%--2.07%) increase of total heart failure mortality and morbidity rate	Shah et al., 2013
Short-term Study: **Systematic Review**	Every 10 µg/m^3 increase in PM$_{10}$ was associated with 0.5% (95% CI = 0.3%--0.7%) increased in total cerebrovascular deaths	Wang et al., 2014
Systematic Review	For the short term effects, cardiovascular mortality and respiratory mortality increased 0.36% (95%CI = 0.24%--0.49%), and 0.42% (95%CI = 0.28%--0.55%) after 10 µg/m^3 increase in PM$_{10}$	Lu et al., 2015

Table 1-1. Summary of the some important studies on both short-term and long-term effects of PM$_{10}$ on the cardiovascular system

1.3.2   PM$_{2.5}$

According to the World Health Organisation, there are approximately 80,000 premature deaths every year caused by the long-term exposure to PM$_{2.5}$, ranking it as the 13th leading cause of death worldwide (Brook et al., 2010). Evidence for the role of PM$_{2.5}$ in cardiovascular disease comes from several studies of short term exposure. One of the difficulties with this type of epidemiological study is the accurate measurement of exposure. Some studies have compared health outcomes between cities based on the average exposure levels in the different cities (Dockery, 1993; Pope et al., 1995; C. Arden Pope et al., 2004). A large cohort study followed-up for 9 years on 8096 people living in 6 U.S cities from 1979 to 1988. PM$_{2.5}$ exposure measurement was based on the city-specific mean concentrations of PM$_{2.5}$. Each elevated 10 μg/m^3 in PM$_{2.5}$ was associated with increased cardiovascular mortality (RR = 1.28; 95% CI = 1.13--1.44) and lung cancer (RR = 1.27; 95% CI = 0.96--1.69) (Laden et al., 2006). However, these approaches miss potentially important effects of more local variations in exposure. To address this, Miller *et al* (2007) assigned exposure data from community level monitors (based on average yearly data from the monitor closest to the subject's address based on ZIP code) to query the role of PM$_{2.5}$ exposure in cardiovascular disease among a cohort of 65,893 postmenopausal women without previous cardiovascular diseases recruited in the U.S and followed up for 6 years from 1994 to 1998. The average yearly exposure concentrations of PM$_{2.5}$ ranged from 3.4 to 28.3 μg/m^3. Every increase of 10 μg/m^3 of PM$_{2.5}$ was associated with a 24% increase in the risk of a cardiovascular event (HR = 1.24; 95% CI = 1.09--1.41) and a 76% increase in the risk of death from cardiovascular disease (HR = 1.76; 95% CI = 1.25--2.47) (Miller et al., 2007).

In a study in Massachusetts, USA, conducted from 2000 to 2008, Kloog *et al* used more sophisticated geographical grid based methods for estimating exposure to $PM_{2.5}$. This approach used air pollution prediction modelling at a solution of 50 m^2 as a basis for studying particle related mortality. The results showed that every 10 $\mu g/m^3$ increase in long-term $PM_{2.5}$ exposure was associated with an OR of 1.6 (95% CI = 1.5--1.8) for particle-related diseases (Kloog et al., 2013). Using a time-series approach to study short term exposure effects, the same study found that for every 10 $\mu g/m^3$ increase in $PM_{2.5}$ exposure there was a 2.8% increase in PM-related mortality (95% CI= 2.3--3.5) (Kloog et al., 2013).

 A Harvard Six Cities Extended Follow-Up study was conducted for 11 additional years. From 2001, average PM2.5 concentration was less than 18 $\mu g/m^3$. Every 10 $\mu g/m^3$ elevation of $PM_{2.5}$ caused 14% (95% CI = 7--22%) increased risk of total mortality, and 26% (95% CI, 14-40%) cardiovascular mortality and 37% (95% CI = 7--75%) lung-cancer mortality (Lepeule et al., 2012). A systemic review focused on 33 Chinese studies of short-term air pollution exposure, every 10 $\mu g/m^3$ elevation of $PM_{2.5}$ was associated with a 0.38% (95% CI = 0.31--0.45) increase in total mortality, a 0.51% (95% CI = 0.30--0.73) in respiratory mortality, and a 0.44% (95% CI = 0.33--0.54) in cardiovascular mortality (Shang et al., 2013). An exposure study of $PM_{2.5}$ in Massachusetts, United States also investigated the short-term exposure effects of on cardiovascular and respiratory diseases. The results indicated that every 10 $\mu g/m^3$ increase in $PM_{2.5}$ exposure there was a 2.8% increase in PM-related mortality (95% CI = 2.0--3.5) (Kloog et al., 2013).

A systemic review of 33 Chinese studies of short-term air pollution exposure, included a meta-analysis that found that every 10 $\mu g/m^3$ elevation of $PM_{2.5}$ was associated with a 0.38% (95%

CI = 0.31--0.45) increase in total mortality, a 0.51% (95% CI = 0.30--0.73) in respiratory mortality, and a 0.44% (95% CI = 0.33--0.54) in cardiovascular mortality (Shang et al., 2013). The authors calculated that reducing $PM_{2.5}$ exposure average to 10 $\mu g/m^3$ would lead to a reduction of premature deaths of between 1.7 and 6.2% in 4 Chinese megacities (Beijing, Shanghai, Guangzhou and Xi'an). A systemic review focused on the association between short term exposures of fine particulate matter and morbidity and mortality rate of heart failure. It showed every 10 $\mu g/m^3$ increase in $PM_{2.5}$ caused 2.12% (95% CI = 1.42%--2.82%) increase of total heart failure mortality and morbidity rate (Shah et al., 2013). Want et al. conducted a systematic review focused on the short term effects of ambient particulate matter on cerebrovascular events which contained all observational human studies from January 1966 to January 2014. Meta-analysis was performed to evaluate the associations that after 10 $\mu g/m^3$ increase in $PM_{2.5,}$ total cerebrovascular deaths increased 1.4% (95% CI = 0.9%--1.9%) (Wang et al., 2014). Another systematic review and meta-analysis focused on the Chinese population and 1464 articles were included from PubMed, Web of Science, and China National Knowledge Infrastructure databases. For the short term effects, after 10 $\mu g/m^3$ increase in $PM_{2.5}$ cardiovascular mortality and respiratory mortality had 0.63% (95%CI = 0.35%--0.91%), and 0.75% (95%CI = 1.39%--1.11%) increased risk, respectively (Lu et al., 2015).

Study	Key Finding	Time	References
Long-term Study: Harvard Six Cities Studies (Extended)	Each elevated 10 μg/m^3 in PM$_{2.5}$ was associated with increased cardiovascular mortality (RR, 1.28; 95% CI = 1.13--1.44) and lung cancer (RR, 1.27; 95% CI = 0.96--1.69).	1979-1988	Laden et al., 2006
Long-term Study : Postmenopausal Women Cohort Study, U.S	Every increase of 10 μg/m^3 of PM$_{2.5}$ was associated with a 24% increase in the risk of a cardiovascular event (HR, 1.24; 95% CI = 1.09--1.41) and a 76% increase in the risk of death from cardiovascular disease (HR, 1.76; 95% CI = 1.25--2.47).	1994-1998	Miller et al., 2007
Long-term Study: Study in Massachusetts, U.S	Every 10 μg/m^3 increase in long-term PM$_{2.5}$ exposure of 1.6 (CI = 1.5--1.8) for particle-related diseases.	2000-2008	Kloog et al., 2013
Short-term Study: Harvard Six Cities Extended Follow-Up Study	Every 10 μg/m^3 elevation of PM$_{2.5}$ caused 14% (95% CI = 7%--22%) increased risk of total mortality, and 26% (95% CI, 14-40%) cardiovascular mortality and 37% (95% CI = 7%--75%) lung-cancer mortality.		Lepeule et al., 2012

Short-term Study: Systemic Review, China	Every 10 μg/m^3 elevation of PM$_{2.5}$ was associated with a 0.38% (95% CI = 0.31--0.45) increase in total mortality, a 0.51% (95% CI = 0.30--0.73) in respiratory mortality, and a 0.44% (95% CI = 0.33--0.54) in cardiovascular mortality.	Shang et al., 2013
Short-term Study: Study in Massachusetts, U.S	Every 10-μg/m^3 increase in PM$_{2.5}$ exposure there was a 2.8% increase in PM-related mortality (95% CI = 2.0–3.5).	Kloog et al., 2013
Short-term Study: Systematic Review	Every 10 μg/m^3 increase in PM$_{2.5}$ caused 2.12% (95% CI = 1.42%--2.82%) increase of total heart failure mortality and morbidity rate.	Shah et al., 2013
Short-term Study: Systematic Review	Every 10 μg/m^3 increase in PM$_{2.5}$ was associated with 1.4% (95% CI = 0.9%--1.9%) increased in total cerebrovascular deaths (Wang et al., 2014).	Wang et al., 2014
Short-term Study: Systematic Review	For the short term effects, after 10 μg/m^3 increase in PM$_{2.5}$ cardiovascular mortality and respiratory mortality had 0.63% (95%CI = 0.35%--0.91%), and 0.75% (95%CI = 1.39%--1.11%) increased risk, respectively.	Lu et al., 2015

Table 1-2.Summary of the some important studies on both short-term and long-term effects of PM$_{2.5}$ on the cardiovascular system

1.3.3   PM$_{0.1}$

Ultrafine particles (below 0.1 µm) are small enough to be potentially taken up into the circulatory system. An *in vivo* human study has confirmed this by using inhaled technetium-99m labelled carbon particles, which are similar in size to ambient ultrafine air pollution particles, to test whether such particles could translocate from the respiratory system to the circulatory system. Through γ-ray camera images, substantial radioactivity was found in the liver and other organs of the body, indicating that the inhaled particles could be able to pass rapidly into the systemic circulation (Nemmar et al., 2002).

Another study showed the potential for ultrafine particles to induce oxidative damage investigated whether the soluble ultrafine particles could induce procoagulant responses in human coronary artery endothelial cells (Snow et al., 2014). The results showed that soluble ultrafine particles could induce procoagulant responses in human coronary artery endothelial cells and result in the increased production of intracellular ROS and activation of the NOX-4 enzyme that regulates tissue factor mRNA (Snow et al., 2014).

There is a study focused on effects of ultrafine petrol exhaust particles on human A549 lung cells and alveolar macrophages (murine RAW 264.7 cells). After 24 hours treatment, the particles induced significant oxidative stress (A549 cell line: 20 and 50 µg/ml; macrophage: 10 and 20 µg/ml) with membrane leakage, lipid peroxidation, cell inflammation and protein release (Durga et al., 2014).

1.3.4   Diesel Particles

Diesel exhaust emission is one kind of the key sources of urban PM_{10} exposure, so the epidemiological studies discussed above have included such PM in the exposure data, as it is difficult to separate out the specific contribution of diesel PM in such studies. There have been experimental studies showing the effects of typical ambient diesel exhaust particles on cardiovascular and respiratory systems.

In a randomized, double-blinded exposure study, 19 healthy young volunteers (mean age, 25 ± 3 years) were divided into three groups that respectively exposed to filtered air, diesel exhaust with particle trap, and diesel exhaust without particle trap for 1 hour (Lucking et al., 2011). Compared to those volunteers who exposed to filtered air, those inhaled diesel exhaust had reduced vasodilatation and increased ex vivo thrombus formation under both low- and high- shear conditions. The diesel exhaust in the presence of particle trap had significantly decreased particle number (150,000 - 300,000/cm^3 to 30 – 300/cm^3) and mass (320 ± 10 to 7.2 ± 2.0 µg/m^3) compared to the diesel exhaust in the absence of particle trap, and showed increased vasodilatation, reduced thrombus formation and increased tPA expression compared to the latter group (Lucking et al., 2011).

Understanding the effects of diesel PM on the types of cells likely to be exposed is another approach to investigating the health effects of such PM. In one study, human primary small airway epithelial cells and human lung carcinoma epithelial A549 cells were treated with diesel particles for 2 hours. Atomic force microscope measurements indicated that short-term diesel particle exposure led to a significant decrease in cell elasticity and a dramatic change in membrane surface adhesion force. The ELISA results showed that DEP-induced

inflammatory responses were found in both cell types after the quantification of cytokines and chemokines production (Tang et al., 2012).

An *in vitro* study from Solomon *et al*. investigated the effects of diesel particle on platelets. The results indicated that diesel particle physically interacted with platelets aggregation, induced signaling and functioning of the activation of platelets, suggesting a possible mechanism to link exposure to diesel particles with platelet driven thrombotic events (Solomon et al., 2013).

1.3.5   Subclinical Pathophysiological Responses

Systemic Inflammation

There is abundant evidence have shown that exposure to PM leads to the elevation of circulating pro-inflammatory biomarkers which indicates a systemic response after PM air pollution inhalation (Brook et al., 2010). After the short-term exposure of ambient PM, acute-phase proteins such as C-reactive protein (CRP), fibrinogen and white blood cells counts increased in young overweight adults (Zeka et al., 2006), and the elderly (Pope et al., 2004); also the tumour necrosis factor-α (TNF-α) and interleukin (IL)-1β increase in children (Calderón-Garcidueñas et al., 2008). Increased ultrafine PM concentration also led to an immediate elevation in soluble CD40-ligand in patients with coronary artery disease (Rückerl et al., 2007). For the long-term PM_{10} exposure, elevated white blood cells count was reported after approximately 1-year exposure in the Third National Health and Nutrition Examination Survey (Brook et al., 2010). Overall, positive associations have been seen between the

exposure of PM and systemic inflammatory response; but there is variation in the strength of changes among the variety of biomarkers and populations (Brook et al., 2010).

Thrombosis and Coagulation

There have been many studies that have reported the associations between PM exposure and thrombosis/coagulation. Early studies demonstrated that plasma viscosity and elevated concentrations of fibrinogen were associated with the PM exposure (Pekkanen et al., 2000; Peters et al., 1997). In Taipei, PM levels were correlated with the increases in plasminogen activator inhibitor (PAI)-1 and fibrinogen levels in healthy adults (Chuang et al., 2007). Increased fibrinogen level is directly correlated with denser fibrin clot structure.

According to Chuang *et al.*, a penal study recruited 76 young, healthy students from University of Taipei to investigate whether biological mechanisms linking air pollution to cardiovascular events. After exposure to $PM_{10,}$ levels of C-reactive protein and fibrinogen were increased which indicated that the urban air pollution was associated with systemic oxidative stress and activation of blood coagulation in young and healthy volunteers (Chuang et al., 2007).

Metassan *et al*. investigated the effect of filtered particulate matter (diameter less than 0.22 µm) on fibrin clot properties *in vitro*. The results showed that after exposure to filtered PM, fibrin clot structure was altered and formed a heterogeneous network according to the formation of clustered fibrin fibres through the generation of reactive oxygen species (ROS). The formation of small clusters of fibrin fibres may break off and block small blood vessels and consequently led to thrombosis (Metassan et al., 2010a).

Atherosclerosis

According to results from the German Heinz Nixdorf Recall Study, the subjects living near the major road traffic had increased coronary artery calcium scores (a surrogate marker for coronary atherosclerosis) compared to those living further away (Hoffmann et al., 2007; Langrish et al., 2012). In another study in Denmark that recruited 1223 subjects, the coronary artery calcium scores were significantly higher in the subjects living in a city centre environment (OD=1.8, 95% CI 1.3-4) who were exposed to 30%-40% higher concentrations of PM_{10} compared to those living outside of the city (Lambrechtsen et al., 2012).

1.4   Haemostasis

Haemostasis is a process which maintains the blood throughout the body under normal physiological conditions that include preventing loss of blood from blood vessels and removal of blood clots following restoration of vascular integrity (Versteeg et al., 2013). From zebra fish to human, the haemostatic system is a highly conserved machinery which tightly regulates the necessary equilibrium (Teruel-Montoya et al., 2014; Versteeg et al., 2013). Haemostasis encompasses four main components, firstly the endothelium, secondly the coagulation cascade, and thirdly platelet activation which is able to accelerate the coagulation cascade, and finally fibrinolysis removes the redundant clots by proteolytic mechanisms (Allford and Machin, 2004; Riddel et al., 2007; Versteeg et al., 2013). The Greek philosopher Plato described the fibres formed from blood approximately 2,000 years age. The word "fibrin" also originated from Plato (Versteeg et al., 2013).

1.4.1 Coagulation Cascade

Blood clot formation involves a cascade of two pathways which are (i) the contact pathway including factor (F) XII (Hageman factor), XI, IX and VIII, and (ii) the tissue factor pathway including FVII activated by tissue factor. In terms of the contact pathway, all the components are present in the blood. But for the tissue factor pathway, tissue factor as an external factor was required, which can be found in the extravascular tissue (Versteeg and Ruf, 2013). These two pathways finally merge into a common pathway involving FX, V, thrombin and fibrinogen (Ajjan and Grant, 2006; Ajjan and Ariens, 2009).

The coagulation cascade can be divided roughly into three phases. In the first or initiation phase, there are only limited amounts of thrombin generated. Then in the second or amplification phase, the coagulation cascade is accelerated. Finally, in the third or propagation phase, fibrin clots are completely formed.
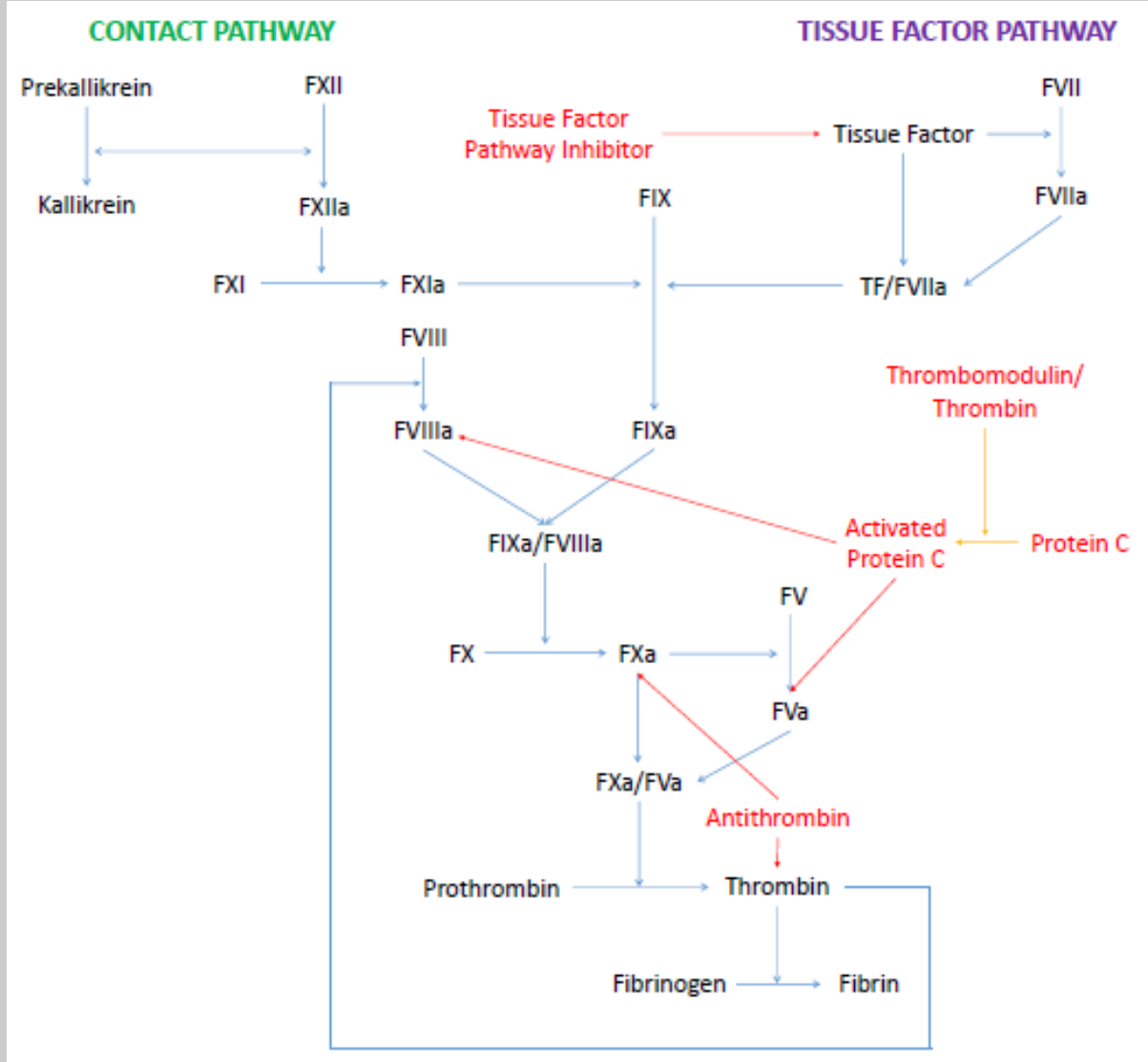
Figure 1-3. Coagulation Cascade

The coagulation cascade consists of two pathways which are (i) the contact pathway including FXII XI, IX and VIII, and (ii) the tissue factor pathway including FVII activated by TF. These two pathways finally merge into a common pathway involving FX, V, thrombin and fibrinogen (Ajjan & Ariens, 2009; Butenas & Mann, 2002; Dahlbäck, 2000; Ajjan & Grant, 2006).

Initiation Phase

The contact pathway becomes activated once blood contacts negatively charged surfaces, FXII starts to get activated and then cleaves prekallikrein into kallikrein, which in turn gives rise to a subsequent activation of FXI, FIX and FX to FXIa, FIXa and FXa respectively. According to Burman et al. (1994), patients with severe FXII deficiency do not have bleeding problems, and as a result FXII is not necessary for thrombin generation (Burman et al., 1994). Therefore, compared to factor XII, tissue factor is emphasized as the main physiological initiator of in vivo coagulation (Adams and Bird, 2009), but FXII and the contact pathway of coagulation may play an important role in thrombosis. In terms of the activation of the tissue factor pathway, classically refers to damage or activation of endothelium in the vessel wall leads to exposure sub-endothelial cells to the blood resulting in the exposure of tissue factor (a transmembrane protein expressed by sub-endothelial smooth muscle cells and fibroblasts) to the blood. Platelets adhere to the site of injury and then become activated by the interaction of von Willebrand factor (VWF) and collagen (Ajjan and Ariens, 2009). TF is a 47 kDa cell-bound transmembrane glycoprotein and member of the class II cytokine superfamily (Adams and Bird, 2009). TF is the key initiator of blood coagulation, which is expressed by sub-endothelial cells (e.g. smooth muscle cells) and cells surrounding blood vessels (e.g. fibroblasts). These two kinds of cells are located outside of the vasculature, i.e., not normally in contact with the circulating blood which is protected from tissue factor exposure by the intact, healthy endothelium (Adams and Bird, 2009; Golino, 2002).

In the initiation phase, FVII accesses TF and is bound to TF with high affinity and specificity, after which FVII is rapidly converted to FVIIa via proteases and auto-activation (Ajjan and

Ariens, 2009; Golino, 2002). Activated TF/FVIIa complexes, on the phospholipids surface of the cell membrane, catalyse the conversion of FIX to FIXa, FX to FXa and FV to FVa (Adams and Bird, 2009; Ajjan and Ariens, 2009; McVey, 1999). FXa and FVa cleave prothrombin to generate trace amounts of thrombin. The duration of the initiation phase is primarily dependent on the concentration of TF/FVIIa and tissue factor pathway inhibitor (TFPI) (Adams and Bird, 2009; Butenas and Mann, 2002).

Amplification Phase

In the amplification phase, the intrinsic tenase complex is formed by FIXa and its thrombin-activated cofactor FVIIIa. The tenase complex FIXa/FVIIIa, aggregating on a membrane surface in the presence of calcium, accelerates FXa production at a 50 to 100 fold higher rate than TF/FVIIa complex and generates more thrombin than FIX alone (Adams and Bird, 2009; Butenas and Mann, 2002). The reaction efficiency of both the intrinsic factor tenase complex and prothrombinase complex is accelerated in the presence of calcium by their co-localization on the surface of platelet with phospholipid membrane (Adams and Bird, 2009; Ajjan and Grant, 2006). The platelets are activated by local collagen at the site of injury in the initial haemostatic plug. Collagen-bond, partially activated platelets are further activated by thrombin through interactions with protease-activated receptor-1 (PAR-1). The fully activated platelets change shape and degranulate. More FVIIIa is generated by thrombin through liberation of FVIII from its complex with von Willebrand factor (FVIII/VWF). Thrombin also activates FXI to FXIa which binds to the surface of platelets. Platelet surface FXa/FVa complexes are the primary activator of prothrombin and lead to the efficient generation of

large amounts of thrombin from prothrombin (Adams and Bird, 2009; Ajjan and Grant, 2006; Butenas and Mann, 2002).

Propagation Phase

The propagation phase depends on the recruitment of activated platelets at the site of injury to generate enough thrombin through the necessary components including intrinsic tenase complex, the prothrombinase complex, calcium and a phospholipid surface. The sufficient amount of thrombin generates fibrinogen to fibrin and forms a stable fibrin clot structure (Adams and Bird, 2009; Ajjan and Grant, 2006; Ajjan and Ariens, 2009).

Except FXII, all other coagulation factors deficiency are associated with bleeding disorders of varying severity. There are three common hereditary bleeding disorders, FVIII deficiency causes haemophilia A, FIX deficiency causes haemophilia B, and VWF deficiency causes von Willebrand diseases (Dahlbäck, 2000; Riddel et al., 2007).

1.4.2 Regulation of Blood Coagulation

Apart from the deficiency of clotting factors, the coagulation cascade can be restricted by several coagulation inhibitors. There are at least four plasma proteins (anti-thrombin, protein C, protein S, and tissue factor pathway inhibitor) and one trans-membrane protein (thrombomodulin) that regulate the anti-coagulant process (Butenas and Mann, 2002). Thrombin has important roles in both pro- and anti-coagulation. As in the initiation phase,

the rate of thrombin generation depends on the concentration of complex TF/FVIIa. Tissue factor pathway inhibitor is the primary inhibitor in the initiation phase (Butenas and Mann, 2002). In the propagation phase, TF/FVIIa complex and TFPI have little effects, while protein C and antithrombin start to play pronounced roles in inhibiting the FVa thus limiting thrombin generation (Butenas and Mann, 2002; Dahlbäck, 2000). Protein C regulates coagulation by restricting the activities of FVIIIa and FVa (Dahlbäck, 2000). Antithrombin can inactive a series of serine proteases (Norris, 2003).

1.4.3   Platelets

Platelets are the smallest blood cells with diameter 2 to 3 μm, also they are the second most numerous corpuscles in the blood (red blood cells are the most abundant) circulating at between 150 x10^9/L and 450 x10^9/L. Their half-life in circulation is around ten days (George, 2000; Harrison, 2005). Generally, concentrations of less than 10,000 platelets/L are defined as extreme thrombocytopenia (Clemetson, 2012), a condition that increases the risk for bleeding. Platelets are biconvex discoid in shape before activation, and they are anucleated cells. Platelets are produced by megakaryocytes in the bone marrow, a large cell that releases platelets by fragmentation of the cell membrane and by packaging mitochondria, dense and alpha granules in the newly formed platelets (Clemetson, 2012; George, 2000; Harrison, 2005). Platelets are multifunctional and participate in many pathophysiological processes such as haemostasis, clot retraction, vessel constriction and repair, and inflammation, of which haemostasis (protection against blood loss) is the most important role of platelets (Clemetson, 2012).

The platelets can be activated by two independent pathways which act in parallel or separately (Furie and Furie, 2008). One of the pathways involves the activation of platelets by the exposure to sub-endothelial collagen. The other pathway in platelets can be initiated by thrombin, generated by tissue factor or present in flowing blood. Although the platelets are activated by different mechanisms, the consequences are the same (Furie and Furie, 2008).

For the first pathway, activation of the platelet by collagen is independent of thrombin. Platelets aggregate to the site of injury, via interactions between platelet glycoprotein VI with collagen and platelet glycoprotein Ib-V-IX with collagen and VWF (Furie and Furie, 2008). Glycoprotein VI is a collagen receptor on platelets, and glycoprotein Ib-V-IX is a cluster of adhesive receptors on platelets (Furie and Furie, 2008). The second pathway of platelet activation occurs through tissue factor driven thrombin generation without disruption of the endothelium. Also, this pathway is independent of VWF and glycoprotein VI. Thrombin is generated through tissue factor pathway that activates FVII and forms the TF/FVIIa complex, which then also activates IX. Thrombin activates platelets by cleaving the PAR-1 on the surface of platelets and causing them to release adenosine diphosphate (ADP), serotonin, and thromboxane A2. Afterwards, these agonists activate other platelets and amplify the signals for thrombus formation (Furie and Furie, 2008).

During the activation, platelets are deformed from their discoid shape to irregular shapes with long dendritic extensions that helps adhesion (George, 2000). Four kinds of secretary granules are released from platelets in activation, but two of them are more important. Firstly the dense granules, also called delta granules, which produce ADP and calcium and promote the platelets aggregation. Secondly the alpha granules secrete a variety of proteins, P-selectin and

fibronectin enhance platelets activation and aggregation to the site of injury; von Willebrand factor, fibrinogen, and coagulation factors V and XIII further assist in the acceleration platelets activation and clots formation (Clemetson, 2012; George, 2000; Harrison, 2005; Lindemann et al., 2007).

1.4.4   Fibrinogen and Fibrin Clot Structure

The Fibrinogen Molecule

Fibrinogen is the most abundant coagulation factor in the blood with an average concentration of 2 to 4 mg/ml (6 – 12 µM) (Ariens, 2013). It is mainly synthesized in the liver, which produces approximately 1.7g to 5g daily (Standeven et al., 2005). Fibrinogen is a 340 kDa glycoprotein and possesses properties of both globular and fibrous proteins (Standeven et al., 2005). The fibrinogen molecule is composed of two sets of three polypeptide chains, denominated Aα, Bβ and γ, cross-linked by 29 disulfide bonds in a dimeric structure with bilateral symmetry (Ariens, 2013; Wolberg, 2007). The central part of the molecule includes the E region, which contains N-termini of all six polypeptide chains. The chains intertwine and connect to two distal D region via α-helical coiled-coil structure which provide elasticity to the molecule (Ariens, 2013; Standeven et al., 2005; Wolberg and Campbell, 2008). The C-terminal region of both the Bβ- and γ- chains end in the D region, however, the Aα-chain protrudes from the D region, form a flexible αC region and extends back to the E region (Ariens, 2013; Standeven et al., 2005; Weisel, 1986).

The Aα-chain contains 610 residues; the Bβ-chain contains 461 residues and the major γ-chain form, γA contains 411 residues. The complete human fibrinogen molecule is therefore made up of 2964 amino acids, yielding a calculated molecular weight of 329 818 (Standeven et al., 2005). There are four carbohydrate clusters present – one on each Bβ- and γ- chain – which contribute another 10 000 in molecular weight, adding up to the total molecular weight of around 340 000 (Standeven et al., 2005). In the γ-chain, the γA chain consists of 411 amino acids and is composed of 10 exons and 9 introns. A minor γ-chain variant termed γ', arises from alternative processing at the exon 9/exon 10 boundaries of the mRNA. The alternative γ'-chain arises when polyadenylation occurs at an alternative polyadenylation signal in intron 9. In this case, intron 9 is not spliced out, leading to the substitution of 4 γA amino acids (γA408-411; AGDV) of exon 10 by a unique 20-amino acid extension (γ'408-427; VRPEHPAETEYDSLYPEDDL) encoded by intron 9 (Campbell et al., 2010; Cooper et al., 2003; Uitte de Willige et al., 2009). The γ'-chain occupies about 8% of the total fibrinogen γ-chain population and the majority of them are in heterodimeric fibrinogen molecules accounting to 15% of plasma fibrinogen molecules. Homodimeric γ'/γ'-molecules are present in circulating fibrinogen molecules in blood at less than 1% (Ariens, 2013; Campbell et al., 2010; Cooper et al., 2003; Uitte de Willige et al., 2009).

Fibrin Clot Formation
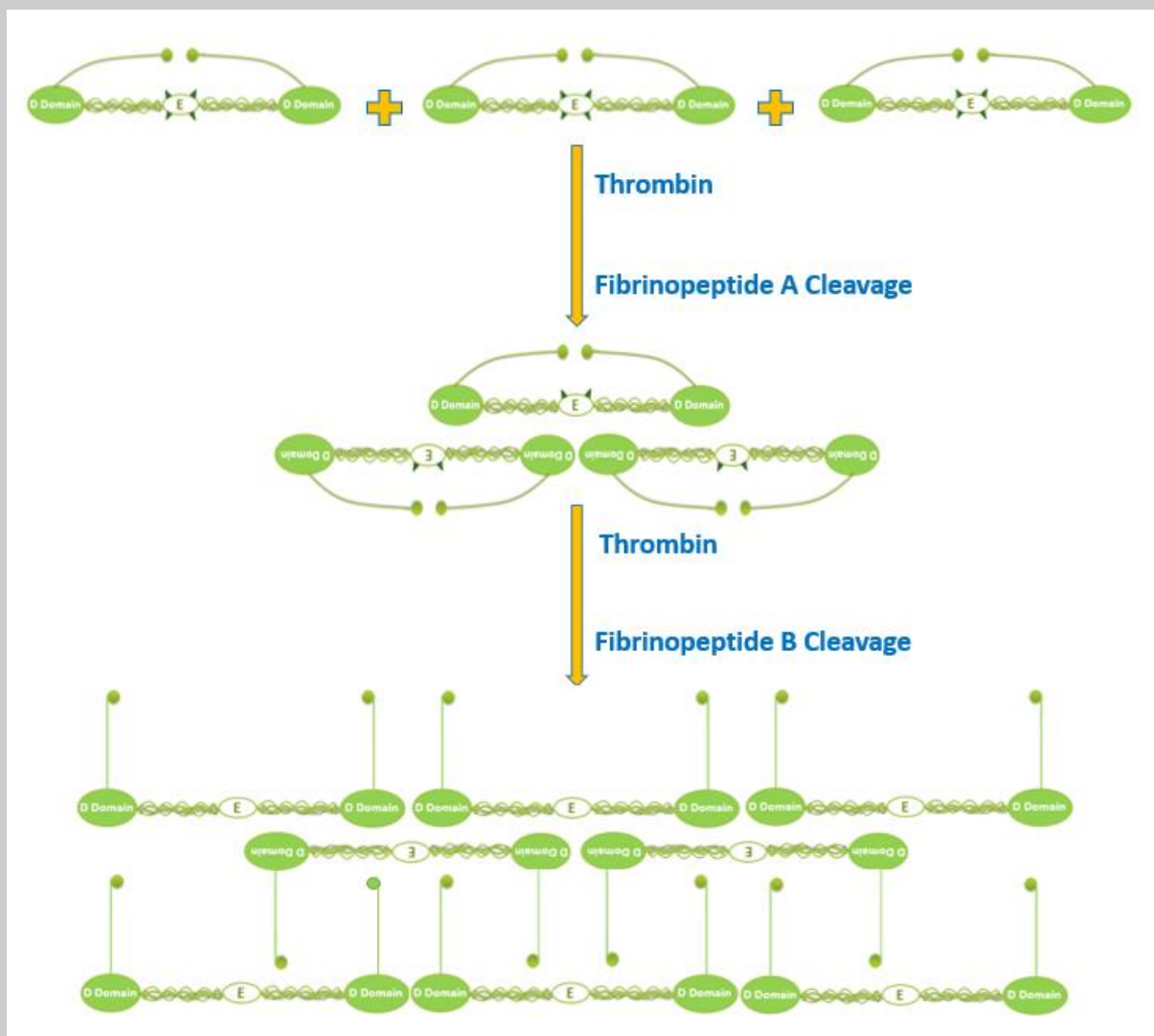
Figure 1-4. Fibrin Clot Formation.

Fibrinogen consists 2Aα, 2Bβ, and 2γ chains. Thrombin firstly cleaves fibrinopeptide A leading the formation of half-staggered and double-stranded twisting protofibrils. FpB is cleaved by thrombin at a slower rate and the cleavage of FpB facilitates the lateral aggregation of protofibrils (Ariens, 2013; Scott et al., 2004; Standeven et al., 2005; Undas & Ariëns, 2011).

Thrombin first cleaves fibrinopeptide A leading to oligomers and protofibrils. Fibrinopeptide B is cleaved at a slower rate and is associated with the release of the αC-region and lateral aggregation of protofibrils into fibers and fiber bundles.

The final stage in the coagulation cascade is conversion of fibrinogen to fibrin and the formation of a fibrin clot (Standeven et al., 2005). The trigger to start the conversion is the thrombin catalysed cleavage of the fibrinopeptide. Thrombin binds to the central E nodule of fibrinogen and removes the N-terminal peptides of the Aα- and Bβ- chains. Firstly, thrombin cleaves the fibrinogen Aα-chain between Arg16 and Gly17, the N-terminal 16 residue peptides (fibrinopeptide A, FpA) are removed and expose a binding site (GPR) which is known as 'A' site in the E region. The 'A' site binds to the 'a' pocket in the γ-chain of the D region of another fibrinogen molecule. These interactions result in the formation of half-staggered and double-stranded twisting protofibrils (Ariens, 2013; Campbell et al., 2010; Standeven et al., 2005; Wolberg, 2007). The length of fibrinogen molecule is 45nm. The half-staggered protofibrils maintain a periodicity of 22.5nm (half the length of the full-length fibrinogen). Fibrils branch out and there are two possible types of branching determining the structure of the clot. The first type of branching supports strength and rigidity in the clot as double-stranded protofibrils align side by side to form a tetra-molecular or bilateral branch-point. The second type of branching is tri-molecular or equilateral which is formed by the combination of three fibrinogen molecules in which three double-stranded protofibrils are connected to each other via 'E:D' associations (shown as figure 1-5). This situation happens when the rate of fibrinopeptide release is slow (Mosesson, 2005; Standeven et al., 2005). Additional fibrin monomers can add longitudinally to the dimer and trimer to form larger oligomers which are long enough for lateral aggregation. The length of a protofibril is approximately 0.5 to 0.6 μm, accordant with 20 to 25 half-staggered fibrin monomers (Weisel and Litvinov I., 2013).
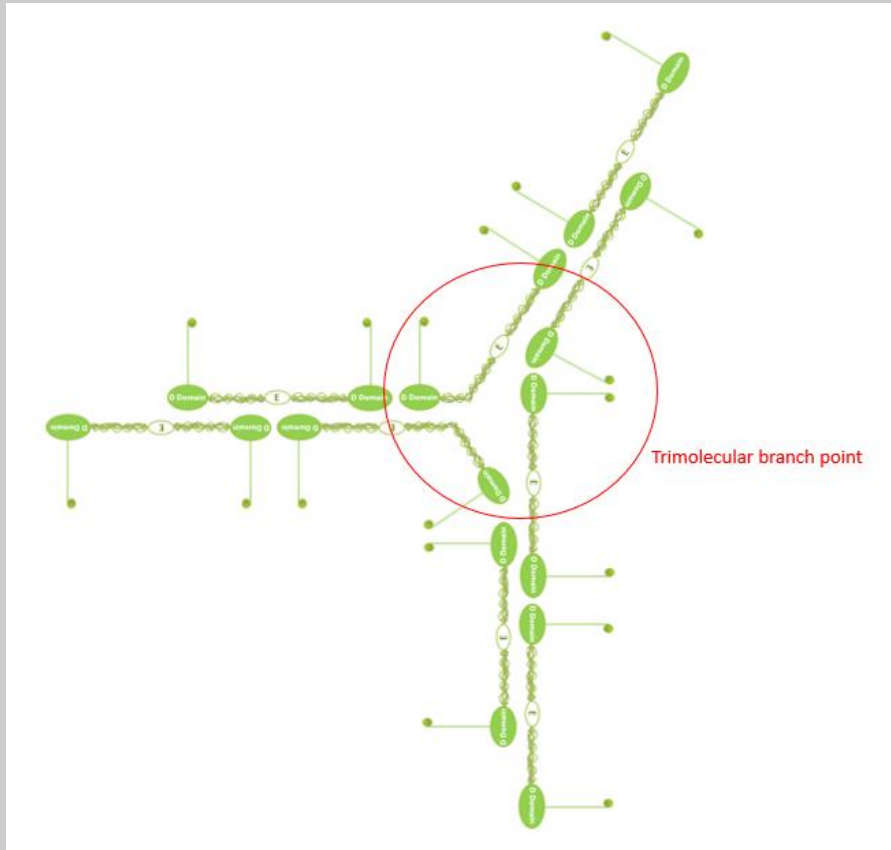
Figure 1-5. Tri-molecular or equilateral branch point.

The tri-molecular branch point is formed by the combination of three fibrinogen molecules in which three double-stranded protofibrils are connected to each other via 'E:D' associations (Mosesson, 2005; Standeven et al., 2005).

Subsequently, the N-terminal 14 residue peptide of the Bβ-chain (fibrinopeptide B, FpB) are removed which expose a second binding site 'B' with the amino acid sequence GHR in the E region. The 'B' site interacts with another specific binding pocket 'b' in the Bβ-chain of the D region of another molecule (Ariens, 2013; Campbell et al., 2010; Standeven et al., 2005; Undas and Ariëns, 2011; Wolberg, 2007). FpB is cleaved by thrombin at a slower rate compared with FpA. In the meantime of removal of FpB occurs, the αC domains are liberated but still interact with the distal D region in fibrinogen (Standeven et al., 2005). The αC domains originate at residue 220 in the D domain and end at Aα610 (Campbell et al., 2010). Interactions of αC

domains change from intramolecular to intermolecular, which promote the lateral aggregation of protofibrils.

The cleavage of FpA is necessary for protofibril formation, nevertheless, the release of FpB in fibrin clot formation is highly controversial. It has been assumed that the cleavage of FpB facilitates the lateral aggregation of protofibrils to form thicker fibres, however, this can actually occur through cleavage of FpA only by several enzymes in the absence of FpB cleavage (Standeven et al., 2005; Wolberg, 2007).

Fibres are twisted structure; the protofibrils need to maintain the periodicity of 22.5nm. When the new protofibrils are added to the growing fibres, they have to undergo a certain degree of stretching. The degree to which a protofibril can be stretched is the determinant of the thickness that the fibres can grow. The growth of the fibril ceases when the energy necessary to stretch an added protofibril exceeds the energy of protofibril bonding (Standeven et al., 2005; Weisel and Litvinov I., 2013).

1.4.5   Factor XIII

Coagulation factor XIII (FXIII), belongs to the enzyme family of transglutaminases, and is the last enzyme to be activated in the blood coagulation pathway (Laudano and Doolittle, 1978). There are two forms of FXIII, the first is a cellular of FXIII (cFXIII), which exists as a dimer (FXIII-A2) in the cytoplasm of certain cells, particularly in platelets, monocytes, and macrophages. In platelets, the amount of FXIII-A2 is 46-82 fg/platelet which amounts to around 3% of total platelet protein. The second form of FXIII is present in the plasma (pFXIII), and is a tetramer

consisting of two catalytic A subunits (FXIII-A) and two carrier/inhibitor B subunits (FXIII-B). In plasma, FXIII circulates as a pro-enzyme (FXIII-A_2B_2), and the concentration in normal conditions is 14-28 mg/L. The A-subunit, containing the catalytic part of the enzyme, is a non-glycosylated single polypeptide chain molecule with 731 amino acid and a molecular weight of 83 kDa (Ariëns et al., 2002). FXIII-A subunit is mainly synthesized in macrophages, megakaryocytes, and placenta with bone marrow origin. The A subunit is constituted by five domains, an activation peptide (AP-FXIII, residues 1-37), a β-sandwich (residues 38-183), a catalytic core region (residues 184-515), and two β-barrels (barrel 1, residues 516-627; barrel 2, residues 628-731). FXIII-B subunit is secreted and synthesized by hepatocytes in liver. The B subunit is a typical mosaic protein which is assembled from ten short consensus repeats, also known as sushi domains, GP-I structure or complement control protein (CCP) module. FXIII-B molecule is constituted by 641 amino acids (each sushi domain contains 60 amino acid) and 8.5% carbohydrate, and the total molecular weight is approximately 80kDa (Weisel & Litvinov, 2013; Bagoly et al., 2012; Bagoly et al., 2012; Ariëns et al., 2002).

The main function of FXIII is the stabilization of the fibrin clot which constitutes the last stage in the coagulation cascade. Plasma FXIII is activated by thrombin and Ca^{2+}. At first, thrombin cleaves off the AP-FXIII by hydrolysing the Arg37-Gly38 peptide bond. Then, in the presence of Ca^{2+}, the carrier FXIII-B subunits dissociate from the catalytically active thrombin-cleaved FXIII-A subunits. The removal of B-subunits from the FXIII complex is necessary for the Ca^{2+}-induced transformation into an active tranglutaminase FXIIIa. The activation process is accelerated 80-100 fold by the presence of fibrin. The fibrin polymer is held together by non-covalent forces at the beginning. After the activation of FXIII by thombin, Ca^{2+} (and fibrin), fibrin is covalently cross-linked by FXIIIa. FXIIIa induces intermolecular ε-(γ-glutamyl)-lysine

covalent bond between the γ406Lys of one γ-chain and the γ398/399Gln of another γ-chain in two adjacent molecules that are aligned in a longitudinal orientation. γ-Chain dimer formation significantly contributes to clot rigidity. α-Chain cross linking plays an important role in regulation of fibrinolysis and enhances fibrin stiffness and viscoelasticity (Bagoly et al., 2012; Ariëns et al., 2002). Alpha-gamma cross-linking is negligible in quantity compared to g-g and a-a. FXIII also cross-links between Gln2 in the amino terminus of α2 antiplasmin and Lys303 in the fibrin α-chains to protect the fibrin clot from lysis (Ariëns et al., 2002). In summary, FXIIIa is able to stabilize the fibrin clot, introducing thinner fibre formation, and increasing the fibre density, as well as protecting from shear stresses and producing a clot with increased resistance to fibrinolysis (Ariëns et al., 2002; Doolittle et al., 1998; Standeven et al., 2007).

1.4.6 Fibrinolysis

The fibrin clot is the essential and primary product of haemostasis. The purpose of fibrinolysis is to remove the excess clot formed either in response to vascular damage or in pathological thrombosis and atherosclerosis (Adams and Bird, 2009; Chapin and Hajjar, 2015). The efficiency of fibrinolysis can be influenced by many factors, including the structure of the clot, the rate of thrombin generation, and the reactivity of thrombin-associated cells. Similarly to the coagulation process, fibrinolysis is also regulated by cofactors, inhibitors and receptors (Chapin and Hajjar, 2015). The key proteolytic enzyme in the fibrinolysis process is plasmin, which can be activated by the hydrolysis of plasminogen by two serine proteases, tissue-type plasminogen activator (tPA) and urokinase-type of plasminogen activator (uPA) (Adams and

Bird, 2009; Chapin and Hajjar, 2015; Lord, 2011). Whereas tPA is produced by endothelial cells, uPA is synthesized by monocytes, macrophages, and urinary epithelial cells (Chapin and Hajjar, 2015). Compared with uPA, tPA has a higher affinity for plasminogen. The rate of plasminogen activation by tPA is increased in the presence of fibrin. Two sites of fibrin are involved in this process, Aα148-160 and γ312-324 (Mosesson, 2005). The cleavage of fibrin by plasmin initiates in the αC domain followed by cleavages in D and E regions (Ajjan and Grant, 2006).

Both the fibrin structure and mechanical properties may affect the rate of fibrinolysis. Individual thicker fibres are lysed slowly compared to the thin fibres, but denser fibrin clots contained thinner fibres with greater number of fibres requires longer fibrinolysis time as denser clot had smaller port sizes which causes prolonged transportation of the fibrinolytic agents through the fibrin clot (Undas et al., 2006).

Several fibrinolysis inhibitors are able to control the excess plasmin and plasminogen activator activities. There are three important serpins in the fibrinolysis, plasminogen activator inhibitor-1, plasminogen activator inhibitor-2, and α2-antiplasmin (A2AP) (Chapin and Hajjar, 2015).

Plasminogen activator inhibitors are produced by endothelial cells, platelets and other cells and released into the circulation. PAI-1 is a linear glycoprotein that consists of 379 amino acids with a molecular weight 48,000. It is the main inhibitor of plasminogen activators tPA and uPA (Binder et al., 2002; Chapin and Hajjar, 2015; Kohler and Grant, 2000). In its free, unbound, active form, PAI-1 is unstable with a half-life of 30 minutes, however, when bound to the matrix protein vitronectin in plasma, PAI-1 stabilizes at the active form and the half-life is prolonged over ten times (Binder et al., 2002; Kohler and Grant, 2000). Fibrinolysis is initiated

when tPA and plasminogen both bind to the fibrin as plasmin is formed when plasminogen is partially cleaved by tPA on the surface of fibrin. This process promotes the activation of plasminogen and acceleration of fibrinolysis (Binder et al., 2002; Chapin and Hajjar, 2015; Kohler and Grant, 2000). In addition, the rate of PAI-1 inhibitory activity was reduced by 80 to 90% in the presence of fibrin. However, once fibrin monomers are cross-linked by activated FXIII, the binding sites for tPA are reduced. PAI-1 rapidly binds to tPA or uPA, forming a 1:1 complex which can be cleared by hepatocytes in the circulation (Chapin and Hajjar, 2015; Kohler and Grant, 2000). PAI-1 can be upregulated by a number of proinflammatory cytokines, as well as thrombin (Binder et al., 2002; Kohler and Grant, 2000). PAI-2 is also a key inhibitor of tPA and uPA but mainly during pregnancy, and the concentration increases as the pregnancy progresses (Chapin and Hajjar, 2015).

A2AP binds plasmin to form an irreversible complex. Once plasmin is bound to fibrin, it is protected from A2AP inhibition (Ajjan and Grant, 2006). There is a non-serpin fibrinolysis inhibitor named thrombin activated fibrinolysis inhibitor (TAFI). TAFI is a carboxypeptidase which removes the C-terminal lysine and arginine residues on fibrin thereby decelerating the plasmin generation by reducing the plasminogen binding sites (Ajjan and Grant, 2006; Chapin and Hajjar, 2015).

1.4.7　Vascular Endothelium

The vascular endothelium is a monolayer that covers the inner surface of the entire vascular system, with a surface area of approximately 1 to 7 m^2 in man (Cines et al., 1998; Esper et al.,

2006). The vascular endothelial surface of an adult human contains approximately 1 to 6 x 10^{13} endothelial cells and the weight is almost 1kg (Cines et al., 1998; Esper et al., 2006; Sumpio et al., 2002). Therefore, the endothelium represents the largest and most important gland of the body (Ajjan and Grant, 2006). It is important to emphasize that endothelial cells exhibit phenotypic variation in different sections of the vasculature. Within an individual, endothelial cells at different locations are not only able to express different markers but can also react differently to the same stimulus. For different individuals, such cells vary greatly in the responses to stimuli (Sumpio et al., 2002).

The endothelial cells have a similar basic structure as other cells in the human body, including the presence of a cytoplasm, nucleus, organelles and cell membrane. The cellular membrane is formed by two layers of phospholipids containing various proteins as receptor or ion channels (Cines et al., 1998; Esper et al., 2006). Many types of contractile proteins, such as actin, myosin, and tropomyosin, cross the cytoplasm and contribute to the motor activities of the cell (Esper et al., 2006). Some of these cells are organised as structure like cortical web and junction-associated actin filament system, and stress fibres (Esper et al., 2006; Sumpio et al., 2002). Cortical web adhering to the internal surface of the sarcolemma, controls the shape and elasticity of the cells, and it changes the stiffness of itself in accordance with the intravascular pressure. The junction-associated actin filament system exists in the intercellular space and the main function is controlling the intercellular space through contraction and dilatation. Stress fibres are myofibril-like straight filament bundles containing actin filaments and myosin filaments, that cross the cytoplasm in all directions. The contraction and relaxation of stress fibres depend on the intracellular Ca^{2+} concentration and presence of adenosine tri-phosphate (ATP). The aim of these fibres is to reduce the possibility

of cell lesions through adjusting the shape of cells based on the forces of blood flow and wall distension (Cines et al., 1998; Esper et al., 2006).

The endothelium, as a barrier of the vessel wall, has a semi-permeable structure that controls the transfer of small and large molecules (Sumpio et al., 2002). The cell membrane is covered by "caveolae", flask-shaped membrane invaginations which occupy 5 to 10% of total cellular surface area. The endothelial caveolae regulate the fluid and transport macromolecules in a transcellular pathway (Esper et al., 2006).

Promotion of vasodilatation
Anti-coagulant effects
Anti-inflammatory effects
Anti-oxidant effects
Inhibition of leukocyte adhesion and migration
Inhibition of smooth muscle cell proliferation and migration
Inhibition of platelet aggregation and adhesion
Pro-fibrinolytic effects

Table 1-3. Healthy Endothelium Functions

Source: adapted from Esper et al., 2006; Cines et al., 1998; Sumpio et al., 2002

The endothelial cells are versatile and multifunctional as shown in the above figure (Sumpio et al., 2002). The major functions of endothelium are providing a mechanical barrier and

regulating the vascular tone (Ajjan and Grant, 2006). Endothelial cells are able to secrete a variety of molecules, vasodilators and vasoconstrictors, procoagulants and anticoagulants, fibrinolytics and anti-fibrinolytics, inflammatory and anti-inflammatory, oxidants and anti-oxidants, to balance the effects of both directions to maintain the integrity of the vascular surface, ensure the protection of the vessel wall and provide healthy blood flow. Endothelial cells play a role in the coagulation process by producing a series of procoagulant agents including VWF, factor V, plasminogen activator inhibitor, and tissue factor (Modena et al., 2002). Endothelial cells also have anticoagulant effects by secreting nitric oxide (NO), postacyclin, tissue plasminogen activator, thrombomodulin (THBD), protein C, and protein S. Nitric oxide works in concert with prostacyclin to restrain the platelet adhesion and aggregation. The expression of THBD causes a transformation of thrombin from a pro-coagulant converter of fibrinogen to fibrin to an anti-coagulation activator of protein C. Activated protein C and protein S synergistically inactivate several clotting factors. Furthermore, endothelial cells have proinflammatory roles through the production of a number of adhesion molecules (e.g. intercellular adhesion molecule-1, ICAM-1) and cytokines (Ajjan and Grant, 2006). Under the healthy environment, endothelium is able to maintain the balance of protein production. However, endothelium damage upsets the balanced secretion of the molecules, reducing the ability to maintain the protection of the vessel wall and ensure healthy blood flow, and initiating the progression of the atherosclerotic process (Ajjan and Grant, 2006).

A sign of endothelial dysfunction is the reduction of bioavailability of vasodilators, especially NO; in addition, the vascular contracting factors are increased (Modena et al., 2002). NO can be found in all tissues and due to its low molecular weight and lipophilic properties, it

permeates easily through cell membranes (Ajjan and Ariens, 2009). Reduced NO production leads to the promotion of platelet adhesion and aggregation, increased leukocytes infiltration, and proliferation of vascular smooth muscle cells (VSMC) (Ajjan and Grant, 2006). Endothelial dysfunction causes the release of VWF which mediate the platelet adhesion on damaged endothelium. The VWF plasma level is a marker of endothelial dysfunction (Ajjan and Grant, 2006; Sumpio et al., 2002; Whincup et al., 2002). TF is also secreted by endothelium only if the cells are dysfunctional. TF cannot be found in normal endothelial cells, but can be detectable in atheromatous plaques, indicating TF is a risk marker of atherosclerosis in diseases pathogenesis (Suefuji et al., 1997). As endothelial dysfunction is characterised as pro-coagulant, pro-inflammatory and proliferation status that contribute to the progression of atherosclerosis, endothelial dysfunction reflects the tendency of an individual to develop atherosclerotic diseases (Cines et al., 1998; Modena et al., 2002).

1.5 Engineered Nanoparticles

As described above, there is a large and growing amount of evidence showing that PM is associated with human health risks, including cardiovascular health risks. Consequently, there is concern that engineered nanoparticles (NPs) which are defined as having at least one, and usually two dimensions less than or equal to 100nm, may also exhibit human health risks (Tiede et al., 2008, Savolainen et al., 2010a, Teow et al., 2011).

1.5.1   ENPs Definition

Engineered nanoparticles (ENPs) are different from the ultrafine particles (UFPs) discussed above. Both of them have similar sizes which are less than 100nm, however, the different sources of these two kinds of particles have different physicochemical properties (Xia et al., 2009). Ultrafine particles are incidental particles arising mainly from combustion. These particles originated from fossil fuel combustion process or through the condensation of semi-volatile substances (Xia et al., 2009). Different from UFPs, ENPs include a variety of particles manufactured from various materials on an industrial scale for a variety of purposes. As a consequence of the small size of the nanoparticles, ENPs possess different physicochemical properties compared to their respective bulk material (Duffin et al., 2007). In some crucial respects, ENPs show different performance physically and chemically compared to UFPs (Kendall and Holgate, 2012). According to Xia et al. (2009), table 1-4 shows the differences and similarities of UFPs and ENPs (Xia et al., 2009). As the UFPs are derived incidentally and ENPs are engineer manufactured, the uniformity for UFPs is low and for ENPs is high. Both of them have high surface to volume ratio. The major exposure route of UFPs is through inhalation. Besides inhalation, ENPs also could be exposed through skin, ingestion, and injection. UFPs have been verified to have adverse health effects on humans, however, the effects of ENPs on humans are still unknown (Xia et al., 2009).

	UFPs	ENPs
Source	Incidental	Engineered
Surface area to volume ratio	High	High
Uniformity	Low	High
Organic chemical content	High	Low
Metal impurities	High	Varies
ROS generation	Yes	Varies
Exposure route	Inhalation	Inhalation, skin, ingestion, injection
Adverse health effects	Yes	Unknown

Table 1-4. Differences between ENPs and nanoparticles

Source: adapted from Xia et al., 2009

When studying ENPs, it is important to fully characterise the particles by measuring various parameters, e.g. size distribution, shape, concentration, dispersion, aggregation, structure, chemical composition, etc (Fanning et al., 2009, Savolainen et al., 2010a).

1.5.2   Functions of ENPs

The functionality of many commercial products has been improved by the nanomaterials that have both novel physical and chemical properties. From the beginning of the 21st century, the unique physicochemical properties of nanoparticles have given rise to applications in many fields, including biomedical and pharmaceutical products, cosmetics, clothing, building materials, electronics, food packaging, food additives, and some personal care products. According to the Nanotechnology Consumer Products Inventory in August 2009, there are

more than 1000 self-claimed nano-products produced by 485 companies in 24 countries. The total worldwide sales revenues for nanotechnology were $11.6billion in 2009, and are expected to increase to more than $26 billion in 2015 (Teow et al., 2011; Xia et al., 2009).

There are some kinds of ENPs which are frequently used, including carbon nanotubes (CNTs); TiO_2, ZnO, CeO_2, Si(O), Fe(O), Ag(O), and Au(O) nanoparticles; fullerenes; nanowires; and Dendrimers (Fanning et al., 2009, Stone et al., 2010). With high exploitation of nanoparticles, people could be exposed to ENPs through many routes. There are few studies focusing on the exposure measurement of ENPs. Measurement and monitoring of the engineered nanoparticle are needed to collect all relevant information about the amount (number, surface area or mass concentration), shape, chemical composition, surface charge, and size distribution, as well as solubility and persistence (Savolainen et al., 2010b). Unfortunately, current available techniques for measuring airborne particulates are not developed enough to measure the exposure to particulates with nanoscale dimensions (Hubbs et al., 2011, Savolainen et al., 2010b).

1.5.3   Exposure

Humans could be exposed to ENPs both intentionally and unintentionally. The unintentional exposure pathways include dermal, respiratory system, gastrointestinal tract, and ocular pathway (Abbott and Maynard, 2010). The human skin could protect from nanoparticles and other chemicals owing to the strong stratum corneum, without sweat glands and hair follicles provide gaps in this barrier that NPs are able to penetrate to the dermis (Xia et al., 2009).

Titanium dioxide nanoparticles are added to sunscreen cream for UV protection, therefore TiO2 NPs is exposed to human through penetrating the skin and reaching hair follicles (Xia et al., 2009). Moreover, nanocrystalline silver has been reported as an anti-bacterial agent added in wound dressings (Hubbs et al., 2011). Where it can directly contact with the wounded area and reach the dermis and epidermis (Hubbs et al., 2011, Cooper et al., 2003, Teow et al., 2011, Savolainen et al., 2010a). The human lung consists of about 2300km of airways and 300 million alveoli. Particles with diameters less than 400nm have higher probability to penetrate the lung epithelial barrier, enter into the blood stream, and transport to different organs afterward (Xia et al., 2009). Nasal cilia and the action of coughing could get rid of coarser particulates (Li et al., 2010, Nemmar et al., 2004). Owing to the size of ENPs, they could easily cross the lung epithelial barrier and penetrate the alveoli. The size and shape of the NPs could affect the region of deposition in the respiratory system; smaller sized particles could penetrate deeper in the lung. Macrophages may not be able to recognize particles with a diameter less than 500nm, and for this reason, NPs could easily enter the blood or the lymphatic system and then transfer to different organs (Teow et al., 2011, Savolainen et al., 2010a). Nanoparticles are applied in food industries as food additives or anti-microbial in food packaging. Silver NPs are used in toothpaste as antibacterials and therefore there may be expose to gastrointestinal tract (Savolainen et al., 2010b). The intentional exposure to ENPs is through targeted drugs that lead to the nanoparticles transport and deposit in organs and tissues (Abbott and Maynard, 2010).

Most ENPs are used without toxicological consideration. They do not need any type of toxicity tests under the law even though they have some novel properties both in physical and chemical respects (Kendall and Holgate, 2012). Focusing on the risk assessment of ENPs,

nanoparticle samples were collected from 40 companies, a survey was carried out in Germany and Switzerland from December 2005 to February 2006. In response to the question "Does your company conduct risk assessments where nano-particulate materials are involved?" 26 (65%) of them answered no, 13 companies (32.5%) implemented risk assessments sometimes or always, and 1 company (2.5%) did not answer the question (Savolainen et al., 2010b). Many of the most serious health and safety concerns about nanoparticles are due to the limited information of health effects and the types of exposure during the production and applications (Savolainen et al., 2010b). Since the increased exploitation of nanoparticles, there is a rising debate concerning the possible risks to human health and the environment (Medina et al., 2007). Therefore, research is focused on unravelling how and why the behaviours of engineered nanoparticles are different from the respective bulk materials.

1.5.4 Silicon Dioxide Nanoparticles

As one of the most important engineered nanoparticles, silicon dioxide NPs have been considered as a kind of ideal material for biomedical applications and are being widely explored as medical diagnostics, biosensor, biomarker, cancer/gene therapy, molecule imaging and DNA/drug delivery (Liu and Sun, 2010). Furthermore, silica NPs are manufactured on an industrial scale as additives to cosmetics, food additives, paints and printer toners (Ahamed, 2013; Yang et al., 2014).

Due to the extremely small size of the SiO_2 NPs widely used in many industries, a concern raised that SiO_2 NPs may directly get into the human body and interact with cells and body fluids (Rim et al., 2013). The effects of SiO_2 NPs were demonstrated as follows.

As SiO_2 NPs can be used as additives in cosmetics and paints, a study by Ahamed and colleges investigated the cytotoxicity of SiO_2 NPs on human skin epithelial cells (A431) and human lung epithelial cells (A549). The results indicated that SiO_2 NPs induced significantly cell death at the concentration of 25 μg/ml on both cell lines after 72 hours treatment and caused dose-dependent cytotoxicity (Ahamed, 2013). Eom and Choi studied the cytotoxicity of SiO_2 NPs on human bronchial epithelial cells (Beas-2B) and demonstrated that after 24 hours incubation, 1 μg/ml of NPs caused 20% cell death compared to control (Eom and Choi, 2009). Another study investigated the toxicity of SiO_2 NPs on human gastric epithelial cells (GES-1) and colorectal adenocarcinoma cells (Caco-2). There was no significant toxicity on both cell line after treatment with 100 μg/ml of SiO_2 NPs for 24 hours incubation. But after longer time and high concentrations, SiO_2 NPs showed dose- and time- dependent effect on these cell lines (Yang et al., 2014). A couple of studies have shown that NPs can translocate from the respiratory tract to the systemic circulation, and thus interact with endothelial cells of the blood vessel (Berry et al., 1977; Guarnieri et al., 2014; Nemmar et al., 2002). A study investigated the effects of SiO_2 NPs on endothelial cells; human dermal microvascular endothelial cells were treated with 5 and 50 μg/ml of SiO_2 NPs for 72 hours, both concentrations did not cause significant cell death compared to the control (Peters et al., 2004).

As the small size of SiO_2 NPs, particles may get into the circulation and interact with cells directly. The cytotoxicity of SiO_2 NPs on cells were detected before, but whether SiO_2 NPs have effects on blood coagulation were largely unknown.

1.6   Aim of Study

The overall aims of this study were to understand how diesel or urban PM can affect clot structure and function and to examine whether engineered nanoparticles may exhibit similar hazard.

Hypotheses:

Particulate matter and diesel particles alter fibrin network structure, mediated by both direct and indirect effects through modulation of endothelial cell function.

Specific aims were to:

1) Determine whether clot structure formed from plasma or purified fibrinogen is affected by presence of PM_{10}, $PM_{0.2}$, diesel particles and filtered diesel particles

2) Determine whether exposure to PM_{10} was associated with changes in clot structure and function in samples from a susceptible population (deep vein thrombosis patients)

3) Determine how exposure of vascular endothelial cells to PM_{10}, $PM_{0.2}$, diesel particles and filtered diesel particles, affects clot formation and investigate changes induced in the endothelial cells as a possible mechanism of action of the particles

4) Determine whether engineered silica nanoparticles induce changes in clot structure

    and function similar to those induced by ultrafine particles

2 Methods

This chapter described the general procedures of each method that were used in this study.

2.1 Materials

Reagent	Preparation/Purchasing Company
Double distilled water	Milli-Q Integral purification system
Human Thrombin	Stock concentration: 250 U/ml Stored at -80˚C (Calbiochem, Merck Chemicals, UK)
Calcium Chloride	Stock concentration: 1M (with double distilled water) Stored at room temperature (Sigma Aldrich, UK)
Permeation buffer	Double distilled water 0.05 M Tris base (Fisher Scientific, UK) 0.1 M NaCl (Sigma Aldrich, UK) pH 7.5 (using 5 M HCl, Sigma Aldrich, UK)
Fluorescein isothiocyanate Alexa Fluor® 488 Protein (FITC)	(Life Technology, UK)
Purified human fibrinogen	(Merck Chemicals, UK)
Normal pooled plasma	Plasma was collected from 30 healthy individuals in University of Leeds

	5ml of sodium citrate and 45ml of whole blood from each individual were transferred to 50ml polypropylene tube.
	The cells were removed from plasma by centrifugation for at least 15 minutes at 2200-2500 RPM at room temperature.
	After the centrifugation, all plasma was immediately transferred into a clean polypropylene tube and mixed together.
	Normal pooled plasma was apportioned into 2ml aliquots and stored at –80°C
Tissue Plasminogen Activator	Stock concentration: 100μg/ml (TechnoClone, UK)
FXII deficiency plasma	(Cambridge Bioscience, UK)
FXII zymogen	(Enzyme Research Laboratories, UK)
Chromogenic substrate S2302	S2302 is a chromogenic substrate for plasma FXIIa and kallikrein. (Instrumentation Laboratory, US)
Triton	(Generon, UK)
Standard Reference Material 2787 particulate matter (<10 μm)	(National Institute of Standards & Technology, NIST, USA)
Standard Reference Material 2975 diesel particulate matter (industrial forklift)	(National Institute of Standards & Technology, NIST, USA)
Silicon Dioxide nano-powder (10 to 20 nm)	(Sigma-Aldrich, UK)

µ-Slides 6 channel slides	(Thistle Scientific, UK)
µ-slide 8 well slides (ibiTreat)	(Thistle Scientific, UK)
Dulbecco's phosphate-buffered saline without calcium and magnesium (DPBS Gibco®)	(Life Technologies, UK)
Endothelial cell growing media	380ml of M199 Media (Sigma-Aldrich, UK) 100 ml of Fetal Bovine Serum (FBS) 10ml of Hepes (Life Technologies, UK) 5ml of Antibiotic Antiomycotic Solution (Life Technologies, UK) 2.5ml of Endothelial Cell Growth Supplements (ECGS) (Sigma-Aldrich, UK) 2.5 ml of 1000 U/ml of Heparin (obtained from St. James University Hospital, Leeds) 1ml of Sodium Pyruvate (Sigma-Aldrich, UK)
Sodium pyruvate solution	It was prepared with 2.75g of sodium pyruvate diluted with 50ml of double distilled water, filtered through 0.2mm diameter filter. The solution was aliquoted to 1ml and stored -20°C.
Trypsin-EDTA	It was diluted with DPBS 1:9. (Lonza, UK)
Human Umbilical Vein Endothelial Cells (HUVEC)	(PromoCell, Germany)
Trypan Blue	(Sigma-Aldrich, UK)

3-(4,5-Dimethylthiazol-2-yl)-2,5-Diphenyltetrazolium Bromide (MTT)	(Life Technologies, UK)
Dimethyl Sulfoxide (DMSO)	(Lonza, UK)
96-Well plate (Corning®)	(Sigma-Aldrich, UK)
Von Willebrand Factor ELISA Kit	(Thermo Fisher Scientific, UK)
Plasminogen Activator Inhibitor-1 ELISA Kit	(Abcam, UK)
PRB322 Plasmid DNA	(Thermo Fisher Scientific, UK)
SYBR GREEN PCR Master Mix	(Thermo Fisher Scientific, UK)
Blue Juice Gel Loading Buffer (10x)	(Thermo Fisher Scientific, UK)
GelRed Nucleic Acid Gel Stain	(Cambridge Bioscience, UK)
Tips and tubes (DNase/RNase free)	(Roche, UK)
96-well plate and 384-well plate for PCR	(Roche, UK)
DNA ladder (100bp and 1kb)	(Thermo Fisher Scientific, UK)

2.1.1   Turbidity Method

Plasma Samples

The kinetics of fibrin formation was evaluated by turbidimetry. The fibrin clot formation is characterised by three parts, which are lag phase, followed by lateral aggregation, and finally

a plateau of maximum absorbency (Metassan et al., 2010a). The lag phase is the time that the optical density value increases up to 0.01. The lag phase of the turbidity curve reflects the time required for fibrin protofibrils to grow up to sufficient length to allow lateral aggregation to occur (Undas et al., 2010). The lag phase starts from the moment that the activation mixture is added. Lateral aggregation is the slope of the turbidity curve, which is determined by the rate of fibrin polymerization. Maximum absorbance at the plateau phase reflects the number of protofibrils per fibre. Polymerisation rate can also be analysed by measuring the slope of the turbidity curve at its steepest or inflexion point.

An aliquot of 25 µl of plasma samples and 75 µl of permeation buffer were transferred in triplicate to the 96-well microplate. Activation mixture contained 0.3 U/ml human thrombin and 15 mM $CaCl_2$. Immediately on addition of 50 µl of activation mix, absorbency was read every 12 seconds at 340 nm for 30 minutes with a Kinetic Plate Reader (Spectramax Plus 384, Molecular Devices, UK). The temperature of the reaction was set at 37 °C. The final concentrations of thrombin and $CaCl_2$ were 0.1 U/ml and 5 mM.
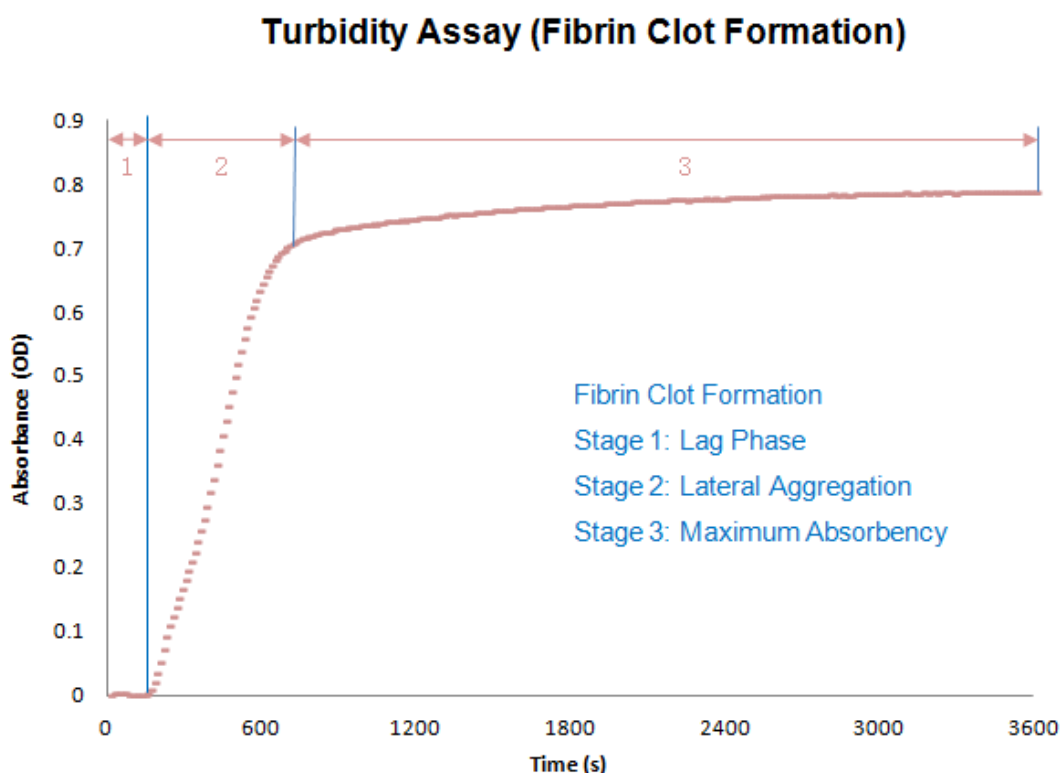
Figure 2-1. Turbidity Assay – Fibrin Clot Formation

The fibrin clot formation is characterised by three parts, which are lag phase, followed by lateral aggregation, and finally a plateau of maximum absorbency (Metassan et al., 2010).

Normal Pooled Plasma

To set up the clot, 25 µl of normal pooled plasma and 25 µl of permeation buffer were added to the 96-well microplate. Four types of particles were used which were PM_{10}, $PM_{0.2}$, total diesel particles and filtered diesel particles. Particles were diluted with permeation buffer to the working concentrations 150 µg/ml, 30 µg/ml, 3 µg/ml, 0.3 µg/ml, and 0.03 µg/ml. 50 µl of different concentrations of particle suspensions were added in triplicate to the microplate. The activation mixture contained 0.3 U/ml human thrombin and 15 mM $CaCl_2$. Immediately

on addition of 50 µl of activation mix, absorbency was read every 12 seconds at 340 nm for 60 minutes with a Kinetic Plate Reader (Spectramax Plus 384, Molecular Devices, UK). The temperature of the reaction was set at 37˚C. The final concentrations of thrombin and $CaCl_2$ were 0.1 U/ml and 5 mM respectively. The concentrations of particles were 50 µg/ml, 10 µg/ml, 1 µg/ml, 0.1 µg/ml, and 0.01 µg/ml.

Purified Human Fibrinogen

50 µl of the human purified fibrinogen was added to each well of the 96-well plate. Same concentrations of particle suspension were used. 50 µl of each concentration of particle suspension were added in triplicate to the microplate. Activation mixture contained 0.3 U/ml human thrombin and 15 mM $CaCl_2$. Immediately on addition of 50 µl of activation mix, absorbency was read every 12 seconds at 340 nm for 30 minutes with a Kinetic Plate Reader (Spectramax Plus 384, Molecular Devices, UK). The temperature of the reaction was set at 37˚C. The final concentration of fibrinogen, thrombin and $CaCl_2$ was 1 mg/ml, 0.1 U/ml and 5 mM. The concentrations of particle suspension were 50 µg/ml, 10 µg/ml, 1 µg/ml, 0.1 µg/ml, and 0.01 µg/ml.

2.1.2   Turbidity Lysis Assay

Normal Pooled Plasma

33.3 µl of normal pooled plasma and 16.7 µl of permeation buffer were added to the 96-well microplate. Particles were diluted with permeation buffer to the working concentrations 200 µg/ml, 40 µg/ml, 4 µg/ml, 0.4 µg/ml, and 0.04 µg/ml. 50 µl of different concentrations of particle suspension were added in triplicate to the microplate. The lysis mixture was consisted of 0.4 µg/ml tPA. The activation mixture contained 0.4 U/ml human thrombin and 20 mM CaCl$_2$. Immediately on addition of 50 µl of lysis mixture and 50 µl of activation mix, absorbency was read every 12 seconds at 340 nm for 60 minutes with a Kinetic Plate Reader (Spectramax Plus 384, Molecular Devices, UK). The temperature of the reaction was set at 37°C. The final concentrations of tPA, thrombin and CaCl2 were 0.1 µg/ml, 0.1 U/ml and 5 mM respectively. The concentrations of particle suspension were 50 µg/ml, 10 µg/ml, 1 µg/ml, 0.1 µg/ml, and 0.01 µg/ml.

Purified Human Fibrinogen

50 µl of 3 mg/ml of purified fibrinogen was added to the 96-well microplate. Particles were diluted with permeation buffer to the working concentrations 150 µg/ml, 30 µg/ml, 3 µg/ml, 0.3 µg/ml, and 0.03 µg/ml. 50 µl of different concentrations of particle suspension were added in triplicate to the microplate. The lysis mixture was consisted of 1.5 µM of Plasminogen. The activation mixture contained 0.6 µg/ml tPA, 0.6 U/ml human thrombin and 30 mM CaCl$_2$. Immediately on addition of 25 µl of lysis mixture and 25 µl of activation mix,

absorbency was read every 12 seconds at 340 nm for 60 minutes with a Kinetic Plate Reader (Spectramax Plus 384, Molecular Devices, UK). The temperature of the reaction was set at 37˚C. The final concentrations of plasminogen, tPA, thrombin and $CaCl_2$ were 0.25 µM, 0.1 µg/ml, 0.1 U/ml and 5 mM respectively. The concentrations of particle suspension were 50 µg/ml, 10 µg/ml, 1 µg/ml, 0.1 µg/ml, and 0.01 µg/ml.

2.2   Laser Scanning Confocal Microscopy

Laser Scanning Confocal Microscopy (LSCM) allows direct quantification of fibrin clot structure by image.

Figure 2-2: Laser Scanning Confocal Microscopy 700 T-PMT ZEISS

2.2.1   Clot Preparation

Plasma Samples

30 µl of plasma samples was added to the microtube. 30 ul of activation mixture which contained 100 µg/ml of human fibrinogen amino terminal labelled with Fluorescein Isothiocyanate (FITC), 0.2 U/ml of human thrombin and 10 mM $CaCl_2$ were introduced into the microtube and mixed with the plasma sample. Fibrin clots were prepared in a total volume of 60 µl, immediately upon the addition of activation mixture, 30 µl was slowly transferred to the channel of µ-slide $VI_{0.4}$. Care was taken to ensure there were no bubbles in the channel. The slides were stored in a humidity chamber to prevent dehydration of the clot and stored at room temperature for 30 minutes. The final concentrations of FITC, thrombin and $CaCl_2$ were 50 µg/ml, 0.1 U/ml and 5 mM respectively.
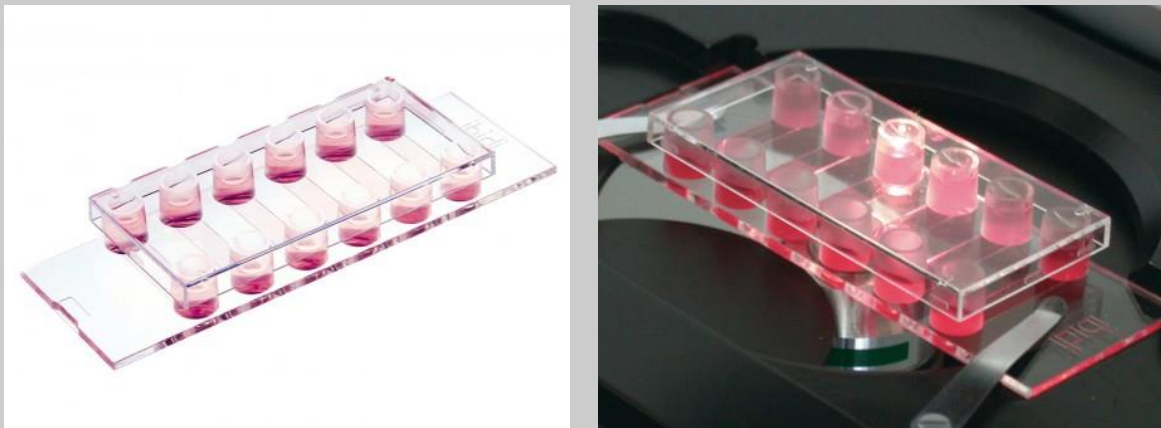
Figure 2-3: 6 channel µ-slide VI0.4 (Ibidi, Martinsried, Germany)

Source: Ibidi Official Website µ-Slide VI 0.4
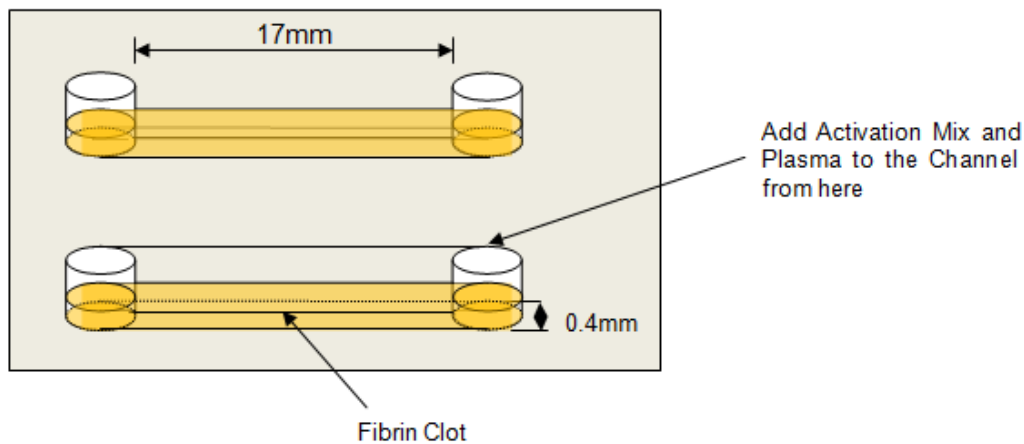
Figure 2-4: Fibrin clot in μ-slide VI

Normal Pooled Plasma

An aliquot of 15 μl of normal pooled plasma mixed with 15 μl of permeation buffer were added to microtube. Silica nanoparticle suspension was prepared to concentrations 150 μg/ml, 30 μg/ml, 3 μg/ml, 0.03 μg/ml, and 0.0003 μg/m. 30 μl of each concentration of SiO2 nanoparticle suspension was added to the plasma sample. 24 μl of activation mixture which contained 150 μg/ml of human fibrinogen amino terminal labelled with Fluorescein Isothiocyanate (FITC) and 15 mM CaCl$_2$ were introduced into the microtube. Finally, 6 μl of 0.3 U/ml of human thrombin added to the tube and mixed with the plasma and nanoparticle suspension in the microtube. Fibrin clots were prepared in a total volume of 90 μl, immediately upon the addition of thrombin 30 μl of solution was slowly transferred to the channel of μ-slide VI$_{0.4}$ (Ibidi, Martinsried, Germany). There should be no bubbles in the channel. The slides were stored in a humidity chamber to prevent dehydration of the clot.

The final concentrations of FITC, thrombin and CaCl$_2$ were 50 µg/ml, 0.1 U/ml and 5 mM respectively. The concentrations of nano-silica suspension were 100 µg/ml, 10 µg/ml, 1 µg/ml, 0.01 µg/ml, and 0.0001 µg/ml.

Purified Human fibrinogen

An aliquot of 30 µl of purified human fibrinogen was introduced into each eppendorf tube. 30 µl of nanoparticle suspensions with concentrations 150 µg/ml, 30 µg/ml, 3 µg/ml, 0.3 µg/ml, and 0.03 µg/ml were added into the eppendorf in duplicate and mixed with the fibrinogen. Activation mixture contained 150 µg/ml of human fibrinogen amino terminal labelled with Fluorescein Isothiocyanate (FITC), 1.5 U/ml of human thrombin and 45 mM CaCl$_2$. 24 µl of activation mixture which contained 150 µg/ml of human fibrinogen amino terminal labelled with Fluorescein Isothiocyanate (FITC) and 15 mM CaCl$_2$ were introduced into the microtube. Finally, 6 µl of 0.3 U/ml of human thrombin added to the tube and mixed with the plasma and nanoparticle suspension in the microtube. Fibrin clots were prepared in a total volume of 90 µl, immediately upon the addition of thrombin 30 µl of solution was slowly transferred to the channel of µ-slide VI0.4 (Ibidi, Martinsried, Germany). Care was taken to ensure there were no bubbles in the channel. The slides were stored in a humidity chamber to prevent dehydration of the clot. The final concentrations of FITC, thrombin and CaCl$_2$ were 50 µg/ml, 0.1 U/ml and 5 mM respectively. The concentrations of nano-silica suspension were 50 µg/ml, 10 µg/ml, 1 µg/ml, 0.1 µg/ml, and 0.01 µg/ml.

2.2.2   Image Analysis

The 3D structure of the clot was visualized by confocal microscopy on a LSM 700 T-PMT ZEISS microscope (ZEISS, Jena, Germany). Clot structure was viewed using 63x oil immersion lens with a 5-W argon laser and 488nm laser filter. The images were collected in the format of 512 x 512 pixels. Fibre density was calculated as the number of fibres crossing a straight line of fixed length across the scanfield. All measurements were performed with Image J version 1.25s software.

Figure 2-5: Fibrin clot image under LSCM

Structure of fibrin clots can be visualized through confocal microscope.

2.3   Permeation Method

2.3.1   Permeability Experimental Apparatus

Fibrin clot permeation involves a gravity-driven tube system as shown in figure 2-6.
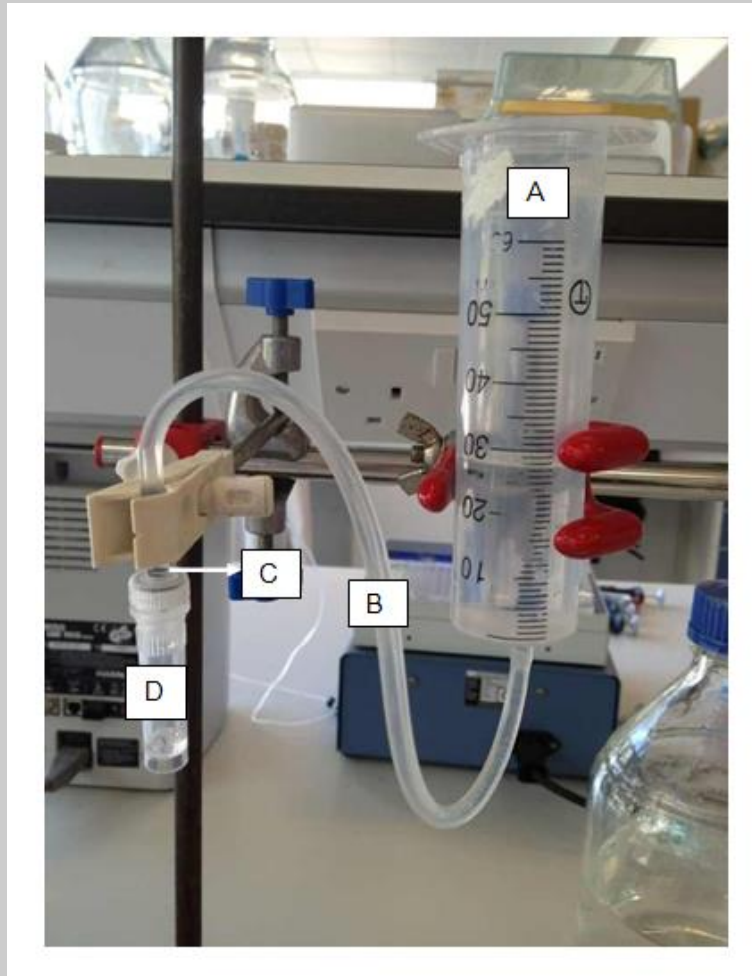
Figure 2-6: Permeability Experimental Apparatus

There are four parts of this apparatus, syringe (A), plastic tube (B), plastic pipette tip (C), and a small plastic microtube (D). The syringe was filled with permeation buffer. The plastic tube was the connection between syringe and the plastic pipette tip. The plastic pipette tip was cut from a disposable plastic pipette. 4.5cm from the tip of the disposable plastic pipette was sheared as the plastic pipette tip. The interior surface of the pipette tip was roughened. The screw cap of the microtube was drilled in the middle with the diameter of the plastic pipette tip. The pipette tip could pass through the cap. The pipette tip and microtube were linked.

The fibrin clot permeation method is used to measure the flow rate of liquid through the fibrin clot. The flow rate represents the pore size of fibrin clot structure.

2.3.2 Clot Preparation

Plasma Samples

Plasma samples were defrosted in the water bath at 37˚C for 3 minutes just before use. After defrosting, plasma samples were agitated briefly to ensure thorough mixing. 100 µl of plasma was transferred to each eppendorf tube. Activation mixture contained 176 mM of $CaCl_2$ and 11 U/ml of thrombin. 10 µl of activation mixture was transferred to each eppendorf tube and mixed with plasma. Fibrin clot started to form. 100 µl of clotting mixture was carefully and immediately transferred from the eppendorf tube to the plastic pipette tip. There should not be any bubbles in the clotting tip. The final concentrations of thrombin and $CaCl_2$ were 1 U/ml and 16 mM. Then the pipette tip was kept in the humidity chamber horizontally for two hours at room temperature. During this time, fibrin gel cross-linking started to occur and stabilise the fibrin clot structure in the humidity chamber horizontally. The humidity chamber was prepared, as follows, before making the fibrin clot, a folded piece of paper towel was soaked with distilled water and placed in the petri dish. After the 2 hours, the plastic pipette tip was connected to the syringe through a plastic tube. The syringe was filled with permeation buffer. The height of the buffer was 4 cm from the bottom of the plastic pipette tip (Fig 2-6). Pressure was created on the clot due to the buffer. The clot was washed by the permeation buffer for 90 to 120 minutes.
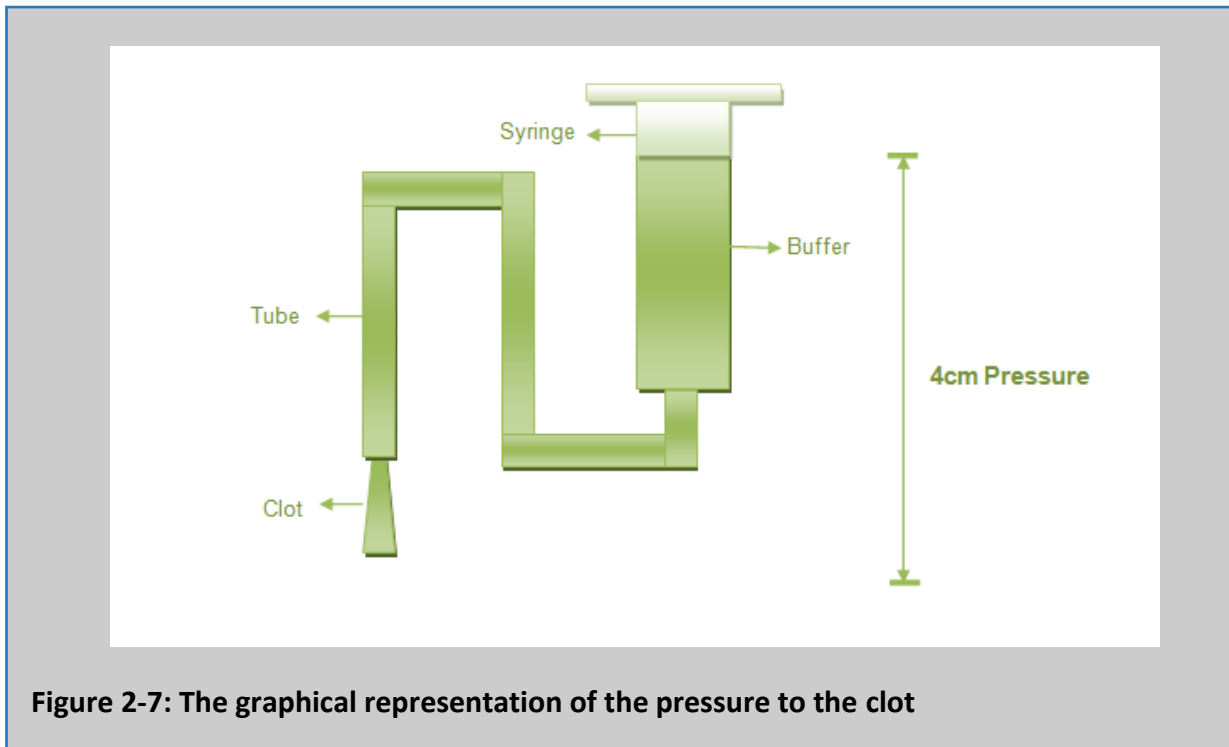
Figure 2-7: The graphical representation of the pressure to the clot

2.3.3   Pore Size Measurement of Fibrin Clot

After 90 to 120 minutes washing, the volume of the permeation buffer through the fibrin clot was measured for the next 120 minutes. The permeation buffer was collected and measured every 30 minutes. To avoid evaporation, the buffer through the fibrin clot dropped into a closed microtube. The microtubes were weighed prior to use, in order to calculate the drops weight accurately. After every 30 minutes, the old microtube was removed and replaced with a new one. After 120 minutes, 4 microtubes were collected. The volume of the permeation buffer through the fibrin clot was calculated (1 g=1 ml).

The permeation coefficient (Darcy constant [Ks]), which indicates the pore size of fibrin clot and represents the surface of the gel allowing flow, was calculated from the equation:

$$Ks = \frac{Q \times L \times \eta}{T \times A \times \Delta P}$$

Ks = Permeability Coefficient

Q = volume of liquid (1ml = 1cm3)

L = the length of fibrin clot gel (1.7cm)

η = viscosity of the liquid (10-2 poise = 10-7 N.s.cm-2)

T = time (second)

A = cross-sectional area (0.071 cm2)

ΔP = pressure drop (density x weight x height = 1 x 980 x 4 = 3920 dyne/cm2 = 0.03920 N.cm-2)

As the constants are substituted, L = 1.7 cm, η = 10-7 N.s.cm-2, A = 0.071, and ΔP = 0.03920 N.cm-2

Ks = Q/T x 6.108 x 10-5

Q = Volume (ml)

T = Time (second)

2.4 Factor XII Activation Test

Method A

Silicon dioxide nanoparticles was diluted with double distilled water and the working concentrations were 150 µg/ml, 30 µg/ml, 3 µg/ml, 0.3 µg/ml, and 0.03 µg/ml. 50 µl of silica suspensions, 25 µl of FXII deficiency plasma and 25 µl of permeation buffer were added in the 96-well plate in triplicates.

The stock concentration of FXII zymogen is 4.1 µg/ml. FXII plasma concentration is 375 nM (30 µg/ml). 1 µl of FXII zymogen was diluted with 136.67 µl of double distilled water. 3.42 µl of FXII zymogen was mixed with 996.58 µl of FXII deficiency plasma. 50 µl of silicon dioxide nanoparticle suspension were added in triplicate. 25 µl of FXII deficiency with plasma FXII zymogen and 25 µl of permeation buffer were added into the 96 well-plate. 50 µl of silica suspensions, 25 µl of normal pooled plasma and 25 µl of permeation buffer were added in triplicate in the 96-well plate as control.

Activation mixture contained 0.3 U/ml human thrombin and 15 mM $CaCl_2$. Immediately on addition of 50 µl of activation mix, absorbency was read every 12 seconds at 340 nm for 60 minutes with a Kinetic Plate Reader (Spectramax Plus 384, Molecular Devices, UK). The temperature of the reaction was set at 37˚C. The final concentrations of thrombin and $CaCl_2$ were 0.1 U/ml and 5 mM respectively. The concentrations of nano-silica suspension were 50 µg/ml, 10 µg/ml, 1 µg/ml, 0.1 µg/ml, and 0.01 µg/ml.
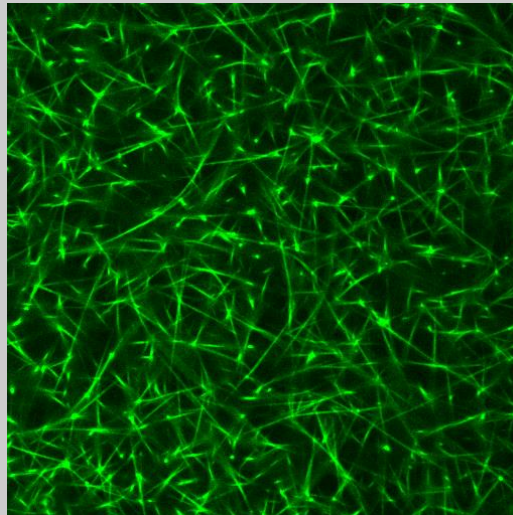
Method B

Silicon dioxide nanoparticles was diluted with double distilled water and the working concentrations were 500 µg/ml, 100 µg/ml, 10 µg/ml, 1 µg/ml, and 0.1 µg/ml. 10 µl of different concentrations of SiO_2 NPs were added to 96-well plate. 0.25% Triton, 625 nM of FXII zymogen, 10 mM S2302 (a kind of chromogenic substrate for plasma kallikrein, factor XIa and factor XIIa) and permeation buffer was added into each well. For a positive control of FXII, PTT automate was added and mixed with 625 nM of FXII zymogen. Absorbency was read every 12 seconds at 340 nm for 180 minutes with a Kinetic Plate Reader (Spectramax Plus 384, Molecular Devices, UK). The temperature of the reaction was set at 37˚C. The final concentrations of Triton, FXII zymogen, and S2302 were 0.05%, 125 nM, and 2 mM respectively. The concentrations of nano-silica suspension were 50 µg/ml, 10 µg/ml, 1 µg/ml, 0.1 µg/ml, and 0.01 µg/ml.

2.5   Endothelial Cell Culture

Endothelial cell growth media (ECGM) was prepared before defrosting the cells. 500 ml of ECGM consisted of 380 ml of M199 media, 100 ml of fetal bovine serum, 10 ml of 1 M Hepes, 5 ml of antibiotic antiomycotic solution, 2.5 ml endothelial cell growth supplements solution, 2.5 ml of 1000 U/ml Heparin, and 1 ml of sodium pyruvate solution. ECGM was stored at -4 degree and prewarmed before use.

Frozen human umbilical vein endothelial cells (HUVEC) were purchased from PromoCell. The vial containing the cells was thawed in a water bath and gently shook for 2 or 3 minutes. Once

the cells were defrosted, they were immediately transferred into a T25 flask containing 9ml pre-warmed ECGM.

Cells were cultured and underwent passaging after 80-90% confluent in the flask. HUVEC were used only between passage 3 to passage 7.

2.5.1 Passaging

When the cells were 80-90% confluent in the T25 flask, they were prepared for passaging. All media was removed completely. The cells were washed once with 5 ml DPBS. Then 1 ml of Trypsin-EDTA (10 fold diluted) was added to the T25 flask which was enough to cover the whole bottom surface of the flask. Cells were incubated for 2 to 3 minutes. Afterwards, all cells should detached from the bottom surface of the flask, 8 ml of pre-warmed ECGM was added to flask to stop trypsinization. Cells were transferred into a sterile 15 ml tube and centrifuged for 5 min at 1000 x g. Then, the supernatant was discarded and the cell pellet was re-suspended with 1 ml of ECGM. Based on the experiment requirements, different number of cells were seeded to either flasks, plates, or slides.

2.5.2   Counting Cells

After the cells were re-suspended with 1 ml fresh ECGM, 10 µl of cell suspension was taken transferred into a small eppendorf and 30 µl of Trypan Blue was added. The haemocytometer was prepared for counting cells by placing cover slip onto the grooves on the glass slide. 10 µl of mixed cell suspension was transferred to one side of the slide under the cover slip. Cells were counted in large square in four corners (Fig 2-8. A parts) of the slide.

$$\text{Number of cell per ml} = \frac{\text{Number of Cells Counted} \times 4 \text{ (Dilution Factor)} \times 10^4}{4}$$

Figure 2-8: Image Showing Haemocytometer

The cells were counted in the area A. For each light blue square, the number of cells in 4 A parts were added up which refers to 'the number of cells counted' in the formula. The number of cells per ml was calculated following the formula.
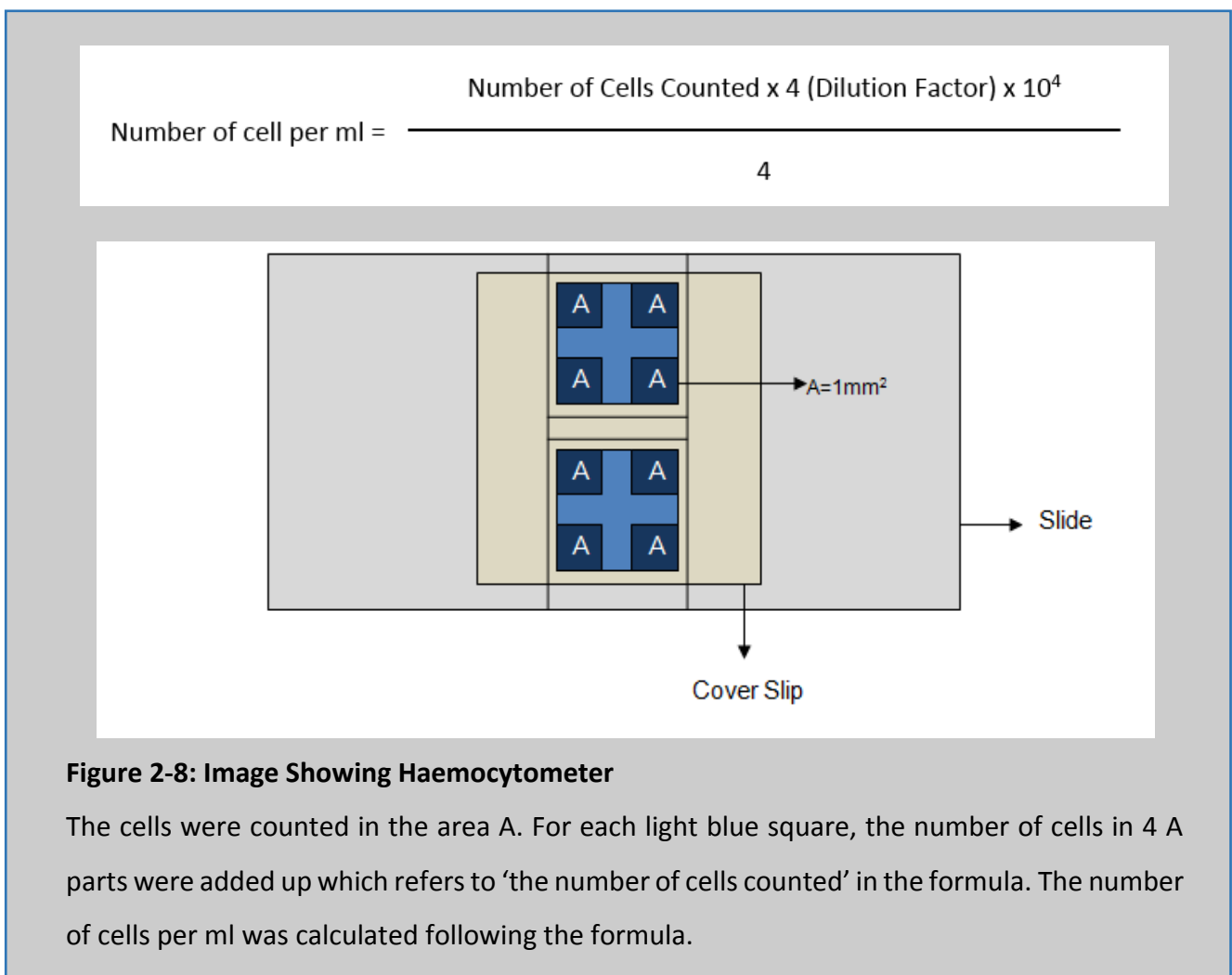
2.5.3　Freezing Cells

The freezing media was prepared with 90% fetal bovine serum and 10% of sterile DMSO. After passaging the cells, 200 μl of cell suspension was transferred to a cryotube (Nunc) containing 800 μl of the freezing mixture. The cell number would be approximately 1.0×10^6 cells per ml. The vials were placed into Nalgene Mr Frosty (Sigma-Aldrich, UK) which is a polycarbonate container holding isopropanol. Isopropanol controls the cooling at a constant rate of 1°C per minute which was required for successful cryopreservation of cells. The Mr Frosty container was placed in the -80°C freezer overnight. Then the vials were moved to the liquid nitrogen storage tank for long term storage. Cells were only frozen until passage three.

2.6　Cytotoxicity Test

The particles cytotoxicity was measured by using the 3-(4, 5-dimerthylthia-zol-2-yl)-2, 5-diphenyltetrazolium bromide (MTT) reduction assay. MTT is a water soluble tetrazolium salt, which can be converted to a purple formazon product by enzymes in living cells. MTT assay is a colorimetric method for cytotoxicity detection that measures the reduction of MTT by mitochondrial succinate dehydrogenase. The MTT entered cells and passed into the mitochondria. Then it became an insoluble, dark purple formazan product. After adding solubilising solution (an organic solvent), the formazan reagent was solubilised and released. Reduction of MTT reagent only occurs in live cells. More mitochondria activities induced the darker colour of cells and indicated more viable cells. The colour was measured spectrophotometrically (Supino, 1995).

For the treatment, cells were seeded into a 96-well plate. Each well contained 2×10^4 cells at the beginning. After the cells were 80 to 90% confluent, cells were ready to be treated with nano-silica. All the media was removed from the well completely. Particle solution was diluted with ECGM without fetal bovine serum. The concentrations were 50 µg/ml, 10 µg/ml, 1 µg/ml, 0.1 µg/ml, 0.01 µg/ml and 0 µg/ml. 100 µl of different concentrations of particle suspension was added to each well in triplicate. The cells were incubated for 24 hours at 37°C with 5% CO_2.

To prepare the MTT, 100 mg of MTT powder was added into a 50 ml falcon tube covered with aluminium foil containing 20 ml of tissue-culture DPBS. The MTT solution was mixed well and incubated in the water bath for 15 minutes at 37°C. The MTT solution was filtered by a 0.2 µm filter in the flow hood without light. The tube containing filtered MTT solution was wrapped with aluminium foil.

The whole process should be conducted in the flow hood without the light on. 10 µl of MTT solution was added to each well without taken the previous treatment solution. 96-well plate was covered with aluminium foil and transferred into the incubator for 4 hours. After incubation, all media was removed completely. 100 ul of sterile DMSO was added to each well for solubilising the MTT reagent. The plate was incubated overnight. The plate was read at 540 nm and 690 nm (reference absorbance) with 10 seconds shaking on the ASCENT software.

2.7   Fibrin Clot Formation on HUVEC

To set up the fibrin clot structure, 300 μl of cell suspension containing 5×10^4 cells were seeded on the μ-slide. After 80 to 90% confluent in the μ-slide, the cells were ready for treatment. The particle suspension was prepared with ECGM without fetal bovine serum for treatment. The concentrations were 50 μg/ml, 10 μg/ml, 1 μg/ml, 0.1 μg/ml, 0.01 μg/ml and 0 μg/ml. 300 μl of each concentration and control were added in duplicate to each well of the slide. The treatment lasted for 24 hours. Then, all solution was removed completely by vacuum pump.

2.7.1   Purified Human fibrinogen

Clot formation were performed on the cells after the treatment. 1 mg/ml of purified fibrinogen was mixed with the activation mixture consisted of 50 μg/ml of FITC, 15mM of $CaCl_2$, 5 U/ml of thrombin and ECGM without fetal bovine serum. 300 μl of the clotting mixture was immediately introduced into the well. The slides were kept in the incubator for 15 to 30 min for the clot to form. The final concentrations of fibrinogen, FITC, thrombin and $CaCl_2$ were 1 mg/ml, 50 μg/ml, 0.5 U/ml and 15 mM respectively.

2.7.2   Normal Pooled Plasma

To set up the clot, 100 μl of normal pooled plasma was mixed with the 200 μl of activation mixture consisted of 0.5 mg/ml of FITC, 150 mM of $CaCl_2$, 5 U/ml of thrombin and M199 media.

300 µl of the clotting mixture was immediately introduced into each well. The slides were kept in the incubator for 30 min allowing the clot formation. The final concentrations of FITC, thrombin and $CaCl_2$ were 50 µg/ml, 0.5 U/ml and 15 mM respectively.

This method was confirmed after trying different concentrations of thrombin and $CaCl_2$, also different reagents (DPBS, permeation buffer, ECGM without serum, M199 media) were used to dilute the activation mixture. M199 media was the most appropriate reagent to mix with thrombin and $CaCl_2$ and setting up the clots.

2.8 Enzyme-Linked Immunosorbent Assay (ELISA)

Enzyme-Linked Immunosorbent Assay (ELISA) was used to measure the concentrations of VWF and Plasminogen Activator Inhibitor-1 (PAI-1) which are secreted by endothelial cells and released into the circulation afterwards.

2.8.1 Von Willebrand Factor

Enzyme-Linked Immunosorbent Assay (ELISA) was used to measure the concentration of Human VWF in the cell culture supernatant. We purchased the Human VWF ELISA Kit from Abcam. 96-well plate had been coated with VWF antibody. The brief procedures were as following. The Standards and samples were added to the wells, incubated and then washed with wash buffer. The VWF biotinylated detection antibody was then added, incubated, and washed by wash buffer. Thirdly, Streptavidin-Peroxidase Conjugates was added, incubated,

and washed with wash buffer. Chromogenic substrate (TMB, 3,3', 5,5;-tetramethylbenzidine) is catalyzed by Streptavidin-Peroxidase to produce a blue color product which was added to visualize Streptavidin-Peroxidase enzymatic reaction. Finally, an acidic stop solution was added and the chromogenic substrate produce color changed to yellow. The density of yellow was measured by a microplate reader and indicated the amount of VWF captured on the plate.

Cell Treatment

HUVEC was treated with different particles with different concentrations 0 μg/ml, 0.01 μg/ml, 0.1 μg/ml, 1 μg/ml, 10 μg/ml, and 50 μg/ml, respectively. The cells were incubated with particle suspension for 24 hours.

Reagent Preparation

All reagents were warmed up to room temperature (18-25°C) prior to use. Diluent N Concentration was diluted 1:10 with MilliQ water and mixed well. Wash Buffer Concentrate was diluted with MilliQ water 1:20 and mixed well.

Von Willebrand Factor Standard was prepared. The stock concentration was 240 mU/ml. The standard were diluted to concentrations 80 mU/ml, 40 mU/ml, 20 mU/ml, 10 mU/ml, 5 mU/ml, 2.5 mU/ml and 0 mU/ml. 50x Biothinylated Von Willebrand Factor Detector Antibody was diluted with Diluent N.

Cell Culture Supernatants Preparation

After the cells were treated for 24 hours, the cell supernatants were transferred to microtubes. The supernatants were centrifuged at 3,000 x g for 10 minutes to remove debris.

ELISA

All materials and prepared reagents were warmed up to room temperature prior to use. 50 µl of standards, controls and samples were added into the wells in triplicate. The plate was covered by a sealing tape and incubated for 2 hours. Each well was inverted and washed five times using 200 µl of 1X Wash Buffer, tapped 4 to 5 times on absorbent paper towel to completely remove the liquid. 50 µl of 1X Biotinylated Von Willebrand Factor Antibody were added to each well and incubated for 2 hours. Plate was washed as described above. Then, 50 µl of 1X SP Conjugate were added to each well and incubated for 30 minutes, followed by plate washing as described above. 50 µl of Chromogen Substrate were added to each well and incubated for 20 minutes and finally 50 µl of Stop Solution were added. The color changed from blue to yellow. Plate was read immediately in microplate reader at a wavelength of 450nm.

Calculation

To generate the standard curve, the graph used the standard concentrations on the x-axis and the corresponding mean 450 nm absorbance on the y-axis. The samples concentrations were calculated from the standard curve.

2.8.2   Plasminogen Activator Inhibitor - 1

Enzyme-Linked Immunosorbent Assay (ELISA) was used to measure the concentration of Human PAI-1 in the cell culture supernatant. Human PAI-1 ELISA Kit was purchased from Life Technologies.

Cell Treatment

HUVEC was treated with different particles with different concentrations from 0 to 50 μg/ml. The cells were incubated with the suspension for 24 hours.

Standard Preparation

PAI-1 Standard was prepared. Each well was added 100 μl of standard. The stock concentration was 4,000 pg/ml. The standard was diluted to 2,000 pg/ml, 1,000 pg/ml, 500 pg/ml, 250 pg/ml, 125 pg/ml, and 0 pg/ml.

Streptavidin-HRP (100X) is in 50% glycerol. Streptavidin-HRP was diluted with Streptavidin-HRP Diluent 1:100. This reagent was prepared within 15 minutes of usage.

Wash Buffer Concentrate (25X) was diluted with MilliQ water 1:25.

Cell Culture Supernatants Preparation

After the cells were treated for 24 hours, the cell supernatants were transferred to microtubes. The supernatants were centrifuged at 3,000 x g for 10 minutes to remove debris.

ELISA

All materials and prepared reagents were warmed up to room temperature prior to use.

All standards, controls and samples were in triplicates. 100 µl of standards were added to each well. Controls and samples were diluted with Standard Diluent Buffer 1:1 (50 µl : 50 µl) and added into each well in triplicate. The plate was covered by a sealing tape and incubated for 2 hours at room temperature. Then, each well was washed with 300 µl of 1X Wash Buffer for four times, tapped 4 to 5 times on absorbent paper towel to completely remove the liquid. 100 µl of Biotinylated Human PAI-1 Biotin Conjugate Solution was added into each well and incubated for another 2 hours at room temperature with sealing tape. The plate was washed as described above. Then 100 µl of Streptavidin-HRP Working Solution was added to each well and incubated for 30 minutes at room temperature with plate cover. The plate was washed 4 times as described above. 100 µl of Stabilized Chromogen was added to each well and incubated for 30 minutes at room temperature in the dark. Finally, 100 µl Stop Solution was added to each well. Read the plate immediately at 450nm.

Calculation

To generate the standard curve, the graph was plotted using the standard concentrations on the x-axis and the corresponding mean 450 nm absorbance on the y-axis. The samples concentrations were calculated from the standard curve.

2.9 Real Time Polymerase Chain Reaction (RT-PCR)

The real time polymerase chain reaction is one of the most useful technologies in molecule biology which can be used to quantify the DNA or RNA in a sample. Specific sequences in a DNA or cDNA template can be amplified thousands to millions fold using sequence specific oligonuceotides. PCR amplifies DNA exponentially, doubling the number of target molecules in each amplification cycle. Fluorescent DNA-binding dyes and real time PCR machine are used to quantify the amplified products by measuring the fluorescence dyes that yield increasing fluorescent signal in direct proportion to the number of PCR product molecules generated.

RT-PCR method was used to quantify the gene expression of tissue factor and thrombomodulin as both of them are membrane proteins secreted by endothelial cells.

2.9.1 Cell Treatment

Human umbilical vein endothelial cells were seeded in T25 flasks with 0.7×10^6. When the T25 flasks were 80 to 90% confluent, cells were treated with different concentrations of particles. Each particles were diluted to six concentrations for cell treatment which were 0 µg/ml, 0.01

μg/ml, 0.1 μg/ml, 1 μg/ml, 10 μg/ml and 50 μg/ml respectively. Cell were treated for 24 hours in the incubator at 37 °C with 5% CO_2. After the treatment, the cells were trypsinzed and collected in the tubes. Then, those cells were washed with DPBS one more time to remove the serum completely. Afterwards, the cells were ready for total RNA extraction.

2.9.2   RNA Extraction

RNeasy Mini Kit from Qiagen (Germany) was used for total RNA extraction from endothelial cells. After treatment, the harvest cell number was approximately $1 - 1.5 \times 10^5$ per flask. Cells were mixed with 350 μl of RLT buffer for 15 minutes with gentle shaking which allowed the cells to be lysed completely. Then, 350 μl of 70% of ethanol was added to the lysate and mixed well by pipetting. 700 μl of each sample was transferred to an RNeasy Mini spin column placed in a 2 ml collection tube. The tubes were centrifuged for 1 min at 4,000 x g, and 5 seconds at 6,000 x g. The flow through was discarded. 700 μl of Buffer RW1 was added to each RNeasy Mini spin column. The tubes were centrifuged for 1 min at 4,000 x g, and 5 seconds at 6,000 x g. The flow through was discarded. 500 μl of Buffer RPE was added to each RNeasy Mini spin column. The tubes were centrifuged for 1 min at 4,000 x g, and 5 seconds at 6,000 x g. The flow through was discarded. Another 500 μl of Buffer RPE was added to each spin column. The tubes were centrifuged for 2 min at 4,000 x g, and 15 seconds at 6,000 x g. The flow through was discarded. The tubes were centrifuged again for 2 min at the maximum speed to dry the membranes. The 2 ml collection tubes were discarded and replaced by the new 1.5 ml collection tubes. Finally, 30 μl of RNase/DNase Free water was added to each spin column membrane. The tubes were centrifuged for 1.5 min at 6000 x g to elute the total RNA.

The quantity and quality of total RNA from each sample was measured by NanoDrop 1000 Spectrophotometer (UK).

2.9.3 Reverse Transcription

For reverse transcriptase from totol RNA to cDNA, we used Taqman Reserve Transcription Reagents (Life Technologies, UK). The total RNA samples were diluted to 100 ng/ul. Each reaction was made up to 20 µl of the reaction volume (as shown below). The enzymes should be kept in the freezer until immediately prior to use.

Component	Volume	Final Concentrations
DNase/RNase Free H_2O	1.6 µl	-
10x RT Buffer	2 µl	1x
25 mM $MgCl_2$	1.4 µl	1.75 mM
10 mM dNTP mix	1 µl	0.5 mM
100 mM DTT	1 µl	5mM
RNase Inhibitor (20 U/µl)	1 µl	1 U/µl
MultiScribe RT (50 U/µl)	1 µl	2.5 U/µl
50 µM Random Hexamers	1 µl	2.5 µM
Template RNA (100 µg/µl)	10 µl	50 µg/ul

Figure 2-9. Reverse Transcription Reagents Preparation

After making up the reaction, the tubes were moved to the PCR machine for incubation in a thermal cycle (as shown below).

Temperature	Time
25 °C	10 minutes
37 °C	30 minutes
95 °C	5 minutes
4 °C	Indefinitely

Figure 2-10. Reverse Transcription thermal cycle setup

After the incubation, the total RNA was reverse transcript to the cDNA and ready for real time PCR.

2.9.4   Primer Design

Good primer design is an important parameter in real time PCR. The primers should be 18 to 24 nucleotides in length and the amplicon length should be between 50 to 150 bp. The primer pairs should have compatible melting temperature (Tm) (within 1 °C) and contain approximately 50% GC content.

We needed to choose primers for housekeeping genes and target genes. There are many common used housekeeping genes. According to the literatures, we chose glyceraldehydes-3-phosphate dehydrogenase (GAPDH) and beta actin (ACTB) as the housekeeping gene. The two target genes were TF and THBD. We found the adaptive primers for each gene from national centre of biotechnology institute (NCBI).

Gene	Primer	Sequence (5' – 3')	Tm	GC%	Amplicon Length
GAPDH NM_001256799.2	Forward	AAGCCTGCCGGTGACTAAC	60 °C	57.89	111 bp
	Reverse	GCATCACCCGGAGGAGAAAT	59.82 °C	55%	
ACTB NM_001101.3	Forward	TCGAGCAAGAGATGGC	62 °C	56%	194 bp
	Reverse	TGAAGGTAGTTTCGTGGATG	66 °C	45%	
TF NM_001178096.1	Forward	AAACCTCGGACAGCCAACAA	60.11 °C	50	116 bp
	Reverse	CCCGGAGGCTTAGGAAAGTG	60.11 °C	60	
THBD NM_000361.2	Forward	AGCCCCTGAACCAAACTAGC	59.96 °C	55	176 BP
	Reverse	GAAACCGTCGTCCAGGATGT	60.04 °C	55	

Figure 2-11. Details of primers of housekeeping genes and target genes

To confirm the specificity of the primers, BLAST® search was used to be sure that the primers were only recognized in the target of interests.

2.9.5   RT-PCR

There were three main steps of real time PCR and the reaction ran for 40 cycles. Before making up the reactions, the LC480 RT-PCR instrument was set up as following.

Program	Analysis Mode	Cycle	Segment	Temperature	Time	Acquisition Mode
Denaturation	None	1		95 °C	10 min	None
Amplification	Quantification	40	Denaturation	95 °C	15 s	None
			Annealing/ Extension	60 °C	1 min	Single
Melting Curves	Melting Curves	1	Denaturation	95 °C	5 s	None
			Annealing/ Extension	60 °C	1 min	None
			Melting	95 °C		Continuous
Cooling	None	1		40 °C	30 s	None

Figure 2-12. Real Time PCR thermal cycle setup

After setting up the instrument, the reactions were prepared as following. SYBR Green Master Mix (Thermo Fisher, UK) was used in the RT-PCR for fluorescence quantification after double stranded DNA binding to the SYBR® Green.

Component	Volume (96-well Plate)	Final Concentrations
2x SYBR Green PCR Master Mix	10 µl	1x
Forward Primer	1 µl	500 nM
Reverse Primer	1 µl	500 nM
cDNA Template	8 µl	40 ng

Figure 2-13. Real Rime PCR reagents preparation

After making up the reactions, the plate was covered by the foil and centrifuged for 2 min at 1,500 x g. Then, the plate was transferred into the instrument LC480 to start the progress immediately.

2.10   Plasmid Strand Break Assay

The plasmid strand break assay was used to investigate the strand breaks in the plasmid DNA caused by exogenous agents such as ionizing radiation, or by endogenously generated reactive oxygen species (Lodge et al., 1989; Schnaith et al., 1994; Smiałek et al., 2009). The pBR supercoiled plasmid DNA was incubated with different concentrations of particles for 12 hours allowing the single strand or double strand breaks to occur and generating nicked or relaxed plasmid DNA. pBR plasmid DNA is 4,361 bp in length. But supercoiled plasmid DNA travels faster than nicked DNA, the relaxed DNA travels the most slowly through an agarose gel during electrophoresis.

2.10.1   Plasmid DNA Precipitation

PBR 322 Plasmid DNA was purchased from Thermo Fisher Scientific and stored in the buffer with 10 mM Tris-HCl and 1mM EDTA. The plasmid need to be precipitated to remove the chelating agent, EDTA, completely.

The pBR 322 supercoiled plasmid DNA was transferred to the RNase/DNase free 1.5 ml tube and then 20 μl of 3M Sodium Acetate buffer was added to the tube. After adding another 500 μl of cold 100% ethanol, the tube was placed in -20 °C freezer for one hour. The plasmid DNA

was centrifuged for 15 minutes at the highest speed (13000 rpm) in a 4°C. The supernatant was removed as much as possible and 250 µl of cold 70% ethanol was added. The plasmid was centrifuged again for 5 minutes in a 4 °C centrifuge at maximum speed. The supernatant was discarded completely. The remaining ethanol was evaporated by using SpeedVac for 10 min. The plasmid DNA pellet was resuspended in 100 µl of DNase/RNase free water. The stock concentration of plasmid DNA was 1 µg/µl and stored in -20°C freezer.

2.10.2   Plasmid Strand Break Assay

PBR322 plasmid was diluted with DNase/RNase free water to 0.2 µg/µl. Different concentrations of particles were prepared for treatment. 5 µl of plasmid DNA was incubated with 5 µl of treatment at room temperature in dark (avoid UV damage of plasmid).

After 12 hours incubation, the gel was prepared with 1 g agarose in 100 ml 1x TBE buffer (0.5M EDTA, Tris Base, Boric Acid), adding 1 µl of gel red. After the gel cooled down, the samples were added. Each sample was mixed with 1 µl of 10x blue juice gel loading buffer and 10 µl of sample was loaded into the gel. Gel electrophoresis was run at 60V for 2 hours with 1x TBE buffer. The gel was visualized. The strand breaks were able to be quantified using BioRad QuantityOne software (Bio-Rad, Hercules, CA) by calculating the proportion of supercoiled plasmid DNA remaining of each sample compared to the control.

3 Effects of Particulate Matter and Diesel Particles on Fibrin Clot Structure

3.1 Introduction

PM has been associated with cardiovascular diseases in many epidemiological studies. Some studies have shown air pollution is associated with increased risks of cardiovascular diseases, such as myocardial infarction, deep vein thrombosis and coronary artery diseases (Franchini and Mannucci, 2007; Langrish et al., 2012; Newby et al., 2014). An epidemiological study from Kloog et al. investigated the short-term and long-term $PM_{2.5}$ exposure effects, the results indicated that every 10 µg/m^3 of $PM_{2.5}$ caused 0.63% (95% CI = 0.03%--1.25%) increase in DVT admissions in short-term exposure and 6.98% (95% CI = 5.65%--8.33%) in long-term exposure. In terms of the pulmonary embolism, 0.38% (95% CI = −0.68%--1.25%) and 2.67% (95% CI = 5.65%--8.33%) increased risks were induced by $PM_{2.5}$ short- and long-term exposure respectively (Kloog et al., 2015). Some studies also confirmed that the alterations in fibrin clot structure, its mechanical properties and resistance to lysis were correlated with different cardiovascular diseases and diseases of both arterial and venous thrombosis. Altered fibrin clot structure with compact, highly branched networks, reduced permeability and prolonged lysis time has been associated with several thromboembolic events, e.g. ischemic stroke and venous thrombosis. The patients with those CVD had altered fibrin clot structure with greater number of fibres and more compact arrangement fibre network (Hooper et al., 2012; Undas and Ariens, 2011; Weisel, 2007). However, the underpinning mechanisms were still unclear. Therefore, in view of the association between exposure to particulate matter and thrombosis,

and of the association between thrombosis and abnormal fibrin clot structure, the aim of this study was to investigate whether particulate matter and diesel particles could induce fibrin clot structure alteration *in vitro*. Normal pooled plasma samples and purified fibrinogen samples were used as *in vitro* models to detect the effects of PM.

3.2   Methods

PM_{10} (SRM 2787) and diesel particles (SRM 2975) was purchased from the National Institute of Standard and Technology (NIST). PM_{10} was collected from an air intake filtration system of a major exhibition centre in Prague, Czech Republic, and generally represents the atmospheric particulate matter obtained from an urban area, which contains polycyclic aromatic hydrocarbons (PAHs), nitro-substituted PAHs (nitro-PAHs), polybrominated diphenyl ether (PBDE) congeners, hexabromocyclododecane (HBCD) isomers, sugars, polychlorinated dibenzo-*p*-dioxin (PCDD) and dibenzofuran (PCDF) congeners, inorganic constituents, and particles-size characteristics in atmospheric particulate material. Total diesel particles was collected from an industrial diesel-powered forklift and contained PAHs and nitro-PAHs in diesel particulate matter.

Both particles were diluted with double distilled water, with a stock concentration of PM_{10} of 1 µg/ml. Both particles were then diluted to 1 µg/ml and centrifuged for 30 min at maximum speed, and then filtered through a 0.2 µm membrane filter respectively. The diameters of the filtered particles were less than 0.2 µm. The mass fraction of $PM_{0.2}$ is 30% of the PM_{10}. And filtered diesel particles is 35% of the total diesel particles.

Five concentrations of particle suspension were used in the experiments; 50 µg/ml, 10 µg/ml, 1 µg/ml, 0.1 µg/ml and 0.01 µg/ml. Different concentrations of PM and diesel particles were added to the normal pooled plasma and fibrinogen samples, respectively. Three methods, turbidity assay, turbidity-lysis assay and laser scanning confocal microscope assay, were used to analyse the fibrin clot structure. The details of the methods were as described in chapter 2.

3.3   Results

3.3.1   Turbidity Assay

The results of the turbidity assay are shown in the following figure (Fig. 3-1 and 3-2). The four types of particles used in experiments in which fibrin clots were formed with 1) normal pooled plasma and 2) purified fibrinogen.

Normal Pooled Plasma Samples

Clots were formed from normal pooled plasma samples in the presence of particles. Compared to the control, the clots formed with particles had no significantly higher absorbance. But, there was a trend that as the concentrations of particles increased, the maximum OD values increased as well (Fig. 3-1).
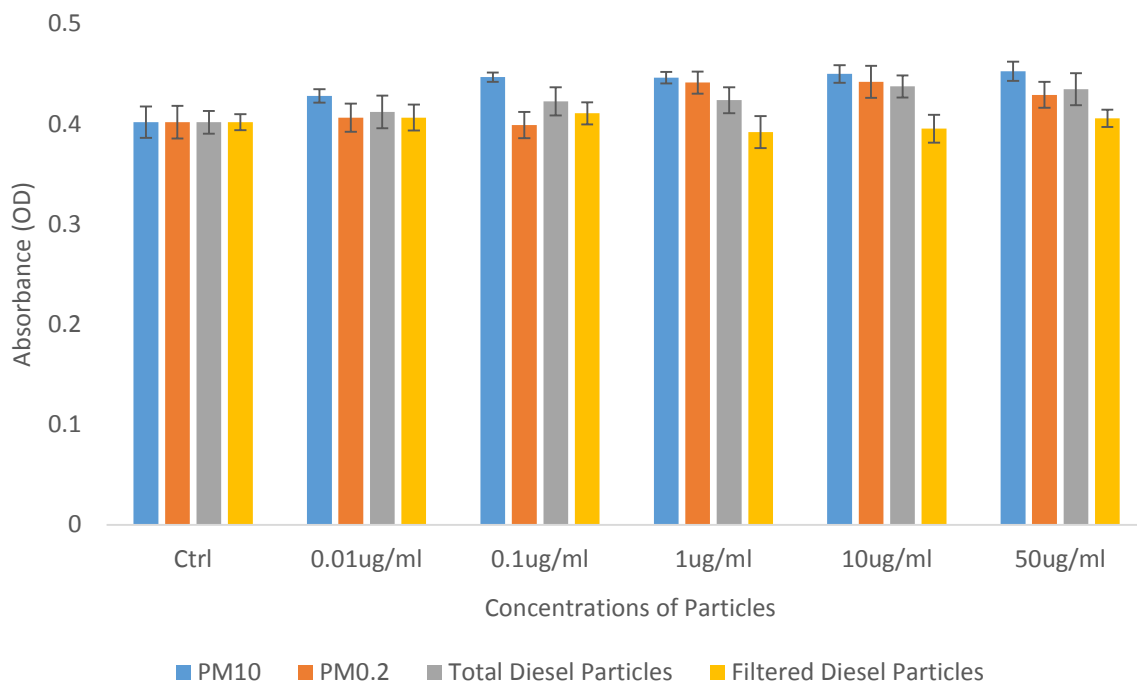
Figure 3-1. Turbidity Assay -- Maximum Absorbance of Plasma Samples Exposed to Different Concentrations of Particles (n=5)

The normal pooled plasma samples were mixed with particle suspension from 0 to 50 μg/ml. The final concentrations of thrombin and $CaCl_2$ were 0.1 U/ml and 5 mM respectively. The maximum absorbance of the clots formed with different concentrations of particles were shown in the figure.

Fibrinogen Samples

In terms of the fibrinogen samples, after the incubation with increased concentrations of PM_{10}, there were no significant differences compared to controls. The total diesel particles showed similar results as PM_{10}. However, for the $PM_{0.2}$ and filtered diesel particles, the maximum fluorescence intensity of the clots showed no changes, even after treatment with 50 μg/ml of particles (Fig. 3-2)
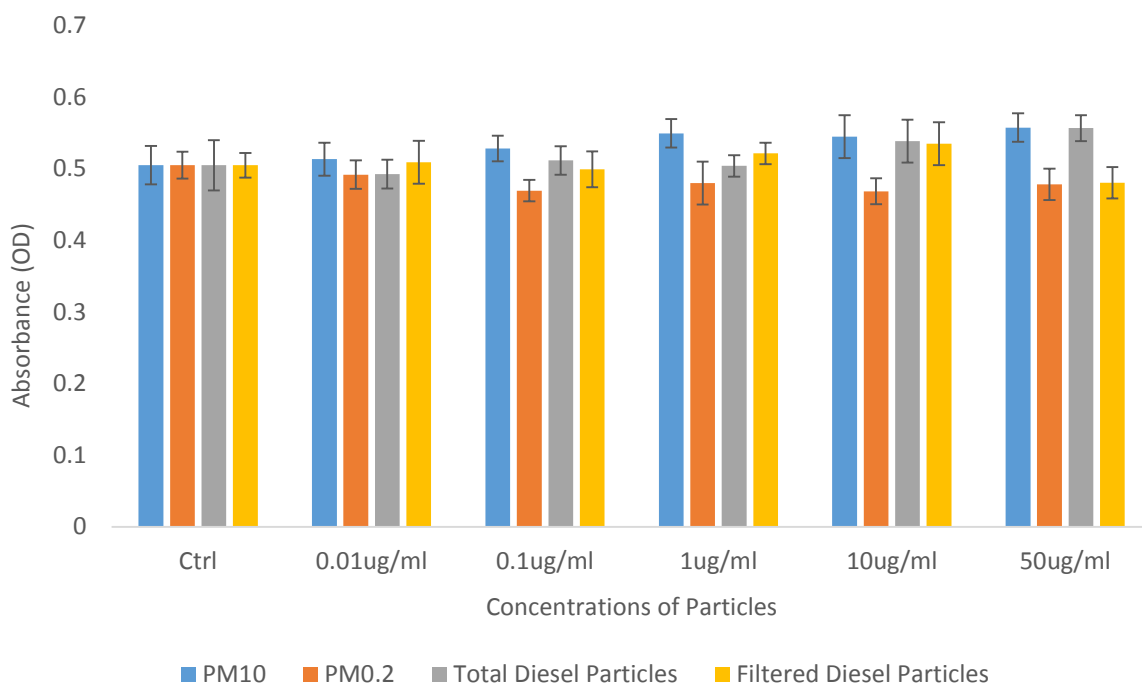
Figure 3-2. Turbidity Assay -- Maximum Absorbance of Fibrinogen Samples Exposed to Different Concentrations of Particles (n=5)

The purified fibrinogen samples were mixed with particle suspension from 0 to 50 µg/ml. The final concentrations of fibrinogen, thrombin and $CaCl_2$ were 1 mg/ml, 0.1 U/ml and 5 mM respectively. The maximum absorbance of the clots formed with different concentrations of particles were shown in the figure.

3.3.2   Turbidity Lysis Assay

Normal Pooled Plasma Samples

In the presence of particles, as the concentrations of particles increased, the $t_{50\%}$ was increased in a dose-dependent manner. Clot lysis time was the time in which absorbance decreased by 50% of the peak value ($t_{50\%}$) (Undas et al., 2014). Higher concentration of particles also had higher OD value and longer $t_{50\%}$. Compared to control, $t_{50\%}$ were significantly

longer at 10 µg/ml of PM_{10} and total diesel particles. $PM_{0.2}$ and filtered diesel particles only caused statistically longer $t_{50\%}$ at 50 µg/ml which were 13.8 and 14.3 min. The results indicated that fibres formed in the presence of particles, especially at the high concentrations, were much less sensitive to fibrinolysis compared to control.
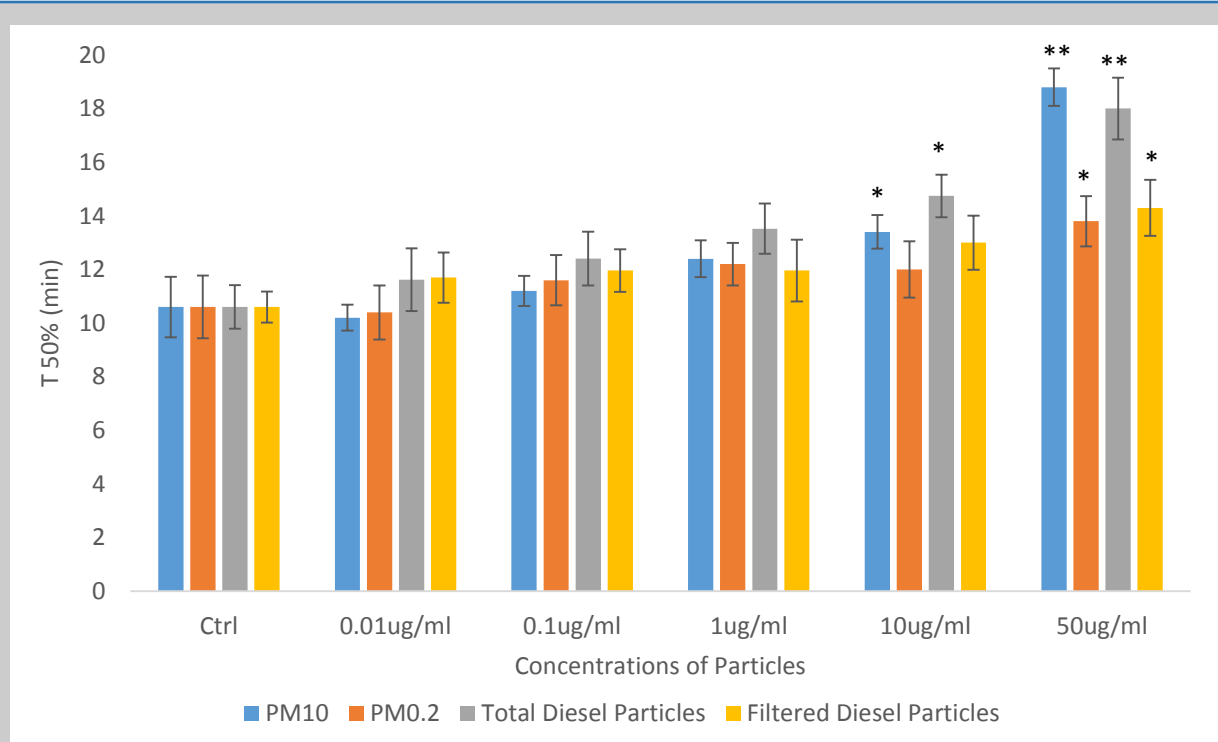
Figure 3-3. Turbidity Lysis Assay – $T_{50\%}$ of Normal Pooled Plasma Samples Exposed to Different Concentrations of Particles (n=3)

*p<0.05; **p<0.001

The clot lysis time was shown based on the concentrations and particle types. The final concentrations of tPA, thrombin and $CaCl_2$ were 0.1 µg/ml, 0.1 U/ml and 5 mM respectively. As the concentrations of particles increased, the $T_{50\%}$ was increased in a dose dependent manner.

Fibrinogen Samples

In terms of the fibrinogen samples, $t_{50\%}$ had no significantly difference between control and high concentrations of particles. The clot lysis time was similar and around 10 to 12 minutes.
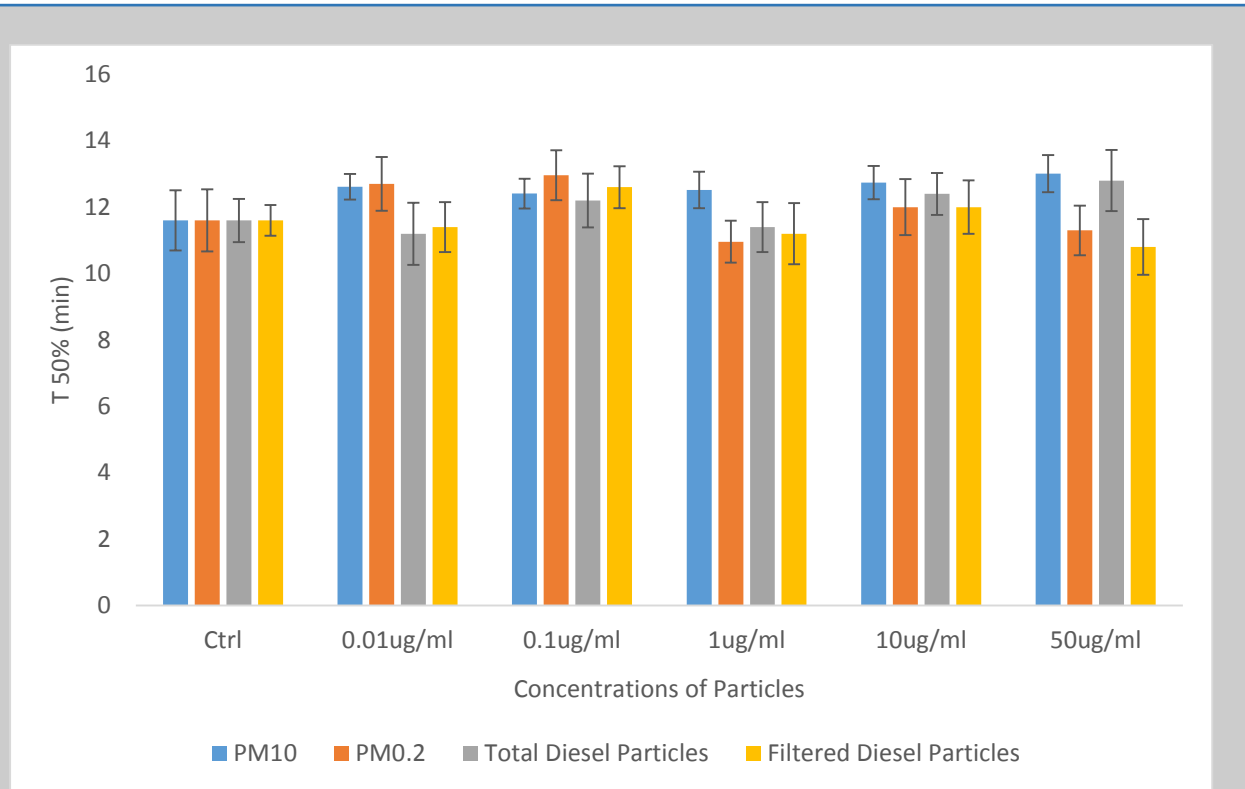
Figure 3-4. Turbidity Lysis Assay – $T_{50\%}$ of Purified Fibrinogen Samples Exposed to Different Concentrations of Particles (n=3)

The clot lysis time was shown based on the concentrations and particle types. The final concentrations of fibrinogen, plasminogen, tPA, thrombin and $CaCl_2$ were 1 mg/ml, 0.25 μM, 0.1 μg/ml, 0.1 U/ml and 5 mM respectively. As the concentrations of particles increased, the $T_{50\%}$ was increased in a dose dependent manner.

3.3.3 Laser Scanning Confocal Microscopy

Normal Pooled Plasma Samples

Fully hydrated fibrin clot structure was analysed under the laser scanning confocal microscope. The four kinds of particles were incubated with plasma samples and the clots formed with 0.1 U/ml of thrombin and 5 mM $CaCl_2$. Fig 3-5 to 3-8 represents the fibrin clot structure of plasma samples with different concentrations of different particles.

Coarse particulate matter were added to the normal pooled plasma samples. The effects of different concentrations of PM_{10} after clots formed from plasma samples were shown in the figures below. Six different concentrations of PM_{10} were incubated with the plasma samples. From 0 µg/ml to 50 µg/ml of PM_{10} (Fig 3-5), the clot structure showed similar fibrin clot structure with similar fibre numbers per µm. Compared to the control, there were no differences after incubation with PM_{10}. The same concentrations of $PM_{0.2}$ were incubated with plasma samples (Fig 3-6). The figures showed fibrin clots formed from plasma samples were similar. The average fibre numbers per um were between 3.10 and 3.43 after treatment with different concentrations of $PM_{0.2}$.

In the normal pooled plasma samples, total diesel particles had almost no effects on fibrin clot structure. Compared to control, 50 µg/ml of total diesel particles lead to slightly denser clot formation but there was no significantly difference (Fig 3-7). In figure 3-8, filtered diesel particles also had no significant effects on alteration of fibrin clot structure formed from normal pooled plasma samples. From 0 µg/ml to 50 µg/ml of filtered diesel particles, the number of fibres was similar.

Fig 3-9 shows that fibre numbers per μm of the clots formed from plasma samples after exposure to different concentrations of particle suspensions. Compared to the control, fibre numbers of the clots with all these four different particles had no difference even at the highest concentration of 50 μg/ml. These four particles did not cause significantly denser fibrin clot structure in the plasma samples.

Control   0.01 μg/ml of PM_{10}

0.1 μg/ml of PM_{10} 1 μg/ml of PM_{10}

10 μg/ml of PM_{10} 50 μg/ml of PM_{10}
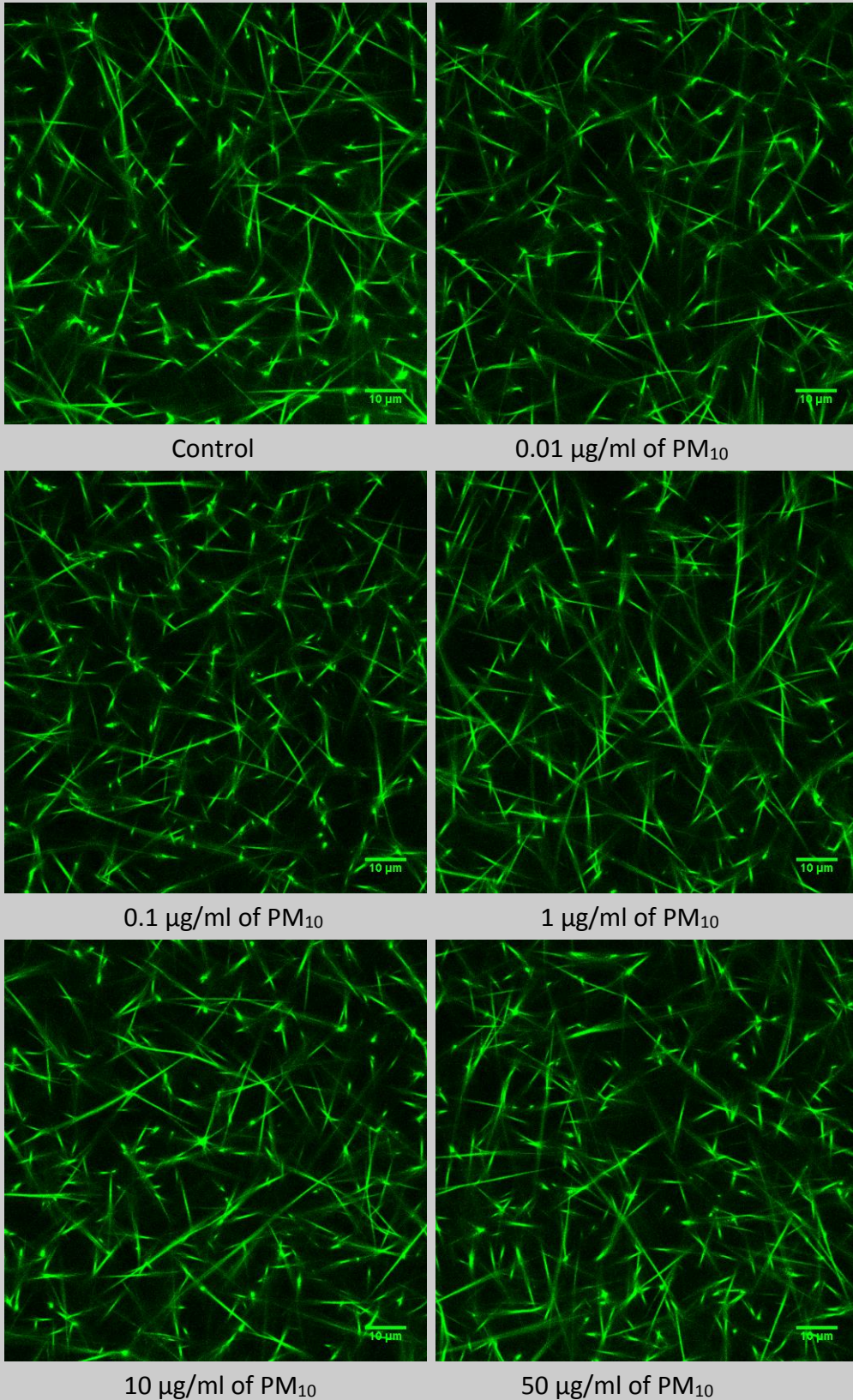
Figure 3-5. LSCM--Effects of PM_{10} on Plasma Samples

The structure of clots formed from plasma samples with PM_{10} from 0 to 50 μg/ml.
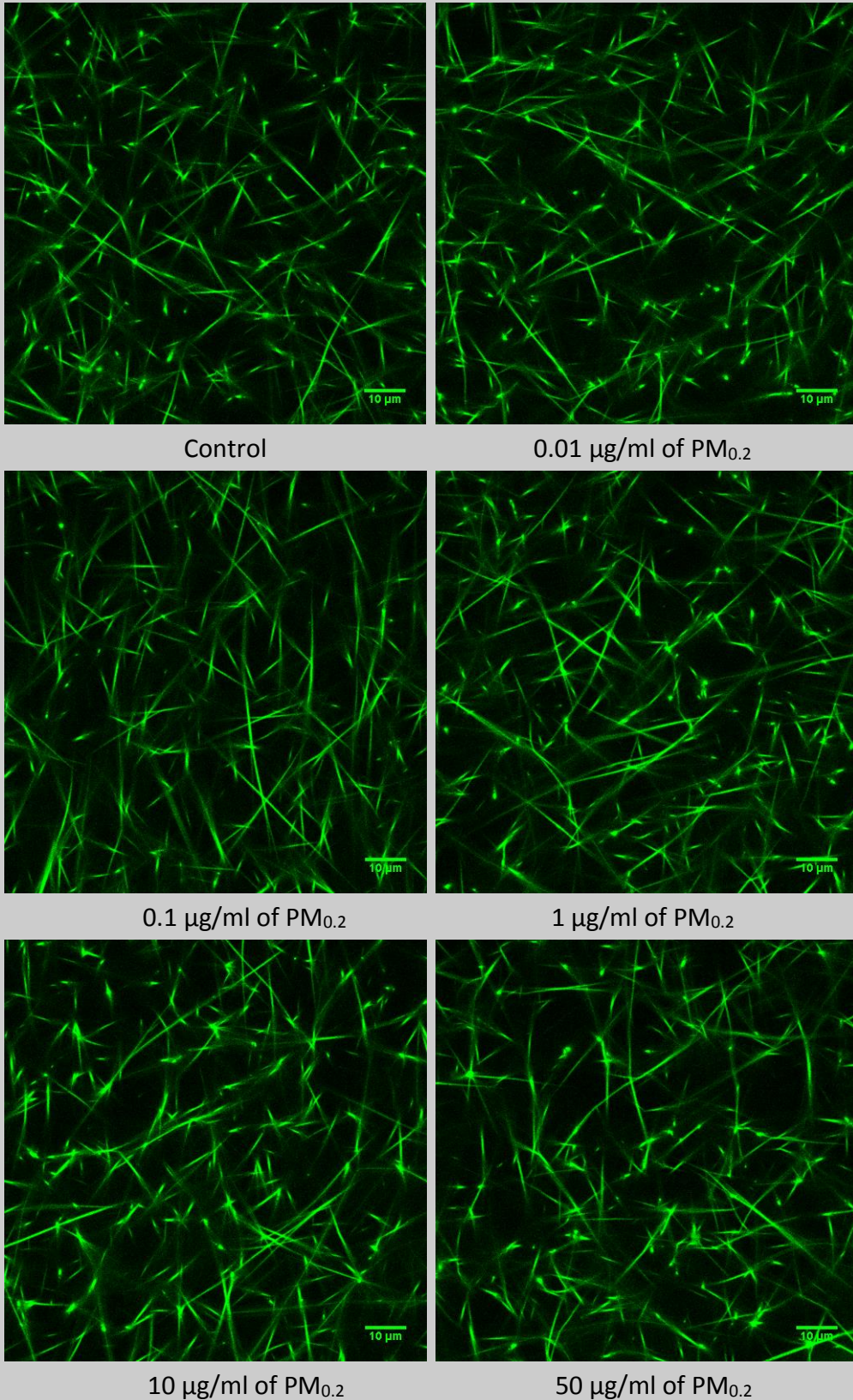
Figure 3-6. LSCM--Effects of PM$_{0.2}$ on Plasma Samples

The structure of clots formed from plasma samples with PM$_{0.2}$ from 0 to 50 μg/ml.

Control

0.01 µg/ml of Total Diesel Particles

0.1 µg/ml of Total Diesel Particles

1 µg/ml of Total Diesel Particles

10 µg/ml of Total Diesel Particles

50 µg/ml of Total Diesel Particles
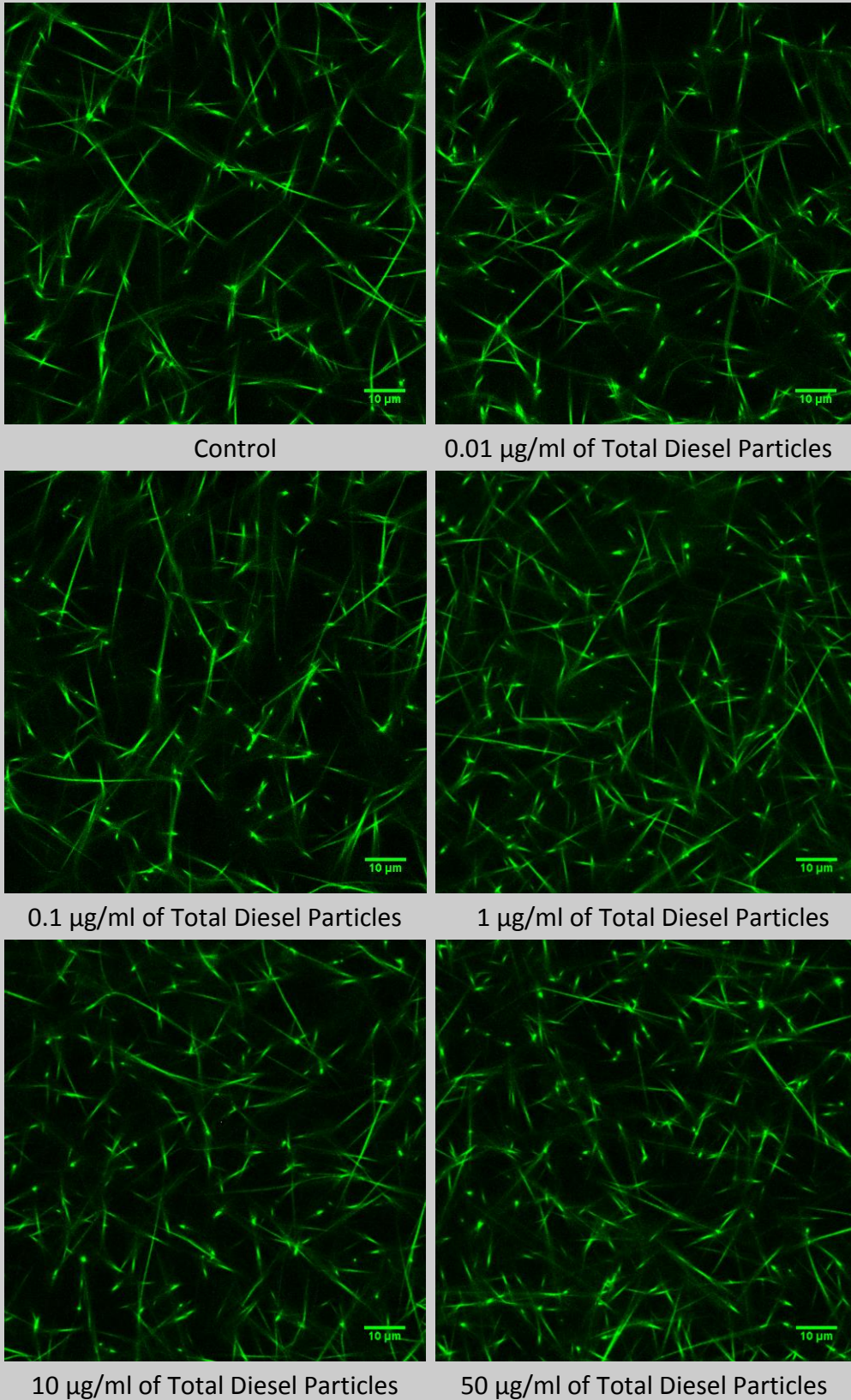
Figure 3-7. LSCM—Effects of Total Diesel Particle on Plasma

The structure of clots formed from plasma with total diesel particles from 0 to 50 µg/ml.

Control

0.01µg/ml of Filtered Diesel Particles

0.1µg/ml of Diesel Particles

1µg/ml of Diesel Particles

10µg/ml of Diesel Particles

50µg/ml of Diesel Particles
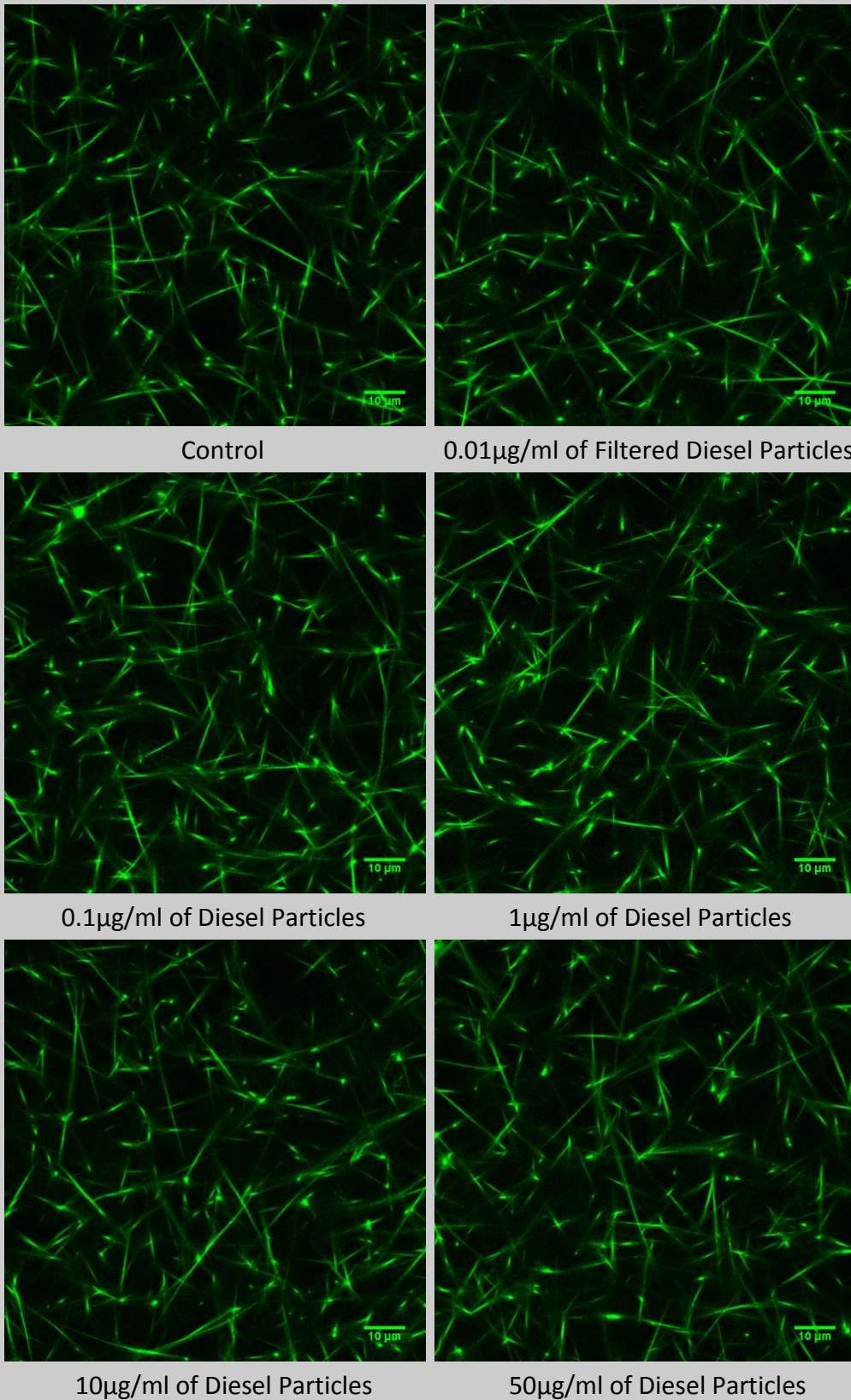
Figure 3-8. LSCM—Effects of Filtered Diesel Particle on Plasma

The structure of clots formed from plasma with total diesel particles from 0 to 50 µg/ml.
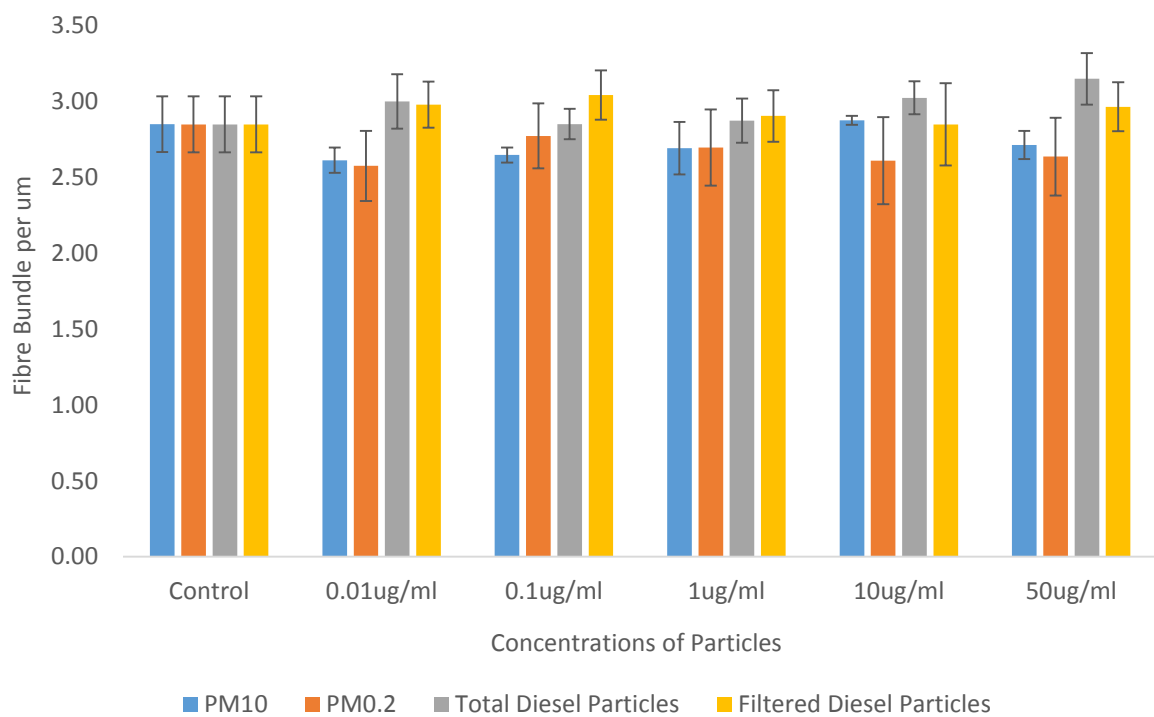
Figure 3-9. Fibre Bundles of Fibrin Clots Formed from Plasma Samples with Different Concentrations of Particles (n=9)

The clots formed from plasma samples with particles from 0 to 50 µg/ml was shown. The final concentrations of thrombin, $CaCl_2$ and FITC were 0.1 U/ml, 5 mM and 50 µg/ml respectively. There were no significant differences in the fibre numbers between the clots with and without particles.

Purified Fibrinogen Samples

Compared to fibrin clots formed from plasma samples, purified fibrinogen samples had looser clot structure with a lower number of fibres per µm (Fig 3-14). To form the clots, the same concentrations of thrombin and $CaCl_2$ were used in plasma and fibrinogen samples. In the normal pooled plasma, there are coagulation factors which may improve the thrombin formation and lead to more fibres produced compared to purified fibrinogen system. The

fibre number of the control was around 2 per µm in the fibrinogen samples, however, in the plasma samples, the fibre number was approximately 3 per µm. In the fibrinogen samples, from 0.1 µ/ml to 50 µg/ml of the particles, there were no significant differences from control.

For the purified fibrinogen samples, same concentrations of PM_{10} were used. In the following figures, it can be seen that there were no significantly differences in the fibrin clot structure formed with or without participation of $PM_{10.}$ The fibre numbers per µm were around 2 (Fig 3-10). Similar as the PM_{10} results, when the clots were formed with $PM_{0.2}$, the clot structure was similar among different concentrations (Fig 3-11).

For the purified fibrinogen samples, the fibrin clot structure was not altered after adding different concentrations of total diesel particles compared to control. The fibre numbers were similar at low and high concentrations of total diesel particles (Fig 3-12). Figure 3-13 shows that filtered diesel particles added in the purified fibrinogen samples did not increased or reduce the fibre numbers per µm compared to the control.

Control   0.01 µg/ml of PM_{10}

0.1 µg/ml of PM_{10} 1 µg/ml of PM_{10}

10 µg/ml of PM_{10} 50 µg/ml of PM_{10}
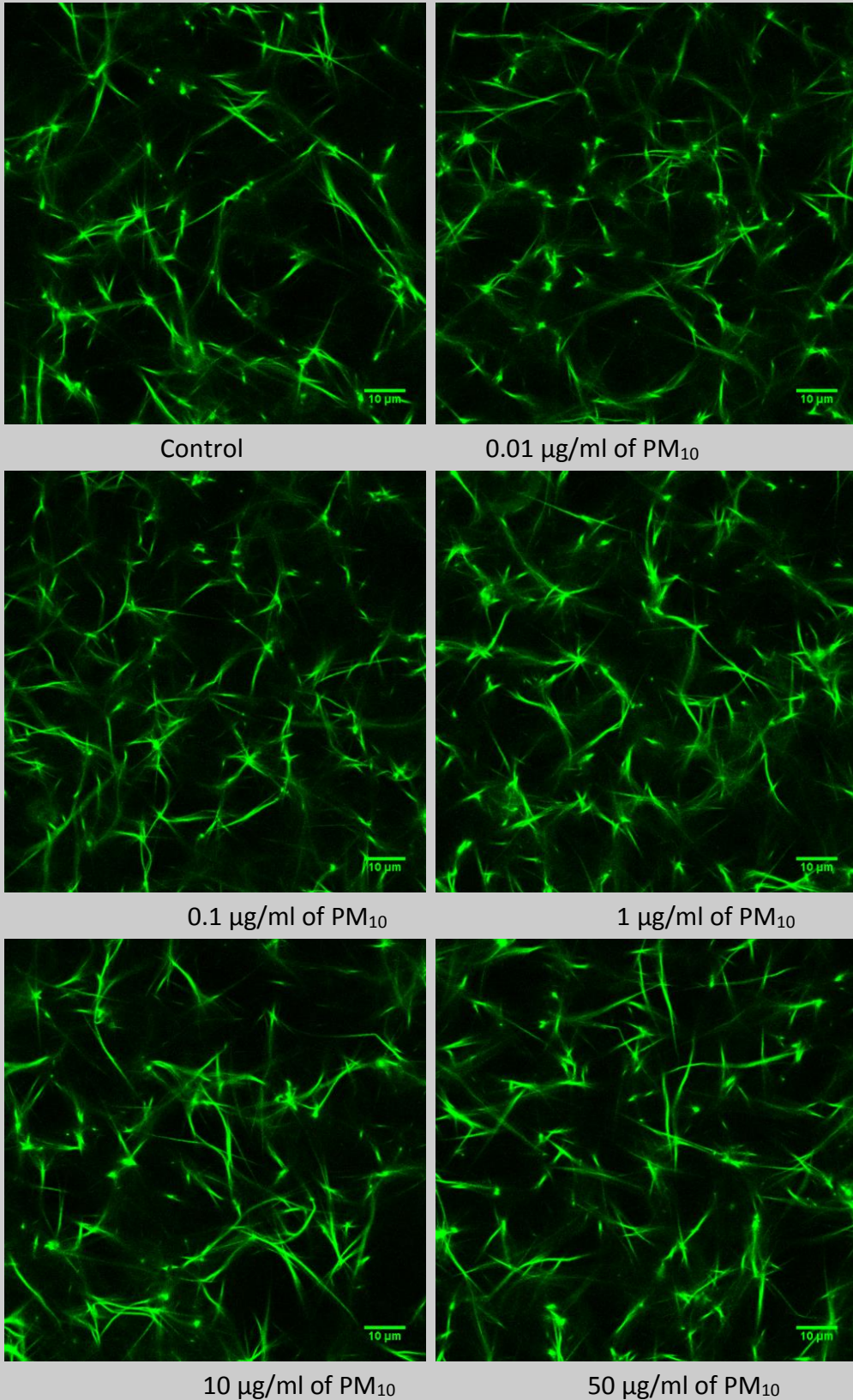
Figure 3-10. LSCM--PM_{10} Effects on Fibrinogen

The structure of clots formed from fibrinogen samples with PM_{10} from 0 to 50 µg/ml.

Control   0.01 µg/ml of $PM_{0.2}$

0.1 µg/ml of $PM_{0.2}$ 1 µg/ml of $PM_{0.2}$

10 µg/ml of $PM_{0.2}$ 50 µg/ml of $PM_{0.2}$
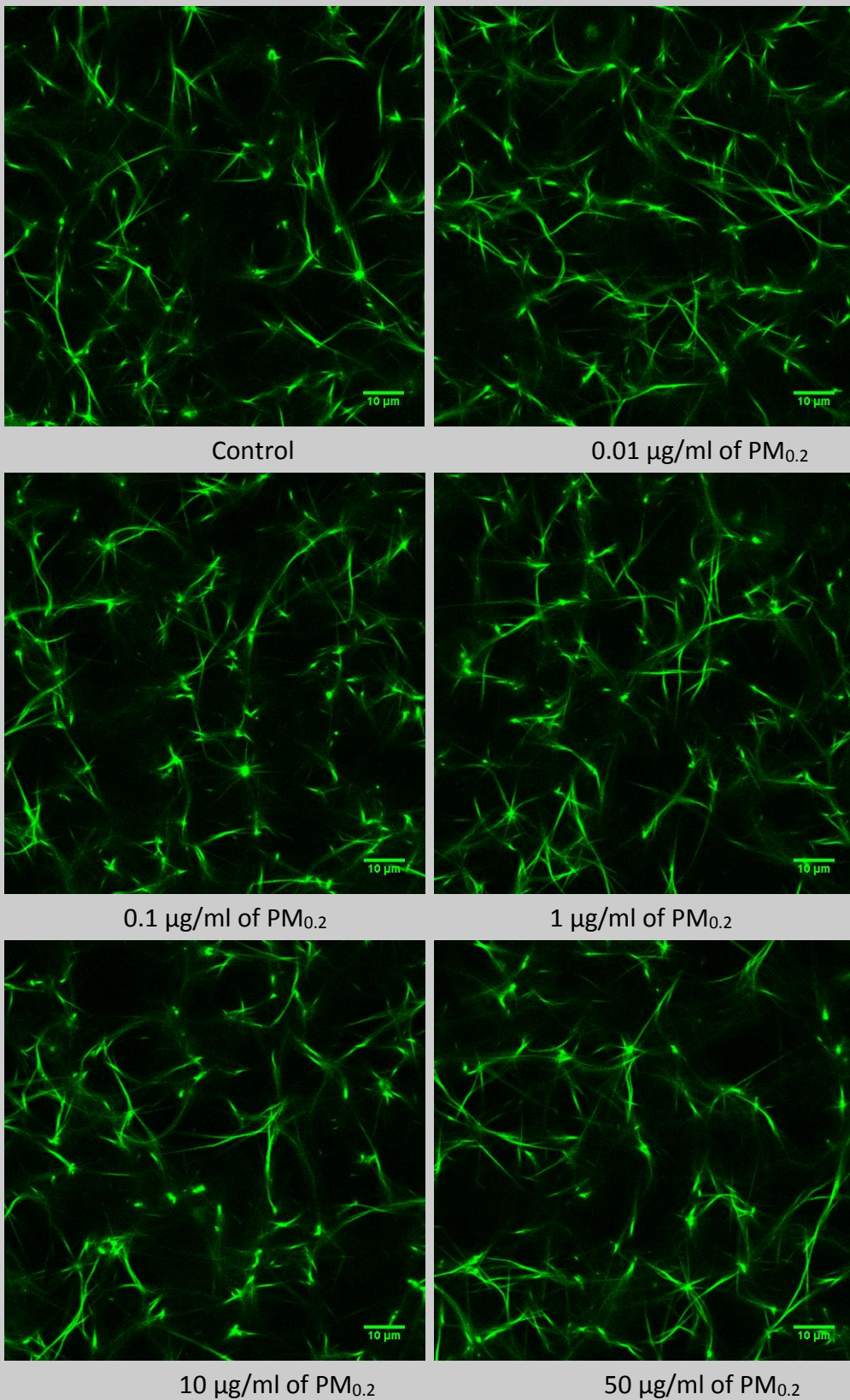
Figure 3-11. LSCM--$PM_{0.2}$ Effects on Fibrinogen

The structure of clots formed from fibrinogen samples with $PM_{0.2}$ from 0 to 50 µg/ml.

Control | 0.01 µg/ml of Total Diesel Particles

0.1 µg/ml of Total Diesel Particles | 1 µg/ml of Total Diesel Particles

10 µg/ml of Total Diesel Particles | 50 µg/ml of Total Diesel Particles
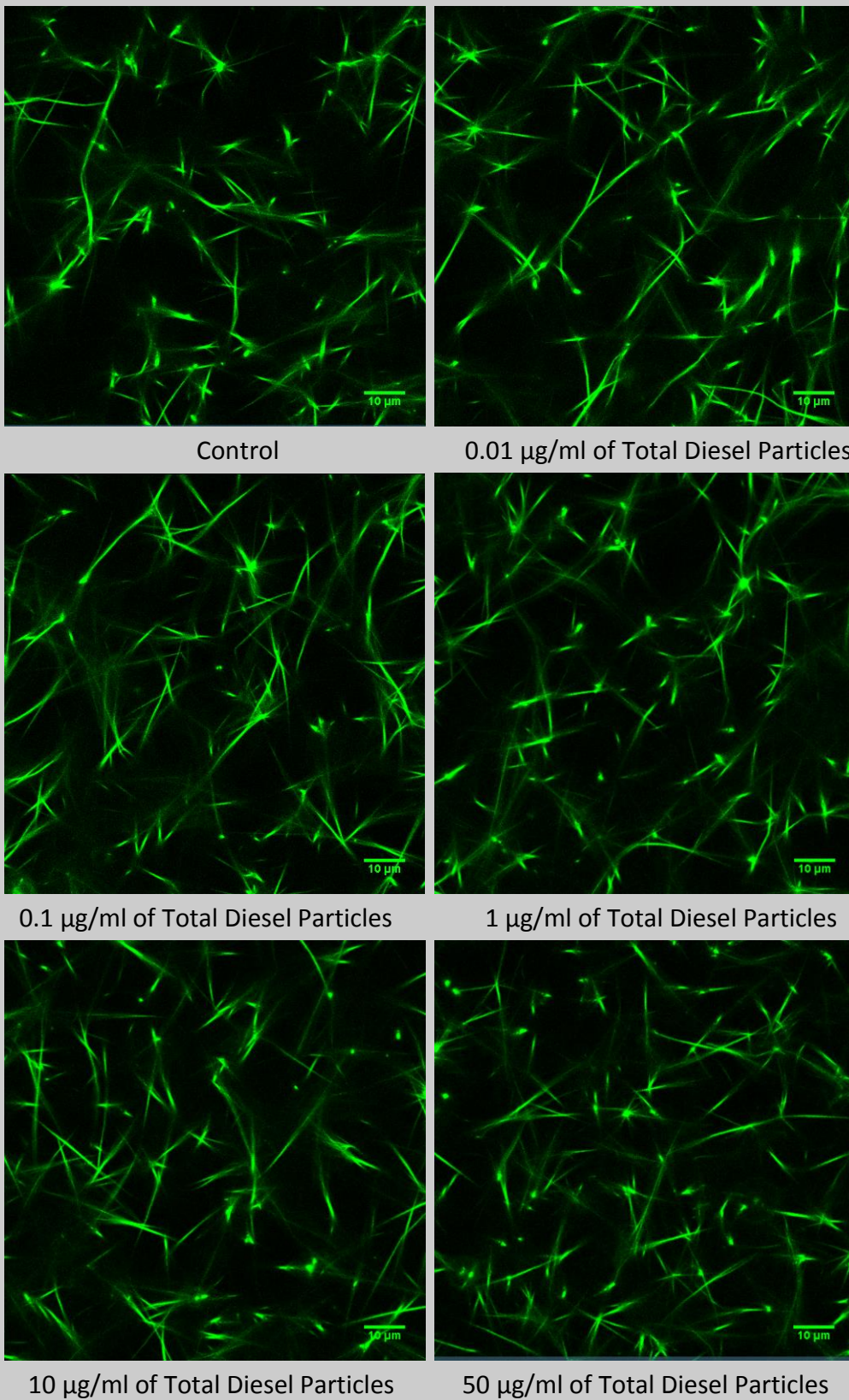
Figure 3-12. LSCM—Effects of Total Diesel Particle on Fibrinogen

The structure of clots formed from fibrinogen with total diesel particles from 0 to 50 µg/ml.

Control

0.01 µg/ml of Filtered Diesel Particles

0.1 µg/ml of Filtered Diesel Particles

1 µg/ml of Filtered Diesel Particles

10 µg/ml of Filtered Diesel Particles

50 µg/ml of Filtered Diesel Particles
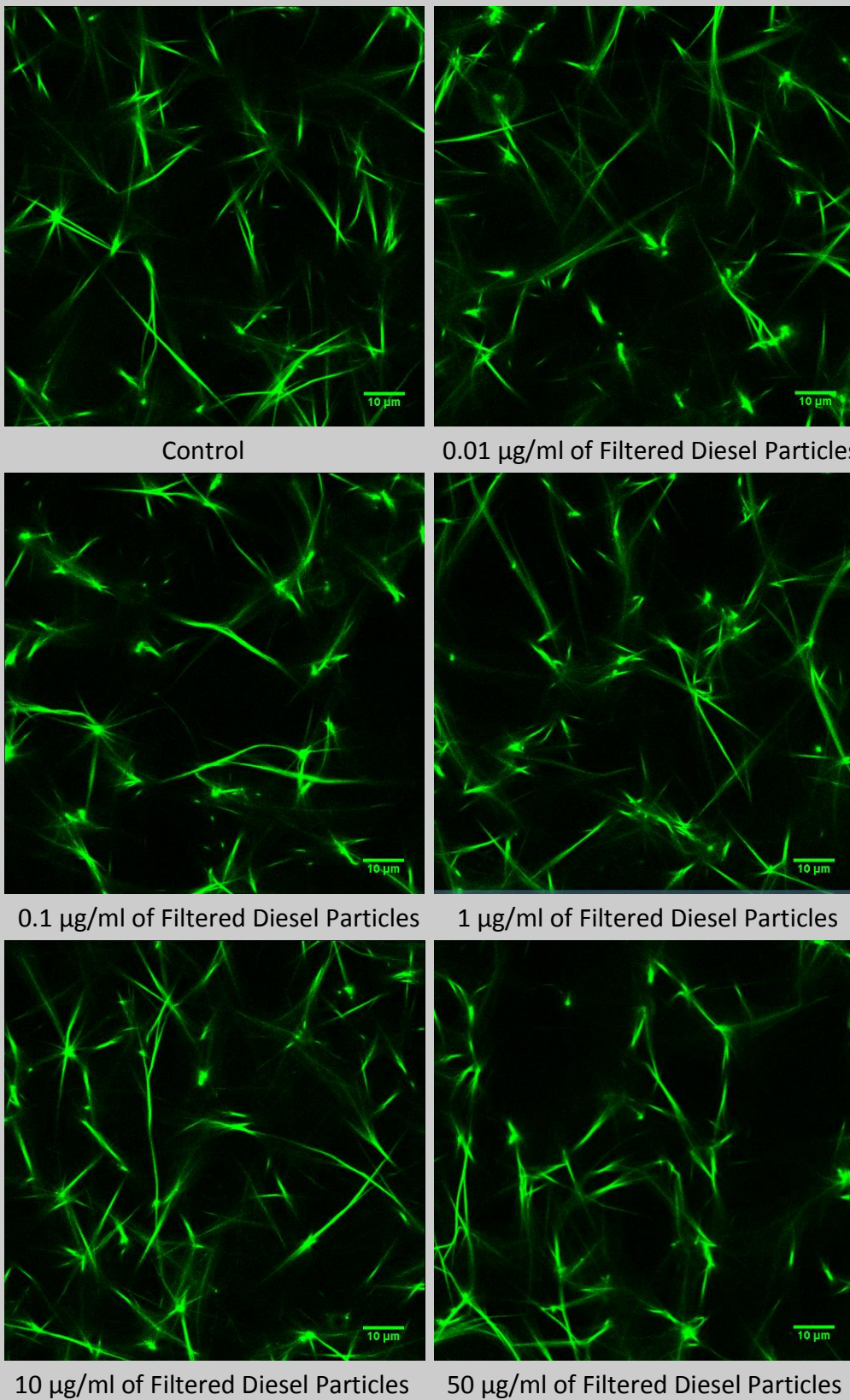
Figure 3-13. LSCM—Effects of Filtered Diesel Particle on Fibrinogen

The structure of clots formed from fibrinogen with filtered diesel particles from 0 to 50 µg/ml.
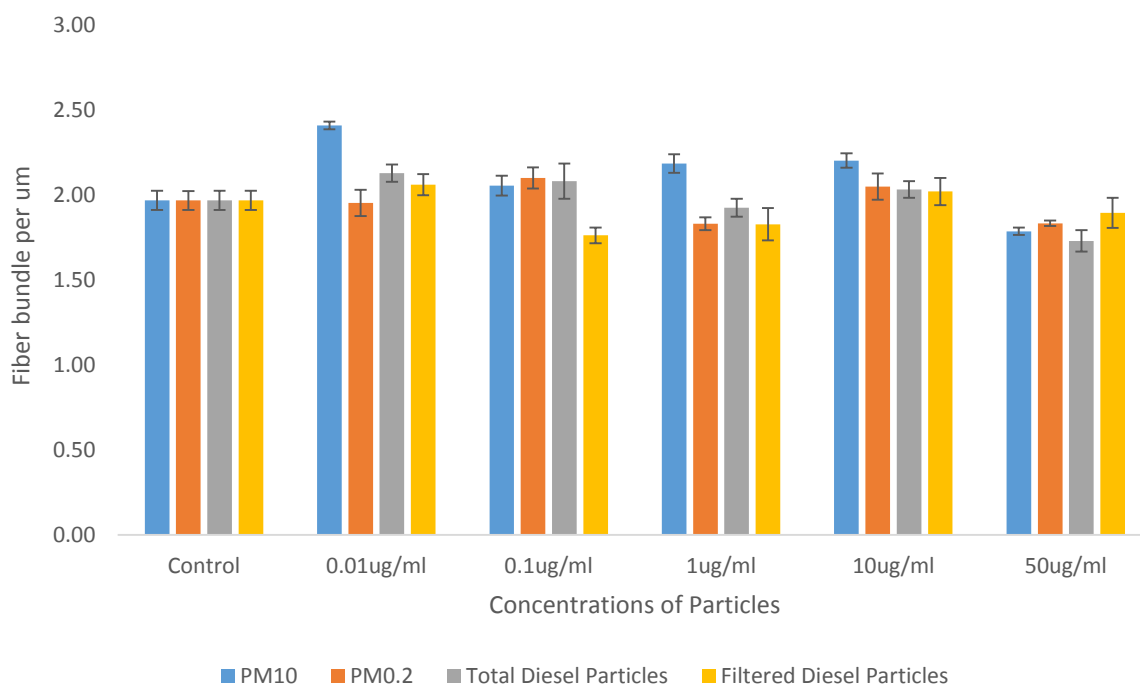
Figure 3-14. Fibre Bundles of Fibrin Clots Formed from Purified Fibrinogen Samples with Different Concentrations of Particles (n=9)

The number of fibres bundles per µm of the clots formed from purified fibrinogen samples with particles from 0 to 50 µg/ml was shown. The final concentrations of fibrinogen, thrombin, $CaCl_2$ and FITC were 1mg/ml, 0.1 U/ml, 5 mM and 50 µg/ml respectively. Figure 3-14 showed that there were no significant differences in the fibre bundles between the clots with and without particles.

3.4   Discussion

In this study, the effects of PM_{10}, $PM_{0.2}$, total diesel particles and filtered diesel particles on fibrin clot structure were investigated. The concentrations chosen were from 0.01 to 50 µg/ml which was different from the other study (Metassan et al., 2010a). In the realistic environment, the highest concentration was measuring 14,000 µg/m^3 (Davis et al., 2002)

which is equal to 0.014 µg/ml in H_2O. Also, as the people keep exposed to particulate matter, it is able to accumulate in the body and the concentrations will increase. Therefore, I chose the start concentration was 0.01 µg/ml and hypothesized that the highest concentration people may have was 50 µg/ml. Three methods were applied to study the effects of particles from air pollution, turbidity assay, turbidity lysis assay and laser scanning confocal microscopy in both normal pooled plasma and purified fibrinogen system. The experiments results from turbidity assay and LSCM assay showed that these four particles did not significantly alter fibrin clot structure formed from normal pooled plasma samples. But the clot lysis time was significantly longer as the concentrations of particles increased. The fibres formed from plasma were getting more resistance to fibrinolysis and $t_{50\%}$ were significantly longer at 50 µg/ml of these four particles compared to control. In terms of the purified fibrinogen system, the clots had similar structure as control even at the highest concentration 50 µg/ml of those particles. In summary, PM_{10} and total diesel particles had more effects on the fibrin clot structure alterations compared to $PM_{0.2}$ and filtered diesel particles. This was because both filtered particles were extracted from the total particles, the mass fraction of $PM_{0.2}$ and filtered diesel particles were only 30% and 35% of PM_{10} and total diesel particles which represented the percentages of filtered particles occupied in the total particles realistically. In other words, at the concentration 10 µg/ml of PM_{10} and total diesel particles, the concentrations of $PM_{0.2}$ and filtered diesel particles were 3 and 3.5 µg/ml respectively.

Fibrin clot structure has been associated with several thromboembolic diseases (Undas and Ariëns, 2011). A large number of case-control studies have reported the associations. Undas et al. (2008) investigated the fibrin clot structure of 40 patients with acute coronary syndromes and 40 controls. The results showed that the patients had faster fibrin

polymerization (p=0.008) and prolonged fibrinolysis time (p<0.001) than controls (Undas et al., 2008). Undas and her collages also measured the fibrin clot structure and functions of the patients with idiopathic venous thromboembolism and their first-degree relatives. The ex vivo plasma was used to form the clots. Compared to healthy controls, those patients with DVT and their relatives were characterized by lower clot permeability (p<0.001), lower compaction (p<0.001), higher maximum clot absorbency (p<0.001), and prolonged clot lysis time (p < 0.001) (Undas et al., 2009). These studies indicated that denser fibrin clot structure with prolong clot lysis time may represent an emerging risk factor for arterial and venous thromboembolism.

A study from the Leeds laboratory showed that PM was able to alter fibrin clot structure and functions in human plasma and purified systems (Metassan et al., 2010a). The concentrations used in the study from Metassan *et al.* were 100 and 200 μg/ml which were higher than the concentrations used in this study. But in this study, the particle did not significantly alter fibrin clot structure. The concentrations used in this study were lower (0.01 μg/ml to 50 μg/ml) compared to the concentrations in the study of Metassan et al (100 μg/ml to 200 μg/ml). There was still a trend that as the concentrations of particles increased, the clot structure was getting denser in a dose-dependent manner. In addition, the clot lysis time were significantly longer compared to control. These results showed that particles from air pollution caused altered fibrin clot structure which possessed similar properties as the clots formed from the plasma of thromboembolic patients. Therefore, air pollution may increase the risks of thrombosis.

The mechanisms of how air pollution increases the risk of thrombosis are not clear. So, for the further investigation, more studies were performed.

4 Italian Cohort Study of Long-term Air Particulate Matter Exposure

4.1 Introduction

Exposure to air pollution is associated with adverse effects on the pulmonary and cardiovascular systems, as reviewed in chapter 1. In particulate, the PM in urban air pollution has been associated with cardiovascular mortality and morbidity, as discussed.

A range of possible mechanisms by which PM may damage the cardiovascular system have been proposed, including atherogenesis and thrombosis as a result of activation of inflammation, oxidative stress, endothelial dysfunction and increased levels of circulating coagulation proteins (eg. factor VIII [FVIII], VWF and fibrinogen) (Baccarelli et al., 2007a, 2007b; Vermylen et al., 2005). Exposure to air pollution particles induces pulmonary inflammation with release of cytokines that are capable of mediating acute-phase proteins and leading to hypercoagulability (Baccarelli et al., 2007a; Esmon, 2004; Seaton et al., 1999). However, the mechanisms underpinning the increased risk of thrombosis after exposure to ambient air pollution are still poorly understood.

In view of these associations between thrombosis and fibrin structure, the effects of particulate matter on fibrin clot structure have previously been investigated in this laboratory. It was found that diesel PM caused changes in fibrin clot structure and function in clots formed from both purified fibrinogen and from human plasma (Metassan et al., 2010a). However, no changes in fibrin clot structure were observed in clots formed from plasma taken

from healthy individuals after 2 hours exposure to PM while performing moderate exercise (Metassan et al., 2010b). The exposure in the latter study was of short duration, so the possibility remained that fibrin clot structure could be affected by long-term exposure to high levels of air pollution, or that susceptible subjects, such as patients with thrombosis could respond differently to the healthy young subjects in the earlier study.

To test this possibility, a sub-study was based on samples from a large cohort study in the Lombardy Region of Italy (Baccarelli et al. 2007; Baccarelli et al. 2009; Baccarelli et al. 2008), which had reported that every 10 μg/m^3 elevation of PM_{10} exposure was associated with a 67% increase of DVT. The aim of this study was to determine the effects of PM_{10} on patient with DVT and healthy controls.

4.2   Methods

Stored plasma samples from an existing large epidemiological study in the Lombardy Region, North Italy (Baccarelli et al., 2007; Baccarelli et al., 2008; Baccarelli et al., 2007; Baccarelli et al., 2009) were used for this study. 224 subjects were randomly chosen from this study. The previous study examined the association between PM_{10} and the risk of deep vein thrombosis. The main result showed that every 10 μg/m^3 elevation of PM_{10} was associated with 67% increased risk of DVT. This sub-study was to investigate the fibrin clot structure alteration after exposure to different concentrations of PM_{10} by analysing the fibrin clot structure formed from the plasma samples of each subject.

4.2.1   Study Population

The study population of patients and controls has been previously described in detail (Baccarelli et al., 2007; Baccarelli et al., 2008; Baccarelli et al., 2007; Baccarelli et al., 2009). Briefly, patients from the Lombardy region, Northern Italy were referred to the Angelo Bianchi Bonomi Thrombosis Centre in Milan from January 1995 to September 2005 for a thrombophilia screening after a first episode of objectively confirmed lower-limb deep vein thrombosis with or without pulmonary embolism. Controls were healthy individuals, friends or partners of the patients referred to the same Thrombosis Centre, who were residents in the Lombardy region and volunteered to undergo thrombophilia screening. All patients and controls provided informed written consent and the duty was approved by the local ethics committee. General characteristics of patients and controls including age, BMI, gender, education, and smoking status, and fibrinogen and FVIII levels were provided by Angelo Bianchi Bonomi Thrombosis Centre. Methods for exposure assignment were previously described in detail (Baccarelli et al., 2008; Baccarelli et al., 2007). Hourly concentrations of PM_{10} were obtained from the Regional Environmental Protection Agency (ARPA Lombardia) which recorded the hourly air pollution data from January 1994 to September 2005 using monitors located at 53 different sites throughout the Lombardy region (Baccarelli et al. 2007).

4.2.2   Method

Three methods were used to analyse the fibrin clots structure formed from ex vivo plasma samples of the patients and controls, permeability assay, turbidity assay and laser scanning

confocal microscope assay. Permeability assay was applied to measure the average pore size of the fibrin clot structure formed from the plasma samples. Fibres arrangements in the clots can be detected through turbidity assay. Laser scanning confocal microscopy method provided a direct 3D visualisation of the clots. The details of each method were as described in chapter 2.

4.3 Results

There were significant correlations between maximum absorbance and the number of fibres ($r = 0.4$, $p < 0.001$), maximum absorbance and Ks ($r = -0.5$, $p < 0.001$), and number of fibres and Ks ($r = -0.5$, $p < 0.001$). Maximum absorbance and fibre number were both positively correlated with age, body mass index (BMI), fibrinogen concentration and plasma level of FVIII, whereas Ks was negatively correlated, indicating that with increasing age, BMI, fibrinogen concentrations and FVIII levels, the fibrin fibres grew thicker, and were more compactly woven in the three-dimensional clot network, and that the clot was less permeable. Except for Ks, both fibre thickness ($r = 0.1$, $p = 0.04$) and fibre number ($r = 0.2$, $p = 0.001$) were associated with PM_{10} concentrations.

	Maximum Absorbance		Fibre Number		Ks	
	Coefficient	P-value	Coefficient	P-value	Coefficient	P-value
Case	0.12	0.07	0.16	0.02	-0.12	0.25
Age (years)	0.23	0.001	0.24	<0.0001	-0.37	<0.0001
Male	0.09	0.18	0.07	0.30	-0. 17	0.12
Non-Smokers	-0.002	0.98	-0.08	0.32	0.06	0.60
BMI	0.33	<0.0001	0. 30	<0.0001	-0. 36	0.001
Fibrinogen (mg/dl)	0.70	<0.0001	0.26	<0.0001	-0. 45	<0.0001
Factor VIII (%)	0.22	0.00	0.17	0.02	-0.33	0.003
PM_{10} Concentration (μg/ml)	0.14	0.04	0.22	0.001	-0.03	0.76
Maximum Absorbance (mOD)	1.00		0.41	<0.0001	-0.51	<0.0001
Fibre Number (per μm)	0.41	<0.0001	1.00		-0. 48	<0.0001
Ks ($x10^{-10}$ cm^2)	-0.51	<0.0001	-0.48	<0.0001	1.00	

Table 4-1. Pearson's and Chi-Square Correlations of Clot Parameters to Other Variables

Correlations between continuous parameters were tested using Pearson's, and between clot structure and categorical variables (case, sex, and smoking) using Chi-Square analysis.
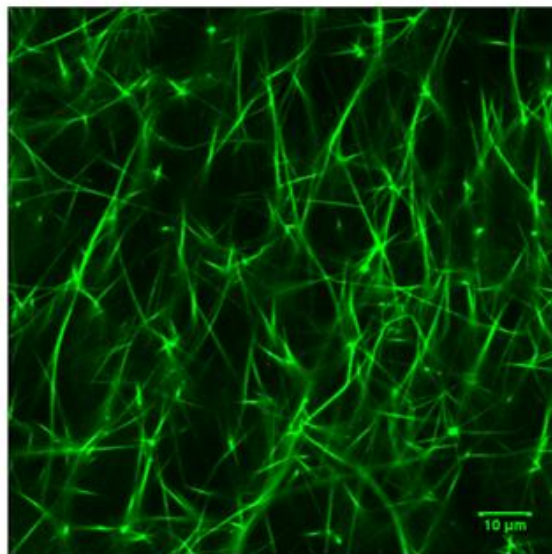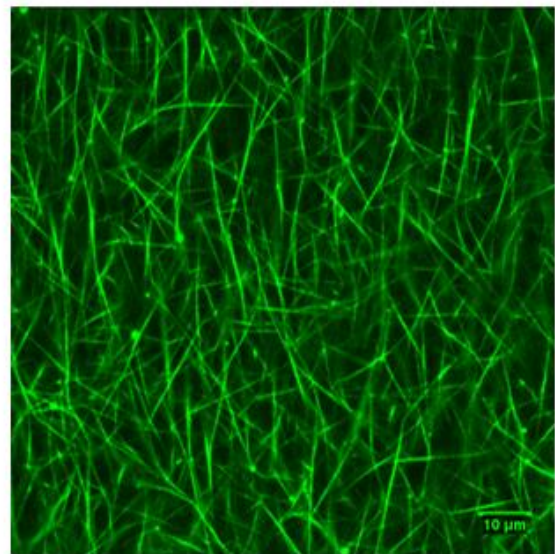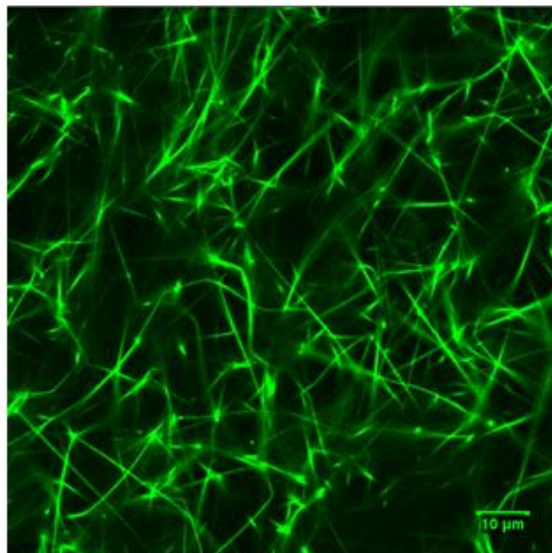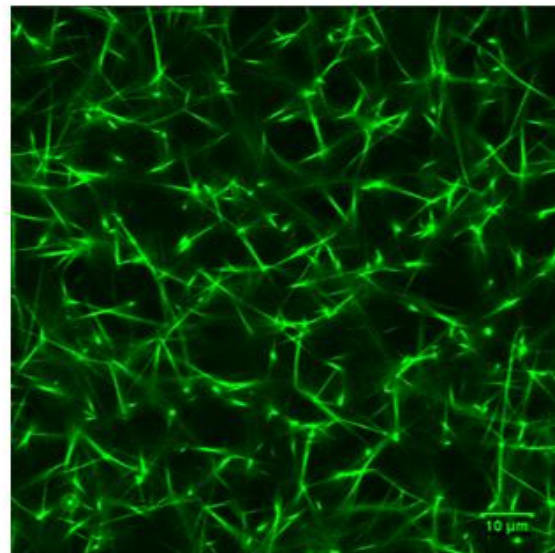
Figure 4-1. Representative fibrin clot structure formed from plasma samples of patients and controls

The fully hydrated fibrin clot were formed with the plasma samples from patients and healthy controls and visualized under laser scanning confocal microscope.

General characteristics, fibrinogen level, factor VIII, thrombophilia abnormalities and fibrin clot structure parameters of patients and controls are shown in Table 4-2. In terms of the general characteristics of these subjects, age was similar between patients and controls. But the BMI and gender were significantly different, the patients had higher BMI compared to healthy controls; and there were more males than females. Fibrinogen concentrations in patients plasma were slightly higher than those in healthy controls (p = 0.070). The patients with DVT had significantly higher FVIII plasma levels compared to controls (p < 0.001). There were more subjects with thrombophilia abnormalities in the patients group (p < 0.001). In terms of the clot structure, only fibre number was significantly different between patients and controls (p = 0.018). However, there was a tendency showed that patients possessed denser fibrin clot structure with thicker fibres, more number of fibres per clot area and less permeable clots compared to controls.

Patients exposed to high levels of air pollution showed higher concentrations of fibrinogen compared to those exposed to low levels, whereas thrombophilia factors did not differ between exposure groups (Table 4-3). We also compared the fibrin clot structure parameters by exposure levels in patients and controls. Patients in the high exposure group had more compactly arranged fibres and less permeable structure compared to those in the low exposure levels. However, in controls only plasma levels of coagulation FVIII were different between the two exposure groups (p = 0.029).

Table 4-4 shows logistic regression analysis of risk factors for DVT. The continuous data age, BMI, fibrinogen concentration, FVIII level were categorized into high and low groups, the cut-off points being 51.9 for age, 24.7 for BMI, 299.7 for fibrinogen, and 125.3 for FVIII,

respectively. The model showed that increased age, BMI and fibrinogen concentrations did not contribute to the development of DVT in this study. Male sex was a risk factor for DVT, as well as FVIII, thrombophilia abnormalities and high level of PM_{10}.

Variables	Patients Mean ±SD or percentage%	Controls Mean ±SD or percentage%	P-Value
Number of subjects	103	121	
Age (years)	53.7 ±14.7	50.4 ±13.9	0.085
Male %	48.5%	25.6%	<0.001
BMI	25.5 ±4.2	24.0 ±4.3	0.014
Non-Smokers %	81.0%	76.9%	0.584
Primary education or below %	70.9%	77.7%	0.187
Fibrinogen (mg/dl)	309.4 ±80.7	290.7 ±50.9	0.070
Factor VIII (%)	141.6 ±43.1	108.1 ±27.4	<0.001
Thrombophilia^ %	40.8%	14%	<0.001
Ks ($\times 10^{-10}$ cm^2)	28.8 ±8.8	31.4 ±12.2	0.248
Fibre Number (per µm)	22.5 ±3.5	21.3 ±3.8	0.018
Maximum Absorbance (mOD)	719.2 ±175.2	679.3 ±156.9	0.073

Table 4-2. Characteristics of patients with DVT and controls

^ Thrombophilia was classified as being positive for at least one of the following: factor V Leiden, prothrombin G20210 mutation, antithrombin-, protein C-, protein S-deficiency, antiphospolipids antibodies and hyperhomocysteinemia.

Variables	Patients			Control		
	Low Exp (n=23)	High Exp (n=80)	P-Value	Low Exp (n=72)	High Exp (n=49)	P-Value
Age (years)	55.3 ±16.5	53.3 ±14.3	0.420	48.7 ±13.7	53.0 ±14.0	0.768
Male[^]	39.1%	51.2%	0.060	29.2%	20.4%	0.027
BMI	24.9 ±3.9	25.7 ±4.3	0.202	24.5 ±4.5	23.4 ±3.8	0.684
Non-Smokers[ᵔ]	84.6%	79.3%	0.416	77.8%	75.5%	0.569
PM_{10} Levels ($\mu g/m^3$)	39.3 ±8.5	48.9 ±2.6	<0.001	41.61 ±4.8	49.20 ±3.0	<0.001
Thrombophilia[≠]	47.8%	38.8%	0.435	12.5%	16.3%	0.552
Factor VIII (%)	132.2 ±38.0	144.2 ±44.3	0.260	114.2 ±30.2	101.7 ±22.9	0.029
Fibrinogen (mg/dl)	277.2 ±81.3	320.4 ±78.1	0.026	283.8 ±64.9	300.4 ±45.3	0.168
Maximum Absorbance (mOD)	626.4 ±155.5	745.8 ±172.2	0.003	675.9 ±171.2	684.2 ±134.7	0.776
Fibre Number (per μm)	20.4 ±3.9	23 ±3.1	0.001	21 ±4	21.7 ±3.4	0.307
Ks ($x10^{-10}$ cm^2)	33.7 ±11.2	26.3 ±6.1	0.006	30.1 ±11.4	35.2 ±14.5	0.236

Table 4-3. General characteristics and clotting parameters (mean ± SD) in patients and controls of high and low PM_{10} exposure

[^]The percentage of male subjects in each group

[ᵔ]The percentage of non-smokers in each group

[≠]The percentage of subjects with positive thrombophilia in each group

Determinants or Variables	OR	95% CI	p-value
Age > 51.9 years	0.70	0.32-1.52	0.368
Men	3.02	1.36-6.74	0.007
BMI > 24.73	0.88	0.39-1.95	0.748
Thrombophilia	2.65	1.16-6.05	0.020
FVIII > 125.27%	5.52	2.52-12.10	<0.001
Fibrinogen > 299.73 mg/dl	1.44	0.65-3.17	0.371
PM_{10} Exposure Level > 45.6 µg/m^3	3.85	1.79-8.28	0.001

Table 4-4. Logistic regression analysis of risk factors for DVT

Finally, we analysed the relative contributions of age, sex, BMI, thrombophilia abnormalities, PM_{10} and interaction of thrombophilia abnormalities and PM_{10} with the variation in maximum absorbance, fibre number and Ks by linear regression in patients and controls, respectively (Table 4-5). In the maximum absorbance model, BMI and PM_{10} exposure both significantly contributed to the formation of thicker fibres in patients only, whereas age was significantly correlated with maximum absorbance in controls. In the fibre number model, PM_{10} and BMI were risk factors for more branched fibre formation for both patients and controls. In the Ks model, exposure to PM_{10} did not contribute to the alterations of clot structure in patients or controls. Permeability of the clot reduced with BMI increased in patients but not in controls. Neither thrombophilia abnormalities nor the interaction of thrombophilia abnormalities and PM_{10} contributed to the alteration of fibrin clot structure in this study. Neither thrombophilia abnormalities nor the interaction of thrombophilia abnormalities and PM_{10} were contributing to the alteration of fibrin clot structure in this study. The reason for the absence of an effect of thrombophilia on clot structure likely reflects the large degree of heterogeneity of the causes of thrombophilia in this group, including deficiencies of antithrombin, protein C, and protein S, hyperhomocysteinemia, antiphospholipids, FV Leiden mutation or prothrombin mutation (table 4-6). Each of these could have differential effects on fibrin clot structure. When we compared the larger subgroups of thrombophilia (i.e. FV Leiden, prothrombin mutation or hyperhomocysteinemia) to patients without thrombophilia there were also no differences in clot structure, likely due to the small sample size. The number of patients with other causes of thrombophilia (i.e. antithrombin, protein C or protein S deficiency, or antiphospholipid syndrome) were too small to perform any meaningful statistical analysis.

Determinants	Maximum Absorbance Correlation Coefficient (95% CI)		Fibre Number Correlation Coefficient (95% CI)		Ks Correlation Coefficient (95% CI)	
	Case	Control	Case	Control	Case	Control
Age (years)	0.47 (-1.75-2.70)	2.30* (0.10-4.49)	-0.02 (-0.07-0.03)	0.09 *** (0.04-0.14)	-0.15 (-0.33-0.02)	-0.26 (-0.52-0.01)
Men	9.01 (-56.58-74.60)	-47.2 (-112.65-18.24)	-0.18 (-1.58-1.22)	-0. 42 (-1.84-1.00)	-1.16 (-6.64-4.33)	3.03 (-5.68-11.74)
BMI	18.12 *** (10.34-25.91)	5.93 (-1.26-13.12)	0.22 * (0.06-0.39)	0.22 ** (0.06-0.37)	-0.65 * (-1.30-(-0.01))	-0.53 (-1.30-0.24)
Thrombophilia	358.56 (-128.83-845.96)	-227.89 (-886.78-431.00)	8.03 (-2.67-18.74)	7.78 (-6.48-22.04)	-16.08 (-48.96-16.81)	-70.42 (-153.83-12.99)
PM$_{10}$ Exposure Level (µg/m^3)	10.07 ** (3.58-16.56)	-1.44 (-6.90-4.03)	0.22 ** (0.08-0.35)	0.12* (0.01-0.24)	-0.32 (-0.75-0.12)	0.41 (-0.48-1.31)
Interaction (Thrombophilia and PM$_{10}$ Exposure)	-7.62 (-17.95-2.71)	4.99 (-9.29-19.26)	-0.157 (-0.38-0.07)	-0.21 (-0.52-0.10)	0.34 (-0.39-1.08)	1.85 (-0.10-3.80)

Table 4-5. Multiple regression analysis of risk factors for Maximum Absorbance, Fibre Number and Ks (cases/controls)

The correlation coefficient is of statistical significance *p<0.05; **p<0.01; ***p<0.001

Patients With/Without Thrombophilia Abnormalities Clotting Parameters	Maximum Absorbance (mOD) Mean (±SD)	Fibre Number (per µm) Mean (±SD)	Ks (x10^{-10} cm^2) Mean (±SD)
Patients without Thrombophilia Abnormalities (n=42)	721.5 (±169.5)	22.2 (±3.8)	29.3 (±9.7)
Patients with Thrombophilia Abnormalities (n=61)[¶]	715.7 (±185.2)	22.8 (±3.0)	28.3 (±7.4)
Patients with Antiphospholipid Antibodies (n=4)	755.0 (±109.3)	25.2 (±1.9)	23.0 (±2.8)
Patients with Antithrombin Deficiency (n=3)	581.0 (±86.7)	22.4 (±2.5)	27.3 (±9.0)
Patients with Factor V Leiden (n=13)	778.8 (±226.5)	21.9 (±3.8)	33.9 (±9.7)
Patients with Hyperhomocysteinemia (n=13)	762.0 (±187.9)	22.9 (±2.4)	27.3 (±7.7)
Patients with Protein C Deficiency (n=2)	558.5 (±1.1)	20.2 (±3.6)	30.4 (±2.9)
Patients with Protein S Deficiency (n=3)	700.3 (±59.6)	23.1 (±2.6)	26.2 (±2.9)
Patients with Prothrombin G20210A (n=10)	620.5 (±141.8)	22.3 (±3.3)	33.9 (±8.8)

Table 4-6. Clotting parameters (mean ± SD) in patients with/without different thrombophilia abnormalities

[¶]Some patients had more than one thrombophilia abnormality.

4.4   Discussion

According to World Health Organisation statistics, air pollution causes 3 million premature deaths each year (World Health Organisation, 2011). So far, it is still very difficult to determine the approximate concentrations of particles that reach the human blood in circulation. The only available data related to PM exposure is the PM mass concentration measured by PM monitors (Baccarelli et al. 2008; Baccarelli et al. 2009; Metassan et al. 2010a).

Consistent with a larger previous study on the association between air pollution and venous thrombosis (Baccarelli et al., 2008), PM_{10} exposure in the current study was a strong risk factor for DVT and men had higher risk of DVT than women. Baccarelli *et al*. (2008) showed that DVT risk was associated with the concentrations of PM_{10} measured during the year before diagnosis. In the current study, sex, levels of factor VIII, thrombophilia abnormalities, and PM_{10} exposure level were all significantly associated with the risk of DVT. Increased levels of coagulation factors, such as factor VIII, have previously been associated with increased risk of thrombosis (Undas et al., 2009). Thrombophilia abnormalities are also contributing factors that modulate fibrin clot structure. The prothrombin G20210 mutation leads to the increase plasma level of prothrombin which triggers the formation of denser clot structure composed of more branched thinner fibres (Wolberg and Campbell, 2008). Age, BMI and fibrinogen concentrations were not significantly associated with DVT.

In table 4-2, it can be seen that the gender and BMI were not balance between patients and healthy controls. There were more women than men, and more subjects with higher BMI in patients compared to controls. Women have higher risks of DVT. Subjects with higher BMI contribute increased risks of thrombosis. Therefore, the group with more women and

subjects with higher BMI may both contribute to the increased risk of DVT and denser clot structure.

Some differences in clot structure between patients and controls were also observed. Clots formed from plasma of patients had denser, less permeable fibrin clot structure containing more, thicker fibres compared to controls, although the differences did not reach statistical significance, possibly due to the relatively small number of subjects studied. These data provide some support to previous studies by Undas et al. (2009), in which plasma from patients with DVT and pulmonary embolism formed clots with lower clot permeability and higher maximum absorbency than controls (Undas et al., 2009). From this study, it also has been found that after long-term and high-level exposure to PM_{10} (concentrations over 45.6 $\mu g/m^3$), patients with deep vein thrombosis had significantly denser fibrin clot structure compared to those living in areas with lower levels of exposure (PM_{10} less than 45.6 $\mu g/m^3$). In the high exposure group, clots from patients possessed more compact fibre arranged fibre networks with thicker fibres and less permeable structure. However, in healthy subjects group, there were no significant differences found in clot structure between high and low exposure levels.

The mechanisms underpinning this difference between patients and healthy controls are unknown but may be related to the differences in susceptibility of fibrin clot structure to air pollution PM exposure. Susceptibility means there will be an aggravating risks of a particular cardiovascular end point or event may occur in a certain group of population (such as subjects with diabetes or old ages) compared to the general population when all of them expose to same concentration of PM to occur for a particulate cardiovascular end event compared with

the general population after the exposure to same concentration of PM (Brook et al., 2010).

In the first American Heart Association scientific statement, the susceptibility factors include the elderly; individuals with diabetes; patients with pre-existing coronary heart disease, chronic lung disease, or heart failure; and individuals with low education or social economic status (Brook et al., 2010). The effects of transient exposure (2 hours) to diesel particle air pollution were previously investigated in a controlled environment in healthy, young individuals. This study provided similar results that fibrin clot structure in plasma from subjects after short-term diesel exhaust exposure was not significantly different compared to those who were exposed to filtered air (Metassan et al., 2010b). It is possible that healthy subjects are more resistant to oxidative stress than patients with venous thrombosis, since the latter may have an enhanced inflammatory state (Franchini and Mannucci, 2011), that increases oxidative stress. Alternatively, due to increased levels of inflammatory proteins and coagulation activation in patients with venous thrombosis, any additional oxidative effects caused by air pollution on fibrin clot structure could be more pronounced, perhaps due to a threshold effect, or a minimum level of oxidative stress needed for effects on clot structure to become apparent. Finally, due to the inflammatory state, pulmonary function may be impaired, leading to translocation of ultrafine PM into the circulation. However, these considerations remain speculative as there currently are no reliable methods to analyse PM in the blood, nor do we have detailed information regarding the pulmonary function in our patients.

Mills et al. reported that diesel exhaust inhalation causes vascular dysfunction and impaired endogenous fibrinolysis (Mills et al., 2005). Furthermore, previous studies have shown that denser fibrin clot structure was associated with prolonged lysis time (Ajjan and Grant, 2006;

Ariens, 2013; Scott et al., 2004; Undas and Ariens, 2011). Therefore, as patients exposed to high levels of air pollution had denser fibrin clot structure, the lysis time compared to those patients exposed to low levels of air pollution is likely to be longer. In Chapter 3, it has been found that after normal pooled plasma exposed to air pollution particles, the clots were getting denser with more compact arrangements and prolonged lysis time. Future studies will be needed to further evaluate the effects of air pollution exposure on fibrinolysis in patients with venous thrombosis.

Possible limitations of this study include the relatively small study sample size (due to the time-consuming nature of fibrin structure analysis), and that we had no information regarding personal levels of air pollution exposure for the participants. The concentrations of PM_{10} in this study were measured according to the area of residence for the subjects, which were different for each subject and spanned several residential areas in Lombardy. Therefore, although exposure to air pollution was not measured with personal monitors, the data obtained did provide average daily, specific and long-term individual exposure to air pollution.

In conclusion, this study shows that patients with venous thrombosis exposed to high level of air pollution had denser fibrin clot structure with thicker fibres (higher maximum absorbance), decreased permeability (lower Ks value) and higher fibre numbers compared to those in the low exposure group, indicative of a prothrombotic clot structure. There were no differences in fibrin clot structure measurements between the two exposure groups in controls, suggesting that air pollution may trigger differences in fibrin clot structure only in patients predisposed to thrombotic diseases.

5 Effects of PM and Diesel Particles on Human Umbilical Vein Endothelial Cells

5.1 Introduction

According to the Italy cohort study in the previous chapter, the results have shown that people exposed to PM_{10} had increased risk of deep vein thrombosis, and that those patients with DVT had denser fibrin clot structure after long term exposure to high level of PM_{10}. Several other epidemiological studies also indicated associations between air pollution and cardiovascular diseases as indicated in the previous chapters. There are a few mechanisms that have been proposed for underpinning this increased cardiovascular risk, which include pulmonary and systemic inflammation, enhanced coagulation, reduced fibrinolysis, and autonomic system dysfunction.

In chapter 3, the effects of PM and diesel particles on plasma or fibrinogen samples were investigated through in vitro experiments. The results showed that particles were not able to alter fibrin clot structure formed from plasma and fibrinogen. But the clot lysis time was significantly longer with particles (50 μg/ml) compared to control. In chapter 4 the Italy *ex vivo* study showed that after high level PM exposure, patients with DVT had significantly denser fibrin clots structure compared to those patients exposure to low level of exposure. Both in vitro and ex vivo studies have shown that particles from air pollution were able to influence the fibrin clot structure formed from plasma samples. Therefore, the possible mechanisms why air pollution particles altered the fibrin clot structure needs to be investigated.

To assess whether air pollutant particles can pass into the systemic circulation, Nemmar et al. measured the distribution of radioactivity after 5 healthy volunteers inhaled the aerosol contains technetium-99m labelled carbon particles (<100 nm). Gamma camera images showed radioactivity was detected in the liver and bladder indicating that ultrafine PM is able to pass into the circulation and directly interfere with endothelial cells (Nemmar et al., 2002). This chapter would focus on the human umbilical vein endothelial cells. It is hypothesized that particulate matter and diesel particles may interfere with the endothelial cells directly and lead to altered fibrin clot structure.

5.2 Methods

HUVECs were cultured as described in chapter 2.3.3. Briefly, cells were treated for 24 hours with different concentrations of PM. Cytotoxicity of the cells was measured by the MTT assay. The same concentrations of PM_{10} and diesel particles were used as for the previous plasma and fibrinogen in vitro study (Chapter 3). The concentrations of particles were chosen which caused less than 20% cell death for further investigation. Cells were seeded on the ibidi μ-slide and incubated with chosen concentrations of particles for 24 hours. The treatment was removed, after which fibrin clots were formed with thrombin and $CaCl_2$ on the cells. Laser scanning confocal microscopy method were used to measure the fibre number of the clots through images. Then, we used Enzyme-linked immune-sorbent assay (ELISA) to quantify the proteins produced by HUVEC after incubation with PM. Some transmembrane proteins may be produced by endothelial cells as well after exposure, but they were not able to be measured by ELISA. To assess changes to gene expression after exposure to the PM for the

genes coding these proteins real time polymerase chain reactions (RT-PCR) were used. The details of each methods were described in chapter 2.

5.3 Results

5.3.1 Cytotoxicity

HUVECs were treated with PM_{10}, $PM_{0.2}$, total diesel particles and filtered diesel particles at 6 different concentrations for 24 hours. The toxicity of these four particles is shown in the following figure. At the highest concentration 50 μg/ml, these four particles caused less than 10% cell death. Compared to diesel particles, PM_{10} and $PM_{0.2}$ had more cytotoxicity. PM_{10} had the most toxicity on HUVEC, but even at the highest concentration this effect was not significant harmful (Fig 5-1).
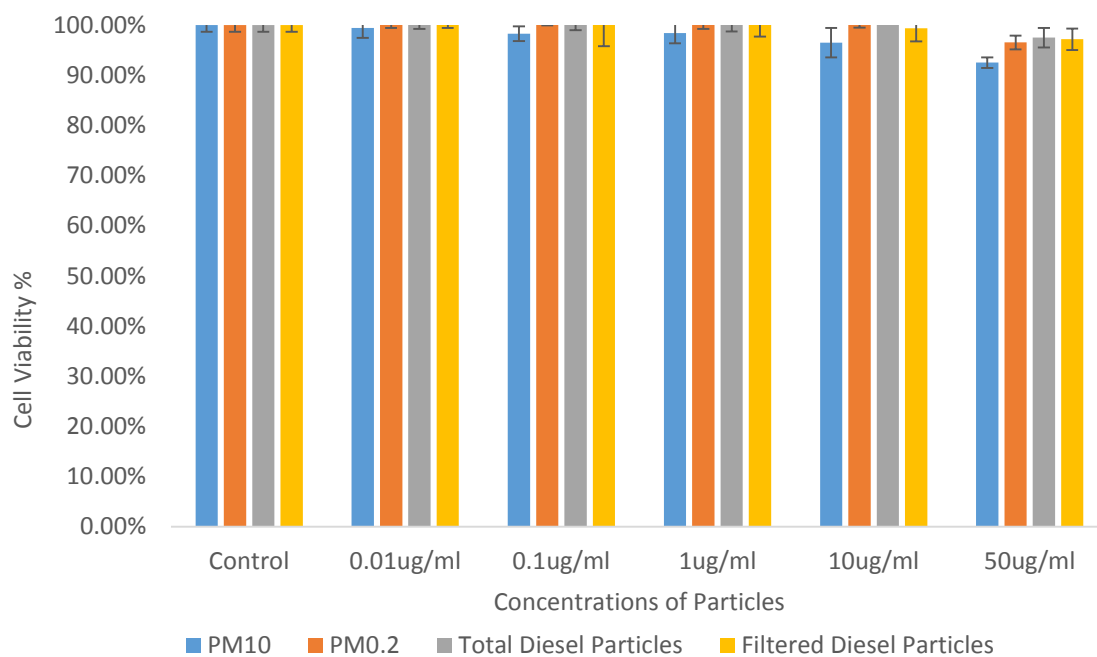
Figure 5-1. Cytotoxicity of Endothelial Cells after 24 hours Particles Exposure (n=10)

HUVEC were treated with different concentrations of different particles for 24 hours. MTT assay was performed to detect the particle cytotoxicity. The results showed that there was no significantly cell death even at the highest concentration 50 μg/ml.

5.3.2 LSCM of Particulate Matter

After the cytotoxicity test, all concentrations of particles could be used in the following experiments as the cell viability was over 80%.

Cells were treated with different concentrations of particles for 24 hours. Then the cell supernatant was removed completely. The fibrin clots were formed from either normal pooled plasma samples or purified fibrinogen with thrombin and CaCl$_2$ in the presence of

treated cells. The clots were incubated at 37 °C for 30 minutes for analysis. The number of fibres was measured through LSCM image.

Normal Pooled Plasma Samples

The fibrin clot structure formed from normal pooled plasma samples with cells exposed to PM_{10}, PM were shown as following. After the cells were treated with particles at concentration of 0.01 µg/ml, 0.1 µg/ml, 1 µg/ml 10 µg/ml and 50 µg/ml, the fibrin clot structure was altered compared to control. These four particles showed a similar trend that as the concentrations of particles increased, the clot structure became denser as the number of fibre per µm increased gradually in a dose-dependent manner.

The following figures represent the fibrin clot structure formed on the cells after treatment with different particles at different concentrations. As the concentrations of PM_{10} increased, the clots were getting much more complex. The clots started to have significantly denser structure after cells treated with 10 µg/ml of PM_{10} compared to control (Fig 5-2).

Figure 5-3 shows that the fibre number increased as the concentration of particles increased. Clots were similar as control after cells were treated with 0.1 µg/ml of $PM_{0.2}$. The fibre number of the clots was significantly higher at 10 µg/ml.

In figure 5-4, it can be seen that when the cells were treated with 0.01 µg/ml of total diesel particles, the clots had similar fibre numbers as control. The increased concentrations of total diesel particles led to increased number of fibres formed in the clots. At 50 µg/ml, total diesel particles caused the densest clots with highest number of fibres.

In terms of the filtered diesel particles, from 10 µg/ml, the fibre numbers were significantly higher compared to control. The clots were getting denser with more branched networking as the concentration of filtered diesel particles increased (Fig 5-5).

Control   0.01 µg/ml of PM_{10}

0.1 µg/ml of PM_{10} 1 µg/ml of PM_{10}

10 µg/ml of PM_{10} 50 µg/ml of PM_{10}
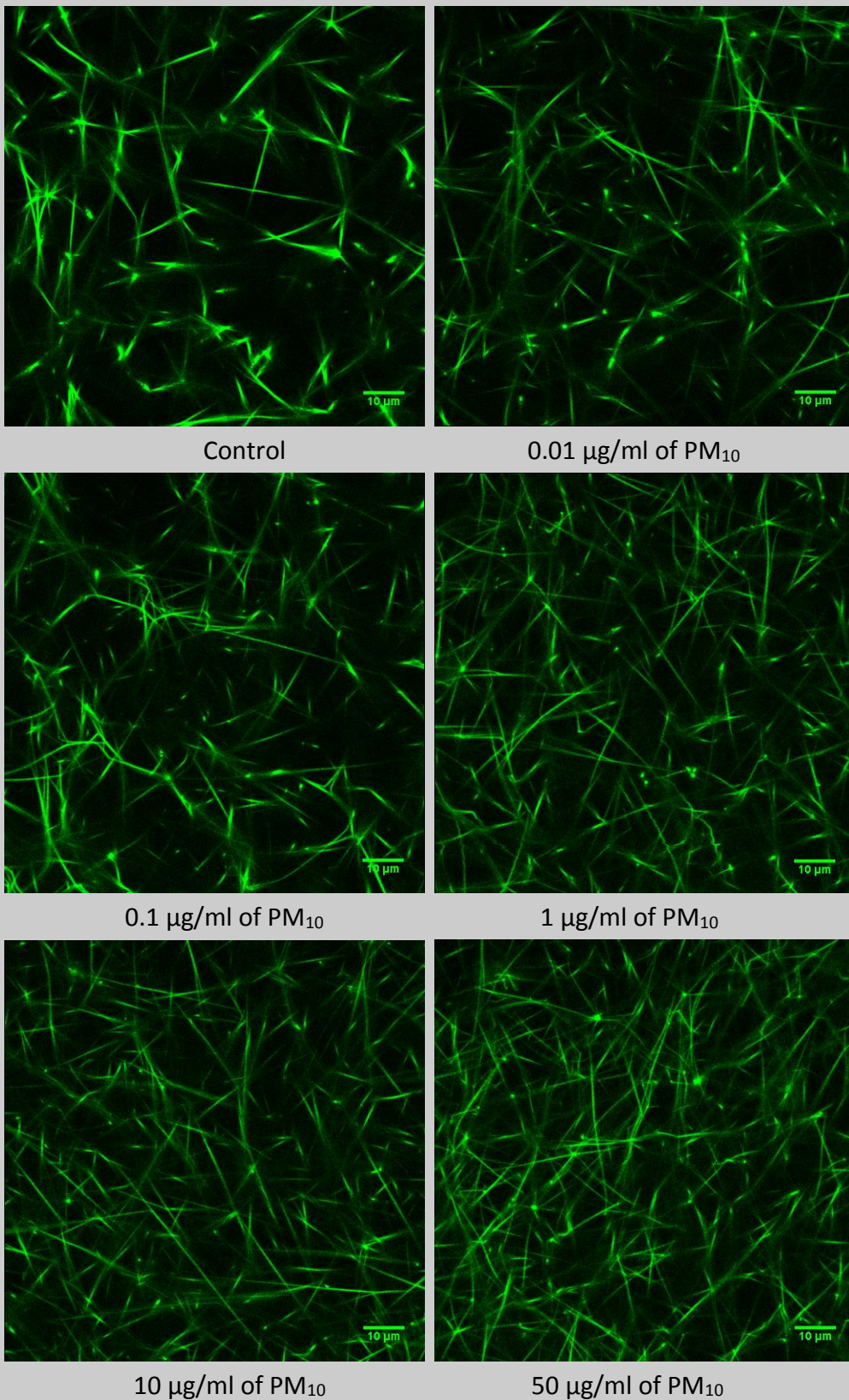
Figure 5-2. LSCM—Effects of PM_{10} on HUVEC (Normal Pooled Plasma)

The fibrin clots were formed with plasma samples in the presence of cells exposed to PM_{10}.

Control   0.01 µg/ml of $PM_{0.2}$

0.1µg/ml of $PM_{0.2}$ 1µg/ml of $PM_{0.2}$

10µg/ml of $PM_{0.2}$ 50µg/ml of $PM_{0.2}$
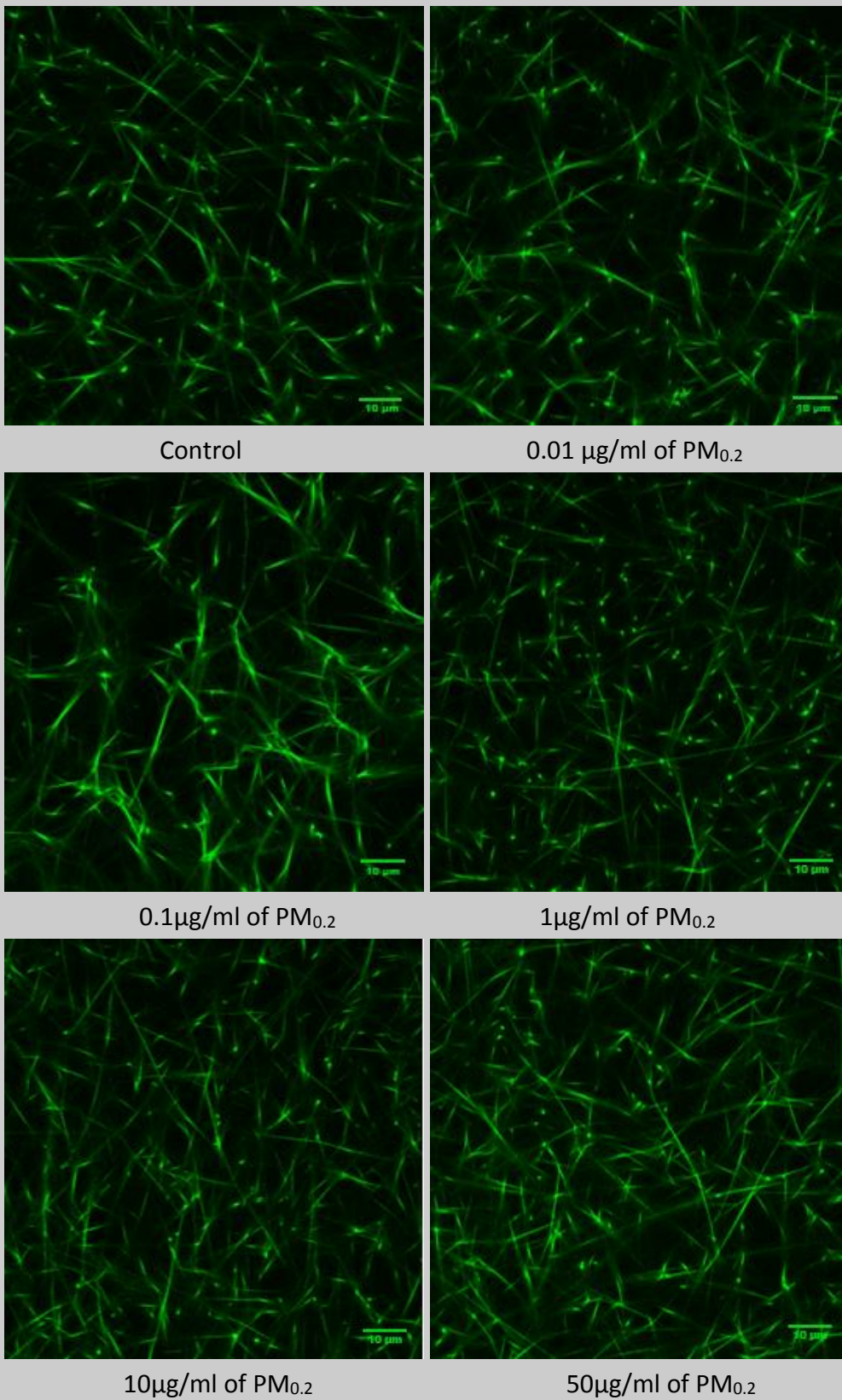
Figure 5-3. LSCM—Effects of $PM_{0.2}$ on HUVEC (Normal Pooled Plasma)

The fibrin clots were formed with plasma samples in the presence of cells exposed to $PM_{0.2}$.

Control   0.01 µg/ml of Total Diesel Particles

0.1 µg/ml of Total Diesel Particles   1 µg/ml of Total Diesel Particles

10µg/ml of Total Diesel Particles   50µg/ml of Total Diesel Particles
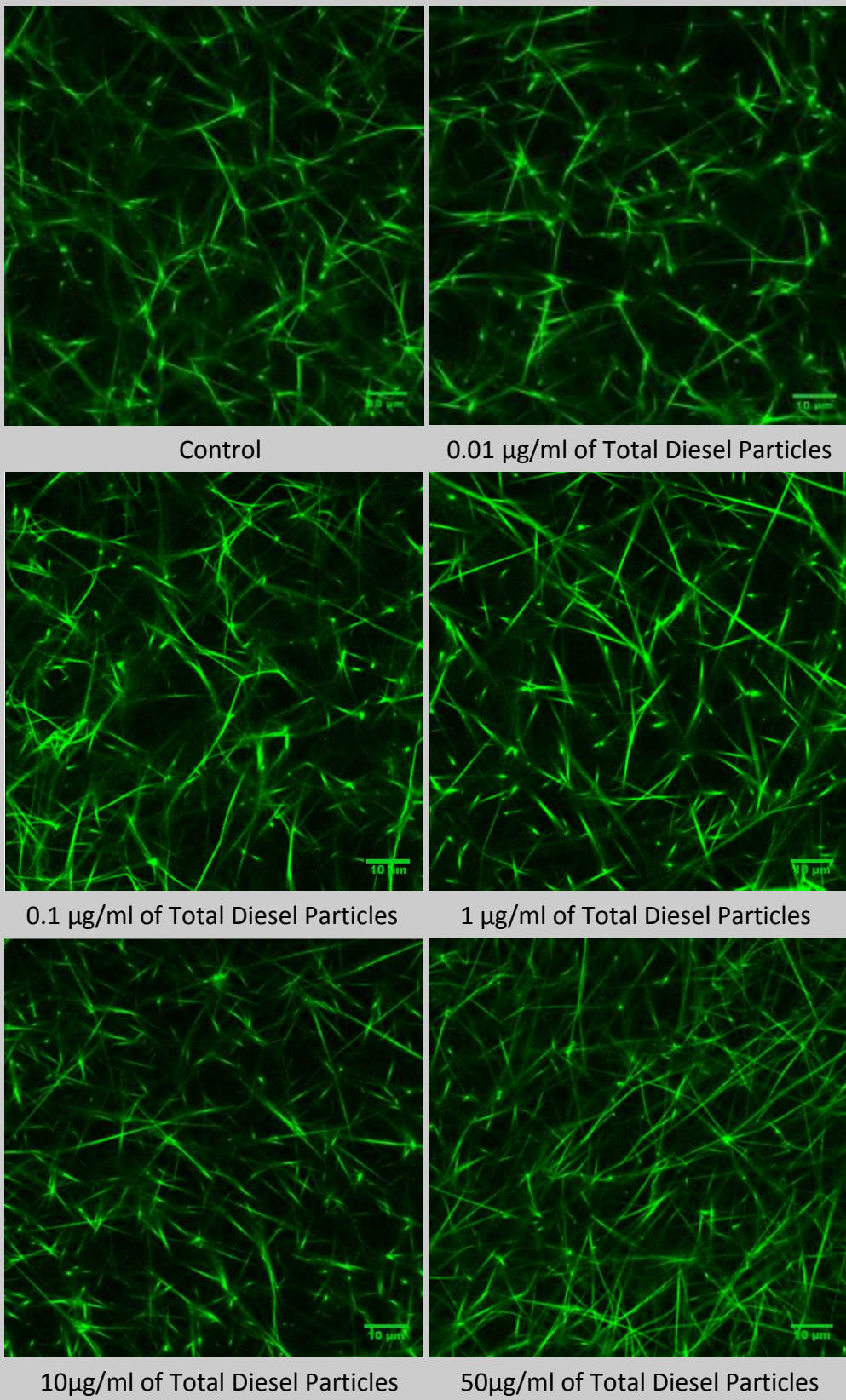
Figure 5-4. LSCM—Effects of Total Diesel Particles on HUVEC (Plasma)

The fibrin clots were formed with plasma in the presence of cells exposed to total DEP.

Control

0.01 µg/ml of Filtered Diesel Particles

0.1 µg/ml of Filtered Diesel Particles

1 µg/ml of Filtered Diesel Particles

10 µg/ml of Filtered Diesel Particles

50 µg/ml of Filtered Diesel Particles
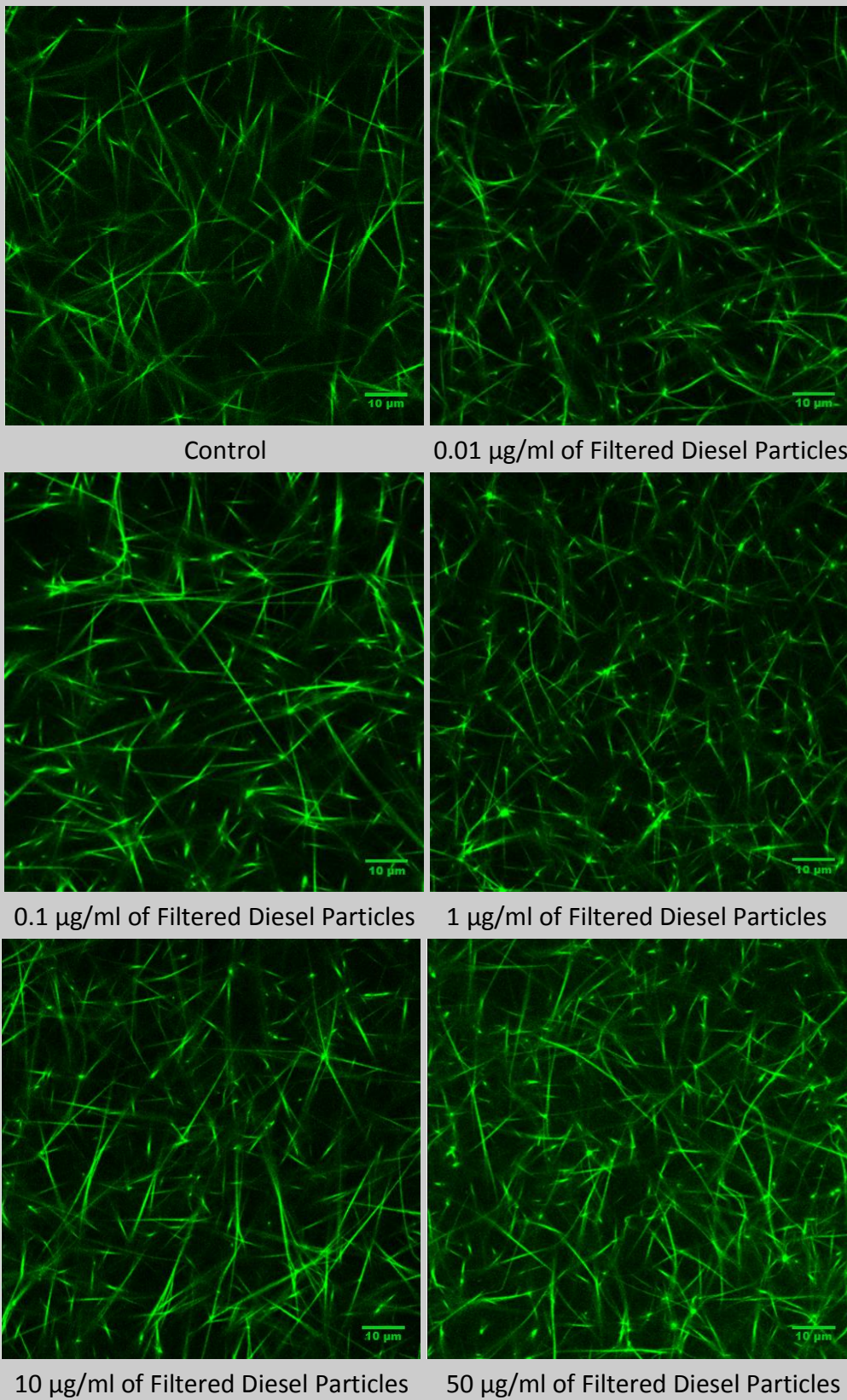
Figure 5-5. LSCM—Effects of Total Diesel Particles on HUVEC (Plasma)

The fibrin clots were formed with plasma in the presence of cells exposed to filtered DEP.

As can be seen from figure 5-2 to 5-6, the clots had significantly denser structure than control at the concentration of 10 µg/ml. The fibre bundles were around 3 per µm after the cells treated with different particles at same concentration. $PM_{0.2}$ and filtered diesel particles had less fibre bundles compared to PM_{10} and total diesel particles (Fig 5-6). The fibre bundles were measured through LSCM images. The details of the calculation were as described in Chapter 2.
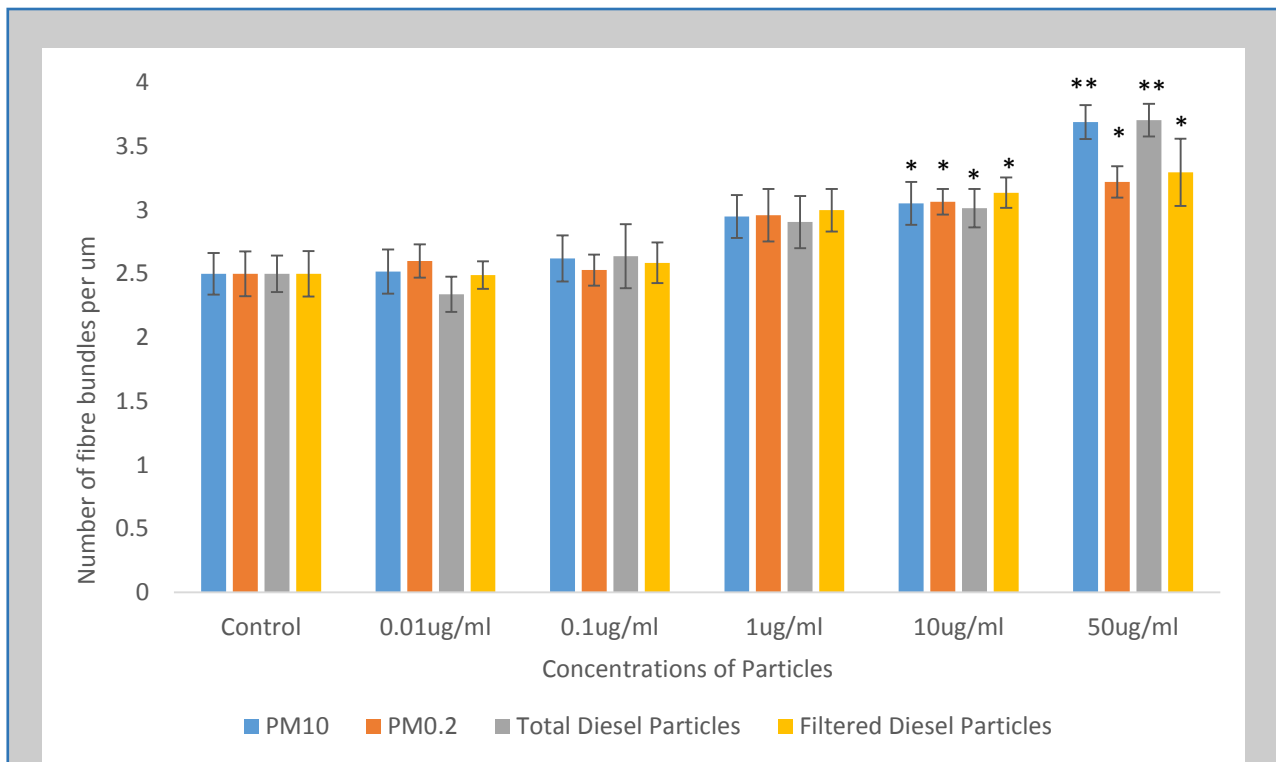
Figure 5-6. Fibre Bundles of Clots Formed from Plasma Samples with Different Concentrations of Particles on HUVEC (n=9)

*p<0.05; **p<0.001

Laser scanning confocal microscope assay was used to measure the fibrin clot structure. After the cells were treated with different concentrations of particles for 24 hours, the fibrin clots were set up with plasma samples in the presence of treated cells. As the concentrations of particles increased, the number of fibre bundles were increased in a dose-dependent manner.

Fibrinogen Samples

For the fibrinogen samples, the clots were set up with purified fibrinogen samples in the presence of endothelial cells exposed to different concentration of particles. The following four figures (5-7 to 5-10) represent the fibrin clot structure formed from purified fibrinogen in the presence of endothelial cells treated with different concentrations of PM_{10}, $PM_{0.2}$, total diesel particles and filtered diesel particles, respectively. The clot structure was similar as control even the cells exposed to the highest concentration of particles. The data (figure 5-11) showed even after the cells treated with the highest concentration of those particles, the fibrin clot structure was still similar as the control. In contrast to the clots formed from plasma, there wasn't any significant difference of the structure between treated and untreated cells.

Control | 0.01μg/ml of PM_{10}

0.1μg/ml of PM_{10} | 1μg/ml of PM_{10}

10μg/ml of PM_{10} | 50 μg/ml of PM_{10}
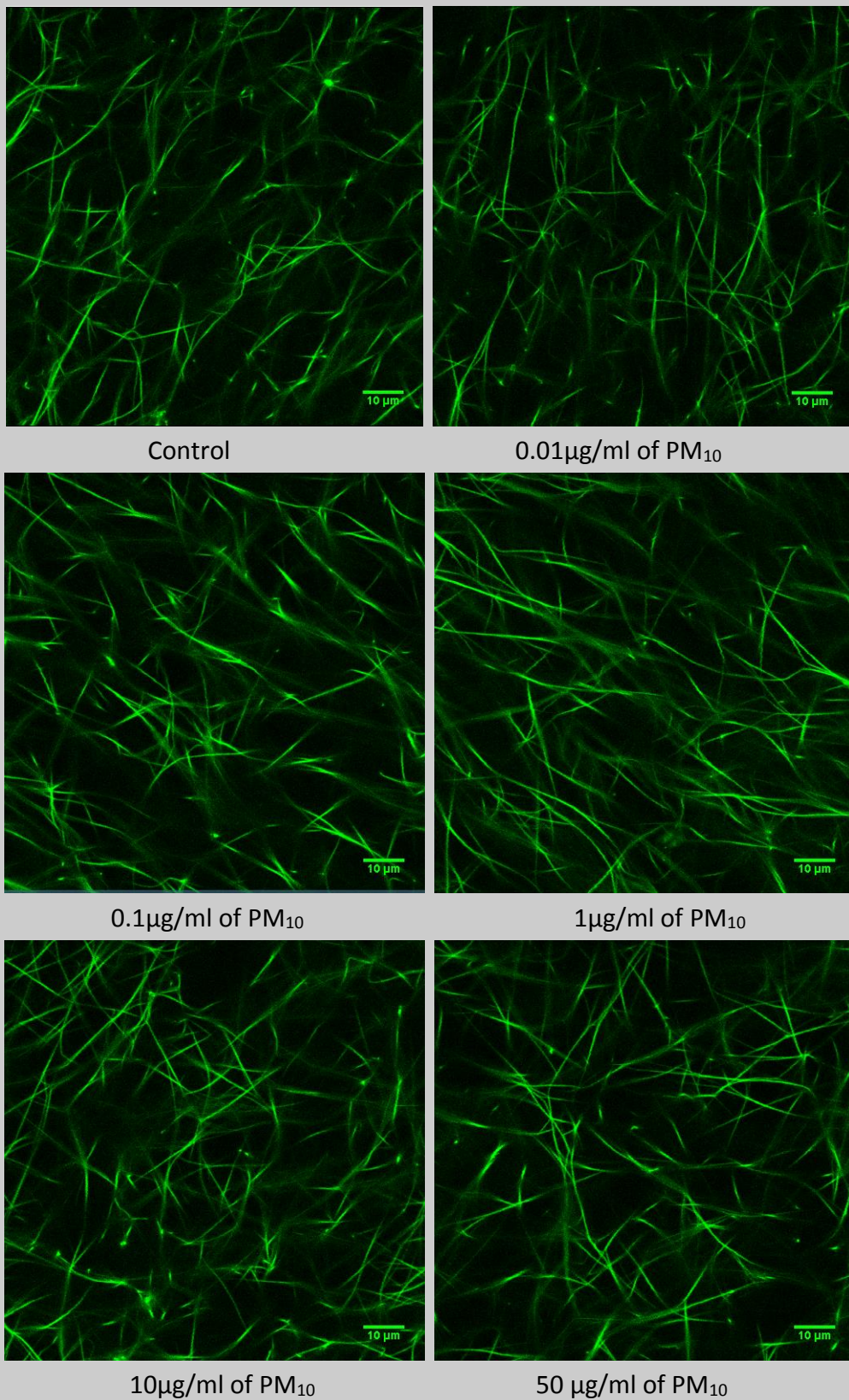
Figure 5-7. LSCM—Effects of PM_{10} on HUVEC (Purified Fibrinogen)

The fibrin clots were formed with fibrinogen samples in the presence of cells exposed to PM_{10}.

Control $0.01\mu g/ml$ of $PM_{0.2}$

$0.1\mu g/ml$ of $PM_{0.2}$ $1\mu g/ml$ of $PM_{0.2}$

$10\mu g/ml$ of $PM_{0.2}$ $50\mu g/ml$ of $PM_{0.2}$
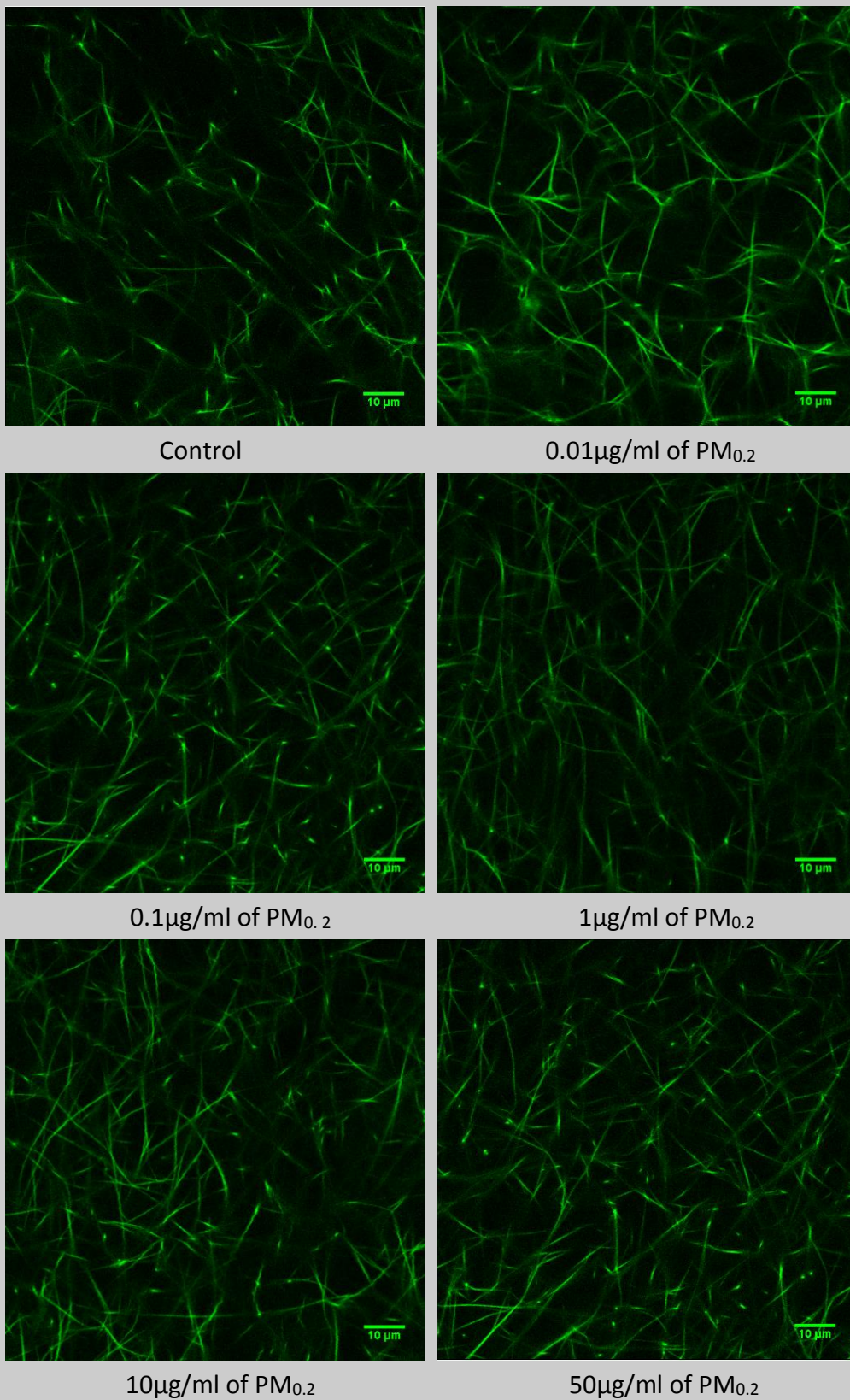
Figure 5-8. LSCM—Effects of $PM_{0.2}$ on HUVEC (Purified Fibrinogen)

The fibrin clots were formed with fibrinogen samples in the presence of cells exposed to $PM_{0.2}$.
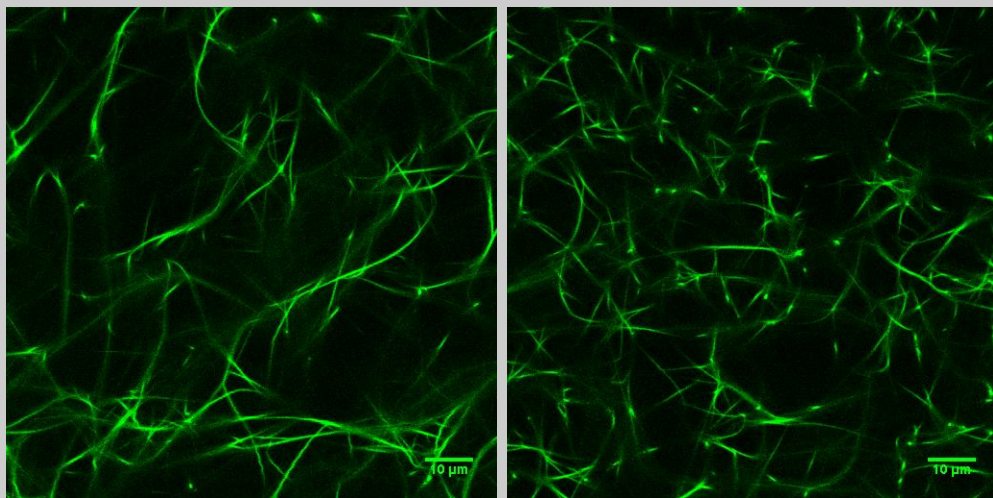
Control   0.01µg/ml of Total Diesel Particles
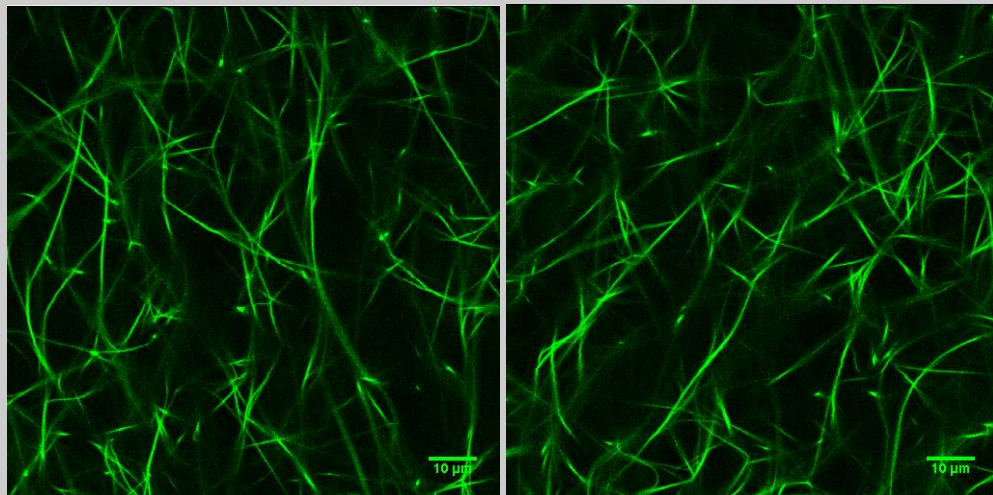
0.1µg/ml of Total Diesel Particles   1µg/ml of Total Diesel Particles
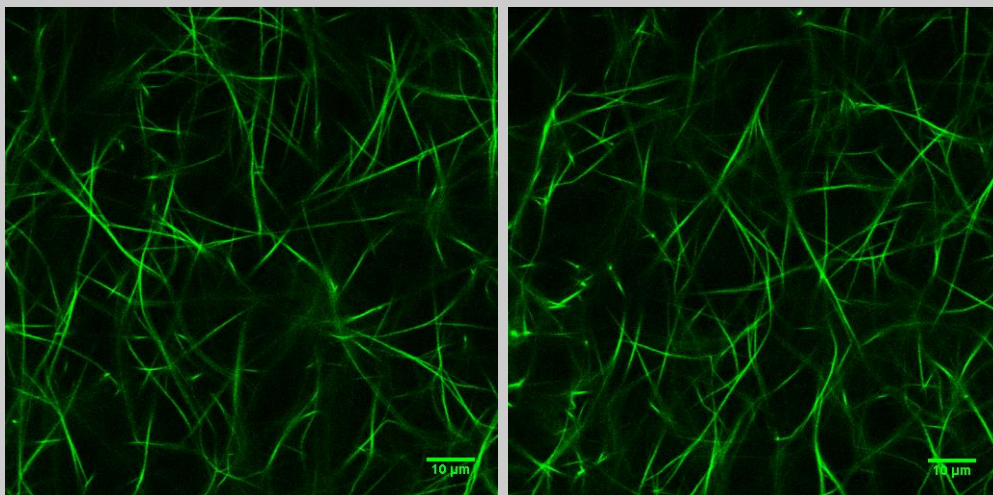
10µg/ml of Total Diesel Particles   50µg/ml of Total Diesel Particles

Figure 5-9. LSCM—Effects of Total Diesel Particles on HUVEC (Purified Fibrinogen)

The fibrin clots were formed with fibrinogen in the presence of cells exposed to total DEP.

Control | 0.01µg/ml of Filtered Diesel Particles

0.1µg/ml of Filtered Diesel Particles | 1µg/ml of Filtered Diesel Particles

10µg/ml of Filtered Diesel Particles | 50µg/ml of Filtered Diesel Particles
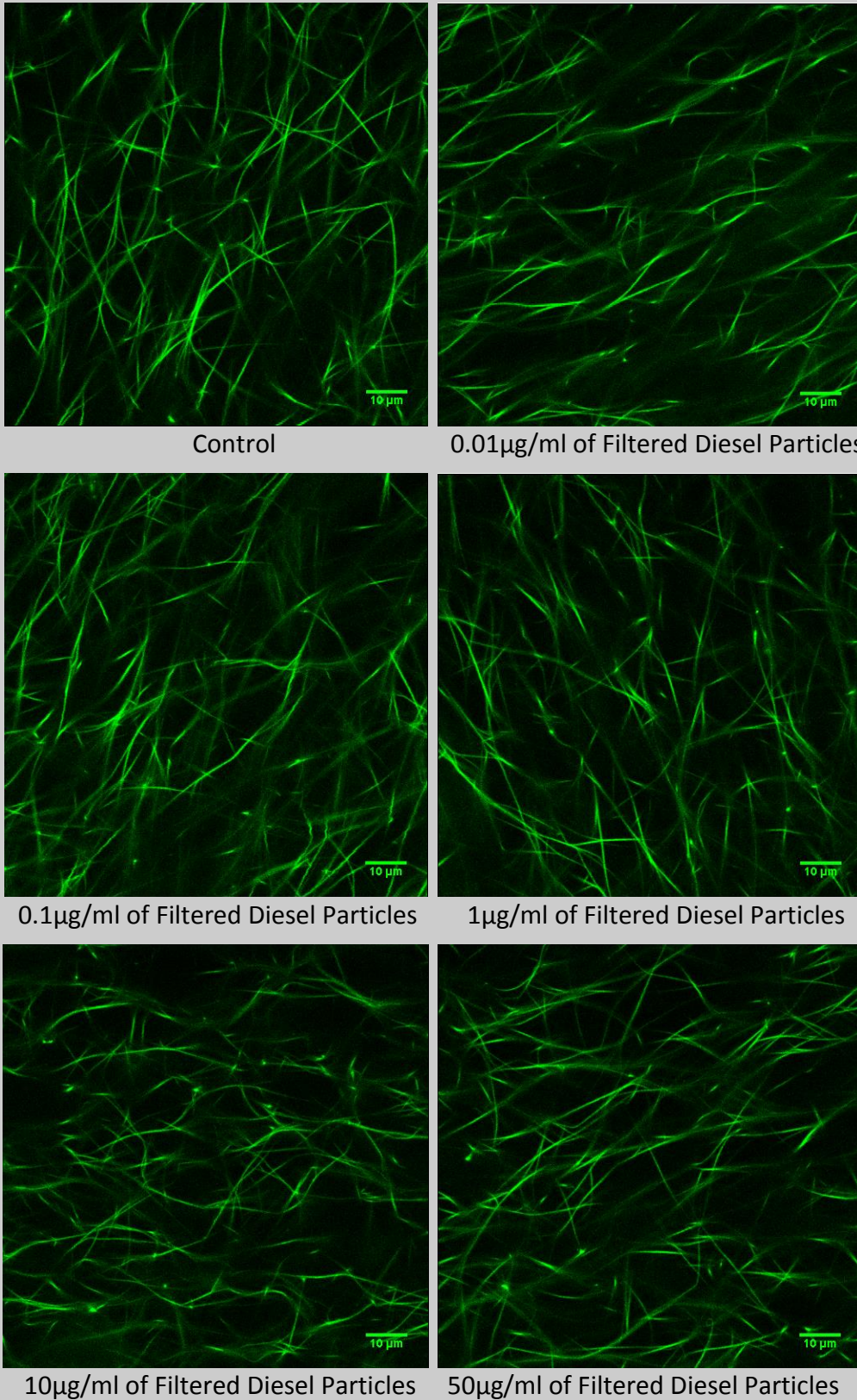
Figure 5-10. LSCM—Effects of Filtered Diesel Particles on HUVEC (Purified Fibrinogen)

The fibrin clots were formed with fibrinogen in the presence of cells exposed to filtered DEP.
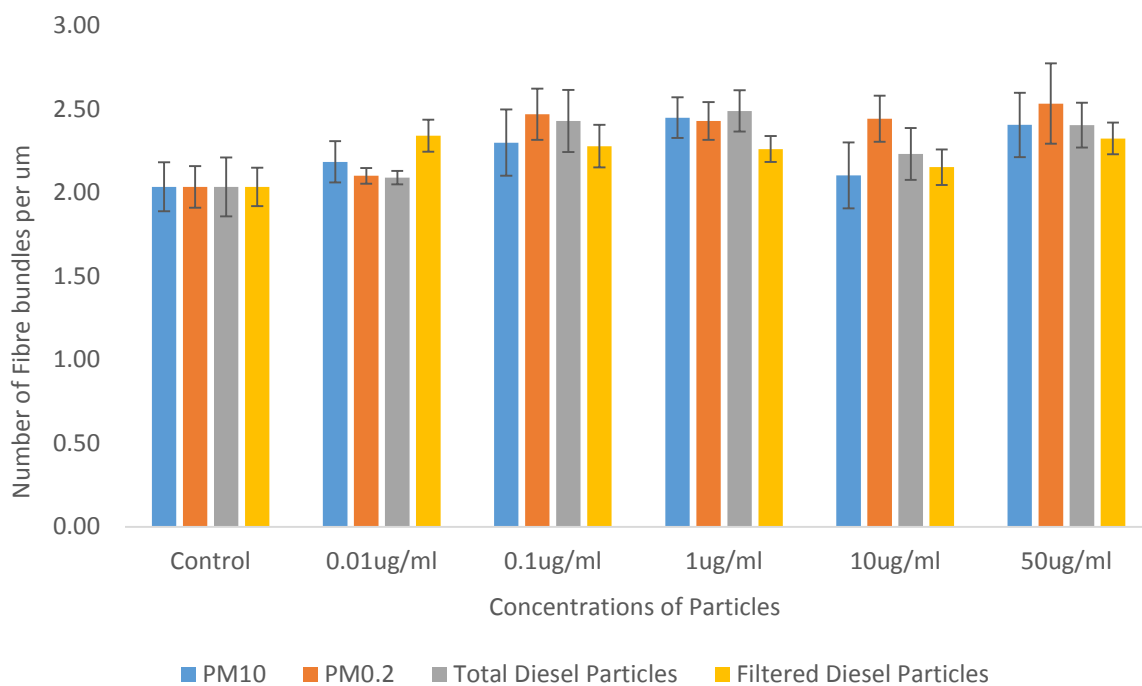
Figure 5-11. Fibre Bundles of Clots Formed from Purified Fibrinogen Samples with Different Concentrations of Particles on HUVEC (n=9)

Laser scanning confocal microscope assay was used to measure the fibrin clot structure. After the cells were treated with different concentrations of particles for 24 hours, the fibrin clots were set up with purified fibrinogen samples in the presence of treated cells. Compared to the control, the fibre numbers of the clots formed with particles treated cells had no significant difference.

5.3.3   RT-PCT

Real time polymerase chain reaction was used to quantify the genes of interests that expressed by endothelial cells after incubation with air pollution particles for 24 hours. Two different genes, tissue factor and thrombomodulin, were measured by RT-PCR.

Tissue Factor

Tissue factor is a transmembrane glycoprotein which is produced by endothelial cells only while exposed to stimuli that activate the endothelial cells such as cytokines. After endothelial cells were incubated with different types and concentrations of particles for 24 hours, the gene of tissue factor was quantified by RT-PCR.

After the cells were treated with PM_{10} and total diesel particles at 0.1 μg/ml, gene expression of tissue factor were significantly higher compared to control. $PM_{0.2}$ caused significantly increased expression of tissue factor gene from 1 μg/ml. Filtered diesel particles had less effect on TF gene expression in comparison with the other three types of particles as shown in the figure. Until 50 μg/ml, all four kinds of particles induced TF mRNA expression significantly more than control. PM_{10} caused three times more tissue factor gene expression compared to control, the other three particles induced 1.85, 1.72, and 1.49 times elevation of TF mRNA, respectively (Fig 5-12).
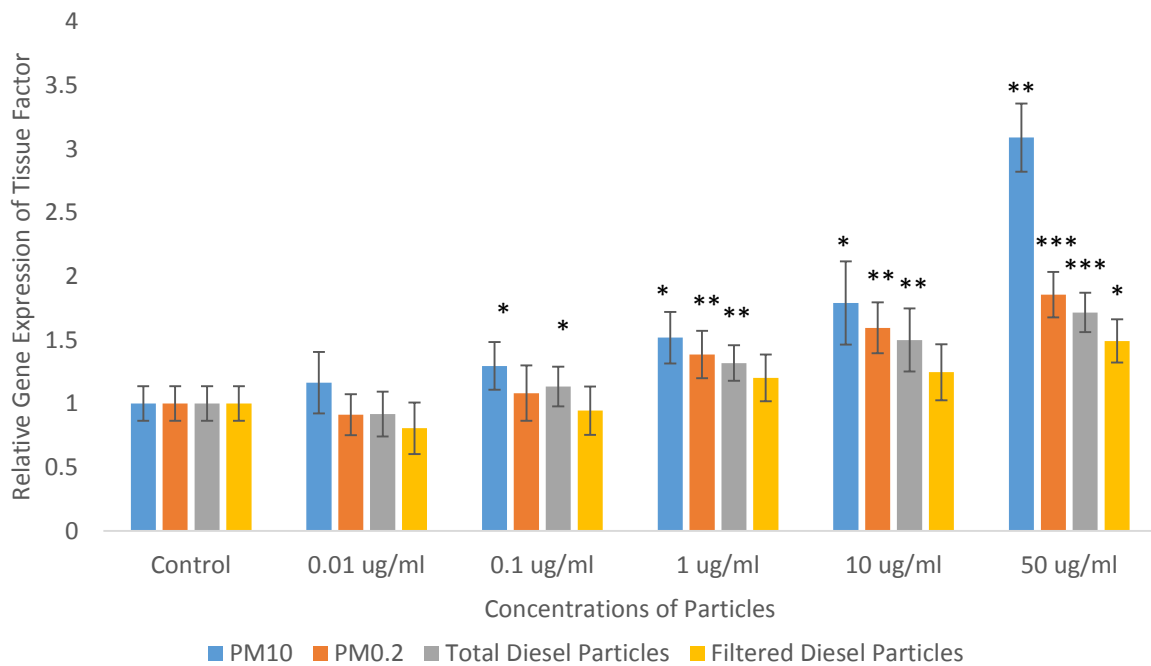
Figure 5-12. Gene Expression Level of Tissue Factor (TF) in Human Umbilical Vein Endothelial Cells after Treatment with the Different Particles (n=3)

*p<0.05; **p<0.001; ***p<0.0001

Relative gene expression level of tissue factor was determined by real-time polymerase chain reaction. As the concentrations of particles increased, the TF mRNA expression level increased as well.

Thrombomodulin

Thrombomodulin is also a membrane protein expressed by endothelial cells. Thrombomodulin binds thrombin and alters its substrate activity so that it activates Protein C (a naturally occurring anticoagulant) rather than fibrinogen. Activated Protein C in turn inactivates activated Factors V and VIII reducing thrombin generation. Therefore, thrombomodulin acts as a potent anticoagulant on intact, healthy endothelial cells. The cells

without particle treatment had the highest level of THBD mRNA expression. As the concentration of particles increased, the gene expression of THBD decreased in a dose-dependent manner. PM_{10}, $PM_{0.2}$ and total diesel particles significantly suppressed THBD mRNA expression by endothelial cells at 1 µg/ml, and followed by filtered diesel particles at 10 µg/ml. At 50 µg/ml, PM_{10} and total diesel particles inhibited the THBD gene expression by 70% reduction compared to control, $PM_{0.2}$ and filtered diesel particles led to approximately 55% less THBD mRNA secretion by HUVECs.
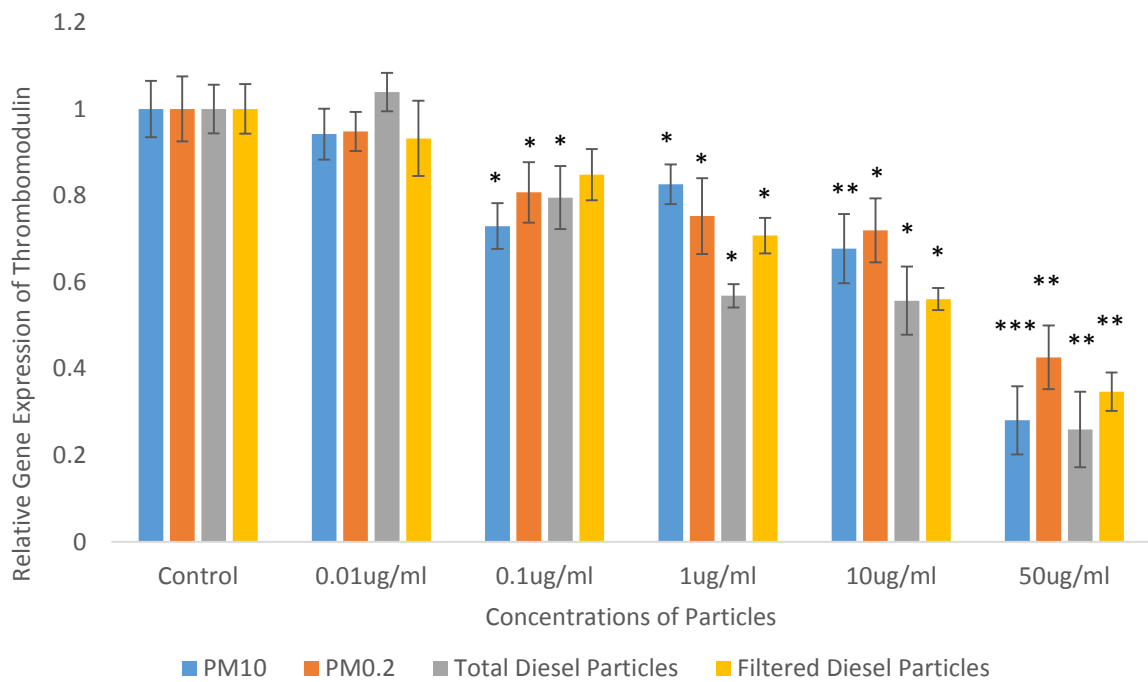
Figure 5-13. Gene Expression Level of Thrombomodulin (THBD) gene in Human Umbilical Vein Endothelial Cells after Treatment with the Different Particles (n=3)

*p<0.05; **p<0.001; ***p<0.0001

Relative gene expression level of thrombomodulin was determined by real-time polymerase chain reaction. As the concentrations of particles increased, the THBD mRNA expression level decreased as well.

5.3.4 ELISA

Enzyme-linked immunosorbent assays were used to quantify the levels of proteins secreted by endothelial cells after incubation with different concentrations of PM. Two proteins were chosen to be measured as both of them were closely correlated with alteration fibrin clot structure and clot fibrinolysis, von Willebrand factor and plasminogen activator inhibitor-1.

Von Willebrand Factor

Endothelial cells were treated for 24 hours, then the cell supernatant was taken for measuring the concentration of VWF. As the concentrations of PM increased, the levels of VWF expressed by treated HUVECs increased in a dose-dependent manner (Fig 5-14). At 50 µg/ml, PM_{10} caused highest concentration of VWF secretion compared to the other three particles, followed by $PM_{0.2}$, total diesel particles and filtered diesel particles.
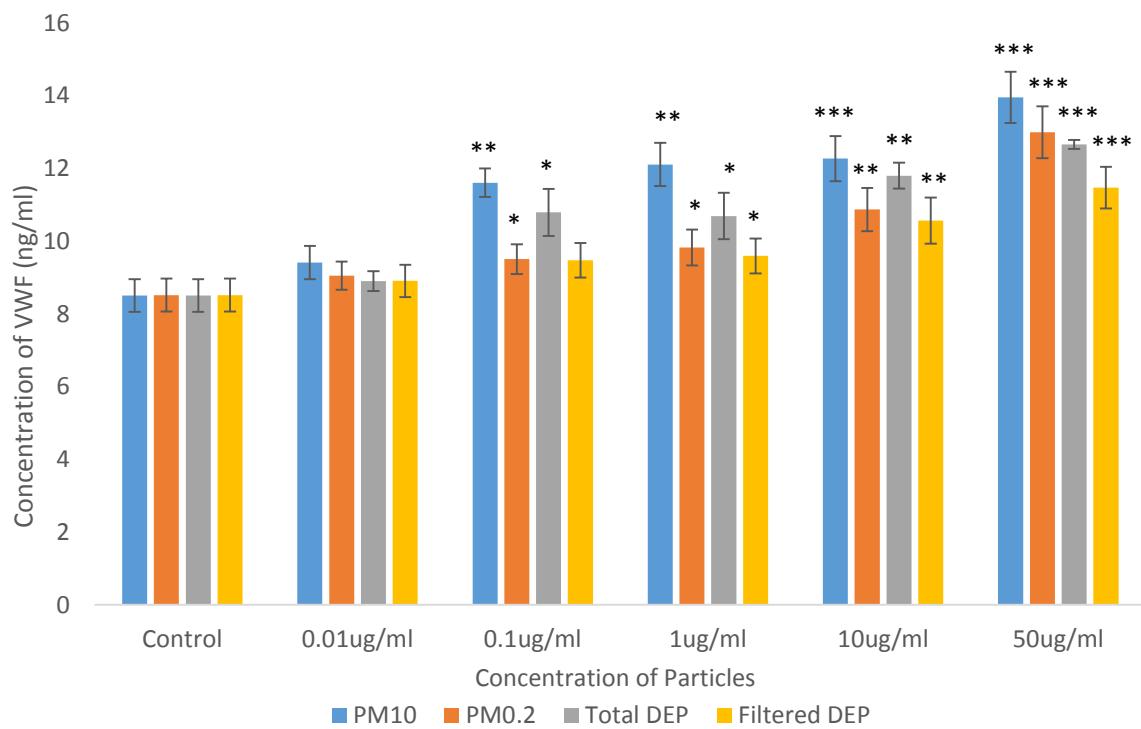
Figure 5-14. Concentrations of Von Willebrand Factor (VWF) from Human Umbilical Vein Endothelial Cells after 24h Treatment with Different Concentrations of Particles (n=5)

*p<0.05; **p<0.001; ***p<0.0001

ELISA was used to measure the VWF protein levels. After the cells were treated with different concentrations of particles for 24 hours, the cell supernatants were taken for measuring the concentrations of VWF secreted by endothelial cells. Compared to control, the VWF concentrations were increased as the concentrations of particles increased in a dose-dependent manner.

Plasminogen Activator Inhibitor–1

PAI-1 as the main inhibitor of tPA was expressed more when endothelial cells were stimulated by PM. At 0.1 µg/ml of PM_{10}, the concentration of PAI-1 increased to approximately 250 pg/ml which was significantly higher compared to control 200 pg/ml. Total diesel particles induced significant PAI- expression at 1 µg/ml (Fig 5-15). $PM_{0.2}$ and filtered diesel particles caused

similar levels of PAI-1 expression after cells were treated with concentrations of 5 and 10 µg/ml.

Figure 5-15. Concentrations of Plasminogen Activator Inhibito-1 (PAI-1) from Human Umbilical Vein Endothelial Cells after 24h Treatment with Different Concentrations of Particles (n=5)

*$p<0.05$; **$p<0.001$; ***$p<0.0001$

ELISA was used to measure the PAI-1 protein levels. Compared to control, the concentrations PAI-1 were increased as the concentrations of particles increased in a dose-dependent manner.

5.3.5   Plasmid Strand Break Assay

Plasmid strand break assay was used to detect the free radicals released from the particles when incubated with supercoiled plasmid DNA.

After 12 hours incubation in the dark, there were more single strand breaks in pBR322 DNA as the concentrations of particles increased (Fig 5-16). PM had more free radicals released compared to the diesel particles. Over 60% of supercoiled plasmid changed to the nicked form induced by PM_{10} and $PM_{0.2}$. In terms of both diesel particles, there were only 35% of nicked plasmid. PM_{10} released the most free radicals and caused significantly more strand breaks at concentration of 10 µg/ml. The other three types of particles caused the significantly nicked DNA at 50 µg/ml.
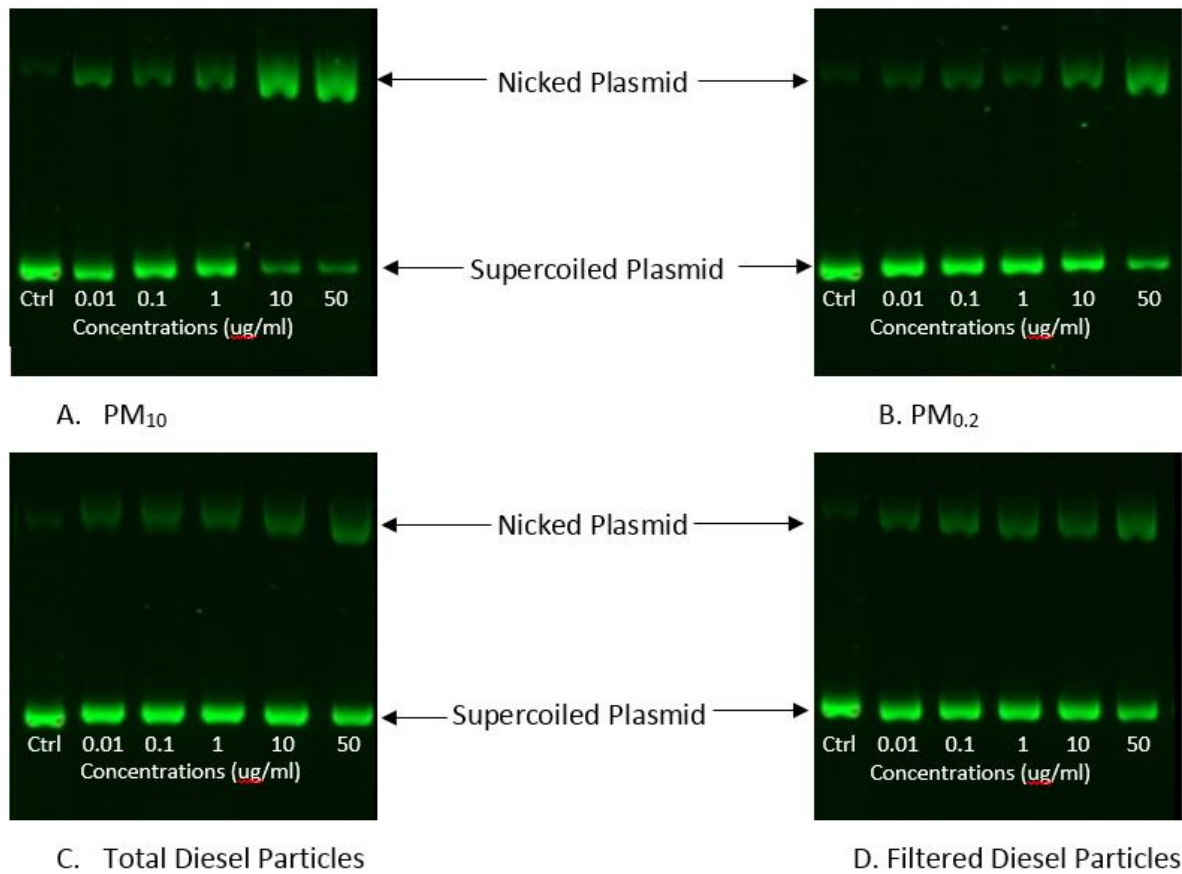
Figure 5-16. Induction of Single Stand Breaks in pBR322 DNA Following Incubation with Different Particles (n=3)

Figure 5-16 showed that gel electrophoresis results of strand breaks induced by different concentrations of particles.
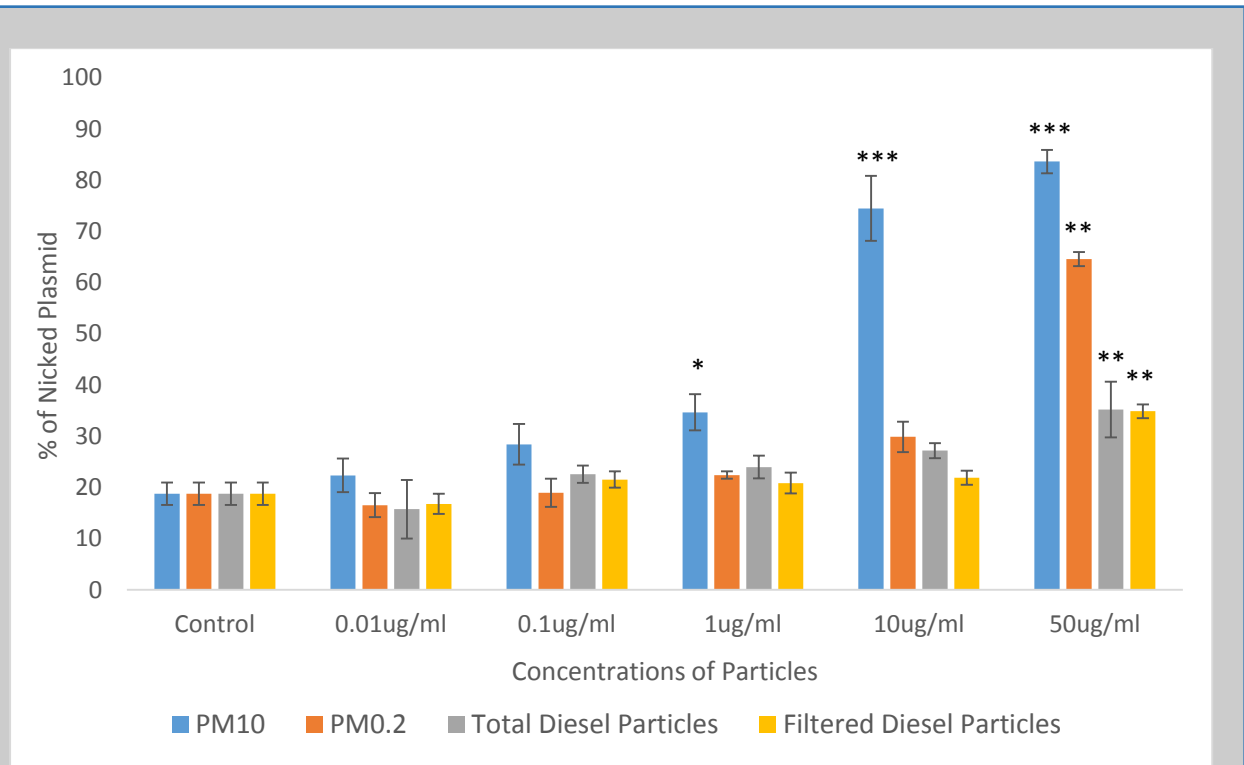
Figure 5-17. Induction of Single Stand Breaks in pBR322 DNA Following Incubation with Different Particles (n=3)

*p<0.05; **p<0.001; ***p<0.0001;

Plasmid DNA was incubated with different concentrations of particles from 0 to 50 µg/ml for 12 hours in the darkness. The induction of strand breaks were assessed and expressed as the percentage of nicked DNA observed. The results indicated that PM_{10} started to induce significantly stand breaks at 10 µg/ml. The other three particles caused damage to plasmid DNA at 50 µg/ml.

5.4 Discussion

In this chapter, the effects of air pollution on human umbilical vein endothelial cells were investigated using five methods, MTT cytotoxicity test, laser scanning confocal microscope, Real-Time PCR, ELISA, and plasmid strand break assay. The results indicated that the particles concentrations used in the study had little cytotoxicity to the cells after 24 hours treatment.

But, the fibrin clots formed on the treated cells were altered compared to the control in plasma samples. In terms of the purified fibrinogen samples, there were no significant differences between treated and untreated cells on the clot structure.

5.4.1 Components of Particles

There were some differences between PM and diesel particles effects on HUVEC as PM had more critical effects compared to the diesel particles due to the differences on the components of these particles. Total diesel particles (SRM 2975) were collected from an industrial diesel-powered forklift and mainly contained PAHs and nitro-PAHs. However, PM_{10} (SRM 2787) contained not only PAHs, nitro-PAHs, but also polybrominated diphenyl ether (PBDE) congeners, hexabronocyclododecane (HBCD) isomers, sugars, polychlorinated dibenzo-p-dioxin (PCDD) and dibenzofuran (PCDF) congeners, inorganic constituents, especially metals, such as Zn, Fe and Cu. The differences of the components may account for the different effects on endothelial cells and clot structure.

5.4.2 Cytotoxicity

Cells were treated with endothelial cell growth media without fetal bovine serum. The serum contains albumin which could act as a metal chelator and thus reduce the effects of PM as both PM_{10} and $PM_{0.2}$ contained metals. After 24 hours treatment, these four particles did not cause any significant cell death. PM_{10} and total diesel particles were more toxic than their own filtered particles, but PM_{10} is the most toxic particle (PM_{10} > $PM_{0.2}$ > Total Diesel Particles >

Filtered Diesel Particles). Similar results were seen by Akhtar et al. (2010), although in a different cell line. In that study, human alveolar epithelial cells (A549) exposed to two particles, SRM 2795 and SRM 1648a (another type of urban particles from NIST), for 24 hours treatment from concentration 10 to 1000 µg/ml. MTT results showed SRM 1648a total urban particles lead to more cell death compared to SRM 2795 total diesel particles. At 50 µg/ml, SRM 2795 had no significant cytotoxicity compared to control (Akhtar et al., 2010). Snow et al. demonstrated ultrafine particles had no toxicity to human coronary artery endothelial cells at 50 µg/ml after 24 hours treatment. Ultrafine particles had similar sizes as $PM_{0.2}$ and filtered diesel particles (Snow et al., 2014). Another study investigated diesel particles cytotoxicity on human aortic endothelial cells and after 50 µg/ml concentration and 24 hours treatment, there was no significant cell death induced by diesel particles (Wu et al., 2012). However, PM and diesel particles can cause cellular death at high concentration and long term treatment; but in these experiments, the concentrations of PM and diesel particles used were non-toxic (cell viability > 80%) which indicated that the endothelial cells changed from normal physiological condition to procoagulant and anti-fibrinolytic status caused by endothelial dysfunction after treatment with PM and diesel particles rather than cell apoptosis.

It has been confirmed that after HUVECs 24 hours exposure to particulate matter and diesel particles, fibrin clots formed from normal pooled plasma samples were significantly denser compared to the controls. These four types of particles caused significantly denser fibrin clot structure from 10 µg/ml compared to control. Increased evidence supports that air pollution is linked with different CVD, and the patients with CVD have altered fibrin clot structure which was mentioned in Chapter 3 that patients with thromboembolic diseases had denser fibrin clot structure with more compact arranged network and prolonged lysis time. A study showed

that patients with peripheral artery disease were characterised by thrombotic fibrin clot phenotype with 32% lower clot permeability (Ks) (P <0.001) and 7% longer clot lysis time ($t_{50\%}$) (P = 0.004) compared with controls (Okraska-Bylica et al., 2012). The other study from Palka et al. also indicated that patients with chronic heart failure predisposed thromboembolic complications with 23% lower permeability (p < 0.0001), 13% less clot compaction (p < 0.001), 15% faster fibrin polymerisation (p < 0.0001) and prolonged lysis time (p = 0.1) compared to control (Palka et al., 2010).

As HUVECs formed denser fibrin clot structure after air pollution particles exposure, several methods were used to detect the underpinning mechanisms of fibrin clot structure alteration which were enzyme-linked immunosorbent assays, real time polymerase chain reaction assays and strand break assays. After 24 hours cells treatment, the gene expression of tissue factor and thrombomodulin were quantified in the RT-PCR experiments. Tissue factor gene expression by endothelial cells significantly increased after exposed to particles compared to control. The level of thrombomodulin mRNA decreased after particles exposure in a dose-dependent manner. ELISA results showed that both von Willebrand factor and plasminogen activator inhibitor-1 increased compared to the control. Through the plasmid strand break assay, free radicals were detected after the plasmid DNA was incubated with particles for 12 hours. The particles induced endothelial dysfunction with increased levels of von Willebrand factor, plasminogen activator inhibitor-1 and tissue factor mRNA expression, decreased level of thrombomodulin mRNA expression and oxidative stress may be caused by free radicals.

5.4.3   Tissue factor & Thrombomodulin

Tissue factor and thrombomodulin both are transmembrane proteins which were measured by using real time PCR.

Tissue Factor, formerly known as thromboplastin, is a key initiator of the coagulation cascade. TF is 47 kDa transmembrane glycoprotein containing 263 amino acids expressed in vascular and non-vascular cells (Napoleone et al., 1997). The TF gene is located on chromosome 1 and consists of 6 exons. Under normal physiological conditions, TF is only expressed in subendothelial cells such as vascular smooth muscle cells in response to the initiation of coagulation cascade when the vessel wall is damaged.

The tissue factor pathway of coagulation cascade is initiated when TF contacts with Factor VII and form the TF/FVIIa complex. Activated TF/FVIIa complexes convert FIX to FIXa, FX to FXa and FV to FVa. FXa and FVa cleave prothrombin to generate thrombin, thereby the fibrin clot is formed (Adams and Bird, 2009; Ajjan and Ariens, 2009; McVey, 1999; Steffel et al., 2006).

Endothelial cells and monocytes only express TF when the cells are exposed to stimuli such as cytokines (Steffel et al., 2006). Endothelial cells express TF when in contact with cytokines, e.g. tumor necrosis factor (TNF) -α, interleukin (IL) -1, or CD40 ligand; or biogenic amines, e.g. serotonin, or histamine; or mediators, e.g. thrombin, oxidized low density lipoprotein, or vascular endothelial growth factor (Steffel et al., 2005; Napoleone et al., 1997; Steffel et al., 2005; Kawano et al., 2001; Drake et al., 1991; Camera et al., 1999; Bavendiek et al., 2002).

The coagulation cascade is activated to protect from blood loss when the vessel wall is injured. Tissue Factor is the key initiator of coagulation cascade. However, heightened activation of

coagulation due to TF expression on endothelial cells and monocytes can cause thrombophilia and atherosclerosis (Steffel et al., 2006). In the RT-PCR experiments, tissue factor mRNA increased in a dose dependent manner. It indicated that air pollution particles act as stimuli when the endothelial cells were treated with particles, cells expressed more TF mRNA, and increased concentrations of particles triggered increased TF gene expression. Increased level of TF mRNA thereby increased the availability for exposure to FVII/FVIIa and more likely to activate the coagulation cascade. Tissue factor as the pathway initiator, forms complex TF/FVIIa with FVII, then in turn activates FIX, FX and FVIII. FXa and FVa cleave prothrombin to thrombin and sufficient amount of thrombin generates fibinogen to fibrin. There were also a few studies focused on the TF gene expression from endothelial cells after exposure to air pollution. Snow et al. Studied the effects of air pollution particles on human coronary arterial endothelial cells. Their results showed that soluble ultrafine particulate matter (diameter less than 0.1 μm) induced a significant 3.8 and 5.1 fold increased gene expression of TF after 50 and 100 μg/m^3 treatment respectively (Snow et al., 2014). Another study demonstrated the TF gene expression after human pulmonary arterial endothelial cells treated with ultrafine particulate matter. Four concentrations of PM$_{0.1}$ were used in this study, 0, 1, 10 and 100 μg/m^3, after treatment for 4 hours, expression level of TF was upregulated in a dose-dependent manner. In the Western blot analysis, as well as the results in RT-PCR, the protein expression of TF was increased after 18 hours particle treatment (Karoly et al., 2007). Milano et al. focused on different cell lines, macrophages, after exposure to different concentrations of PM$_{10}$, TF mRNA levels were consistantly increased from 10 to 100 μg/m^3 compared to the control in a dose-dependent manner (Milano et al., 2015).

Increased levels of TF expression is associated with elevated risks of procoagulability and increased tendency of thrombosis (Chu, 2005). Tissue factor initiates the extracellular coagulation which provokes the intracellular inflammation signalling. The coagulation factors (FVIIa, FXa, and thrombin) and fibrin are proinflammatory, all of which can activate the cells independently (Chu, 2005). Inflammation boosts coagulation through feedback upregulation on TF expression that sustains the coagulation TF pathway and coagulation dependent inflammation to refuel the coagulation-inflammation cycle. Therefore, regulation of TF expression is crucial in inhibition of coagulation-dependent inflammation (Chu, 2005).

Thrombomodulin, a transmembrane protein produced by endothelial cells, causes a transformation of thrombin from a pro-coagulant converter of fibrinogen to fibrin to an anti-coagulation activator of protein C. Activated protein C synergistically deactivates the coagulation cascade by supressing the activities of FVa and FVIIIa (Fuentes-Prior et al., 2000; Li et al., 2012). In this study, after endothelial cells were treated with different concentrations of PM, the results showed the mRNA level of thrombomodulin decreased in a dose-dependent manner. The reduced level of thrombomodulin may cause low level of activated protein C. In a cross-sectional study conducted in 2009-2010, after the healthy subjects were exposed to different levels of air pollution over 6 months, mRNA of THBD was measured. It indicated that the participants who exposed to high levels of PM_{10} had reduced level of THBD compared to those exposed to low levels of PM_{10}, although the difference was not significant (Poursafa et al., 2011). In an *in vitro* study, human coronary artery endothelial cells were incubated with 10, 50, and 100 μg/ml of soluble Ultrafine PM for 6 and 24 hours. The results showed that even after 24 hours and highest concentration of PM treatment, the level of THBD produced by treated cells were similar as untreated cells (Snow et al., 2014).

Besides the anti-coagulant function, thrombin-thrombomodulin complex also inhibits fibrinolysis by activating the thrombin activatable fibrinolysis inhibitor (TAFI) (Fuentes-Prior et al., 2000). TAFIa is activated by thrombin from TAFI. TAFIa removes COOH-terminal lysine residues from partially degraded fibrin and causes impaired fibrinolysis (Versteeg et al., 2013).

5.4.4   Von Willebrand Factor & Plasminogen Activator Inhibitor-1

Von Willebrand factor is a large glycoprotein which plays a pivotal role in haemostasis, circulating in human plasma at concentrations of 10 µg/ml. VWF is synthesized by vascular endothelial cells and encoded by a gene on chromosome 12 (Lenting et al., 2012; Mannucci, 1998; Vischer, 2006). VWF is secreted from endothelial cells in a bipolar manner, through both the luminal and abluminal membranes. When secreted through the luminal membrane, VWF directly reaches the bloodstream; when it is secreted through the abluminal membrane, VWF is deposited on the sub-endothelium as an extracellular matrix protein that helps to aggregate and activate platelets when the endothelium is disrupted (Mannucci, 1998).

VWF mediates platelet aggregation and adhesion to the site of vascular injuries, which is particularly important under high shear stress (Mannucci, 1998; Vischer, 2006). There are two platelets receptors for VWF in the platelets which are glycoprotein (GP) Ibα in the GP Ib-IX-V complex and the integrin $\alpha_{IIb}\beta_3$ (GP IIb-IIIa complex) (Ruggeri and Ruggeri ZM, 2003). VWF also acts as a plasma carrier for factor VIII and protects it from degradation and cellular uptake, when not bound to VWF the plasma half-life of FVIII is reduced from 12 hours to 1 to 2 hours

(Meyer et al., 2009; Ruggeri and Ruggeri ZM, 2003; Vischer, 2006). Pro-VWF is expressed in endothelial cells and platelets and stored in Weibel-Palade bodies and α-granules respectively.

An animal study investigated the effects of diesel particles on rats after exposed to 5 hours/day, 1 day/week for 16 weeks, the results demonstrated that as the mRNA levels pf TF, PAI-1 and VWF as the biomarkers of thrombosis were increased in the aorta (Kodavanti et al., 2011).

VWF contributes with atherothrombotic diseases and venous thromboembolism (Lenting et al., 2012). The connection between VWF and these two diseases was related to FVIII. VWF as the FVIII protein carrier, the levels of VWF and FVIII were closely correlated that high level of VWF induce high level of FVIII, which, contributes to atherothrombotic diseases and venous thromboembolism (Koster et al., 1995; Lenting et al., 2012, 1998). Several animal studies also provided evidence that inhibition and genetic deficiency of VWF protects against venous thrombosis (Brill et al., 2011; Chauhan et al., 2007; Lenting et al., 2012; Yamamoto et al., 1998).

Plasmin is the main fibrinolytic enzyme which can be activated by two serine proteases, tPA and uPA. PAI-1 supresses the fibrinolysis by inhibiting tPA and uPA. High plasma PAI-1 concentration is associated with many thrombotic disorders, thus it is considered as astrong marker of reduced fibrinolytic function (Kohler and Grant, 2000; Su et al., 2006). In this study, the results showed that, after endothelial cells were treated with those particles, the protein levels of PAI-1 increased in a dose-dependent manner. All types of particles, PM_{10}, $PM_{0.2}$, total diesel particles and filtered diesel particles induced significantly increased levels of PAI-1 expression from 10 μg/ml.

In an animal study, Budinger *et al*. indicated that after exposed to $PM_{2.5}$, mice had increased levels of PAI-1 mRNA and protein compared to the mice only exposed to filtered air (Budinger et al., 2011). In a panel study from Taiwan investigated the effects of urban air pollution on human. The results showed that after exposure to PM_{10} or $PM_{2.5}$ in single-pollutant models, healthy young humans had increased high-sensitivity C reactive protein, PAI-1, fibrinogen, and decreased heart rate variability, which indicated the potential mechanisms that urban air pollution was associated with inflammation, oxidative stress, blood coagulation and autonomic dysfunction (K. Chuang et al., 2007). However, Su et al. showed slightly different results that compared to the patients, PAI-1 levels were significantly elevated in the patients with CHD exposed to high level of air pollution. However, the PAI-1 levels in the participants with multiple CHD risk factors were not different whether exposed to high or low level of air pollution. This may suggest that urban air pollution probably caused adverse effects in plasma fibrinolytic function in the susceptible population (Su et al., 2006).

Fibrinolysis initiates when tPA and plasminogen both bind to the fibrin as plasmin is formed when plasminogen is partially cleaved by tPA on the surface of fibrin. The elevated level of PAI-1 effectively supresses fibrinolysis through inhibiting tPA and uPA, less plasmin is activated and impair fibrinolytic function, resulting in fibrin deposition in the vessel wall, thus facilitating thrombosis (Kohler and Grant, 2000). An impaired fibrinolytic system also contributes to thrombosis formation and propagation. Mills et al. recruited 30 healthy men in a double-blind, randomized, cross-over study to study the effects of diluted diesel particles. The level of tPA secreted from endothelial cells showed significant reductions after exposure to the diluted diesel exhaust compared with controls. The fibrinolytic function was impaired

and persisted for 6 hours after the exposure (Franchini and Mannucci, 2011; Mills et al., 2007, 2005). The reduction of tPA was possibly due to the increased secretion of PAI-1.

Elevated levels of PAI-1 are an independent risk factors for cardiovascular diseases in large prospective studies such as Northwick Park Heart Studies (Carter, 2005; Kohler and Grant, 2000).

5.4.5 Oxidative Stress

Plasmid strand break assay was used to test whether there were free radicals released from particles. Free radicals refer to the molecules possessing one or more unpaired electron (Bahorun et al., 2006; Halliwell and Gutteridge, 2007; Pham-Huy et al., 2008). Air pollutants are able to induce oxidative stress and inflammatory responses as pro-oxidants of lipids and proteins or as free radicals generators (Kampa and Castanas, 2008; Menzel, 1994; Rahman and MacNee, 2000). A previous study from this lab showed that diesel particles released free radicals. Therefore, plasmid strand break assay was used to detect whether particles triggered the free radicals. In accordance with the literature, the results showed that PM_{10}, $PM_{0.2}$, total diesel particles and filtered diesel particles released different amounts of free radicals in a dose-dependent manner that higher concentrations of particles lead to more plasmid DNA strand breaks. The free radicals released from those particles may be formed via the breakage of a chemical bond or via redox reactions (Halliwell and Gutteridge, 2007; Pham-Huy et al., 2008). Free radicals have adverse effects on cellular lipids, proteins, and also interfere with signalling pathways within the cells (Kampa and Castanas, 2008; Valko et al., 2007). PM and

diesel particles cause oxidative stress mainly through oxidant hydrogen peroxide (H_2O_2), free radical superoxide ($\cdot O_2-$), and free radical hydroxyl radical ($OH\cdot$) (Akhtar et al., 2010).

Free radicals are not only released from the air pollutants but also continuously produced during human normal metabolism and in response to exogenous environmental exposure. The cells used oxygen to generate energy, adenosine triphosphate (ATP) and free radicals are produced by the mitochondria as the consequence (Kampa and Castanas, 2008; Pham-Huy et al., 2008). The human body is able to produce antioxidants either in situ or externally supplied by food or supplements to neutralize the oxidative stress (Pham-Huy et al., 2008). As the concentration of free radicals increases and the imbalance between the two antagonistic effects comes into being, oxidative stress is generated and gradually plays the major role in a range of diseases, such as atherosclerosis, chronic inflammatory diseases, central nervous system disorders, age related disorders and finally cancer (Kampa and Castanas, 2008; Pham-Huy et al., 2008). As the components of these particles were different, among those components, PM were enriched in metals, such as Cu, Fe, and Zn which induced high concentrations of free radicals than diesel engine particles (Akhtar et al., 2010). Heavy metals also can induce free radical release and cause DNA damage (Kampa and Castanas, 2008).

5.4.6   Summary

This chapter focused on the effects of air pollution on human umbilical vein endothelial cells. These cells are in contact with blood and more likely to receive air pollution components when they get into the blood stream. These results provide a potential pathogenic role of PM

and diesel particles in endothelial cell system and imply that PM had more adverse effects compared to diesel particles. Furthermore, PM and diesel particles can cause cellular death at high concentration and long term treatment; but in these experiments, the concentrations of PM and diesel particles used were non-toxic (cell viability > 80%) which indicated that the endothelial cells changed from normal physiological condition to procoagulant and anti-fibrinolysis status were caused by endothelial dysfunction after treatment with PM and diesel particles rather than cell apoptosis.

This is the first study that investigated the structure of fibrin clots setting upon on the HUVEC after cells exposed to PM and diesel particles. The procoagulant and proinflammatory proteins and fibrinolysis inhibitors released from endothelial cells after 24 hours treatment with exposure to air pollution all contribute to endothelial dysfunction, fibrin clot structure alteration and prothrombotic tendency. The results in this study demonstrated that both PM and diesel particles caused impaired endothelial function with pro-inflammatory and oxidative state, thus induced the changes of fibrin clot structure formed from plasma samples.

Healthy endothelial cells have several functions such as anti-coagulation, anti-inflammation, anti-oxidation and pro-fibrinolysis. However, after the cells were exposed to air pollution particles, the endothelial cells were pro-inflammatory with increased TF gene expression, anti-fibrinolysis with increased levels of PAI-1 and decreased thrombomodulin mRNA expression and pro-oxidation. Also, as the increased VWF expression, platelets were promoted to aggregate. The significant elevation and reduction of levels of protein or gene expression expressed by HUVEC after exposed to air pollution particles not only indicated endothelial dysfunction but also contributed to the denser fibrin clot structure formation.

Many studies have confirmed that patients with thrombotic diseases had abnormal fibrin clot structure such as thinner fibres, more compact arrangements and prolonged lysis time. These features are in accordance with the clots formed from plasma samples on HUVEC after exposed to air pollution particles. Therefore, air pollution may contribute to the denser fibrin clot structure formation, thereby inducing a prothrombotic state.

6 Effects of Silicon Dioxide Nanoparticles on Fibrin Clot Structure

6.1 Introduction

Silicon dioxide nanoparticles (SiO_2 NP) are one the most widely applied engineered nanoparticles. SiO_2 NPs can be used as additives to cosmetics, printer toners, and varnishes. In addition, silica NPs are applied in biotechnological applications such as gene therapy, drug delivery, DNA transfection, and enzyme immobilization (Duan et al., 2014a; Napierska et al., 2010).

Owing to the wide applications, the cytotoxicity and other effects of SiO_2 NP were worth to be investigated. Some studies had shown that SiO_2 NP had does- and time- dependent manner on cell cytotoxicity (Ahamed, 2013; Eom and Choi, 2009; Napierska et al., 2010; Peters et al., 2004; Yang et al., 2014). Malvindi et al. documented that silica NPs had good biocompatibility when applied in a reasonable concentration, under 2.5 nM (Guo et al., 2015; Malvindi et al., 2012). However, as the diameter of nanoparticles are less than some of the cellular organelles, particles may penetrate the plasma membrane, deposit in mitochondria or nucleus, and finally lead to cell death (Guo et al., 2015; Liang et al., 2014; Zhu et al., 2013). The cardiovascular system may be affected by nanoparticles through direct interaction with vasculature, blood, and the heart (Guo et al., 2015; Nemmar et al., 2002). However, there were few related research focused on SiO_2 NPs. Therefore, this chapter would either confirm or deny that SiO_2 NPs was able to alter fibrin clot structure and cause endothelial dysfunction.

6.2 Methods

Silicon dioxide nanoparticle powder with size 10-20 nm was purchased from Sigma Aldrich. Particles were diluted with double distilled water, and the stock concentration was 1 mg/ml. Different concentrations of particle suspensions were used in the experiments which included 50 μg/ml, 10 μg/ml, 1 μg/ml, 0.1 μg/ml and 0.01 μg/ml. Different concentrations of SiO_2 NPs were added to normal pooled plasma and purified fibrinogen samples, respectively. Three methods, turbidity assay, turbidity lysis assay and laser scanning confocal microscope assay were used to analyse the fibrin clot structure formed with or without SiO_2 NPs. The details of the methods were as described in chapter 2.

Human umbilical vein endothelial cells were also used to investigate the effects of SiO_2 NPs. Particle cytotoxicity was firstly measured using MTT assay. Then, the clots were formed with plasma or fibrinogen samples on the cells. LSCM was used direct visualisation of fibrin clot structure.

To detect the mechanisms that how SiO_2 NP affected the fibrin clot structure, coagulation factors activation test, plasmid strand break assay, ELISA and RT-PCR were used.

6.3 Results

### 6.3.1 Effects of SiO_2 NPs on Fibrin Clot Structure

Three methods, turbidity assay, turbidity lysis assay, and laser scanning confocal microscope assay, were used to investigate the effects of SiO_2 NPs on fibrin clot structure.

Turbidity Assay

These figures represent the kinetic curves of the clots formation from plasma samples and purified fibrinogen samples with different concentrations of SiO_2 NPs. The curves showed a lag period before clots started to form (in some cases is this very short), an exponential growth phase during the clot rapidly formed and finally a plateau when the clots formed completely and reached the maximum OD value.

Normal Pooled Plasma Samples

In the normal pooled plasma samples, control had highest OD value and SiO_2 NPs caused decreased OD value as the concentration increased. But it is hard to say whether the fibre is thicker or thinner, as clots formed from plasma sample can lead to same OD value with either more number of thinner fibres or less number of thicker fibres.
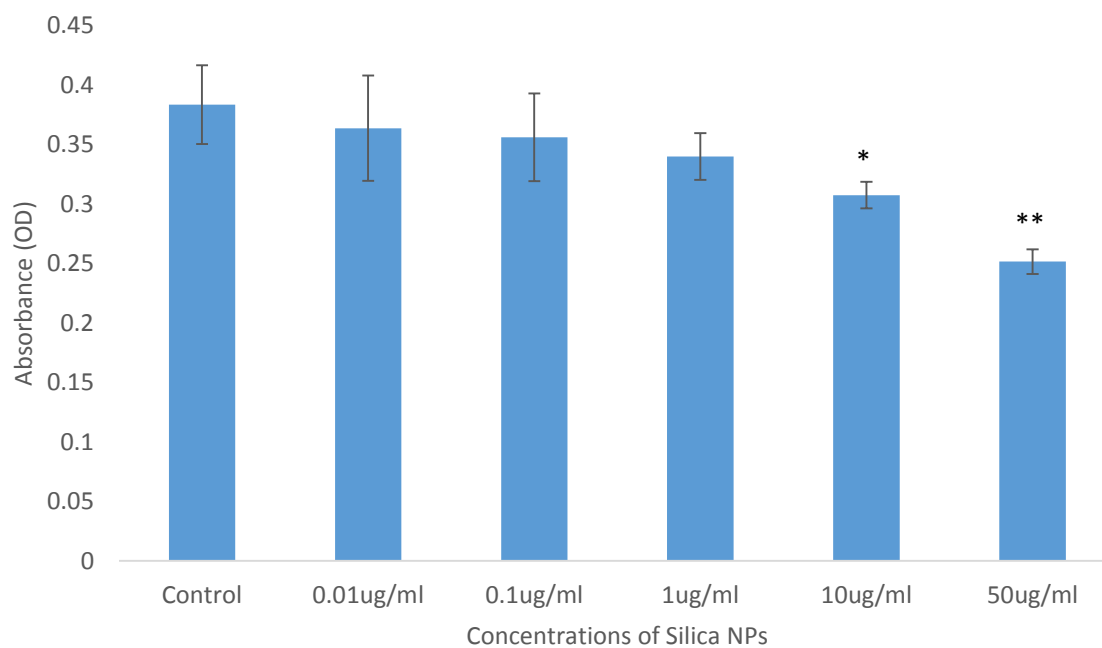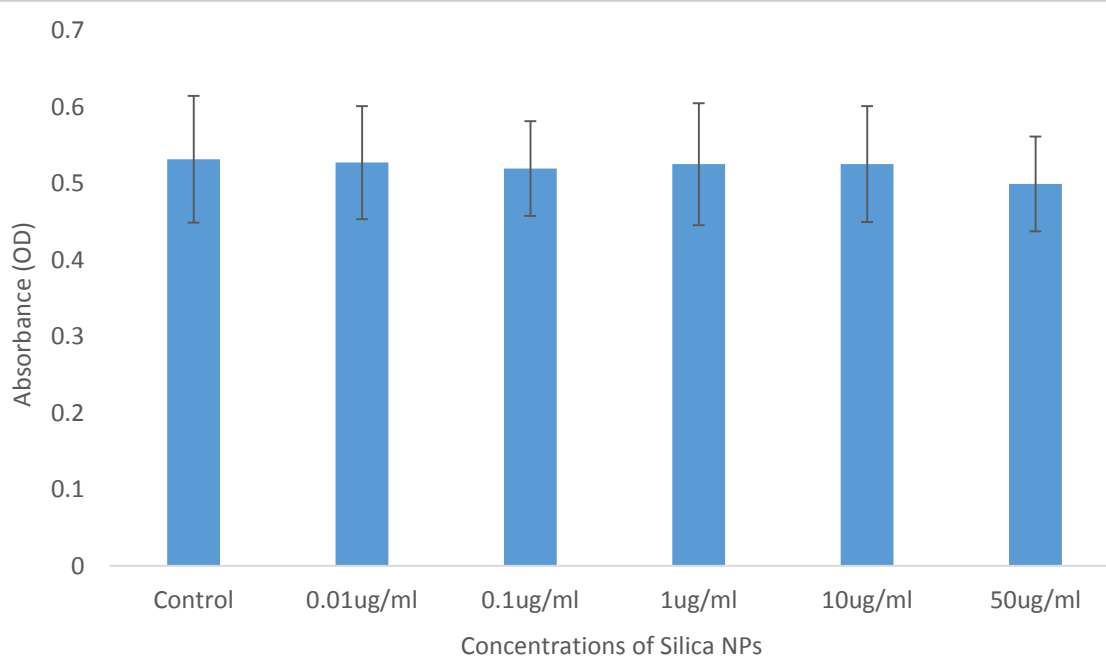
Figure 6-1. Turbidity Assay of SiO$_2$ NPs with Plasma Samples (n=5)

*$p<0.05$; **$p<0.001$

Fibrin clots were formed with plasma samples in the presence of silica nanoparticles. The final concentrations of thrombin and CaCl$_2$ were 0.1 U/ml and 5 mM respectively. The figure shows the maximum absorbance of the clots with different concentrations of particles.

Fibrinogen Samples

In the purified fibrinogen samples, there were no differences in the fibrin clot structure between different concentrations of SiO$_2$ NPs. The highest concentration of SiO$_2$ NPs and control had similar maximum OD value. The clots were formed similar structure even with different concentrations of SiO$_2$ NPs. This figure illustrated that silica nanoparticles had no effects on the fibrin clot structure formed from purified fibrinogen samples (Fig 6-2).

Figure 6-2. Turbidity Assay of SiO$_2$ NPs with Purified Fibrinogen Samples (n=5)

Fibrin clots were formed with purified fibrinogen samples in the presence of silica nanoparticles. The final concentrations of fibrinogen, thrombin and CaCl$_2$ were 1 mg/ml, 0.1 U/ml and 5 mM respectively. The figure shows the kinetic curve of the clots formation and maximum absorbance with different concentrations of particles.

Turbidity Lysis Assay

Normal Pooled Plasma Samples

The rate of clots degradation was measured by turbidity lysis assay. In the presence of particles, the maximum OD value was decreased as the concentrations of particles increased; but the time to 50% fibrinolysis (t$_{50\%}$) was similar between control and other concentrations of particles (figure 6-3).
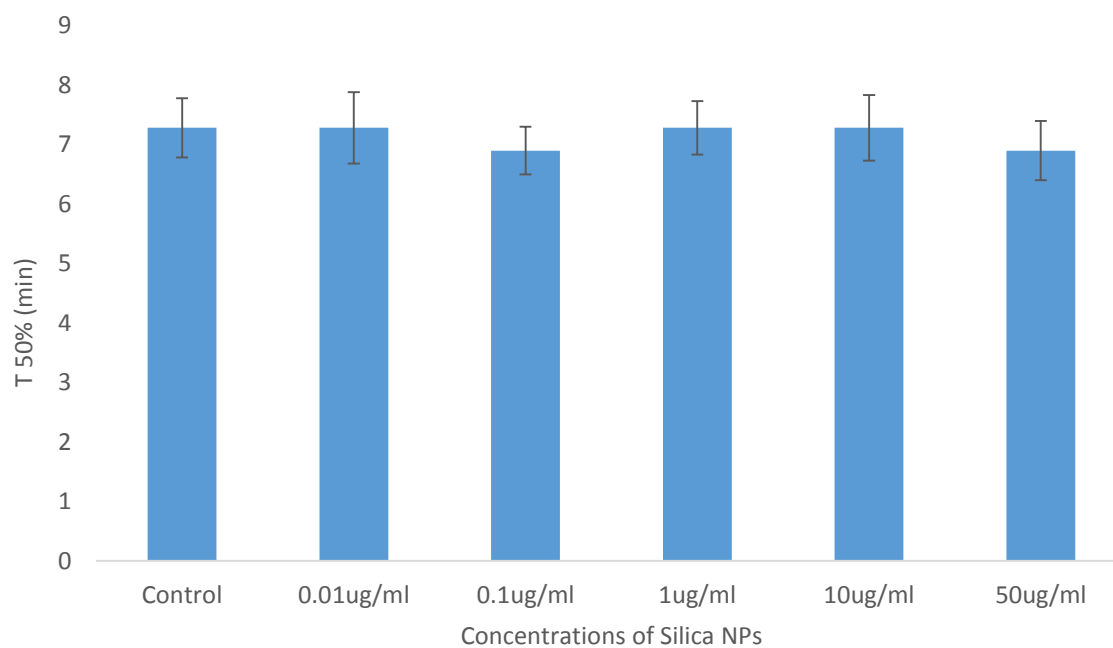
Figure 6-3. Turbidity Lysis Assay of SiO$_2$ NPs with Plasma Samples (n=3)

The T$_{50\%}$ were shown in the figure. The final concentrations of tPA, thrombin and CaCl$_2$ were 0.1 µg/ml, 0.1 U/ml and 5 mM respectively.

Purified Fibrinogen Samples

Similar results was found in the purified fibrinogen samples in that t$_{50\%}$ was similar between control and other concentrations of particles (figure 6-4). The silica nanoparticles did not cause any prolonged lysis time.
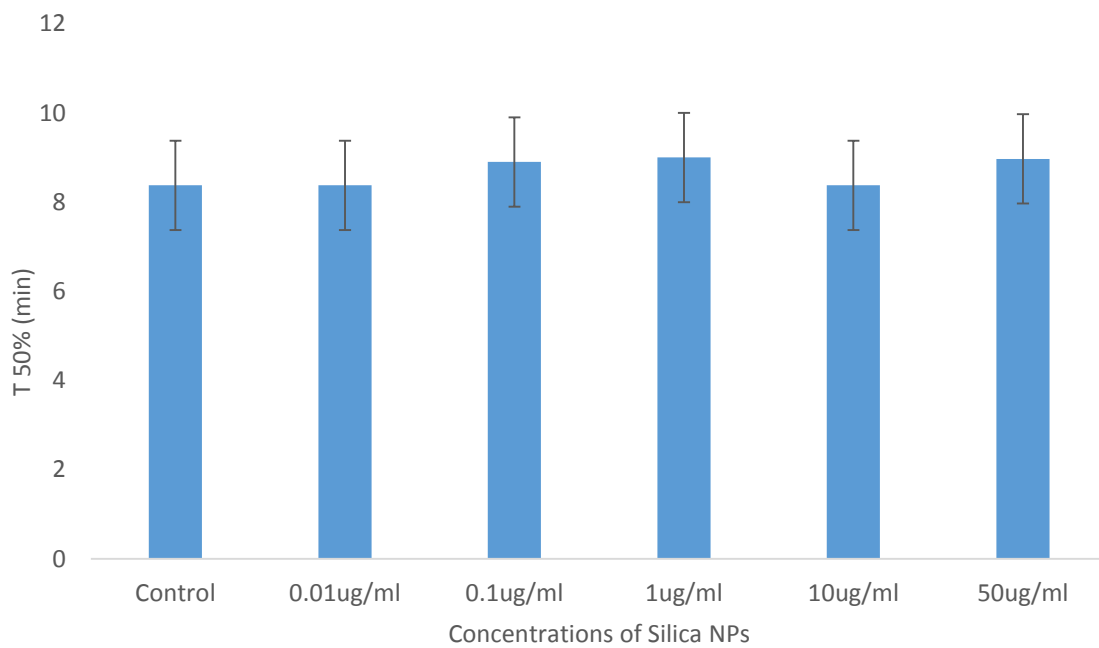
Figure 6-4. Turbidity Lysis Assay of SiO$_2$ NPs with Purified Fibrinogen Samples (n=3)

The clot lysis time was shown based on the concentrations and particle types. The final concentrations of fibrinogen, plasminogen, tPA, thrombin and CaCl$_2$ were 1 mg/ml, 0.25 µM, 0.1 µg/ml, 0.1 U/ml and 5 mM respectively.

LSCM

Fibrin clots were formed with either plasma or fibrinogen samples with different concentrations of SiO$_2$ NPs. The clot structure was visualised by LSCM and measured using Image J.

Normal Pooled Plasma Samples

In the normal pooled plasma samples, after adding the nanoparticles suspension, fiber bundles was increased as the concentration of particles increased. From 10 μg/ml, SiO_2 NPs caused significantly denser fibrin clot structure formation with increased numbers of fibers. Combined with the turbidity assay results, lower OD value indicated the denser fibrin clot structure formed from plasmas with different concentrations of SiO_2 NPs.
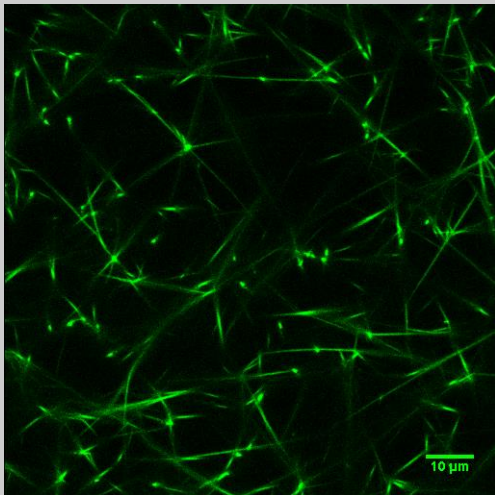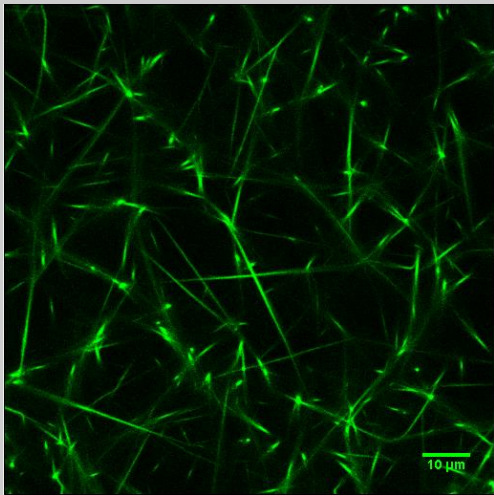
Control   0.01 µg/ml of SiO₂ NPs
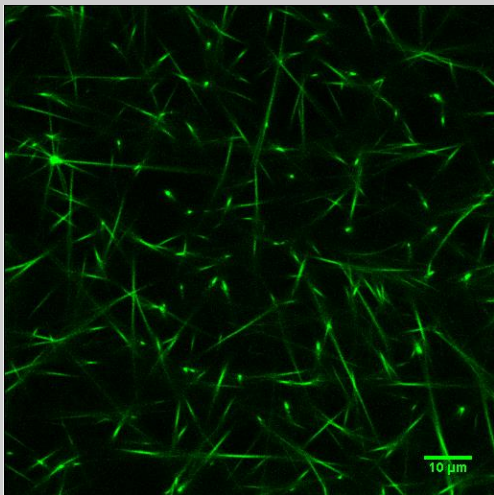
0.1 µg/ml of SiO₂ NPs   1 µg/ml of SiO₂ NPs
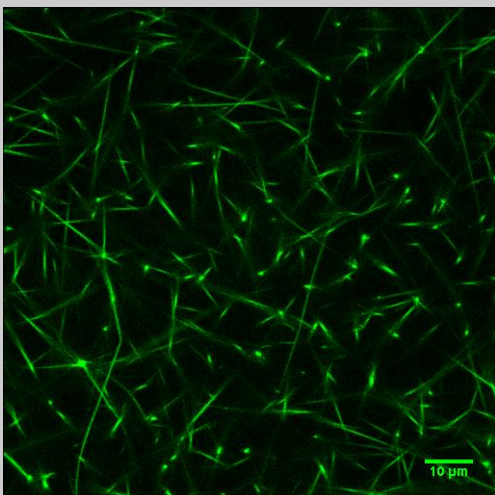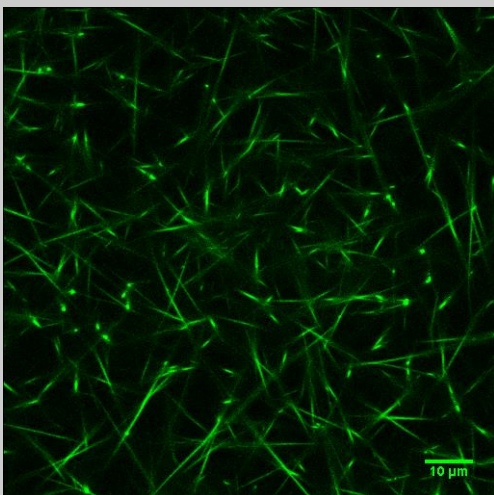
10 µg/ml of SiO₂ NPs   50 µg/ml of SiO₂ NPs
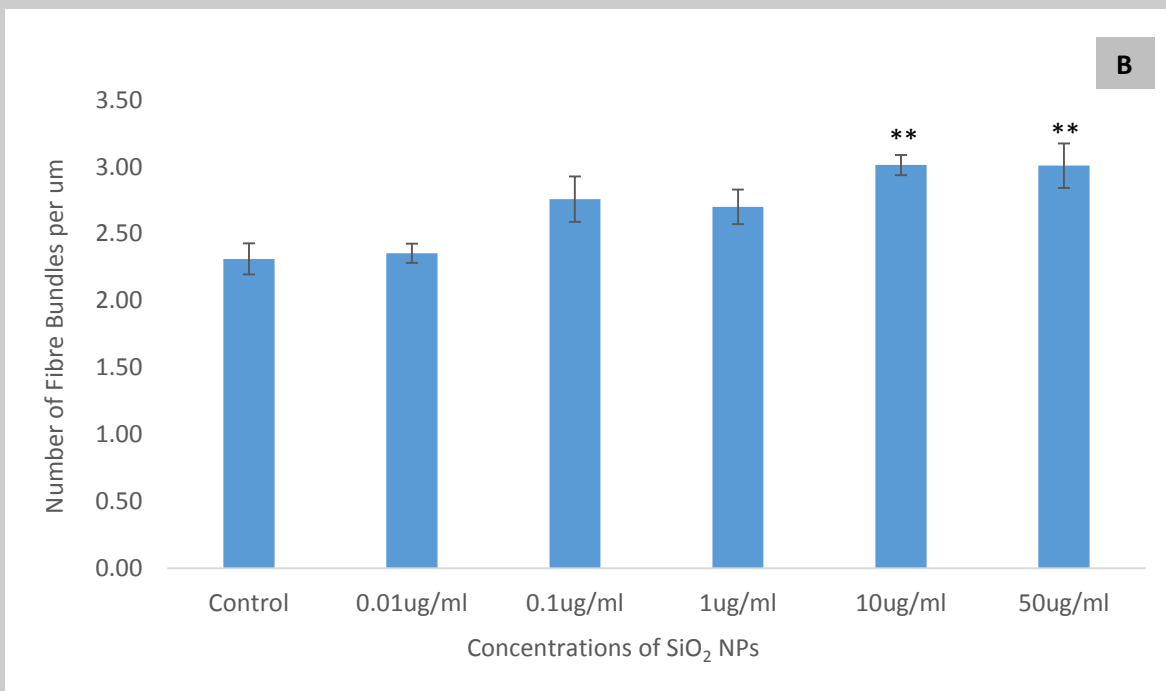
Figure 6-5 (A): LSCM—Clot Structure Formed from Plasma Samples with Different Concentrations of SiO₂ NPs;

Figure 6-6 (B): LSCM—Number of Fibre Bundles from Plasma Samples with Different Concentrations of SiO₂ NPs (n=9)

**p<0.001

The clots formed from plasma samples with SiO₂ NPs from 0 to 50 µg/ml. The final concentrations of thrombin, CaCl₂ and FITC were 0.5 U/ml, 15 mM and 50 µg/ml respectively.

Purified Fibrinogen Samples

In the purified fibrinogen samples, there were no significant differences between the clots with and without SiO₂ NPs which indicated that silica had no effects on purified fibrinogen system (Fig 6-6). The result in LSCM was consistent with the turbidity result.
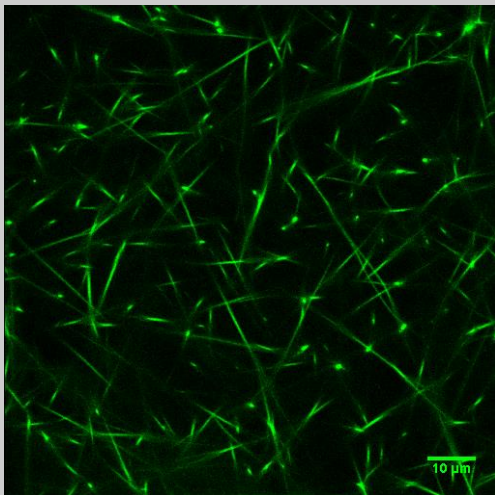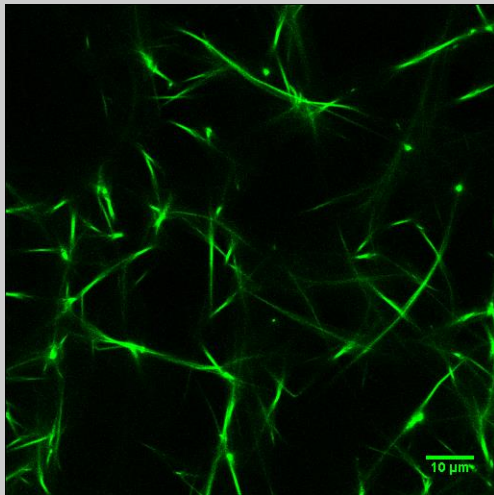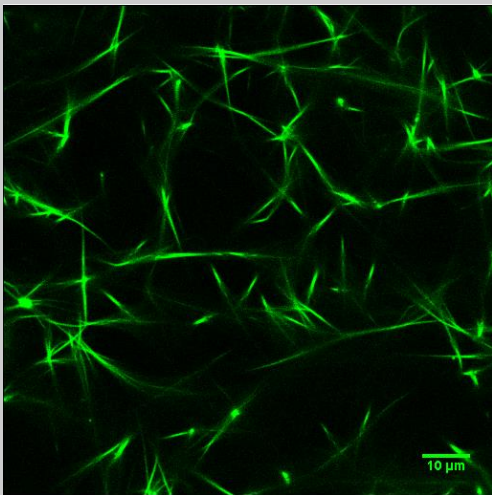
Control
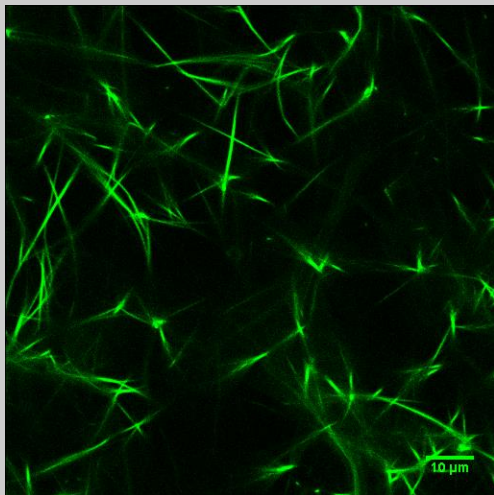
0.01 µg/ml of SiO$_2$ NPs
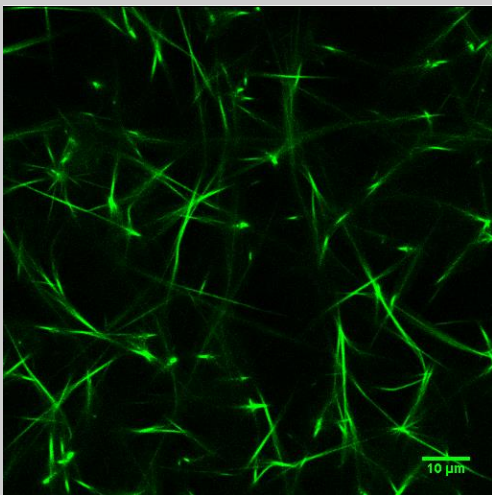
0.1 µg/ml of SiO$_2$ NPs
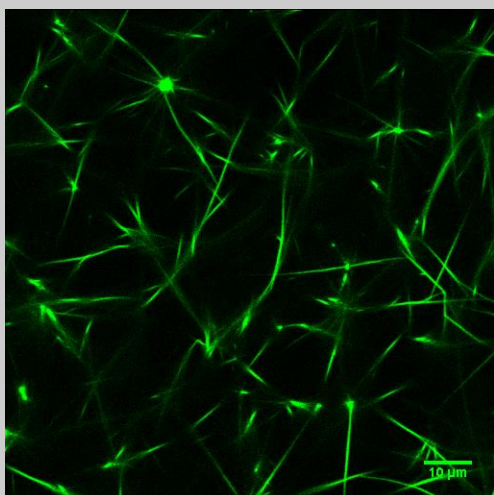
1 µg/ml of SiO$_2$ NPs
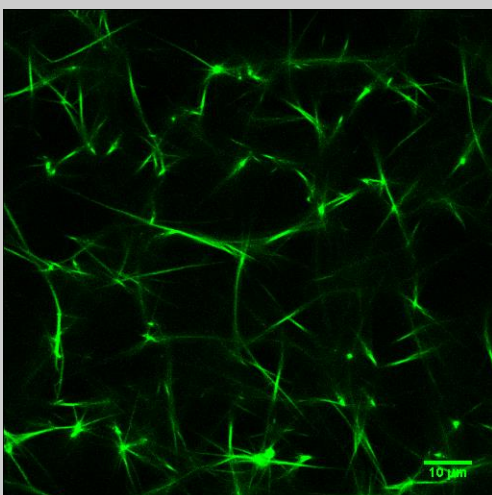
10 µg/ml of SiO$_2$ NPs

50 µg/ml of SiO$_2$ NPs
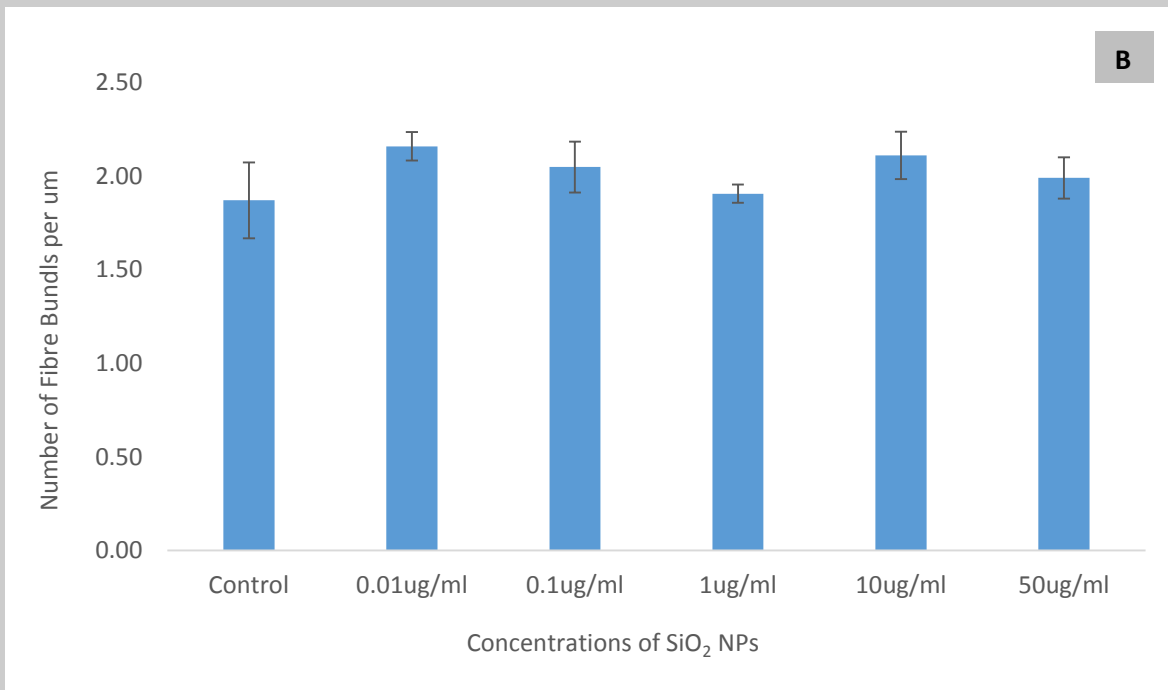
Figure 6-6 (A): LSCM—Clot Structure Formed from Purified Fibrinogen with Different Concentrations of SiO₂ NPs;

Figure 6-6 (B): LSCM—Number of Fibre Bundles from Purified Fibrinogen with Different Concentrations of SiO₂ NPs (n=9)

**p<0.001

The clots formed from purified fibrinogen with SiO_2 NPs from 0 to 50 µg/ml. The final concentrations of fibrinogen, thrombin, $CaCl_2$ and FITC were 1 mg/ml, 0.5 U/ml, 15 mM and 50 µg/ml respectively.

Factor XII Activation Test

The results of fibrin clot formed from plasma showed that the clots had become denser as the concentrations of silicon dioxide nanoparticles increased. A possible mechanism could be that the coagulation factors in plasma caused the dose-dependent effects which needed to be further investigated. Factor XII was tested to explore the reasons for denser fibrin clot formation as FXII is activated by negatively charged surfaces.

In the first method, FXII deficient plasma was used. In figure 6-7, the fibrin clots were formed from FXII deficient plasma with different concentrations of silicon dioxide nanoparticles and activation mixture. There was a trend that increased concentrations of SiO_2 NPs caused decreased OD value which were similar as the clot structure formed from normal pooled plasma. In figure 6-8, FXII zymogen was added to the clots with the presence of FXII deficient plasma, different concentrations of silicon dioxide nanoparticles and activation mixture. Similar trend was found as the clots formed from FXII deficient plasma without FXII zymogen. But in the presence of FXII zymogen, the clots were getting into the maximum absorbance faster with higher OD value. However, FXII zymogen seemed no effect on fibrin clot structure in the presence of SiO_2 NPs.
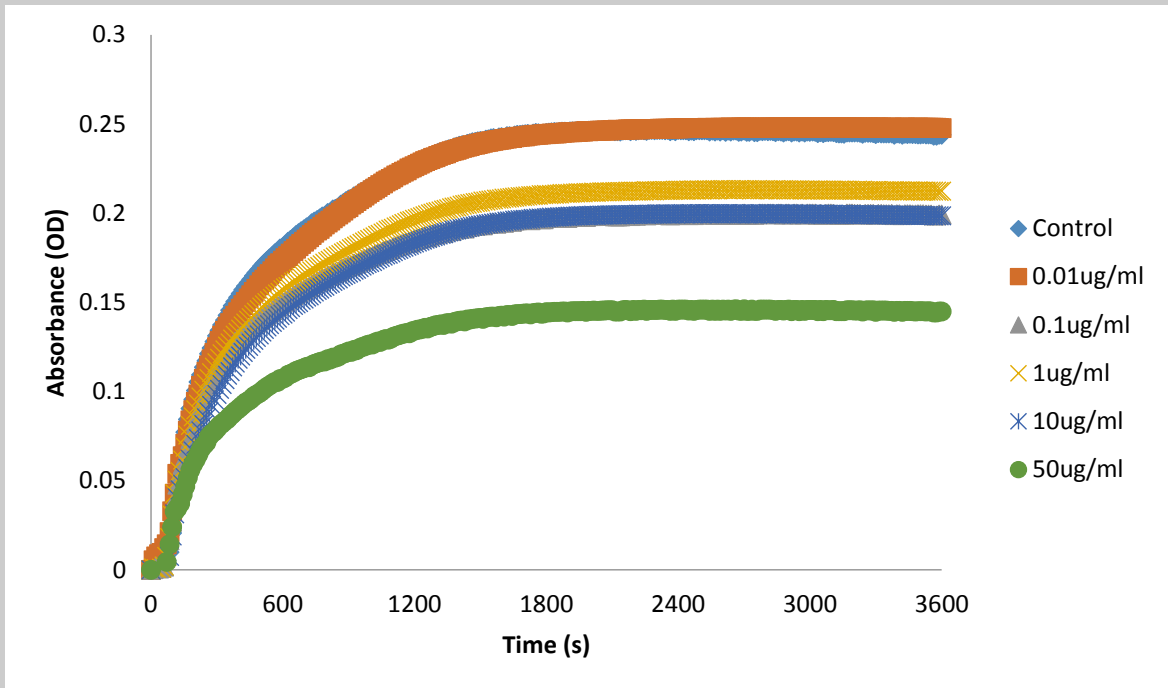
Figure 6-7: Turbidity Assay -- SiO₂ NPs with FXII deficient plasma (n=3)

The clots were formed with FXII deficient plasma and SiO₂ NPs 0 to 50 µg/ml.
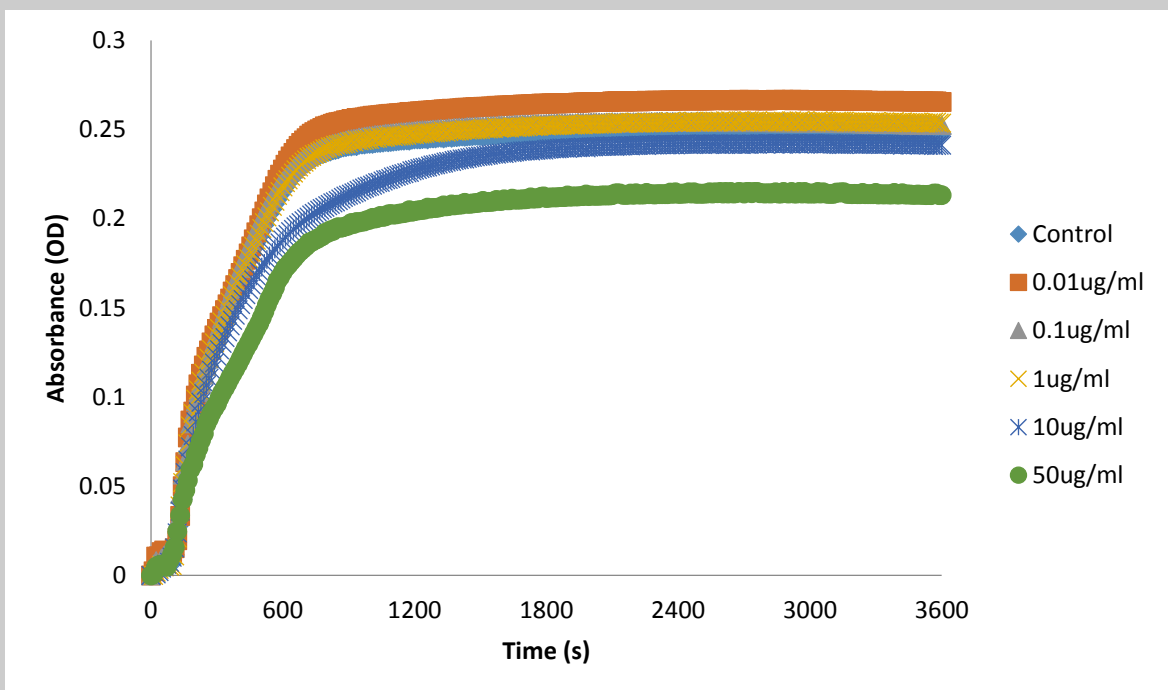
Figure 6-8: Turbidity Assay -- SiO₂ NPs with FXII deficient plasma and FXII zymogen (n=3)

The clots were formed with FXII deficient plasma, FXII zymogen and SiO₂ NPs 0 to 50 µg/ml.

In the second method, different concentrations of silica NPs were mixed with and without FXII zymogen. PTT automate as the positive control was added to FXII zymogen. Compared to the positive control in figure 6-9 (C), figure 6-9 (A) and 6-10 (B) illustrated silicon dioxide nanoparticle were not able to activate FXII zymogen. The OD value for the positive control was approximately 3.5 at 30 min. However, after 1 hour's interaction, the OD value was only 0.5 even with the highest concentration, 50 μg/ml. This method also showed the SiO₂ NPs was not able to activate FXII zymogen.
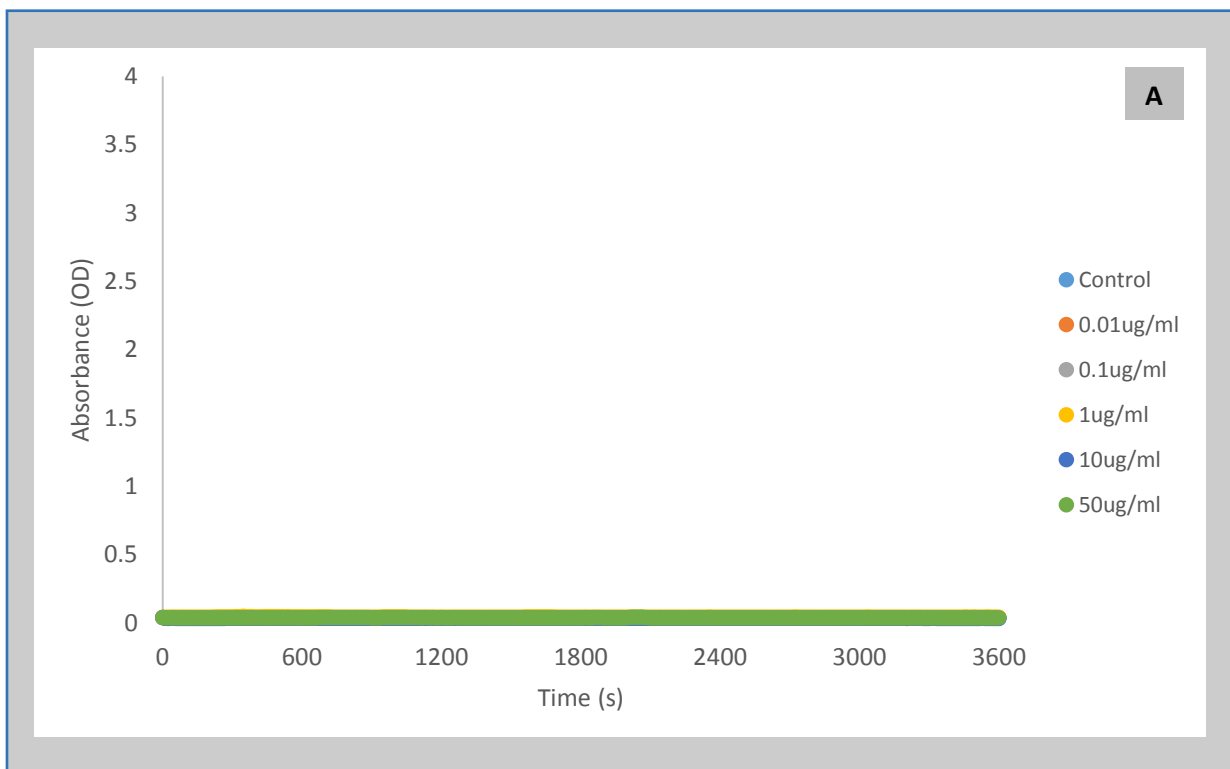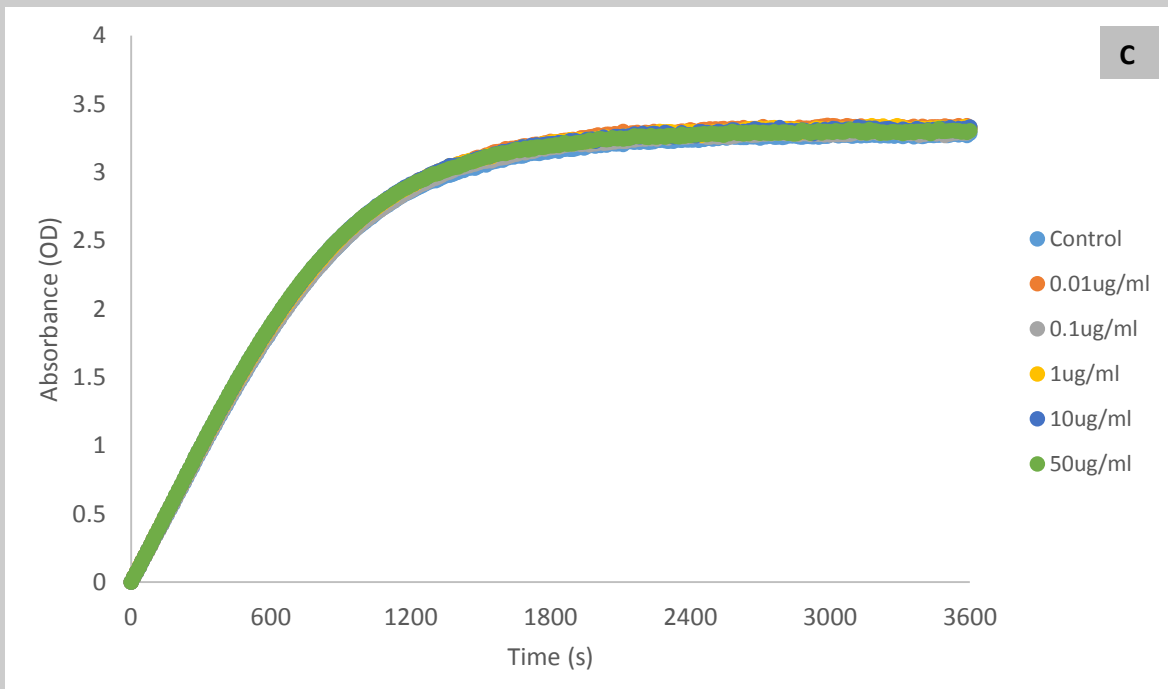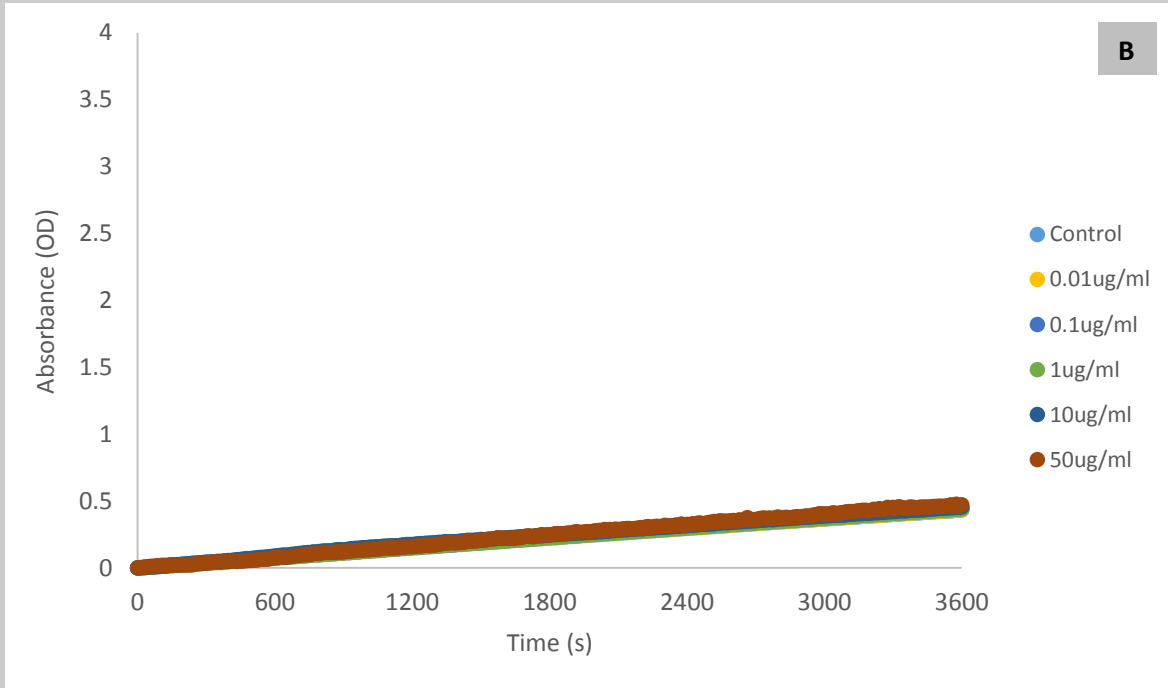
Figure 6-9 (A): Turbidity Assay -- SiO₂ NPs without FXII Zymogen (n=3);

Figure 6-10 (B): Turbidity Assay -- SiO₂ NPs with FXII Zymogen (n=3);

Figure 6-11 (C): Turbidity Assay -- SiO₂ NPs with PTT Automate and FXII Zymogen (n=3)

In Figure 6-9 (A), there were no clots formed as only SiO₂ NPs were added into the plate. In Figure 6-9 (B), SiO₂ NPs were mixed with FXII zymogen, the final concentration of FXII zymogen was 125 nM. In Figure 6-9 (C), PTT was added to the mixture as the positive control.

Therefore, these two methods confirmed that silica NPs did not react with FXII, thus FXII was not the reason for denser fibrin clot structure in the presence of SiO_2 NPs.

Plasmid Strand Break Assay

Plasmid strand break assay was used to detect the free radicals released from the silicon dioxide nanoparticles when they were incubated with supercoiled plasmid DNA.

After 12 hours incubation in the dark, silica NPs did not have more free radical released compared to control (Fig 6-10). The nicked plasmid was between 10 to 20% after the plasmid pBR322 incubated with 0 to 50 µg/ml of SiO_2 NPs. This result indicated that silicon dioxide nanoparticles were not able to release free radicals.
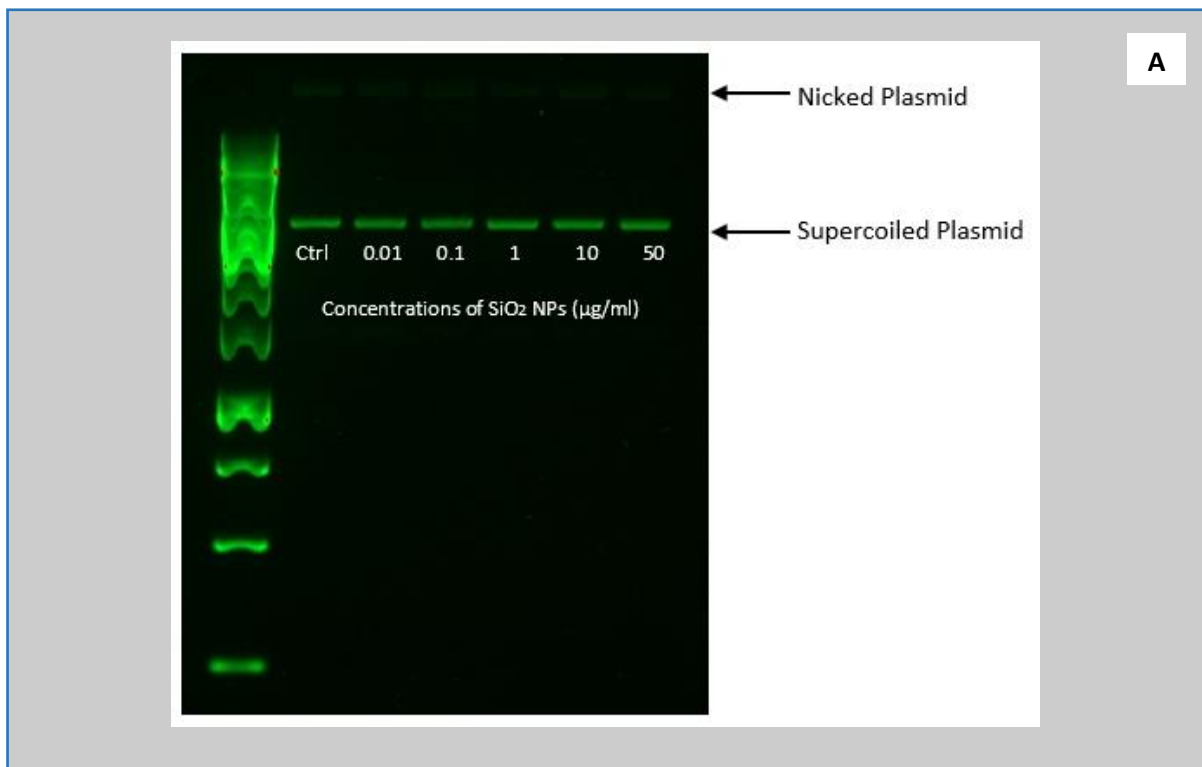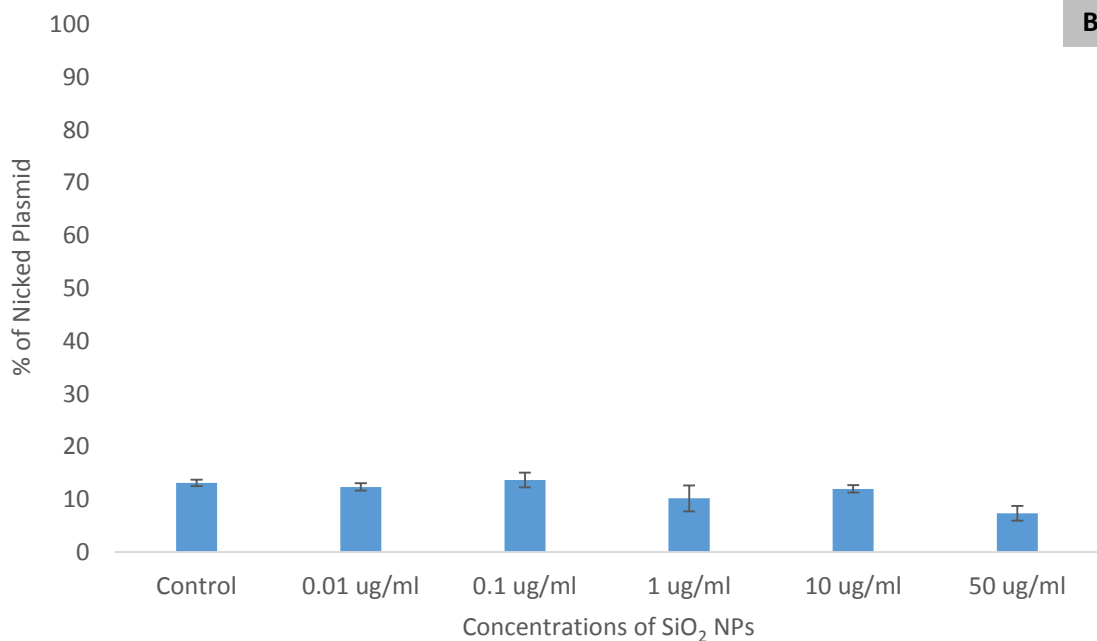
Figure 6-12. Induction of Single Stand Breaks in pBR322 DNA following Incubation with SiO₂ NPs (n=6)

Plasmid DNA was incubated with SiO_2 NPs from 0 to 50 µg/ml for 12 hours in the darkness. The induction of strand breaks were assessed and expressed as the percentage of nicked DNA observed. The results indicated that there were no significantly higher number of stand breaks caused by SiO_2 NPs.

6.3.2   Effects of SiO₂ NPs on HUVEC

To investigate the effects of SiO_2 NPs on fibrin clot structure formed from plasma and fibrinogen samples were not enough, which was not able to represent the in vivo environment. Human umbilical vein endothelial cells were used to develop mechanisms of the effects of SiO_2 NP.

Endothelial Cell Cytotoxicity

Human umbilical vein endothelial cells were treated with 50 μg/ml, 10 μg/ml, 1 μg/ml, 0.1 μg/ml, and 0.01 μg/ml of silicon dioxide nanoparticles for 24 hours.

Figure 6-13. Cytotoxicity of Endothelial Cells after 24 hours SiO₂ NPs Treatment (n=9)
Cells were treated for 24 hours with different concentrations of SiO₂ NPs. After the cells exposed to 10 μg/ml of particles, there were approximately 10% cell death which was significantly more compared to control.
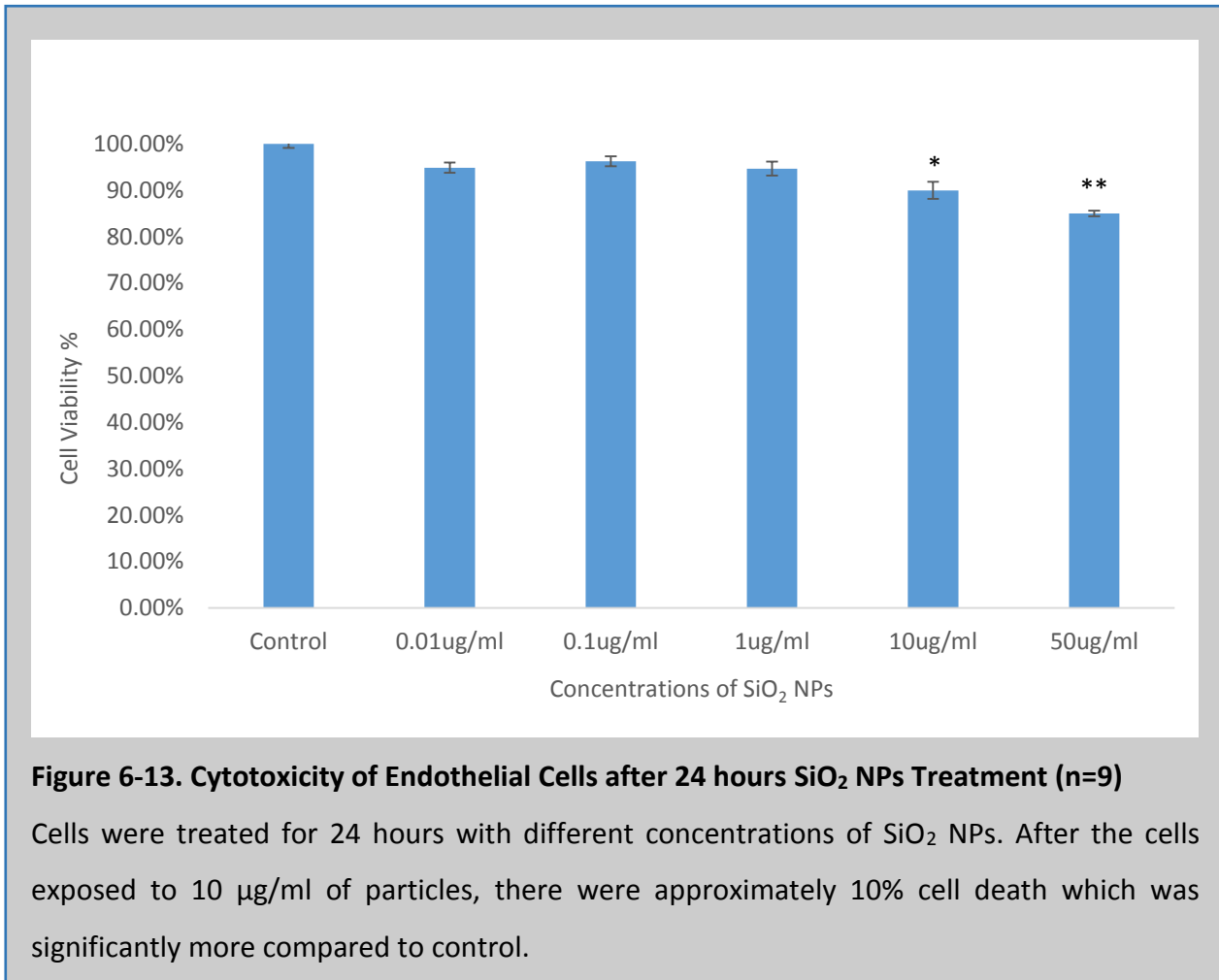
Fibrin Clot Formation on Endothelial Cells

After the cell cytotoxicity test, LSCM was used to investigate the fibrin clot structure. The clots were set up on the cells after HUVECs were treated with different concentrations of SiO₂ NPs for 24 hours. Cell supernatant was removed completely and the clots were formed from

either normal pooled plasma samples or purified fibrinogen with thrombin and $CaCl_2$ upon the treated cells. The slides were incubated at 37 degree for 30 minutes which allowing the clots for form completely. The structure of the fibrin was analysed through confocal microscope.

Normal Pooled Plasma Samples

The fibrin clot structure formed from normal pool plasma samples in the presence of treated cells are shown below. After the cells were treated with SiO_2 NPs at concentration of 0.01 µg/ml, 0.1 µg/ml, 1 µg/ml 10 µg/ml and 50 µg/ml, the fibrin clot structure was altered compared to control. As the concentration of particles increased, the clot structure became much denser with increased number of fibres per µm in a dose-dependent manner. The clots had significant denser structure from the concentration of 1 µg/ml.
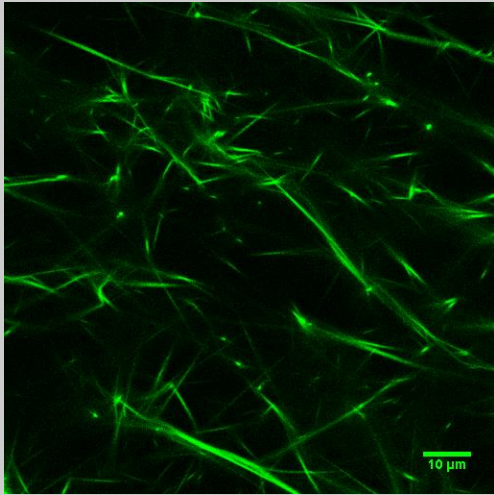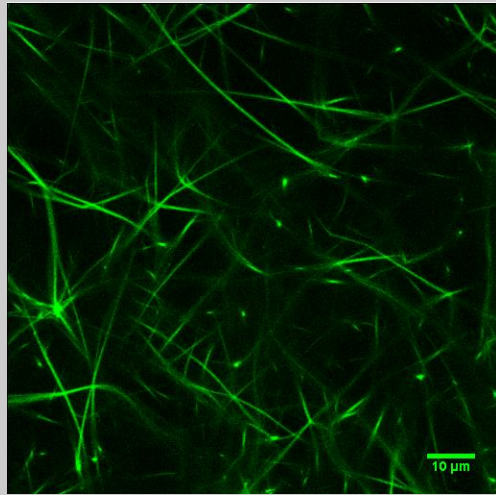
Control
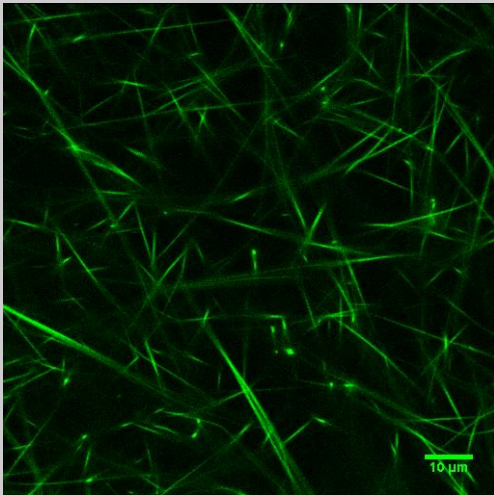
0.01 µg/ml of SiO$_2$ NPs
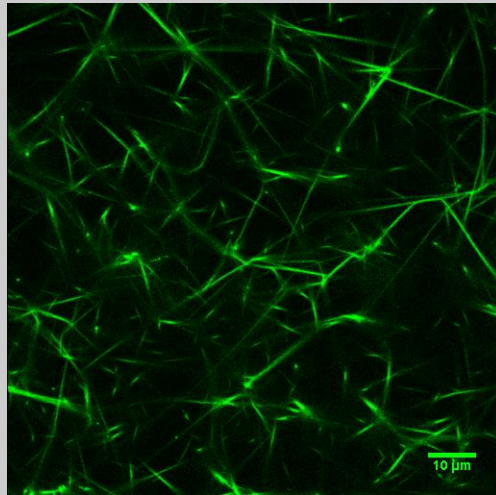
0.1 µg/ml of SiO$_2$ NPs
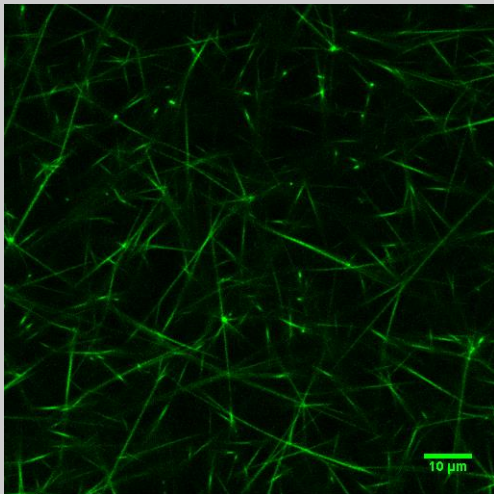
1 µg/ml of SiO$_2$ NPs
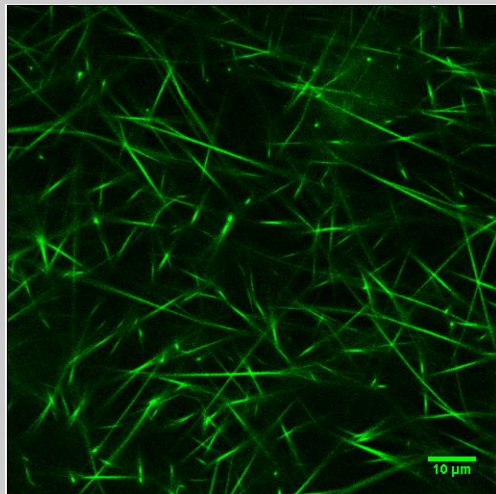
10 µg/ml of SiO$_2$ NPs

50 µg/ml of SiO$_2$ NPs
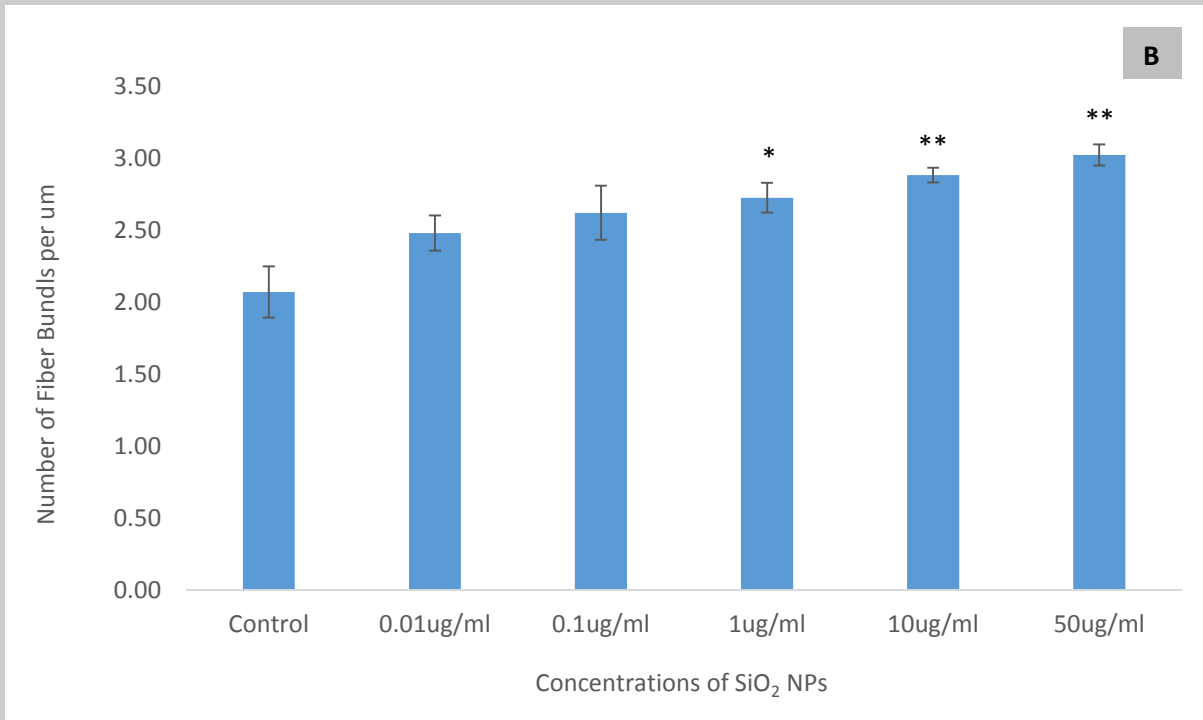
Figure 6-14 (A): LSCM—Clot Structure Formed from Plasma Samples on Human Umbilical Vein Endothelial Cells after Treatment with Different Concentrations of SiO₂ NPs;

Figure 6-15 (B): LSCM—Number of Fibre Bundles from Plasma Samples on Human Umbilical Vein Endothelial Cells after Treatment with Different Concentrations of SiO₂ NPs (n=9)

*$p<0.05$; **$p<0.001$

The clots formed from plasma samples in the presence of cells exposed to SiO_2 NPs s from 0 to 50 µg/ml. The final concentrations of thrombin, $CaCl_2$ and FITC were 0.5 U/ml, 15 mM and 50 µg/ml respectively.

Purified Fibrinogen Samples

For the fibrinogen samples, the clots were formed with purified fibrinogen samples in the presence of treated endothelial cells. The data showed even after the cells treated with the highest concentration of those particles, the fibrin clot structure was similar as the control. In contrast to the clots formed from plasma, the clots formed from purified fibrinogen did not have any significant difference in the structure between treated and untreated cells.
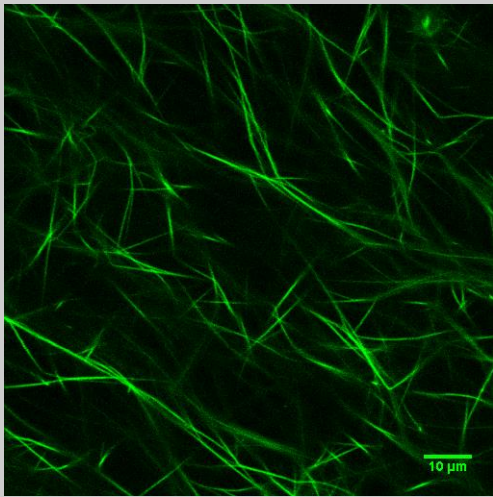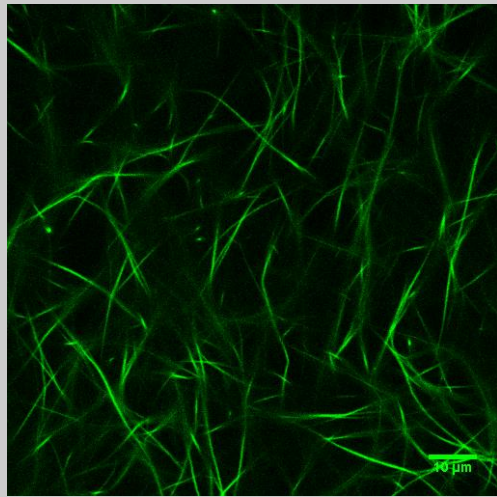
Control   0.01 µg/ml of SiO$_2$ NPs
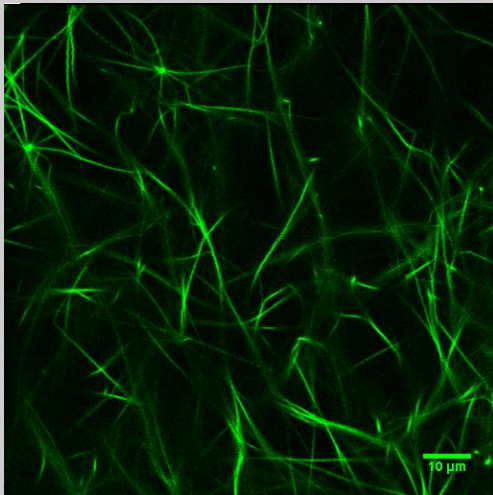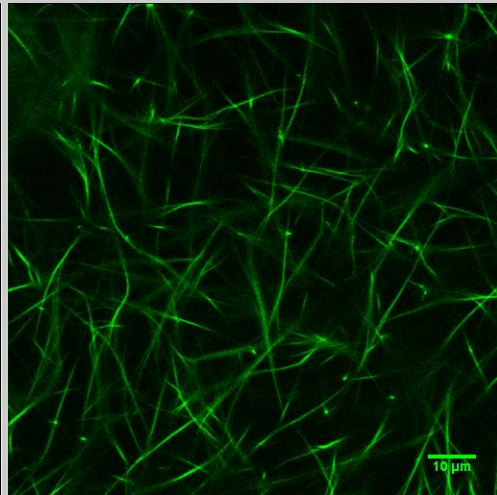
0.1 µg/ml of SiO$_2$ NPs   1 µg/ml of SiO$_2$ NPs
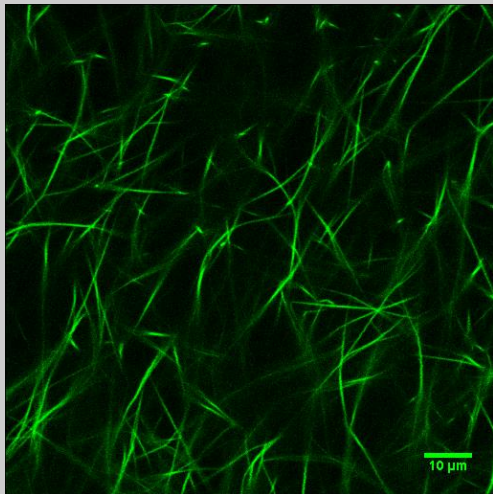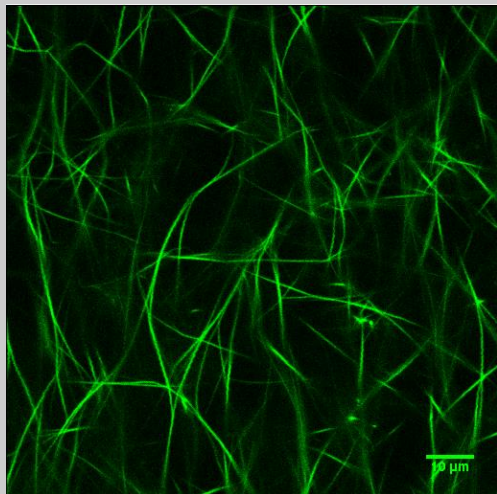
10 µg/ml of SiO$_2$ NPs   50 µg/ml of SiO$_2$ NPs
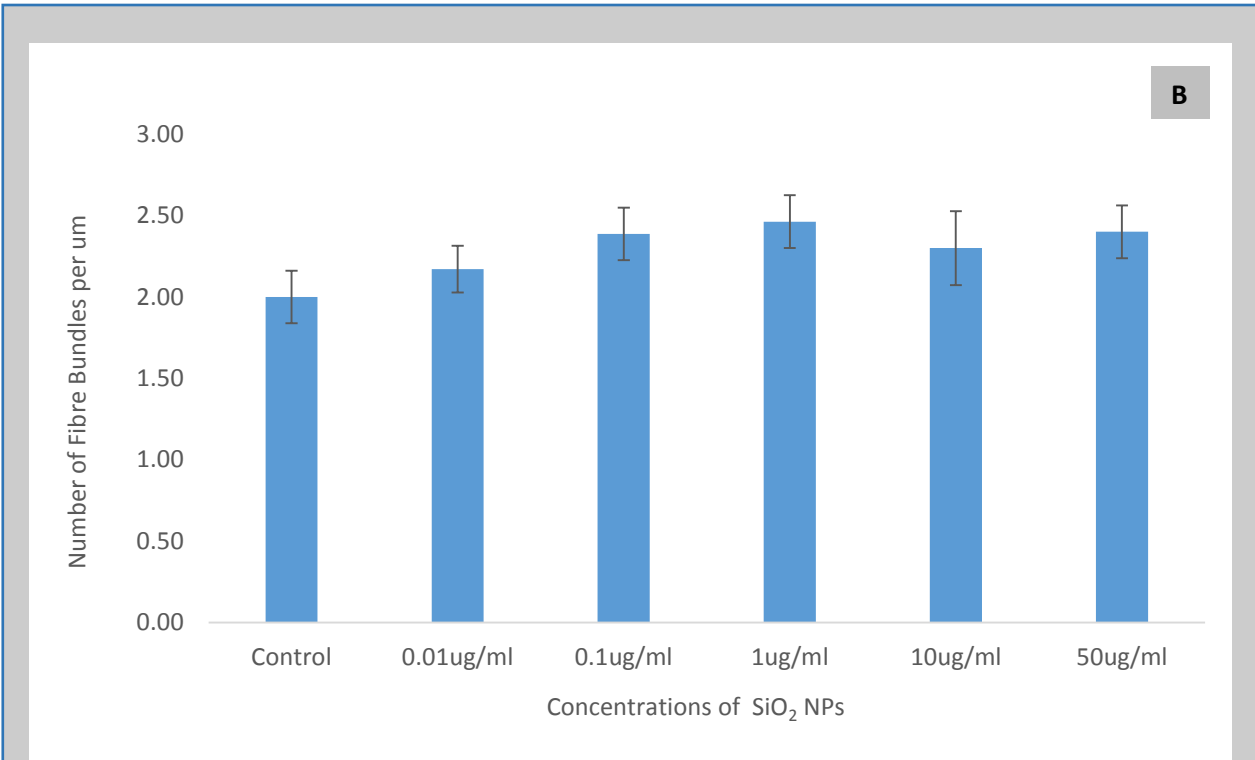
Figure 6-16 (A): LSCM—Clot Structure Formed from Purified Fibrinogen on Human Umbilical Vein Endothelial Cells after Treatment with Different Concentrations of SiO₂ NPs;

Figure 6-17 (B): LSCM—Number of Fibre Bundles from Purified Fibrinogen on Human Umbilical Vein Endothelial Cells after Treatment with Different Concentrations of SiO₂ NPs (n=9)

The clots formed from purified fibrinogen in the presence of cells exposed to SiO$_2$ NPs s from 0 to 50 μg/ml. The final concentrations of fibrinogen, thrombin, CaCl$_2$ and FITC were 1 mg/ml, 0.5 U/ml, 15 mM and 50 μg/ml respectively.

RT-PCR

Real time polymerase chain reaction was used to quantify the genes of interests that released from endothelial cells after incubation with silicon dioxide nanoparticles for 24 hours. Two different genes, tissue factor and thrombomodulin, were measured by RT-PCR.

Tissue Factor

Tissue factor is a transmembrane glycoprotein. After endothelial cells were incubated with the particles for 24 hours, the gene expression of tissue factor was quantified by RT-PCR. Concentrations of SiO_2 NPs were 0.01 µg/ml, 0.1 µg/ml, 1 µg/ml, 10 µg/ml and 50 µg/ml were used. Compared to control, there were no significant difference in the TF gene expression after HUVEC treated with SiO_2 NPs.

Figure 6-18. Relative Gene Expression Level of Tissue Factor (TF) in Human Umbilical Vein Endothelial Cells after Treatment with Different Concentrations of SiO_2 NPs (n=3)

Relative gene expression level of tissue factor was determined by real-time polymerase chain reaction.
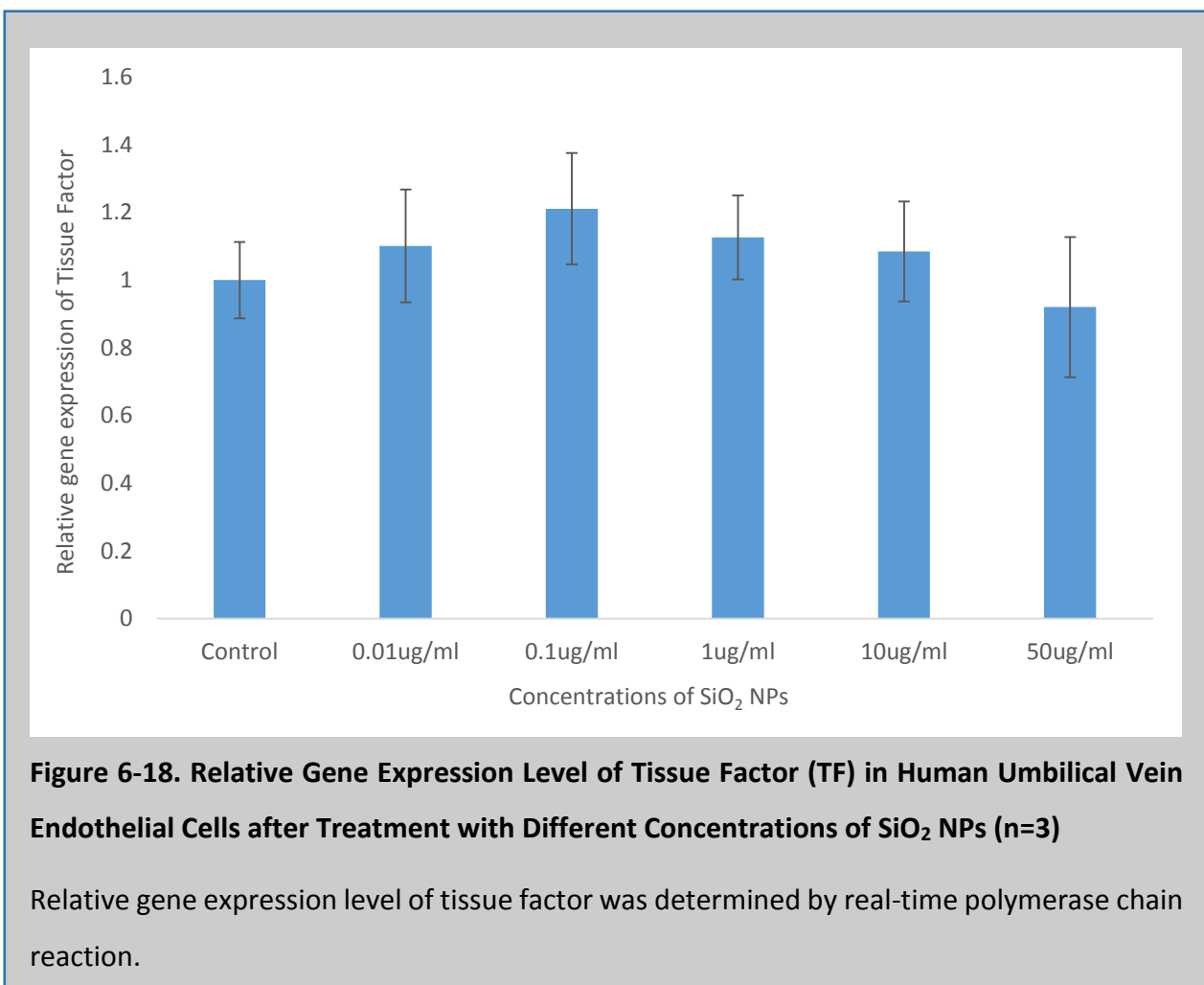
Thrombomodulin

Thrombomodulin is produced by endothelial cells. After the cells were treated with SiO_2 NPs, increased concentrations of SiO_2 NPs caused decreased thrombomodulin mRNA secretion with a dose-dependent manner. From 10 µg/ml of SiO_2 NPs, the level of THBD gene expression was decreased significantly compared to control. Figure 6-15 showed that SiO_2 NPs inhibited the THBD gene expression on HUVEC.
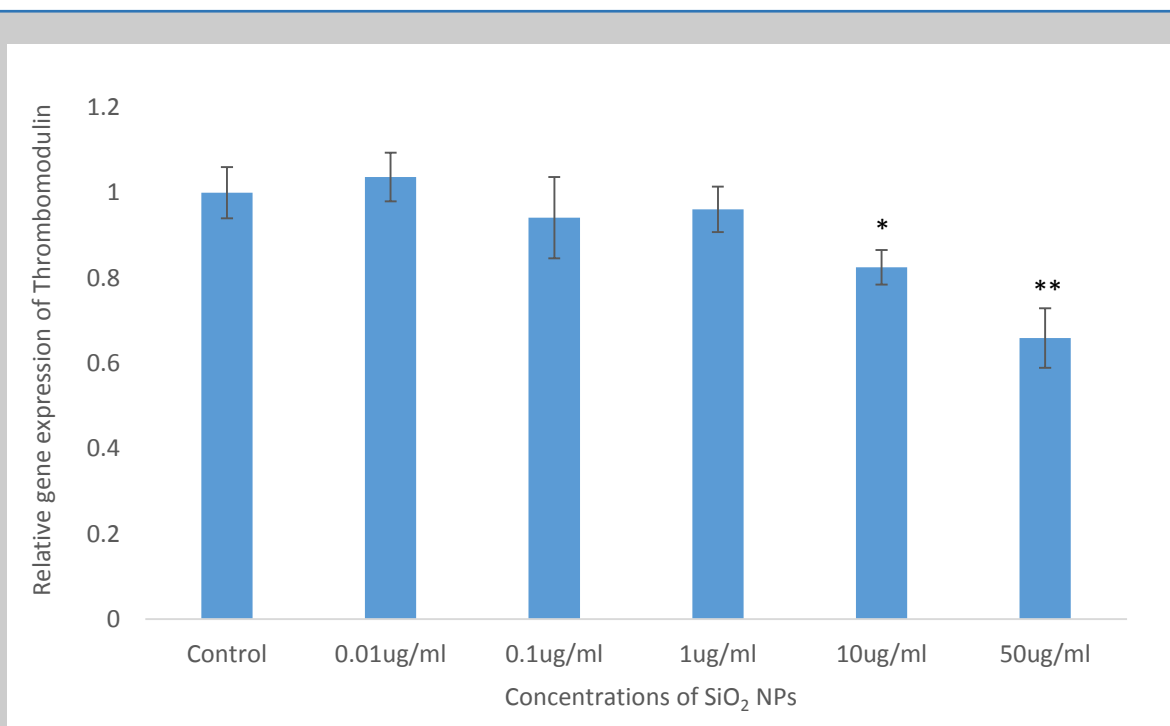
Figure 6-19. Relative Gene Expression Level of Thrombomodulin (THBD) in Human Umbilical Vein Endothelial Cells after Treatment with Different Concentrations of SiO_2 NPs (n=3)

Relative gene expression level of thrombomodulin was determined by real-time polymerase chain reaction. The THBD mRNA level was decreased as the concentrations of SiO_2 NPs increased.

ELISA

ELISA was used to quantify the protein level of von Willebrand factor and plasminogen activator inhibitor-1 produced by endothelial cells after the stimuli by air pollution particles.

Von Willebrand Factor

HUVEC were treated with different concentrations of SiO_2 NPs for 24 hours. The cell supernatant was taken for the measurement of protein levels of VWF produced by cells. Figure 6-12 showed that after 10 μg/ml of SiO_2 NPs treatment, endothelial cells produced significantly high levels of VWF with concentration of 9.8 ng/ml. From 0.01 μg/ml to 50 μg/ml of SiO_2 NPs, VWF secretion increased gradually in a dose-dependent manner.
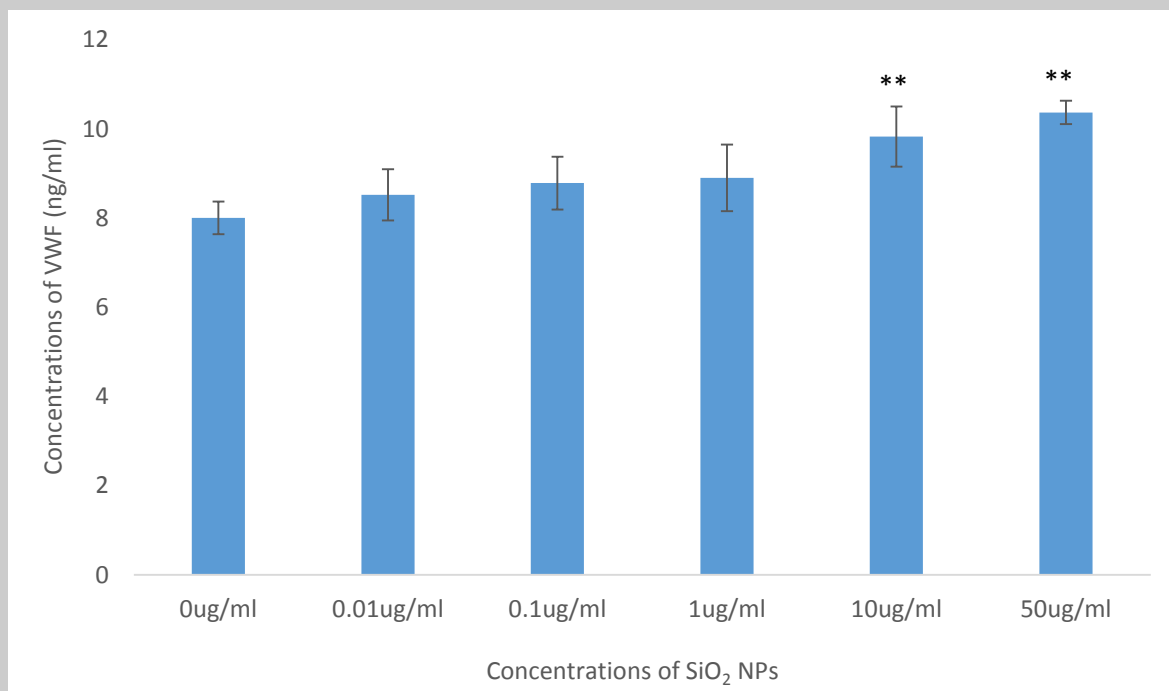
Figure 6-20. ELISA -- Concentrations of Von Willebrand Factor (VWF) from Human Umbilical Vein Endothelial Cells after 24h Treatment with Different Concentrations of SiO₂ NPs (n=3) **p<0.001

ELISA was used to measure the VWF protein levels. After the cells were treated different concentrations of SiO_2 NPs for 24 hours, the cell supernatant was taken and measured the concentrations of VWF released from cells. From 10 μg/ml, SiO_2 NPs induced significantly more VWF secretion from endothelial cells.

Plasminogen Activator Inhibitor - 1

After the endothelial cells were treated with different concentrations of silica nanoparticles, PAI-1 was produced at similar levels. There were no significant higher concentrations of PAI-1 secreted by treated cells compared to control (as shown in figure 6-13).
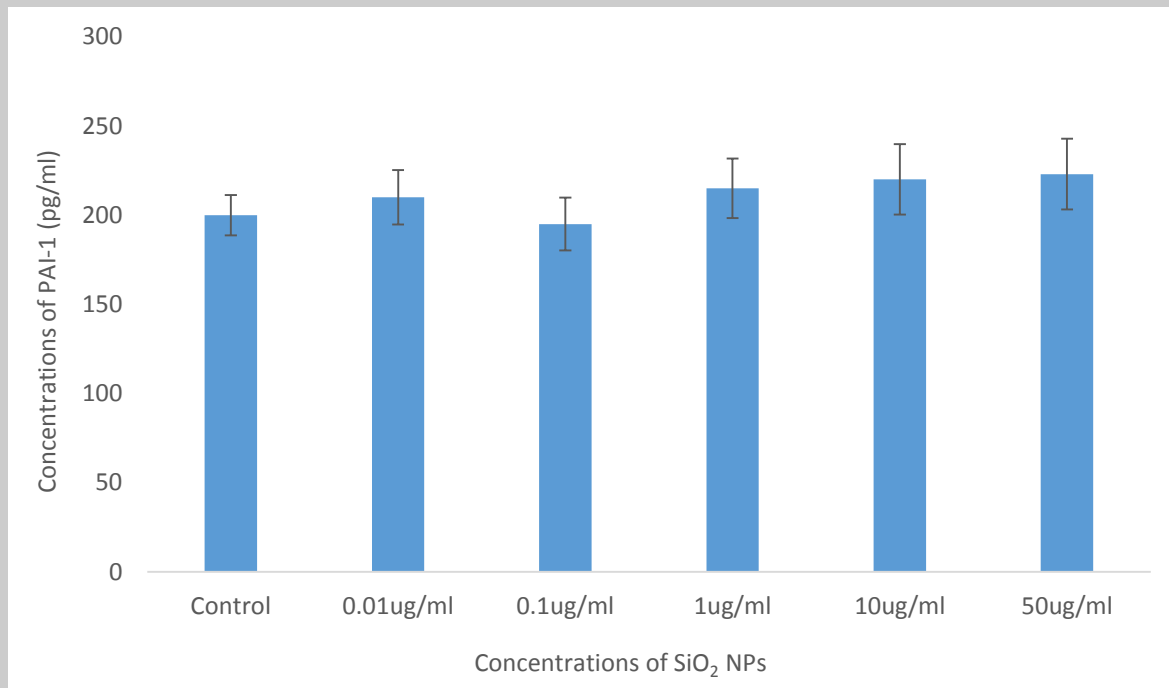
Figure 6-21. ELISA -- Concentrations of Plasminogen Activator Inhibitor-1 (PAI-1) from Human Umbilical Vein Endothelial Cells after 24h Treatment with Different Concentrations of SiO$_2$ NPs (n=3)

ELISA was used to measure the PAI-1 protein levels. After the cells were treated different concentrations of SiO$_2$ NPs for 24 hours, the cell supernatant was taken and measured the concentrations of PAI-1 released from cells.

6.4   Discussion

Silicon dioxide nanoparticles caused denser fibrin structure in clots made from normal pooled plasma, but not from purified fibrinogen. The plasma turbidity results showed that as the concentrations of particles increased, the OD values decreased. Combined the results from confocal microscope, plasma samples formed increased denser fibrin clot structure with increased concentrations of SiO$_2$ NPs. It indicated that the lower OD value represented thinner fibre but more compact fibre arrangement. This is different from results of air

pollution particles. Air particulate matter and diesel particles showed plasma samples formed denser fibrin clot structure with higher OD value. Compared with previous data, there was a discrepancy in the results linking clot maximum absorbance with network density and there are two potential explanations for this. Clot maximum absorbance is a composite measure of both clot density and fibre thickness; therefore lower maximum absorbance does not necessarily mean less compact clots but may simply reflect thinner fibres. Alternatively, it is possible the SiO_2 NPs directly affect clot maximum absorbance, resulting in this discrepancy. These findings further emphasise the importance of complementing turbidimetric analyses with clot visualisation techniques such as confocal microscopy. The fibrin clot lysis time was prolonged as the concentration of silica NP increased in plasma samples. In the *in vitro* cell work, silica NPs induced significantly endothelial cell death from 10 μg/ml with a dose-dependent manner. In addition, fibrin clots formed from normal pooled plasma in the presence of SiO_2 NPs treated cells were getting denser as the concentrations of NPs increased and showed prothrombotic tendency. Real time PCR results indicated that the gene expression of thrombomodulin was inhibited by SiO_2 NPs, but there were no significant difference in the tissue factor mRNA expression between control and treated cells. ELISA results showed silica NPs caused increased concentration of von Willebrand factor produced by endothelial cells, however, PAI-1 was not influenced by SiO_2 NPs.

Plasma contains not only fibrinogen, but also other coagulation factors, such as cascade initiators, factor XII. These factors may interact with the nanoparticles and induced the denser fibrin clot structure formation and longer fibrin lysis time. FXII was chosen to be tested as FXII can be activated by negatively charged surfaces such as silica and glass. However, FXIIa did not interact with SiO_2 NPs.

According to the literature, silicon dioxide nanoparticles are able to trigger oxidative stress (Duan et al., 2013a; Eom and Choi, 2009; Liu and Sun, 2010; Park and Park, 2009), therefore, plasmid strand break assay was used to detect the free radicals releasing from SiO_2 NPs. The results showed that silica did not produce significantly more free radicals compared to control which means that SiO_2 NPs may cause ROS through other pathways.

The effects of SiO_2 NPs on human umbilical vein endothelial cells were also investigated. Silicon dioxide nanoparticles were able to cause different extent of cell death according to the treatment time and different cell lines. For the human umbilical vein endothelial cell, Duan et al. found that SiO_2 NPs caused cell death in a dose- and time-dependent manner. After 24 hours treatment, 50 µg/ml of SiO_2 NPs triggered approximately 15% cell death (Duan et al., 2013a) which was in accordance with the findings of the cytotoxicity of SiO_2 NPs in this study. Similar results were found in another study that showed after 24 hours incubation with 50 µg/ml of SiO_2 NPs, HUVEC viability was 83.49% (Duan et al., 2013b). There is also a study that demonstrated that 50 µg/ml of SiO_2 NPs exerted toxicity and led to 10% reduction of live cells after 48 hours treatment (Peters et al., 2004). Cuo et al. investigated the cytotoxicity of SiO_2 NPs on HUVEC. The results showed that after 24 hours treatment, SiO_2 NPs caused significant cell death at 25 µg/ml (Guo et al., 2015). In most of the studies, SiO_2 NPs caused significantly endothelial cell death from 50 µg/ml after 24 hours treatment. Some studies confirmed that silicon dioxide nanoparticles are able to enter the cells easily through endocytosis (Corbalan et al., 2011; Guo et al., 2015; He et al., 2009). Silica NPs were internalised by the cells and distributed in the cytoplasm and deposited in mitochondria (Guarnieri et al., 2014). As the concentrations of particles increased, the endocytosis of endothelial cells increased (Guo et al., 2015). Duan et al. also mentioned that the endothelial

cell death was caused by both apoptosis and necrosis, and that release of lactate dehydrogenase as an indicator of necrosis was increased from 25 µg/ml of SiO$_2$ NPs treatment, while apoptosis rate was significantly elevated at 50 µg/ml of SiO$_2$ NPs (Duan et al., 2014). Endothelial cells apoptosis significantly contributed to atherothrombosis (Duan et al., 2013; Tedgui & Mallat, 2003).

It has been shown that endothelial cell death would cause the decrease of cell integrity and increased in vascular permeability. Monocytes and adhesion molecules will migrate into the vessels and increase the expression of chemokines, thus contributing to the initiation of atherosclerosis (Guo et al., 2015). Guo et al. (2015) and Duan et al. (2014) indicated that SiO$_2$ NPs induced inflammatory response as the mRNA expression for IL-1β, IL-6, IL-8, TNF-α, ICAM-1, VCAM-1, and MCP-1 by endothelial cells were increased after the treatment (Guo et al., 2015; Duan et al., 2014). IL-6 not only increases CRP in the liver but also fibrinogen and PAI-1. IL-1 also triggers the synthesis of PAI-1 (Esper et al., 2006).

In this study, there was no significantly increased free radicals release detected from SiO$_2$ NPs, but many studies demonstrated that SiO$_2$ NPs induced oxidative stress. According to the literature, silica NPs lead to redox imbalance and inflammation response which is possibly through other pathways, such as MARK-Nrf2 and Nf-kB signalling pathway (Guo et al., 2015).

The fibrin clots were produced on top of endothelial cells after treatment with different concentrations of SiO$_2$ NPs. The clots formed with plasma samples in the presence of treated cells were getting denser as the concentrations of treatment increased. There was no difference in the clots formed from purified fibrinogen between control and treated cells. To get a closer insight into the Silica NPs effects, real time PCR and ELISA were used for further

investigation on the effects of SiO$_2$ NPs on endothelial cells and the mechanisms of denser fibrin clot structure formation as endothelial dysfunction can be evaluated by quantifying circulation adhesion molecules, proatherogenic substances and antifibrinolytics (Esper et al., 2006). Von Willebrand factor, tissue factor, and plasminogen activator inhibitors are all procoagulant proteins secreted by endothelial cells. In this study, silica NPs had no effects on tissue factor mRNA and PAI-1 protein expression even in cells exposed to the highest concentration 50 μg/ml for 24 hours. Von Willebrand factor increased after particle treatment and the gene expression of thrombomodulin decreased in a dose-dependent manner. Significantly decreased mRNA thrombomodulin and increased VWF expression indicated the endothelial dysfunction after HUVEC were exposed to SiO$_2$ NPs. Increased level of VWF promotes coagulation and platelets activation and aggregation. The reduced level of thrombomodulin caused low level of activated protein C (Sofat et al., 2010). VWF plays an important role in haemostasis and thrombosis. VWF not only stabilizes the FVIII activities, but also promotes platelet aggregation (Wu and Thiagarajan, 1996). Especially at high shear stress, VWF binds to platelets glycoprotein IIb-IIIa to support agonist-induced platelet aggregation (Wu and Thiagarajan, 1996). In addition, thrombomodulin is able to inhibit a number of procoagulant activities of thrombin, for example, fibrinogen, activation of FV and FXIII, and inactivation of protein S. Therefore, increased VWF protein expression and decreased thrombomodulin both may lead to denser fibrin clot structure formation.

In conclusion, SiO$_2$ nanoparticles caused alterations of fibrin clot structure with denser clot structure, more compact arrangement, and prolonged lysis time from normal pooled plasma. There was no effects found in purified fibrinogen. In the in vitro cell work, silica NPs triggered significant endothelial cell death from 10 μg/ml in a dose-dependent manner. In addition,

fibrin clots formed from normal pooled plasma in the presence of SiO_2 NPs treated cells were getting denser as the concentrations of NPs increased and showed prothrombotic tendency. The gene expression of thrombomodulin was inhibited by SiO_2 NPs, but there were no significant difference in the tissue factor mRNA expression between control and treated cells. Silica NPs caused increased concentrations of von Willebrand factor produced by endothelial cells, PAI-1 was not influenced by SiO_2 NPs. This adds to existing evidence as to the hazards associated with such NPs.

7 Discussion

A number of pathological mechanisms by which air pollution exposure may impact cardiovascular disease have been proposed, with the most relevant being the induction of oxidative stress, systemic inflammation, endothelial dysfunction, atherothrombosis, and arrhythmogenesis (Newby et al., 2014).

There are three possible pathways that the exposure to particles may be capable of affecting remote cardiovascular territories. Pathway 1: after exposure to the particles, pro-oxidative/proinflammatory mediators (e.g. cytokines or activated immune cells) and vasculoactive molecules (e.g. histamine or microparticles) are released from the lungs, which in turn have indirect effects on cardiovascular system. Pathway 2: an imbalance of the autonomic nervous system (parasympathetic nervous system withdraw and/or sympathetic nervous system activation) is caused by the interaction between particles and nerves. Pathway 3: nano-sized particles, soluble PM and particles constituents (e.g. organic compounds or metals) may directly get into the blood circulation (Brook, 2008).

These three pathways may be activated at different time points or overlap temporally, also can act alone or together to prompt some cardiovascular event (Brook, 2008). Hyperacutely (within minutes to hours), pulmonary inflammation and autonomic system imbalance are the most probable dominant pathways. Acute and sub-acute responses (hours to days) may be applied through pathways 2 and 3 firstly and induce systemic oxidative stress and inflammation secondarily. The chronic actions, such as enhancement of atherosclerosis and thrombosis generation, are plausibly induced by the chronic pro-oxidative and pro-inflammatory state.

Particles' sizes and types also can determine the pathways. Ultrafine particles and the soluble components of larger particles may be able to get into the circulation directly. Whereas the coarse particles or larger fine particles may have effects on the cardiovascular system only through acquired secondary pro-oxidative or inflammatory responses by activation and irritation of the lung alveolae (Brook, 2008).

The investigations from this study focused on the first and third pathway. For the first pathway, air pollution may contribute to the development of thrombosis involve local pulmonary inflammatory and oxidative responses with the release of prothrombotic factors and inflammatory cytokines into the circulation after the inhalation of particles (Emmerechts and Hoylaerts, 2012; Mills et al., 2009; Newby et al., 2014). Previous animal studies showed that PM_{10} caused lung inflammation following intrapulmonary instillation of PM and inhalation of concentrated ambient particles (Donaldson et al., 2005; Elder et al., 2004; Mills et al., 2009). In clinical studies, pulmonary inflammation occurred after inhalation of both concentrated ambient particulate matter and dilute diesel particles (Donaldson et al., 2005; Fujii et al., 2002; Mills et al., 2009). After exposure, plasma concentrations of pro-inflammatory cytokines such as interleukin (IL) - 1β, IL-6 and tumour necrosis factor-α increased (Elder et al., 2004; Mills et al., 2009; Schwartz, 2001). In both animal and clinical studies, exposure of PM also led to the elevation of fibrinogen concentrations. High concentrations of fibrinogen shorten the lag phase of polymerisation, increase branch point densities, fibre thickness and clot rigidity, with concurrent increases in the resistance of the clot to fibrinolysis (Scott et al., 2004; Weisel, 2007).

For the third pathway, airborne particles are capable direct translocation from the pulmonary alveoli into the blood circulation, crossing the pulmonary epithelium and vascular endothelium barrier (Emmerechts and Hoylaerts, 2012; Mills et al., 2009; Newby et al., 2014). PM and diesel particles would affect fibrin clot structure and interfere with endothelial cells. Particles with diameters less than 10 μm can be inhaled deeply into the lungs. A number of other factors may influence the possible translocation of PM, including charge, chemical composition, and propensity to form aggregates (Mills et al., 2009). The size and shape of the particles could affect the region of deposition in the respiratory system, with smaller sized particles penetrating deeper into the lung. Macrophages may not be able to recognize particles with a diameter less than 500 nm, and for this reason, ultrafine PM may enter the blood or lymphatic systems more easily and transfer to different organs (Teow et al., 2011). Once in the circulation, the particles could interact with vascular endothelial cells and have direct effects on the atherosclerotic plaque, platelets and fibrin clot formation, structure and stability (Lauer et al., 2009; Mills et al., 2009).

In this study, the effects of PM_{10}, $PM_{0.2}$, total diesel particles and filtered diesel particles on fibrin clot structure were investigated. Standard Reference Materials were used in the study which were directly purchased from NIST. There are some advantages to use SRMs for the investigation. Firstly, the components of the SRMs had been measured and certified. Secondly, based on the collection method of SRMs, several studies had confirmed that SRMs were able to represent the urban/diesel PM (Akhtar et al., 2010; Boland et al., 2001; Hetland et al., 2004). Thirdly, compared to the particles that were obtained from different areas in various studies, SRMs were more homogenous, thus increasing the consistency in the measurement of

different biological endpoints and promoting the reproducibility of the same biological endpoint (Akhtar et al., 2010).

It is difficult to compare airborne exposure concentrations with concentrations used in *in vitro* experiments. According to the World Health Organisation statistics, the guideline values for PM$_{10}$ and PM$_{2.5}$ are 50 µg/m^3 and 25 µg/m^3 for the 24-hour mean concentration; 20 µg/m^3 and 10 µg/m^3 for the annual concentration (World Health Organisation, 2011). The PM$_{10}$ level in the Great Smog in London in 1952 was from 3,000 to 14,000 µg/m^3. Some *in vitro* studies chose concentrations of air pollution particles above 50 µg/ml which is too high compared to the level at which people may be exposed. Therefore, based on those data, the concentrations of PM chosen to investigate the effects on fibrin clot structure and human endothelial cells in this study were from very low concentrations (0.01 µg/ml) to intermediate and high, which may better reflect environmental exposures.

In this study, the effects of PM$_{10}$, PM$_{0.2}$, total diesel particles and filtered diesel particles on fibrin clot structure were investigated. Three methods were applied to study the effects of particles from air pollution, turbidity assay, turbidity lysis assay and laser scanning confocal microscopy in both normal pooled plasma and purified fibrinogen system. The experiments results from turbidity assay and LSCM assay showed that for clots formed from pooled plasma, there was a trend that higher concentrations of particles led to denser fibrin clot structure formation compared to control. The results from turbidity lysis provided more obvious consequences that as the concentrations of particles increased, the fibres formed from plasma were getting less sensitive to fibrinolysis and times to 50% lysis were significantly longer at 50 µg/ml of these four particles compared to control. In terms of the purified

fibrinogen system, the clots had similar structure as control even at the highest concentration 50 µg/ml of those particles. The results demonstrated these four particles were able to alter the fibrin clot structure. Filtered PM ($PM_{0.2}$) and filtered diesel particles with diameter than less than 200 nm represented the ultrafine particles which were able to get into the circulation (Nemmar et al., 2002). These two types of filtered particles had less effect on fibrin clot structure alterations and endothelial dysfunction compared to the larger particles, as $PM_{0.2}$ and filtered diesel particles occupied 30% and 35% of PM_{10} and total diesel particles, respectively.

In view of the associations between thrombosis and fibrin structure, the effects of particulate matter on fibrin clot structure have previously been investigated in this laboratory. It was found that diesel PM caused changes in fibrin clot structure and function in clots formed from both purified fibrinogen and from human plasma (Metassan et al., 2010a). However, no changes in fibrin clot structure were observed in clots formed from plasma taken from healthy individuals after 2 hours exposure to PM while performing moderate exercise (Metassan, et al., 2010b). The exposure in the latter study was of short duration, so the possibility remained that fibrin clot structure could be affected by long-term exposure to high levels of air pollution, or that susceptible subjects, such as patients with thrombosis could respond differently to the healthy young subjects in the earlier study.

To test this possibility, a sub-study was performed using samples from a large cohort study in the Lombardy Region of Italy (Baccarelli et al. 2007; Baccarelli et al. 2009; Baccarelli et al. 2008), which had reported that every 10 µg/m^3 elevation of PM_{10} exposure was associated with a 67% increased risk of DVT. The aim of the sub-study was, therefore, to investigate the

possible association between fibrin clot structure and PM_{10} levels in a well-characterized group of patients with DVT and healthy controls. The sub-study results showed that after long-term and high-level exposure to air pollution (PM_{10} concentrations over 45.6 $\mu g/m^3$), patients with DVT had significantly denser fibrin clot structure compared to those living in areas with lower levels of exposure (PM_{10} less than 45.6 $\mu g/m^3$). In the high exposure group, clots from patients contained thicker fibres, more compact fibre arrangements and less permeable clot structure. There were no significant differences in fibrin clot structure between the two exposure levels in healthy subjects. This shows that patients with existing prothrombotic susceptibility may be affected by PM exposure. This raises the possibility that high PM exposure contributes to the onset of the DVT through changes to clot structure. The observation in this and a previous study (Metassan et al., 2010b) that there were no changes in clot structure in healthy individuals suggests that only people with an existing risk show changes to clot structure in response to PM exposure.

As the endothelial cell plays an important role in modulating thrombosis in blood vessels, the effects of PM exposure on endothelial cells was studied. At 50 $\mu g/ml$ of PM that did not induce significant cell death after 24 hours exposure, the fibrin clots formed from pooled plasma on the treated cells were altered compared to the controls. For the clots formed from purified fibrinogen samples, there were no significant differences on the clot structure between treated and untreated cells. Changes in expression of TF, THBD, VWF and PAI-1 following PM exposure of HUVECs were consistent with changes observed in clot structure, which adds evidence for PM affecting thrombosis via influences on endothelial cells.

Whilst there is an acknowledged risk of increased CVD associated with air pollution, and PM in particular, there is currently no epidemiological evidence of risk associated with engineered nanoparticles in the same size range. Nevertheless, there is a body of data showing that engineered nanoparticles such as silica NPs induce toxicity, including cytotoxicity and genotoxicity, and silica nanoparticles are widely used in many industries. It was therefore decided to investigate whether silica NPs induced changes to clot structure similar to those seen for PM.

Silica nanoparticles caused denser fibrin structure in clots formed only from normal pooled plasma, but not from purified fibrinogen. Also, the fibrin clot lysis time was prolonged as the concentration of silica NP increased in plasma samples. These results are consistent with those seen for PM, which suggests the potential for silica NPs to be toxic to the cardiovascular system in an analogous manner. In the cell experiments, silica NPs induced significant endothelial cell death from 10 μg/ml in a dose-dependent manner. In addition, fibrin clots formed from normal pooled plasma in the presence of SiO_2 NPs treated cells were getting denser as the concentrations of NPs increased and showing a prothrombotic tendency. Real time PCR results indicated that the gene expression of thrombomodulin was inhibited by SiO_2 NPs, but there were no significant difference in the TF mRNA expression between control and treated cells. ELISA results showed silica NPs caused increased concentration of VWF produced by endothelial cells, but PAI-1 was not influenced by SiO_2 NPs. It can be seen that not all results mirrored those seen with diesel PM, but there were some similar results, raising the potential for toxicity of silica NPs on these cells. It is known that PM can release free radicals in solution, as a result of metal ions associated with the PM. This was confirmed for the PM used in this study, raising the possibility that oxidative stress could be one mechanism

responsible for changes induced in endothelial cells. Such free radical production was not observed in solution for the silica NPs, but it may be that free radicals were released within the cellular environment as this was not measured in this study.

The comparison of effects of air particulate matter and silicon dioxide nanoparticles are shown as following tables.

Fibrin Clot Structure		PM$_{10}$	PM$_{0.2}$	Total Diesel Particles	Filtered Diesel Particles	SiO$_2$ NPs
Plasma	**Maximum Absorbance**	No difference^	No difference^	No difference^	No difference^	Decreased From 10 µg/ml¶
	Lysis Time	Increased From 10 µg/ml¶	Increased From 50 µg/ml¶	Increased From 10 µg/ml¶	Increased From 50 µg/ml¶	No difference^
	Fibre Number	No difference^	No difference^	No difference^	No difference^	Increased From 10 µg/ml¶
Fibrinogen	**Maximum Absorbance**	No difference^	No difference^	No difference^	No difference^	No difference^
	Lysis Time	No difference^	No difference^	No difference^	No difference^	No difference^
	Fibre Number	No difference^	No difference^	No difference^	No difference^	No difference^

Table 7-1. Summary of Parameters of Fibrin Clot formed from Plasma or Purified Fibrinogen Samples

¶ Concentrations: Parameters significantly increased/decreased after different concentrations of particles treatment

^There were no significant difference found after particles treatment from control.

	PM$_{10}$	PM$_{0.2}$	Total Diesel Particles	Filtered Diesel Particles	SiO$_2$ NPs
Von Willebrand Factor	Increased From 0.1 µg/ml¶	Increased From 0.1 µg/ml¶	Increased From 0.1 µg/ml¶	Increased From 1 µg/ml¶	Increased From 1 µg/ml¶
Plasminogen Activator Inhibitor-1	Increased From 0.1 µg/ml¶	Increased From 10 µg/ml¶	Increased From 1 µg/ml¶	Increased From 10 µg/ml¶	No difference^
Tissue Factor mRNA	Increased From 0.1 µg/ml¶	Increased From 1 µg/ml¶	Increased From 0.1 µg/ml¶	Increased From 50 µg/ml¶	No difference^
Thrombomodulin mRNA	Decreased From 0.1 µg/ml¶	Decreased From 0.1 µg/ml¶	Decreased From 0.1 µg/ml¶	Decreased From 1 µg/ml¶	Decreased From 10 µg/ml¶
Free Radicals	Increased From 10 µg/ml¶	Increased From 50 µg/ml¶	Increased From 50 µg/ml¶	Increased From 50 µg/ml¶	No difference^
Fibre Number--Plasma	Increased From 10 µg/ml¶	Increased From 10 µg/ml¶	Increased From 10 µg/ml¶	Increased From 10 µg/ml¶	Increased From 1 µg/ml¶
Fibre Number--Fibrinogen	No difference^	No difference^	No difference^	No difference^	No difference^

Table 7-2. Summary of Proteins/Gene Expression and Fibrin Clot Structure of HUVEC after Treatment with Different Particles

¶ Concentrations of Particles: Proteins/Gene expressions or fibre numbers significantly increased or decreased after different concentrations of particles treatment

^There were no significant difference found after particles treatment from control.

There is increasing recognition that PM in air pollution is associated with cardiovascular mortality and morbidity. The results presented here show that PM can induce changes to clot structure and function, and that changes in gene expression induced in endothelial cells may be a mechanism by which a prothrombotic state is induced in response to PM exposure. Furthermore, some, but not all, similar changes were observed in clots and cells exposed to silica NPs, raising the possibility that such engineered nanoparticles may also have the potential to contribute to cardiovascular toxicity. This adds to existing evidence as to the hazards associated with such NPs.

8 Bibliography

Aaronson, P.I., Ward, J.P.T., 2007. The Cardiovascular System at a Glance. Blackwell, Oxford, UK.

Adams, R.L., Bird, R.J., 2009. Review article: Coagulation cascade and therapeutics update: relevance to nephrology. Part 1: Overview of coagulation, thrombophilias and history of anticoagulants. Nephrol. 14, 462–470. doi:10.1111/j.1440-1797.2009.01128.x

Ahamed, M., 2013. Silica nanoparticles-induced cytotoxicity, oxidative stress and apoptosis in cultured A431 and A549 cells. Hum. Exp. Toxicol. 32, 186–95. doi:10.1177/0960327112459206

Ajjan, R., Grant, P.J., 2006. Coagulation and atherothrombotic disease. Atherosclerosis 186, 240–259. doi:10.1016/j.atherosclerosis.2005.10.042

Ajjan, R.A., Ariens, R.A., 2009. Cardiovascular disease and heritability of the prothrombotic state. Blood Rev 23, 67–78. doi:10.1016/j.blre.2008.07.001

Akhtar, U.S., McWhinney, R.D., Rastogi, N., Abbatt, J.P.D., Evans, G.J., Scott, J. a, 2010. Cytotoxic and proinflammatory effects of ambient and source-related particulate matter (PM) in relation to the production of reactive oxygen species (ROS) and cytokine adsorption by particles. Inhal. Toxicol. 22 Suppl 2, 37–47. doi:10.3109/08958378.2010.518377

Allford, S.L., Machin, S., 2004. Haemostasis. Surg. doi:10.1383/surg.22.8.200a.43067

Ariens, R.A., 2013. Fibrin(ogen) and thrombotic disease. J Thromb Haemost 11 Suppl 1, 294–305. doi:10.1111/jth.12229

Ariëns, R.A.S., Lai, T.S., Weisel, J.W., Greenberg, C.S., Grant, P.J., 2002. Role of factor XIII in fibrin clot formation and effects of genetic polymorphisms. Blood. doi:10.1182/blood.V100.3.743

Baccarelli, A., Martinelli, I., Pegoraro, V., Melly, S., Grillo, P., Zanobetti, A., Hou, L., Bertazzi, P.A., Mannucci, P.M., Schwartz, J., 2009. Living near major traffic roads and risk of deep vein thrombosis. Circulation 119, 3118–3124. doi:10.1161/CIRCULATIONAHA.108.836163

Baccarelli, A., Martinelli, I., Zanobetti, A., Grillo, P., Hou, L.F., Bertazzi, P.A., Mannucci, P.M., Schwartz, J., 2008. Exposure to particulate air pollution and risk of deep vein thrombosis. Arch Intern Med 168, 920–927. doi:10.1001/archinte.168.9.920

Baccarelli, A., Zanobetti, A., Martinelli, I., Grillo, P., Hou, L., Giacomini, S., Bonzini, M., Lanzani, G., Mannucci, P.M., Bertazzi, P.A., Schwartz, J., 2007a. Effects of exposure to air pollution on blood coagulation. J Thromb Haemost 5, 252–260. doi:10.1111/j.1538-7836.2007.02300.x

Baccarelli, A., Zanobetti, A., Martinelli, I., Grillo, P., Hou, L., Lanzani, G., Mannucci, P.M.,

Bertazzi, P.A., Schwartz, J., 2007b. Air pollution, smoking, and plasma homocysteine. Env. Heal. Perspect 115, 176–181. doi:10.1289/ehp.9517

Bagoly, Z., Katona, E., Muszbek, L., 2012a. Factor XIII and inflammatory cells. Thromb. Res. 129 Suppl , S77–81. doi:10.1016/j.thromres.2012.02.040

Bagoly, Z., Koncz, Z., Hársfalvi, J., Muszbek, L., 2012b. Factor XIII, clot structure, thrombosis. Thromb. Res. doi:10.1016/j.thromres.2011.11.040

Bahorun, D.T., Soobrattee, M.M., Luximon-Ramma, M. V, Prof. OI Aruoma*, 2006. Free radicals and antioxidants in cardiovascular health and disease. Internet J. Med. Updat. 1, 25–41. doi:10.4314/ijmu.v1i2.39839

Bavendiek, U., Libby, P., Kilbride, M., Reynolds, R., Mackman, N., Schonbeck, U., 2002. Induction of tissue factor expression in human endothelial cells by CD40 ligand is mediated via activator protein 1, nuclear factor kappa B, and Egr-1. J. Biol. Chem. 277, 25032–25039. doi:10.1074/jbc.M204003200\rM204003200 [pii]

Berry, J., Arnoux, B., Stanislas, G., Galle, P., Chretien, J., 1977. A microanalytic study of particles transport across the alveoli: role of blood platelets. Biomedicine 27, 354–357.

Bertina, R.M., Koeleman, B.P., Koster, T., Rosendaal, F.R., Dirven, R.J., de Ronde, H., van der Velden, P.A., Reitsma, P.H., 1994. Mutation in blood coagulation factor V associated with resistance to activated protein C. Nature 369, 64–7. doi:10.1038/369064a0

Binder, B.R., Christ, G., Gruber, F., Grubic, N., Hufnagl, P., Krebs, M., Mihaly, J., Prager, G.W., 2002. Plasminogen activator inhibitor 1: physiological and pathophysiological roles. News Physiol. Sci. 17, 56–61.

Boland, S., Baeza-Squiban, a, Bonvallot, V., Houcine, O., Pain, C., Meyer, M., Marano, F., 2001. Similar cellular effects induced by diesel exhaust particles from a representative diesel vehicle recovered from filters and Standard Reference Material 1650. Toxicol. In Vitro 15, 379–85. doi:10.1016/S0887-2333(01)00040-6

Bouma, B.N., Mosnier, L.O., 2006. Thrombin activatable fibrinolysis inhibitor (TAFI) - How does thrombin regulate fibrinolysis? Ann. Med. 38, 378–388. doi:10.1080/07853890600852898

Brill, A., Fuchs, T.A., Chauhan, A.K., Yang, J.J., De Meyer, S.F., K??llnberger, M., Wakefield, T.W., L??mmle, B., Massberg, S., Wagner, D.D., 2011. Von Willebrand factor-mediated platelet adhesion is critical for deep vein thrombosis in mouse models. Blood 117, 1400–1407. doi:10.1182/blood-2010-05-287623

British Heart Foundation, 2012. Coronary Heart Disease Statistics 2012 .

Brook, R.D., 2008. Cardiovascular effects of air pollution. Clin Sci 115, 175–187. doi:10.1042/CS20070444

Brook, R.D., Franklin, B., Cascio, W., Hong, Y., Howard, G., Lipsett, M., Luepker, R., Mittleman, M., Samet, J., Smith, S.C., Tager, I., 2004. Air pollution and cardiovascular disease: A statement for healthcare professionals from the expert panel on population and

prevention science of the American Heart Association. Circulation. doi:10.1161/01.CIR.0000128587.30041.C8

Brook, R.D., Rajagopalan, S., Pope 3rd, C.A., Brook, J.R., Bhatnagar, A., Diez-Roux, A. V., Holguin, F., Hong, Y., Luepker, R. V., Mittleman, M.A., Peters, A., Siscovick, D., Smith Jr., S.C., Whitsel, L., Kaufman, J.D., Pope, C.A., Smith, S.C., 2010. Particulate matter air pollution and cardiovascular disease: An update to the scientific statement from the american heart association. Circulation 121, 2331–2378. doi:10.1161/CIR.0b013e3181dbece1

Budinger, G.R.S., McKell, J.L., Urich, D., Foiles, N., Weiss, I., Chiarella, S.E., Gonzalez, A., Soberanes, S., Ghio, A.J., Nigdelioglu, R., Mutlu, E. a., Radigan, K. a., Green, D., Kwaan, H.C., Mutlu, G.M., 2011. Particulate Matter-Induced Lung Inflammation Increases Systemic Levels of PAI-1 and Activates Coagulation Through Distinct Mechanisms. PLoS One 6, e18525. doi:10.1371/journal.pone.0018525

Burman, J.F., Chung, H.I., Lane, D.A., Philippou, H., Adami, A., Lincoln, J.C., 1994. Role of factor XII in thrombin generation and fibrinolysis during cardiopulmonary bypass. Lancet 344, 1192–1193.

Butenas, S., Mann, K.G., 2002. Blood coagulation. Biochem. 67, 3–12.

Calderón-Garcidueñas, L., Villarreal-Calderon, R., Valencia-Salazar, G., Henríquez-Roldán, C., Gutiérrez-Castrellón, P., Torres-Jardón, R., Osnaya-Brizuela, N., Romero, L., Torres-Jardón, R., Solt, A., Reed, W., 2008. Systemic inflammation, endothelial dysfunction, and activation in clinically healthy children exposed to air pollutants. Inhal. Toxicol. 20, 499–506. doi:10.1080/08958370701864797

Camera, M., Giesen, P.L., Fallon, J., Aufiero, B.M., Taubman, M., Tremoli, E., Nemerson, Y., 1999. Cooperation between VEGF and TNF-alpha is necessary for exposure of active tissue factor on the surface of human endothelial cells. Arterioscler. Thromb. Vasc. Biol. 19, 531–537. doi:10.1161/01.ATV.19.3.531

Campbell, R.A., Aleman, M., Gray, L.D., Falvo, M.R., Wolberg, A.S., 2010. Flow profoundly influences fibrin network structure: implications for fibrin formation and clot stability in haemostasis. Thromb Haemost 104, 1281–1284. doi:10.1160/TH10-07-0442

Carter, A.M., 2005. Inflammation, thrombosis and acute coronary syndromes. Diab. Vasc. Dis. Res. 2, 113–21. doi:10.3132/dvdr.2005.018

Celinska-Lowenhoff, M., Iwaniec, T., Alhenc-Gelas, M., Musial, J., Undas, A., 2011. Arterial and venous thrombosis and prothrombotic fibrin clot phenotype in a Polish family with type 1 antithrombin deficiency (antithrombin Krakow). Thromb Haemost 106, 379–381. doi:10.1160/TH11-02-0066

Chapin, J.C., Hajjar, K.A., 2015. Fibrinolysis and the control of blood coagulation. Blood Rev. 29, 17–24. doi:10.1016/j.blre.2014.09.003

Chauhan, A.K., Kisucka, J., Lamb, C.B., Bergmeier, W., Wagner, D.D., 2007. Von Willebrand factor and factor VIII are independently required to form stable occlusive thrombi in

injured veins. Blood 109, 2424–2429. doi:10.1182/blood-2006-06-028241

Chu, A.J., 2005. Tissue factor mediates inflammation. Arch. Biochem. Biophys. 440, 123–32. doi:10.1016/j.abb.2005.06.005

Chuang, K.J., Chan, C.C., Su, T.C., Lee, C.T., Tang, C.S., 2007. The effect of urban air pollution on inflammation, oxidative stress, coagulation, and autonomic dysfunction in young adults. Am J Respir Crit Care Med 176, 370–376. doi:10.1164/rccm.200611-1627OC

Chuang, K.-J., Chan, C.-C., Su, T.-C., Lee, C.-T., Tang, C.-S., 2007. The effect of urban air pollution on inflammation, oxidative stress, coagulation, and autonomic dysfunction in young adults. Am J Respir Crit Care Med 176, 370–6. doi:10.1164/rccm.200611-1627OC

Cines, D.B., Pollak, E.S., Buck, C.A., Loscalzo, J., Zimmerman, G.A., McEver, R.P., Pober, J.S., Wick, T.M., Konkle, B.A., Schwartz, B.S., Barnathan, E.S., McCrae, K.R., Hug, B.A., Schmidt, A.M., Stern, D.M., 1998. Endothelial cells in physiology and in the pathophysiology of vascular disorders. Blood 91, 3527–3561.

Clemetson, K.J., 2012. Platelets and primary haemostasis. Thromb. Res. 129, 220–224. doi:10.1016/j.thromres.2011.11.036

Cooper, A. V, Standeven, K.F., Ariens, R.A., 2003. Fibrinogen gamma-chain splice variant gamma' alters fibrin formation and structure. Blood 102, 535–540. doi:10.1182/blood-2002-10-3150

Corbalan, J.J., Medina, C., Jacoby, A., Malinski, T., Radomski, M.W., 2011. Amorphous silica nanoparticles trigger nitric oxide/peroxynitrite imbalance in human endothelial cells: inflammatory and cytotoxic effects. Int. J. Nanomedicine 6, 2821–2835. doi:10.2147/IJN.S25071

Dahlbäck, B., 2000. Blood coagulation. Lancet 355, 1627–1632. doi:10.1016/S0140-6736(00)02225-X

Dahlbäck, B., Villoutreix, B.O., 2005. The anticoagulant protein C pathway. FEBS Lett. doi:10.1016/j.febslet.2005.03.001

Davis, D.L., Bell, M.L., Fletcher, T., 2002. A look back at the London smog of 1952 and the half century since. Env. Heal. Perspect 110, A734–5.

Dockery, D.W., 1993. Epidemiologic study design for investigating respiratory health effects of complex air pollution mixtures. Env. Heal. Perspect 101 Suppl , 187–191.

Donaldson, K., Mills, N., MacNee, W., Robinson, S., Newby, D., 2005. Role of inflammation in cardiopulmonary health effects of PM. Toxicol Appl Pharmacol 207, 483–488. doi:10.1016/j.taap.2005.02.020

Doolittle, R.F., Spraggon, G., Everse, S.J., 1998. Three-dimensional structural studies on fragments of fibrinogen and fibrin. Curr Opin Struct Biol 8, 792–798.

Drake, T.A., Hannani, K., Fei, H.H., Lavi, S., Berliner, J.A., 1991. Minimally oxidized low-density lipoprotein induces tissue factor expression in cultured human endothelial cells. Am. J.

Pathol. 138, 601–607.

Duan, J., Yu, Y., Li, Y., Yu, Y., Li, Y., Zhou, X., Huang, P., Sun, Z., 2013a. Toxic effect of silica nanoparticles on endothelial cells through DNA damage response via Chk1-dependent G2/M checkpoint. PLoS One 8, e62087. doi:10.1371/journal.pone.0062087

Duan, J., Yu, Y., Li, Y., Yu, Y., Sun, Z., 2013b. Cardiovascular toxicity evaluation of silica nanoparticles in endothelial cells and zebrafish model. Biomaterials 34, 5853–5862. doi:10.1016/j.biomaterials.2013.04.032

Duan, J., Yu, Y., Yu, Y., Li, Y., Huang, P., Zhou, X., Peng, S., Sun, Z., 2014a. Silica nanoparticles enhance autophagic activity, disturb endothelial cell homeostasis and impair angiogenesis. Part. Fibre Toxicol. 11, 50. doi:10.1186/s12989-014-0050-8

Duan, J., Yu, Y., Yu, Y., Li, Y., Wang, J., Geng, W., Jiang, L., Li, Q., Zhou, X., Sun, Z., 2014b. Silica nanoparticles induce autophagy and endothelial dysfunction via the PI3K/Akt/mTOR signaling pathway. Int. J. Nanomedicine 9, 5131–41. doi:10.2147/IJN.S71074

Durga, M., Nathiya, S., Rajasekar, A., Devasena, T., 2014. Effects of ultrafine petrol exhaust particles on cytotoxicity, oxidative stress generation, DNA damage and inflammation in human A549 lung cells and murine RAW 264.7 macrophages. Environ. Toxicol. Pharmacol. 38, 518–30. doi:10.1016/j.etap.2014.08.003

Elder, A.C.P., Gelein, R., Azadniv, M., Frampton, M., Finkelstein, J., Oberdörster, G., 2004. Systemic effects of inhaled ultrafine particles in two compromised, aged rat strains. Inhal. Toxicol. 16, 461–471. doi:10.1080/08958370490439669

Elliot Wagland, 2013. 11 Incredible Pictures From The Great Smog Of 1952. Huffingt. Post.

Emmerechts, J., Hoylaerts, M.F., 2012. The effect of air pollution on haemostasis. Hamostaseologie 32, 5–13. doi:10.5482/ha-1179

Eom, H.-J., Choi, J., 2009. Oxidative stress of silica nanoparticles in human bronchial epithelial cell, Beas-2B. Toxicol. In Vitro 23, 1326–1332. doi:10.1016/j.tiv.2009.07.010

Esmon, C.T., 2009. Basic mechanisms and pathogenesis of venous thrombosis. Blood Rev. 23, 225–229. doi:10.1016/j.blre.2009.07.002

Esmon, C.T., 2004. Interactions between the innate immune and blood coagulation systems. Trends Immunol. doi:10.1016/j.it.2004.08.003

Esper, R.J., Nordaby, R.A., Vilarino, J.O., Paragano, A., Cacharron, J.L., Machado, R.A., 2006. Endothelial dysfunction: a comprehensive appraisal. Cardiovasc Diabetol 5, 4. doi:10.1186/1475-2840-5-4

Franchini, M., Mannucci, P.M., 2012. Air pollution and cardiovascular disease. Thromb Res 129, 230–234. doi:10.1016/j.thromres.2011.10.030

Franchini, M., Mannucci, P.M., 2011. Thrombogenicity and cardiovascular effects of ambient air pollution. Blood 118, 2405–2412. doi:10.1182/blood-2011-04-343111

Franchini, M., Mannucci, P.M., 2007. Short-term effects of air pollution on cardiovascular

diseases outcomes and mechanisms. J. Thromb. Haemost. 2169–2174.

Frayn, K.N., Stanner, S., British Nutrition, F., 2005. Cardiovascular disease: diet, nutrition and emerging risk factors : the report of a British Nutrition Foundation task force. Blackwell Publishing.

Fuentes-Prior, P., Iwanaga, Y., Huber, R., Pagila, R., Rumennik, G., Seto, M., Morser, J., Light, D.R., Bode, W., 2000. Structural basis for the anticoagulant activity of the thrombin-thrombomodulin complex. Nature 404, 518–525. doi:10.1038/35006683

Fujii, T., Hayashi, S., Hogg, J.C., Mukae, H., Suwa, T., Goto, Y., Vincent, R., Van Eeden, S.F., 2002. Interaction of alveolar macrophages and airway epithelial cells following exposure to particulate matter produces mediators that stimulate the bone marrow. Am. J. Respir. Cell Mol. Biol. 27, 34–41. doi:10.1165/ajrcmb.27.1.4787

Furie, B.B.C., Furie, B.B.C., 2008. Mechanisms of thrombus formation. N. Engl. J. Med. 359, 938–949. doi:10.1056/NEJMra0801082

Gehring, U., Heinrich, J., Kramer, U., Grote, V., Hochadel, M., Sugiri, D., Kraft, M., Rauchfuss, K., Eberwein, H.G., Wichmann, H.E., 2006. Long-term exposure to ambient air pollution and cardiopulmonary mortality in women. Epidemiology 17, 545–551. doi:10.1097/01.ede.0000224541.38258.87

George, J.N., 2000. Platelets. Lancet 355, 1531–1539. doi:10.1016/S0140-6736(00)02175-9

Gold, D.R., Samet, J.M., 2013. Air Pollution, Climate, and Heart Disease. Circulation 128, e411–e414. doi:10.1161/CIRCULATIONAHA.113.003988

Golino, P., 2002. The inhibitors of the tissue factor:factor VII pathway. Thromb Res 106, V257–65.

Guarnieri, D., Malvindi, M.A., Belli, V., Pompa, P.P., Netti, P., 2014. Effect of silica nanoparticles with variable size and surface functionalization on human endothelial cell viability and angiogenic activity. J. Nanoparticle Res. 16. doi:10.1007/s11051-013-2229-6

Guo, C., Xia, Y., Niu, P., Jiang, L., Duan, J., Yu, Y., Zhou, X., Li, Y., Sun, Z., 2015. Silica nanoparticles induce oxidative stress, inflammation, and endothelial dysfunction in vitro via activation of the MAPK/Nrf2 pathway and nuclear factor-κB signaling. Int. J. Nanomedicine 10, 1463–77. doi:10.2147/IJN.S76114

Hales, S., Blakely, T., Woodward, A., 2012. Air pollution and mortality in New Zealand: cohort study. J Epidemiol Community Heal. 66, 468–473. doi:10.1136/jech.2010.112490

Halliwell, B., Gutteridge, J.M.C., 2007. Free Radicals in Biology and Medicine, Free Radical Biology and Medicine. doi:10.1016/0891-5849(91)90055-8

Harrison, P., 2005. Platelet function analysis. Blood Rev. 19, 111–123. doi:10.1016/j.blre.2004.05.002

He, Q., Zhang, Z., Gao, Y., Shi, J., Li, Y., 2009. Intracellular localization and cytotoxicity of

spherical mesoporous silica nano- and microparticles. Small 5, 2722–9. doi:10.1002/smll.200900923

Heinrich, J., Thiering, E., Rzehak, P., Kramer, U., Hochadel, M., Rauchfuss, K.M., Gehring, U., Wichmann, H.E., 2013. Long-term exposure to NO2 and PM10 and all-cause and cause-specific mortality in a prospective cohort of women. Occup Env. Med 70, 179–186. doi:10.1136/oemed-2012-100876

Helfand, W.H., Lazarus, J., Theerman, P., 2001. Donora, Pennsylvania: an environmental disaster of the 20th century. Am J Public Heal. 91, 553.

Hetland, R.., Cassee, F.., Refsnes, M., Schwarze, P.., Låg, M., Boere, A.J.., Dybing, E., 2004. Release of inflammatory cytokines, cell toxicity and apoptosis in epithelial lung cells after exposure to ambient air particles of different size fractions. Toxicol. Vitr. 18, 203–212. doi:10.1016/S0887-2333(03)00142-5

Hoffmann, B., Moebus, S., Möhlenkamp, S., Stang, A., Lehmann, N., Dragano, N., Schmermund, A., Memmesheimer, M., Mann, K., Erbel, R., Jöckel, K.H., 2007. Residential exposure to traffic is associated with coronary atherosclerosis. Circulation 116, 489–496. doi:10.1161/CIRCULATIONAHA.107.693622

Hooper, J.M., Stuijver, D.J., Orme, S.M., van Zaane, B., Hess, K., Gerdes, V.E., Phoenix, F., Rice, P., Smith, K.A., Alzahrani, S.H., Standeven, K.F., Ajjan, R.A., 2012. Thyroid dysfunction and fibrin network structure: a mechanism for increased thrombotic risk in hyperthyroid individuals. J Clin Endocrinol Metab 97, 1463–1473. doi:10.1210/jc.2011-2894

Jones, A.P., 1999. Indoor air quality and health. Atmos. Environ. doi:10.1016/S1352-2310(99)00272-1

Kampa, M., Castanas, E., 2008. Human health effects of air pollution. Environ. Pollut. 151, 362–367. doi:10.1016/j.envpol.2007.06.012

Karoly, E.D., Li, Z., Dailey, L. a, Hyseni, X., Huang, Y.-C.T., 2007. Up-regulation of tissue factor in human pulmonary artery endothelial cells after ultrafine particle exposure. Environ. Health Perspect. 115, 535–40. doi:10.1289/ehp.9556

Katsouyanni, K., Touloumi, G., Samoli, E., Gryparis, a, Le Tertre, a, Monopolis, Y., Rossi, G., Zmirou, D., Ballester, F., Boumghar, a, Anderson, H.R., Wojtyniak, B., Paldy, a, Braunstein, R., Pekkanen, J., Schindler, C., Schwartz, J., 2001. Confounding and effect modification in the short-term effects of ambient particles on total mortality: results from 29 European cities within the APHEA2 project. Epidemiology 12, 521–531. doi:10.1097/00001648-200109000-00011

Kawano, H., Tsuji, H., Nishimura, H., Kimura, S., Yano, S., Ukimura, N., Kunieda, Y., Yoshizumi, M., Sugano, T., Nakagawa, K., Masuda, H., Sawada, S., Nakagawa, M., 2001. Serotonin induces the expression of tissue factor and plasminogen activator inhibitor-1 in cultured rat aortic endothelial cells. Blood 97, 1697–1702. doi:10.1182/blood.V97.6.1697

Kloog, I., Ridgway, B., Koutrakis, P., Coull, B. a, Schwartz, J.D., 2013. Long- and short-term exposure to PM2.5 and mortality: using novel exposure models. Epidemiology 24, 555–

61. doi:10.1097/EDE.0b013e318294beaa

Kloog, I., Zanobetti, a, Nordio, F., Coull, B., Baccarelli, A., Schwartz, J., 2015. Effects of airborne fine particles (PM2.5) on Deep Vein Thrombosis Admissions in North Eastern United States. J. Thromb. Haemost. n/a–n/a. doi:10.1111/jth.12873

Kodavanti, U.P., Thomas, R., Ledbetter, A.D., Schladweiler, M.C., Shannahan, J.H., Wallenborn, J.G., Lund, A.K., Campen, M.J., Butler, E.O., Gottipolu, R.R., Nyska, A., Richards, J.E., Andrews, D., Jaskot, R.H., McKee, J., Kotha, S.R., Patel, R.B., Parinandi, N.L., 2011. Vascular and cardiac impairments in rats inhaling ozone and diesel exhaust particles. Env. Heal. Perspect 119, 312–318. doi:10.1289/ehp.1002386

Kohler, H.P., Grant, P.J., 2000. Plasminogen activator inhibitor type 1 and coronary artery disease. N. Engl. J. Med. 342, 1792–1801.

Koster, T., Blann, a D., Briët, E., Vandenbroucke, J.P., Rosendaal, F.R., 1995. Role of clotting factor VIII in effect of von Willebrand factor on occurrence of deep-vein thrombosis. Lancet 345, 152–155. doi:10.1016/S0140-6736(95)90166-3

Laden, F., Schwartz, J., Speizer, F.E., Dockery, D.W., 2006. Reduction in fine particulate air pollution and mortality: Extended follow-up of the Harvard Six Cities study. Am J Respir Crit Care Med 173, 667–672. doi:10.1164/rccm.200503-443OC

Lambrechtsen, J., Gerke, O., Egstrup, K., Sand, N.P., Nørgaard, B.L., Petersen, H., Mickley, H., Diederichsen, A.C.P., 2012. The relation between coronary artery calcification in asymptomatic subjects and both traditional risk factors and living in the city centre: A DanRisk substudy. J. Intern. Med. 271, 444–450. doi:10.1111/j.1365-2796.2011.02486.x

Langrish, J.P., Bosson, J., Unosson, J., Muala, A., Newby, D.E., Mills, N.L., Blomberg, A., Sandstrom, T., Sandström, T., 2012. Cardiovascular effects of particulate air pollution exposure: Time course and underlying mechanisms. J Intern Med 272, 224–239. doi:10.1111/j.1365-2796.2012.02566.x

Laudano, A.P., Doolittle, R.F., 1978. Synthetic peptide derivatives that bind to fibrinogen and prevent the polymerization of fibrin monomers. Proc Natl Acad Sci U S A 75, 3085–3089.

Lauer, E., Kipen, H., Gandhi, S., Ohman-Strickland, P., Philipp, C., Rich, D., 2009. Acute Platelet Responses to Ambient Particulate Matter. Epidemiology 20, S208–S209 10.1097/01.ede.0000362699.44458.26.

Le Tertre, A., Medina, S., Samoli, E., Forsberg, B., Michelozzi, P., Boumghar, A., Vonk, J.M., Bellini, A., Atkinson, R., Ayres, J.G., Sunyer, J., Schwartz, J., Katsouyanni, K., 2002. Short-term effects of particulate air pollution on cardiovascular diseases in eight European cities. J. Epidemiol. Community Health 56, 773–9. doi:10.1136/jech.56.10.773

Lenting, P.J., Casari, C., Christophe, O.D., Denis, C. V., 2012. von Willebrand factor: The old, the new and the unknown. J. Thromb. Haemost. 10, 2428–2437. doi:10.1111/jth.12008

Lenting, P.J., van Mourik, J. a, Mertens, K., 1998. The life cycle of coagulation factor VIII in view of its structure and function. Blood 92, 3983–3996.

Lepeule, J., Laden, F., Dockery, D., Schwartz, J., 2012. Chronic exposure to fine particles and mortality: an extended follow-up of the Harvard Six Cities study from 1974 to 2009. Env. Heal. Perspect 120, 965–970. doi:10.1289/ehp.1104660

Levick, J.R., 2003. An introduction to cardiovascular physiology. London: Arnold.

Levy, M.N., Pappano, A.J., Berne, R.M., 2007. Cardiovascular physiology. Philadelphia: Mosby Elsevier.

Li, Y.-H., Kuo, C.-H., Shi, G.-Y., Wu, H.-L., 2012. The role of thrombomodulin lectin-like domain in inflammation. J. Biomed. Sci. 19, 34. doi:10.1186/1423-0127-19-34

Liang, H., Jin, C., Tang, Y., Wang, F., Ma, C., Yang, Y., 2014. Cytotoxicity of silica nanoparticles on HaCaT cells. J. Appl. Toxicol. 34, 367–72. doi:10.1002/jat.2953

Libby, P., Theroux, P., 2005. Pathophysiology of coronary artery disease. Circulation 111, 3481–3488. doi:10.1161/CIRCULATIONAHA.105.537878

Lindemann, S., Krämer, B., Seizer, P., Gawaz, M., 2007. Platelets, inflammation and atherosclerosis. J. Thromb. Haemost. 5, 203–211. doi:10.1111/j.1538-7836.2007.02517.x

Liu, X., Sun, J., 2010. Endothelial cells dysfunction induced by silica nanoparticles through oxidative stress via JNK/P53 and NF-kappaB pathways. Biomaterials 31, 8198–8209. doi:10.1016/j.biomaterials.2010.07.069

Lodge, J.K., Kazic, T., Berg, D.E., 1989. Formation of supercoiling domains in plasmid pBR322. J. Bacteriol. 171, 2181–7.

Lord, S.T., 2011. Molecular mechanisms affecting fibrin structure and stability. Arterioscler. Thromb. Vasc. Biol. 31, 494–499. doi:10.1161/ATVBAHA.110.213389

Lu, F., Xu, D., Cheng, Y., Dong, S., Guo, C., Jiang, X., Zheng, X., 2015. Systematic review and meta-analysis of the adverse health effects of ambient PM2.5 and PM10 pollution in the Chinese population. Environ. Res. 136, 196–204. doi:10.1016/j.envres.2014.06.029

Lucking, A.J., Lundback, M., Barath, S.L., Mills, N.L., Sidhu, M.K., Langrish, J.P., Boon, N.A., Pourazar, J., Badimon, J.J., Gerlofs-Nijland, M.E., Cassee, F.R., Boman, C., Donaldson, K., Sandstrom, T., Newby, D.E., Blomberg, A., 2011. Particle traps prevent adverse vascular and prothrombotic effects of diesel engine exhaust inhalation in men. Circulation 123, 1721–1728. doi:10.1161/CIRCULATIONAHA.110.987263

Lucking, A.J., Lundbäck, M., Barath, S.L., Mills, N.L., Sidhu, M.K., Langrish, J.P., Boon, N.A., Pourazar, J., Badimon, J.J., Gerlofs-Nijland, M.E., Cassee, F.R., Boman, C., Donaldson, K., Sandstrom, T., Newby, D.E., Blomberg, A., 2011. Particle traps prevent adverse vascular and prothrombotic effects of diesel engine exhaust inhalation in men. Circulation 123, 1721–1728. doi:10.1161/CIRCULATIONAHA.110.987263

Mackman, N., 2012. New insights into the mechanisms of venous thrombosis. J. Clin. Invest. 122, 2331–2336. doi:10.1172/JCI60229.paralysis

Madden, E.F., Fowler, B.A., 2000. Mechanisms of nephrotoxicity from metal combinations: a review. Drug Chem. Toxicol. 23, 1–12. doi:10.1081/DCT-100100098

Mahmood, S., 2009. Pathophysiology of Coronary Artery Disease, in: Movahed, A., Gnanasegaran, G., Buscombe, J., Hall, M. (Eds.), Integrating Cardiology for Nuclear Medicine Physicians. Springer Berlin Heidelberg, pp. 23–30. doi:10.1007/978-3-540-78674-0_2

Malvindi, M.A., Brunetti, V., Vecchio, G., Galeone, A., Cingolani, R., Pompa, P.P., 2012. SiO2 nanoparticles biocompatibility and their potential for gene delivery and silencing. Nanoscale 4, 486. doi:10.1039/c1nr11269d

Mannucci, P.M., 1998. von Willebrand Factor A Marker of Endothelial Damage? Arter. Thromb Vasc Biol 1359–1362. doi:10.1901/jaba.2010.43-350

McVey, J.H., 1999. Tissue factor pathway. Baillieres Best Pr. Res Clin Haematol 12, 361–372.

Meijers, J.C., Tekelenburg, W.L., Bouma, B.N., Bertina, R.M., Rosendaal, F.R., 2000. High levels of coagulation factor XI as a risk factor for venous thrombosis. N. Engl. J. Med. 342, 696–701. doi:10.1056/NEJM200003093421004

Meltzer, M.E., Doggen, C.J.M., de Groot, P.G., Rosendaal, F.R., Lisman, T., 2007. Fibrinolysis and the risk of venous and arterial thrombosis. Curr. Opin. Hematol. 14, 242–8. doi:10.1097/MOH.0b013e3280dce557

Menzel, D., 1994. The toxicity of air pollution in experimental animals and humans: the role of oxidative stress. Toxicol. Lett. 72, 269–277. doi:10.1016/0378-4274(94)90038-8

Metassan, S., Charlton, A.J., Routledge, M.N., Scott, D.J., Ariens, R.A., 2010a. Alteration of fibrin clot properties by ultrafine particulate matter. Thromb Haemost 103, 103–113. doi:10.1160/TH09-05-0330

Metassan, S., Routledge, M.N., Lucking, A.J., Uitte de Willige, S., Philippou, H., Mills, N.L., Newby, D.E., Ariens, R.A., 2010b. Fibrin clot structure remains unaffected in young, healthy individuals after transient exposure to diesel exhaust. Part Fibre Toxicol 7, 17. doi:10.1186/1743-8977-7-17

Meyer, S.F. De, Deckmyn, H., Vanhoorelbeke, K., 2009. von Willebrand factor to the rescue. Current 113, 5049–5057. doi:10.1182/blood-2008-10-165621.

Milano, M., Dongiovanni, P., Artoni, a, Gatti, S., Rosso, L., Colombo, F., 2015. Particulate matter phagocytosis induces tissue factor in differentiating macrophages. J. Appl. Toxicol. doi:10.1002/jat.3156

Miller, K.A., Siscovick, D.S., Sheppard, L., Shepherd, K., Sullivan, J.H., Anderson, G.L., Kaufman, J.D., 2007. Long-term exposure to air pollution and incidence of cardiovascular events in women. N Engl J Med 356, 447–458. doi:10.1056/NEJMoa054409

Mills, N.L., Donaldson, K., Hadoke, P.W., Boon, N.A., MacNee, W., Cassee, F.R., Sandstrom, T., Blomberg, A., Newby, D.E., 2009. Adverse cardiovascular effects of air pollution. Nat Clin Pr. Cardiovasc Med 6, 36–44. doi:10.1038/ncpcardio1399

Mills, N.L., Törnqvist, H., Gonzalez, M.C., Vink, E., Robinson, S.D., Söderberg, S., Boon, N.A., Donaldson, K., Sandström, T., Blomberg, A., Newby, D.E., 2007. Ischemic and thrombotic effects of dilute diesel-exhaust inhalation in men with coronary heart disease. N. Engl. J. Med. 357, 1075–1082. doi:10.1056/NEJMoa066314

Mills, N.L., Törnqvist, H., Robinson, S.D., Gonzalez, M., Darnley, K., MacNee, W., Boon, N.A., Donaldson, K., Blomberg, A., Sandstrom, T., Newby, D.E., 2005. Diesel exhaust inhalation causes vascular dysfunction and impaired endogenous fibrinolysis. Circulation 112, 3930–3936. doi:10.1161/CIRCULATIONAHA.105.588962

Modena, M.G., Bonetti, L., Coppi, F., Bursi, F., Rossi, R., 2002. Prognostic role of reversible endothelial dysfunction in hypertensive postmenopausal women. J Am Coll Cardiol 40, 505–510.

Morris, R.D., 2001. Airborne particulates and hospital admissions for cardiovascular disease: a quantitative review of the evidence. Env. Heal. Perspect 109 Suppl , 495–500.

Mosesson, M.W., 2005. Fibrinogen and fibrin structure and functions. J Thromb Haemost 3, 1894–1904. doi:10.1111/j.1538-7836.2005.01365.x

Mu, L., Deng, F., Tian, L., Li, Y., Swanson, M., Ying, J., Browne, R.W., Rittenhouse-Olson, K., Zhang, J.J., Zhang, Z.F., Bonner, M.R., 2014. Peak expiratory flow, breath rate and blood pressure in adults with changes in particulate matter air pollution during the Beijing Olympics: a panel study. Env. Res 133, 4–11. doi:10.1016/j.envres.2014.05.006

Napierska, D., Thomassen, L.C.J., Lison, D., Martens, J. a, Hoet, P.H., 2010. The nanosilica hazard: another variable entity. Part. Fibre Toxicol. 7, 39. doi:10.1186/1743-8977-7-39

Napoleone, E., Di Santo, A., Lorenzet, R., 1997. Monocytes upregulate endothelial cell expression of tissue factor: a role for cell-cell contact and cross-talk. Blood 89, 541–549.

Nemery, B., Hoet, P.H., Nemmar, A., 2001. The Meuse Valley fog of 1930: an air pollution disaster. Lancet 357, 704–708. doi:10.1016/S0140-6736(00)04135-0

Nemmar, A., Hoet, P.H.M., Vanquickenborne, B., Dinsdale, D., Thomeer, M., Hoylaerts, M.F., Vanbilloen, H., Mortelmans, L., Nemery, B., 2002. Passage of inhaled particles into the blood circulation in humans. Circulation 105, 411–414. doi:10.1161/hc0402.104118

Newby, D.E., Mannucci, P.M., Tell, G.S., Baccarelli, a. a., Brook, R.D., Donaldson, K., Forastiere, F., Franchini, M., Franco, O.H., Graham, I., Hoek, G., Hoffmann, B., Hoylaerts, M.F., Kunzli, N., Mills, N., Pekkanen, J., Peters, a., Piepoli, M.F., Rajagopalan, S., Storey, R.F., 2014. Expert position paper on air pollution and cardiovascular disease. Eur. Heart J. 36, 83–93. doi:10.1093/eurheartj/ehu458

Norris, L.A., 2003. Blood coagulation. Best Pract. Res. Clin. Obstet. Gynaecol. 17, 369–383. doi:10.1053/S1521-6934(03)00014-2

Okraska-Bylica, A., Wilkosz, T., Słowik, L., Bazanek, M., Konieczyńska, M., Undas, A., 2012. Altered fibrin clot properties in patients with premature peripheral artery disease. Pol. Arch. Med. Wewn. 122, 608–615.

Palka, I., Nessler, J., Nessler, B., Piwowarska, W., Tracz, W., Undas, A., 2010. Altered fibrin clot properties in patients with chronic heart failure and sinus rhythm: a novel prothrombotic mechanism. Heart 96, 1114–1118. doi:10.1136/hrt.2010.192740

Park, E.J., Park, K., 2009. Oxidative stress and pro-inflammatory responses induced by silica nanoparticles in vivo and in vitro. Toxicol Lett 184, 18–25. doi:10.1016/j.toxlet.2008.10.012

Pekkanen, J., Brunner, E.J., Anderson, H.R., Tiittanen, P., Atkinson, R.W., 2000. Daily concentrations of air pollution and plasma fibrinogen in London. Occup. Environ. Med. 57, 818–822. doi:10.1136/oem.57.12.818

Peters, A., 2005. Particulate matter and heart disease: evidence from epidemiological studies. Toxicol Appl Pharmacol 207, 477–482. doi:10.1016/j.taap.2005.04.030

Peters, A., Döring, A., Wichmann, H.E., Koenig, W., 1997. Increased plasma viscosity during an air pollution episode: A link to mortality? Lancet 349, 1582–1587. doi:10.1016/S0140-6736(97)01211-7

Peters, K., Unger, R.E., Kirkpatrick, C.J., Gatti, A.M., Monari, E., 2004. Effects of nano-scaled particles on endothelial cell function in vitro: Studies on viability, proliferation and inflammation. J. Mater. Sci. Mater. Med. 15, 321–325. doi:10.1023/B:JMSM.0000021095.36878.1b

Pham-Huy, L.A., He, H., Pham-Huy, C., 2008. Free radicals, antioxidants in disease and health. Int. J. Biomed. Sci. 4, 89–96.

Polichetti, G., Cocco, S., Spinali, A., Trimarco, V., Nunziata, A., 2009. Effects of particulate matter (PM(10), PM(2.5) and PM(1)) on the cardiovascular system. Toxicology 261, 1–8. doi:10.1016/j.tox.2009.04.035

Pönkä, a, Savela, M., Virtanen, M., 2010. Mortality and air pollution in Helsinki. Arch. Environ. Health 53, 281–6. doi:10.1080/00039899809605709

Pope 3rd, C.A., 2009. The expanding role of air pollution in cardiovascular disease: does air pollution contribute to risk of deep vein thrombosis? Circulation 119, 3050–3052. doi:10.1161/CIRCULATIONAHA.109.870279

Pope, C. a, Thun, M.J., Namboodiri, M.M., Dockery, D.W., Evans, J.S., Speizer, F.E., Heath, C.W., 1995. Particulate air pollution as a predictor of mortality in a prospective study of U.S. adults. Am. J. Respir. Crit. Care Med. 151, 669–74. doi:10.1164/ajrccm/151.3_Pt_1.669

Pope, C.A., Burnett, R.T., Thurston, G.D., Thun, M.J., Calle, E.E., Krewski, D., Godleski, J.J., Pope 3rd, C.A., Burnett, R.T., Thurston, G.D., Thun, M.J., Calle, E.E., Krewski, D., Godleski, J.J., 2004. Cardiovascular Mortality and Long-Term Exposure to Particulate Air Pollution: Epidemiological Evidence of General Pathophysiological Pathways of Disease. Circulation 109, 71–77. doi:10.1161/01.CIR.0000108927.80044.7F

Pope, C.A., Hansen, M.L., Long, R.W., Nielsen, K.R., Eatough, N.L., Wilson, W.E., Eatough, D.J., 2004. Ambient particulate air pollution, heart rate variability, and blood markers of inflammation in a panel of elderly subjects. Environ. Health Perspect. 112, 339–345.

doi:10.1289/ehp.6588

Poursafa, P., Kelishadi, R., Lahijanzadeh, A., Modaresi, M., Javanmard, S.H., Assari, R., Amin, M.M., Moattar, F., Amini, A., Sadeghian, B., 2011. The relationship of air pollution and surrogate markers of endothelial dysfunction in a population-based sample of children. BMC Public Health 11, 115. doi:10.1186/1471-2458-11-115

Rahman, I., MacNee, W., 2000. Oxidative stress and regulation of glutathione in lung inflammation. Eur. Respir. J. 16, 534–54. doi:10.1034/j.1399-3003.2000.016003534.x

Rajagopalan, S., Brook, R.D., 2012. THE INDOOR-OUTDOOR AIR-POLLUTION CONTINUUM AND THE BURDEN OF CARDIOVASCULAR DISEASE: AN OPPORTUNITY FOR IMPROVING GLOBAL HEALTH. Glob. Heart 7, 207–213. doi:10.1016/j.gheart.2012.06.009

Rajzer, M., Wojciechowska, W., Kawecka-Jaszcz, K., Undas, A., 2012. Plasma fibrin clot properties in arterial hypertension and their modification by antihypertensive medication. Thromb Res 130, 99–103. doi:10.1016/j.thromres.2011.08.022

Riddel, J.P., Aouizerat, B.E., Miaskowski, C., Lillicrap, D.P., 2007. Theories of blood coagulation. J. Pediatr. Oncol. Nurs. 24, 123–31. doi:10.1177/1043454206298693

Rim, K.T., Song, S.W., Kim, H.Y., 2013. Oxidative DNA damage from nanoparticle exposure and its application to workers' health: A literature review. Saf. Health Work 4, 177–186. doi:10.1016/j.shaw.2013.07.006

Rosendaal, F.R., Reitsma, P.H., 2009. Genetics of venous thrombosis. J. Thromb. Haemost. doi:10.1111/j.1538-7836.2009.03394.x

Routledge, H.C., Ayres, J.G., 2005. Air pollution and the heart. Occup Med 55, 439–447. doi:10.1093/occmed/kqi136

Rückerl, R., Phipps, R.P., Schneider, A., Frampton, M., Cyrys, J., Oberdörster, G., Wichmann, H.E., Peters, A., 2007. Ultrafine particles and platelet activation in patients with coronary heart disease--results from a prospective panel study. Part. Fibre Toxicol. 4, 1. doi:10.1186/1743-8977-4-1

Ruggeri, Z.M., Ruggeri ZM, 2003. Von Willebrand factor, platelets and endothelial cell interactions. J. Thromb. Haemost. 1, 1335–42. doi:260 [pii]

Samet, J.M., Dominici, F., Curriero, F.C., Coursac, I., Zeger, S.L., 2000. Fine particulate air pollution and mortality in 20 U.S. cities, 1987-1994. N. Engl. J. Med. 343, 1742–9. doi:10.1056/NEJM200012143432401

Schnaith, L.M., Hanson, R.S., Que, L., 1994. Double-stranded cleavage of pBR322 by a diiron complex via a "hydrolytic" mechanism. Proc. Natl. Acad. Sci. U. S. A. 91, 569–73. doi:10.1073/pnas.91.2.569

Schwartz, J., 2001. Air pollution and blood markers of cardiovascular risk. Environ. Health Perspect. 109, 405–409. doi:10.2307/3434788

Schwartz, J., 1997. Air pollution and hospital admissions for cardiovascular disease in Tucson.

Epidemiology 8, 371–377.

Schwartz, J., Morris, R., 1995. Air pollution and hospital admissions for cardiovascular disease in Detroit, Michigan. Am J Epidemiol 142, 23–35.

Scott, E.M., Ariens, R.A., Grant, P.J., 2004. Genetic and environmental determinants of fibrin structure and function: relevance to clinical disease. Arter. Thromb Vasc Biol 24, 1558–1566. doi:10.1161/01.ATV.0000136649.83297.bf

Seaton, A., Soutar, A., Crawford, V., Elton, R., McNerlan, S., Cherrie, J., Watt, M., Agius, R., Stout, R., 1999. Particulate air pollution and the blood. Thorax 54, 1027–1032. doi:10.1136/thx.54.11.1027

Shah, A.S., Langrish, J.P., Nair, H., McAllister, D.A., Hunter, A.L., Donaldson, K., Newby, D.E., Mills, N.L., 2013. Global association of air pollution and heart failure: a systematic review and meta-analysis. Lancet 382, 1039–1048. doi:10.1016/S0140-6736(13)60898-3

Shang, Y., Sun, Z., Cao, J., Wang, X., Zhong, L., Bi, X., Li, H., Liu, W., Zhu, T., Huang, W., 2013. Systematic review of Chinese studies of short-term exposure to air pollution and daily mortality. Environ. Int. doi:10.1016/j.envint.2013.01.010

Simkhovich, B.Z., Kleinman, M.T., Kloner, R. a., 2008. Air Pollution and Cardiovascular Injury. Epidemiology, Toxicology, and Mechanisms. J Am Coll Cardiol 52, 719–726. doi:10.1016/j.jacc.2008.05.029

Smiałek, M. a, Moore, S. a, Mason, N.J., Shuker, D.E.G., 2009. Quantification of radiation-induced single-strand breaks in plasmid DNA using a TUNEL/ELISA-based assay. Radiat. Res. 172, 529–36. doi:10.1667/RR1684.1

Smith, R.A., 1872. Air and Rain. The Beginning of a Chemical Climatology. Longmans, Green, and Co., London.

Snow, S.J., Cheng, W., Wolberg, A.S., Carraway, M.S., 2014. Air pollution upregulates endothelial cell procoagulant activity via ultrafine particle-induced oxidant signaling and tissue factor expression. Toxicol Sci 140, 83–93. doi:10.1093/toxsci/kfu071

Sofat, R., Hingorani, A.D., Smeeth, L., Humphries, S.E., Talmud, P.J., Cooper, J., Shah, T., Sandhu, M.S., Ricketts, S.L., Boekholdt, S.M., Wareham, N., Khaw, K.T., Kumari, M., Kivimaki, M., Marmot, M., Asselbergs, F.W., van der Harst, P., Dullaart, R.P., Navis, G., van Veldhuisen, D.J., Van Gilst, W.H., Thompson, J.F., McCaskie, P., Palmer, L.J., Arca, M., Quagliarini, F., Gaudio, C., Cambien, F., Nicaud, V., Poirer, O., Gudnason, V., Isaacs, A., Witteman, J.C., van Duijn, C.M., Pencina, M., Vasan, R.S., D'Agostino Sr., R.B., Ordovas, J., Li, T.Y., Kakko, S., Kauma, H., Savolainen, M.J., Kesaniemi, Y.A., Sandhofer, A., Paulweber, B., Sorli, J. V, Goto, A., Yokoyama, S., Okumura, K., Horne, B.D., Packard, C., Freeman, D., Ford, I., Sattar, N., McCormack, V., Lawlor, D.A., Ebrahim, S., Smith, G.D., Kastelein, J.J., Deanfield, J., Casas, J.P., 2010. Separating the mechanism-based and off-target actions of cholesteryl ester transfer protein inhibitors with CETP gene polymorphisms. Circulation 121, 52–62. doi:10.1161/CIRCULATIONAHA.109.865444

Solomon, A., Smyth, E., Mitha, N., Pitchford, S., Vydyanath, A., Luther, P.K., Thorley, A.J.,

Tetley, T.D., Emerson, M., 2013. Induction of platelet aggregation after a direct physical interaction with diesel exhaust particles. J. Thromb. Haemost. 11, 325–334. doi:10.1111/jth.12087

Stafoggia, M., Zauli-Sajani, S., Pey, J., Samoli, E., Alessandrini, E., Basagaña, X., Cernigliaro, A., Chiusolo, M., Demaria, M., Díaz, J., Faustini, A., Katsouyanni, K., Kelessis, A.G., Linares, C., Marchesi, S., Medina, S., Pandolfi, P., Pérez, N., Querol, X., Randi, G., Ranzi, A., Tobias, A., Forastiere, F., Study Group, M.-P., 2015. Desert Dust Outbreaks in Southern Europe: Contribution to Daily PM10 Concentrations and Short-Term Associations with Mortality and Hospital Admissions. Environ. Health Perspect. doi:10.1289/ehp.1409164

Standeven, K.F., Ariens, R.A., Grant, P.J., 2005. The molecular physiology and pathology of fibrin structure/function. Blood Rev 19, 275–288. doi:10.1016/j.blre.2005.01.003

Standeven, K.F., Carter, A.M., Grant, P.J., Weisel, J.W., Chernysh, I., Masova, L., Lord, S.T., Ariens, R.A., 2007. Functional analysis of fibrin {gamma}-chain cross-linking by activated factor XIII: determination of a cross-linking pattern that maximizes clot stiffness. Blood 110, 902–907. doi:10.1182/blood-2007-01-066837

Steffel, J., Akhmedov, A., Greutert, H., Lüscher, T.F., Tanner, F.C., 2005a. Histamine induces tissue factor expression: Implications for acute coronary syndromes. Circulation 112, 341–349. doi:10.1161/CIRCULATIONAHA.105.553735

Steffel, J., Hermann, M., Greutert, H., Gay, S., Lüscher, T.F., Ruschitzka, F., Tanner, F.C., 2005b. Celecoxib decreases endothelial tissue factor expression through inhibition of c-Jun terminal NH 2 kinase phosphorylation. Circulation 111, 1685–1689. doi:10.1161/01.CIR.0000160358.63804.C9

Steffel, J., Lüscher, T.F., Tanner, F.C., 2006. Tissue factor in cardiovascular diseases: Molecular mechanisms and clinical implications. Circulation. doi:10.1161/CIRCULATIONAHA.105.567297

Su, T.-C., Chan, C.-C., Liau, C.-S., Lin, L.-Y., Kao, H.-L., Chuang, K.-J., 2006. Urban air pollution increases plasma fibrinogen and plasminogen activator inhibitor-1 levels in susceptible patients. Eur. J. Cardiovasc. Prev. Rehabil. 13, 849–52. doi:10.1097/01.hjr.0000219116.25415.c4

Suefuji, H., Ogawa, H., Yasue, H., Kaikita, K., Soejima, H., Motoyama, T., Mizuno, Y., Oshima, S., Saito, T., Tsuji, I., Kumeda, K., Kamikubo, Y., Nakamura, S., 1997. Increased plasma tissue factor levels in acute myocardial infarction. Am Hear. J 134, 253–259.

Sumpio, B.E., Riley, J.T., Dardik, A., 2002. Cells in focus: endothelial cell. Int J Biochem Cell Biol 34, 1508–1512.

Sun, Q., Hong, X., Wold, L.E., 2010. Cardiovascular effects of ambient particulate air pollution exposure. Circulation 121, 2755–2765. doi:10.1161/CIRCULATIONAHA.109.893461

Supino, R., 1995. MTT assays. Methods Mol. Biol. 43, 137–149. doi:10.2307/302397

Tang, M., Li, Q., Xiao, L., Li, Y., Jensen, J.L., Liou, T.G., Zhou, A., 2012. Toxicity effects of short term diesel exhaust particles exposure to human small airway epithelial cells (SAECs) and

human lung carcinoma epithelial cells (A549). Toxicol. Lett. 215, 181–192. doi:10.1016/j.toxlet.2012.10.016

Tedgui, A., Mallat, Z., 2003. Apoptosis, a major determinant of atherothrombosis. Arch Mal Coeur Vaiss 96, 671–675.

Teow, Y., Asharani, P. V, Hande, M.P., Valiyaveettil, S., 2011. Health impact and safety of engineered nanomaterials. Chem Commun 47, 7025–7038. doi:10.1039/c0cc05271j

Teruel-Montoya, R., Rosendaal, F.R., Martínez, C., 2014. MicroRNAs in hemostasis. J. Thromb. Haemost. 1–12. doi:10.1111/jth.12788

Thron, R.W., 1996. Direct and indirect exposure to air pollution, ,. Otolaryngol. - Head Neck Surg. 114, 281–285. doi:10.1016/S0194-5998(96)70184-5

Uitte de Willige, S., Standeven, K.F., Philippou, H., Ariens, R.A., 2009. The pleiotropic role of the fibrinogen gamma' chain in hemostasis. Blood 114, 3994–4001. doi:10.1182/blood-2009-05-217968

Undas, A., Ariens, R.A., 2011. Fibrin clot structure and function: a role in the pathophysiology of arterial and venous thromboembolic diseases. Arter. Thromb Vasc Biol 31, e88–99. doi:10.1161/ATVBAHA.111.230631

Undas, A., Ariëns, R.A.S., 2011. Fibrin clot structure and function: A role in the pathophysiology of arterial and venous thromboembolic diseases. Arterioscler. Thromb. Vasc. Biol. doi:10.1161/ATVBAHA.111.230631

Undas, A., Brozek, J., Jankowski, M., Siudak, Z., Szczeklik, A., Jakubowski, H., 2006. Plasma homocysteine affects fibrin clot permeability and resistance to lysis in human subjects. Arter. Thromb Vasc Biol 26, 1397–1404. doi:10.1161/01.ATV.0000219688.43572.75

Undas, A., Podolec, P., Zawilska, K., Pieculewicz, M., Jedlinski, I., Stepien, E., Konarska-Kuszewska, E., Weglarz, P., Duszynska, M., Hanschke, E., Przewlocki, T., Tracz, W., 2009. Altered fibrin clot structure/function in patients with cryptogenic ischemic stroke. Stroke 40, 1499–1501. doi:10.1161/STROKEAHA.108.532812

Undas, A., Szu??drzynski, K., Stepien, E., Zalewski, J., Godlewski, J., Tracz, W., Pasowicz, M., Zmudka, K., 2008. Reduced clot permeability and susceptibility to lysis in patients with acute coronary syndrome: Effects of inflammation and oxidative stress. Atherosclerosis 196, 551–557. doi:10.1016/j.atherosclerosis.2007.05.028

Undas, A., Zawilska, K., Ciesla-Dul, M., Lehmann-Kopydłowska, A., Skubiszak, A., Ciepłuch, K., Tracz, W., 2009. Altered fibrin clot structure/function in patients with idiopathic venous thromboembolism and in their relatives. Blood 114, 4272–4278. doi:10.1182/blood-2009-05-222380

Undas, A., Zubkiewicz-Usnarska, L., Helbig, G., Woszczyk, D., Kozi??ska, J., Dmoszy??ska, A., Podolak-Dawidziak, M., Kuliczkowski, K., 2014. Altered plasma fibrin clot properties and fibrinolysis in patients with multiple myeloma. Eur. J. Clin. Invest. 44, 557–566. doi:10.1111/eci.12269

Utell, M.J., Frampton, M.W., Zareba, W., Devlin, R.B., Cascio, W.E., 2002. Cardiovascular effects associated with air pollution: potential mechanisms and methods of testing. Inhal Toxicol 14, 1231–1247. doi:10.1080/08958370290084881

Valko, M., Leibfritz, D., Moncol, J., Cronin, M.T.D., Mazur, M., Telser, J., 2007. Free radicals and antioxidants in normal physiological functions and human disease. Int. J. Biochem. Cell Biol. 39, 44–84. doi:10.1016/j.biocel.2006.07.001

van Hylckama Vlieg, a, van der Linden, I.K., Bertina, R.M., Rosendaal, F.R., 2000. High levels of factor IX increase the risk of venous thrombosis. Blood 95, 3678–82.

Vermylen, J., Nemmar, A., Nemery, B., Hoylaerts, M.F., 2005. Ambient air pollution and acute myocardial infarction. J. Thromb. Haemost. 3, 1955–1961. doi:10.1111/j.1538-7836.2005.01471.x

Versteeg, H.H., Heemskerk, J.W., Levi, M., Reitsma, P.H., 2013. New fundamentals in hemostasis. Physiol Rev 93, 327–358. doi:10.1152/physrev.00016.2011

Versteeg, H.H., Ruf, W., 2013. New helpers in TF-dependent migration. J Thromb Haemost 11, 1877–1879. doi:10.1111/jth.12378

Vischer, U.M., 2006. von Willebrand factor, endothelial dysfunction, and cardiovascular disease. J. Thromb. Haemost. 4, 1186–93. doi:10.1111/j.1538-7836.2006.01949.x

Wang, Y., Eliot, M.N., Wellenius, G. a., 2014. Short-term Changes in Ambient Particulate Matter and Risk of Stroke: A Systematic Review and Meta-analysis. J. Am. Heart Assoc. 3, e000983–e000983. doi:10.1161/JAHA.114.000983

Weisel, J.W., 2007. Structure of fibrin: impact on clot stability. J Thromb Haemost 5 Suppl 1, 116–124. doi:10.1111/j.1538-7836.2007.02504.x

Weisel, J.W., 1986. Fibrin assembly. Lateral aggregation and the role of the two pairs of fibrinopeptides. Biophys J 50, 1079–1093. doi:10.1016/S0006-3495(86)83552-4

Weisel, J.W., Litvinov I., R., 2013. Mechanisms of fibrin polymerization and clinical implications. Blood Coagul Fibrinolysis 121, 1712–1719.

Wellenius, G.A., Schwartz, J., Mittleman, M.A., 2006. Particulate air pollution and hospital admissions for congestive heart failure in seven {United States} cities. Am J Cardiol 97, 404–408. doi:S0002-9149(05)01831-X [pii]\n10.1016/j.amjcard.2005.08.061

Whincup, P.H., Danesh, J., Walker, M., Lennon, L., Thomson, A., Appleby, P., Rumley, A., Lowe, G.D., 2002. von Willebrand factor and coronary heart disease: prospective study and meta-analysis. Eur Hear. J 23, 1764–1770.

Wichmann, H.-E., Peters, A., 2000. Epidemiological evidence of the effects of ultrafine particle exposure. Philos. Trans. R. Soc. A Math. Phys. Eng. Sci. 358, 2751–2769. doi:10.1098/rsta.2000.0682

Wolberg, A.S., 2007. Thrombin generation and fibrin clot structure. Blood Rev 21, 131–142. doi:10.1016/j.blre.2006.11.001

Wolberg, A.S., Campbell, R.A., 2008. Thrombin generation, fibrin clot formation and hemostasis. Transfus. Apher. Sci. 38, 15–23. doi:10.1016/j.transci.2007.12.005

World Health Organisation, 2015a. WHO | Background information on urban outdoor air pollution.

World Health Organisation, 2015b. WHO | Household air pollution and health.

World Health Organisation, 2014. WHO | Ambient (outdoor) air pollution in cities database 2014.

World Health Organisation, 2011. Air quality and health [WWW Document]. URL http://www.who.int/mediacentre/factsheets/fs313/en/

Wu, K.K., Thiagarajan, P., 1996. Role of endothelium in thrombosis and hemostasis. Annu. Rev. Med. 47, 315–331. doi:10.1146/annurev.med.47.1.315

Wu, Y., Yu, T., Gilbertson, T. a., Zhou, A., Xu, H., Nguyen, K.T., 2012. Biophysical assessment of single cell cytotoxicity: Diesel exhaust particle-treated human aortic endothelial cells. PLoS One 7, 1–10. doi:10.1371/journal.pone.0036885

Xia, T., Li, N., Nel, A.E., 2009. Potential health impact of nanoparticles. Annu Rev Public Heal. 30, 137–150. doi:10.1146/annurev.publhealth.031308.100155

Yamamoto, H., Vreys, I., Stassen, J.M., Yoshimoto, R., Vermylen, J., Hoylaerts, M.F., 1998. Antagonism of vWF inhibits both injury induced arterial and venous thrombosis in the hamster. Thromb. Haemost. 79, 202–210.

Yang, Y.X., Song, Z.M., Cheng, B., Xiang, K., Chen, X.X., Liu, J.H., Cao, A., Wang, Y., Liu, Y., Wang, H., 2014. Evaluation of the toxicity of food additive silica nanoparticles on gastrointestinal cells. J Appl Toxicol 34, 424–435. doi:10.1002/jat.2962

Zeka, A., Sullivan, J.R., Vokonas, P.S., Sparrow, D., Schwartz, J., 2006. Inflammatory markers and particulate air pollution: Characterizing the pathway to disease. Int. J. Epidemiol. 35, 1347–1354. doi:10.1093/ije/dyl132

Zhang, L.W., Chen, X., Xue, X.D., Sun, M., Han, B., Li, C.P., Ma, J., Yu, H., Sun, Z.R., Zhao, L.J., Zhao, B.X., Liu, Y.M., Chen, J., Wang, P.P., Bai, Z.P., Tang, N.J., 2014. Long-term exposure to high particulate matter pollution and cardiovascular mortality: a 12-year cohort study in four cities in northern China. Env. Int 62, 41–47. doi:10.1016/j.envint.2013.09.012

Zhang, P., Dong, G., Sun, B., Zhang, L., Chen, X., Ma, N., Yu, F., Guo, H., Huang, H., Lee, Y.L., Tang, N., Chen, J., 2011. Long-term exposure to ambient air pollution and mortality due to cardiovascular disease and cerebrovascular disease in Shenyang, China. PLoS One 6, e20827. doi:10.1371/journal.pone.0020827

Zhou, M., Liu, Y., Wang, L., Kuang, X., Xu, X., Kan, H., 2014. Particulate air pollution and mortality in a cohort of Chinese men. Env. Pollut 186, 1–6. doi:10.1016/j.envpol.2013.11.010

Zhu, J., Liao, L., Zhu, L., Zhang, P., Guo, K., Kong, J., Ji, C., Liu, B., 2013. Size-dependent cellular

uptake efficiency, mechanism, and cytotoxicity of silica nanoparticles toward HeLa cells. Talanta 107, 408–415. doi:10.1016/j.talanta.2013.01.037